

RADC-TR-90-211
In-House Report
July 1990



(2)

AD-A226 493

SYNTHESIS OF MULTICHANNEL AUTOREGRESSIVE RANDOM PROCESSES AND ERGODICITY CONSIDERATIONS

James H. Michels

DTIC
ELECTE
SEP 18 1990
S B D

APPROVED FOR PUBLIC RELEASE; DISTRIBUTION UNLIMITED.

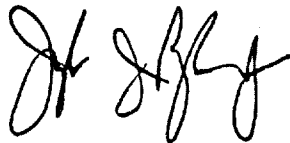
**Rome Air Development Center
Air Force Systems Command
Griffiss Air Force Base, NY 13441-5700**

90 09 17 075

This report has been reviewed by the RADC Public Affairs Division (PA) and is releasable to the National Technical Information Services (NTIS) At NTIS it will be releasable to the general public, including foreign nations.

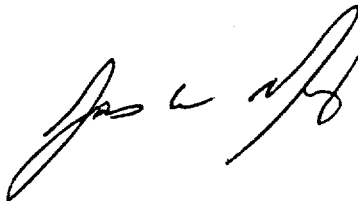
RADC-TR-90-211 has been reviewed and is approved for publication.

APPROVED:



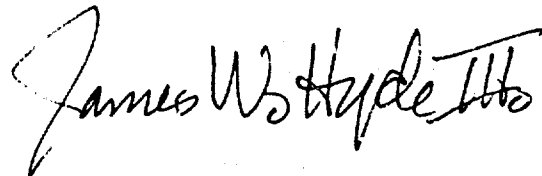
JOSEPH J. POLNIASZEK
Acting Chief, Surveillance Technology Division
Directorate of Surveillance

APPROVED:



James W. Youngberg, LtCol, USAF
Deputy Director of Surveillance

FOR THE COMMANDER:



JAMES W. HYDE III
Directorate of Plans and Programs

If your address has changed or if you wish to be removed from the RADC mailing list, or if the addressee is no longer employed by your organization, please notify RADC (OCTM) Griffiss AFB NY 13441-5700. This will assist us in maintaining a current mailing list.

Do not return copies of this report unless contractual obligations or notices on a specific document require that it be returned.

REPORT DOCUMENTATION PAGE

Form Approved
OPM No. 0704-0188

Public reporting burden for this collection of information is estimated to average 1 hour per response, including the time for reviewing instructions, searching existing data sources, gathering and maintaining the data needed, and completing and reviewing the collection of information. Send comments regarding this burden estimate or any other aspect of this collection of information, including suggestions for reducing the burden, to Washington Headquarters Services, Directorate for Information Operations and Reports, 1215 Jefferson Davis Highway, Suite 1204, Arlington, VA 22202-4302, and to the Office of Management and Budget, Paperwork Project, Washington, DC 20503.

1. AGENCY USE ONLY (Leave Blank)		2. REPORT DATE July 1990	3. REPORT TYPE AND DATES COVERED In-House Aug 89 - May 90	
4. TITLE AND SUBTITLE Synthesis of Multichannel Autoregressive Random Processes and Ergodicity Considerations			5. FUNDING NUMBERS PE - 62702F PR - 4506 TA - 17 WU - 67	
6. AUTHOR(S) James H. Michels				
7. PERFORMING ORGANIZATION NAME(S) AND ADDRESS(ES) Rome Air Development Center (OCTM) Griffiss AFB NY 13441-5700			8. PERFORMING ORGANIZATION REPORT NUMBER RADC-TR-90-211	
9. SPONSORING/MONITORING AGENCY NAME(S) AND ADDRESS(ES) Rome Air Development Center (OCTM) Griffiss AFB NY 13441-5700			10. SPONSORING/MONITORING AGENCY REPORT NUMBER	
11. SUPPLEMENTARY NOTES RADC Project Engineer: James H. Michels/OCTM/(315) 330-4432				
12a. DISTRIBUTION/AVAILABILITY STATEMENT Approved for public release; distribution unlimited.			12b. DISTRIBUTION CODE	
13. ABSTRACT (Maximum 200 words) In this paper, a method is presented for synthesizing multichannel autoregressive random processes. The procedure allows for variable temporal and cross-correlation properties subject to specific constraint conditions for correlation functions. Expressions for the ergodic series are also developed providing a performance measure to specify the sample integration sizes required to achieve a specific variance of the time-averaged correlation function estimates. A unique aspect of this development is the determination of the functional dependence of the ergodic series in terms of the temporal correlation and variances of the processes. As a result, this analysis provides an analytic description which quantitatively assesses the ergodicity of the auto- and cross-correlation functions in terms of these fundamental process parameters. Thus, the variation of the process statistics based on time averages from those based on ensemble averages is given a more quantitative description than previously noted.				
14. SUBJECT TERMS Random Processes, Autoregressive Processes, Multichannel Processes, Ergodicity, Parameter Estimation			15. NUMBER OF PAGES 210	
			16. PRICE CODE	
17. SECURITY CLASSIFICATION OF REPORT UNCLASSIFIED	18. SECURITY CLASSIFICATION OF THIS PAGE UNCLASSIFIED	19. SECURITY CLASSIFICATION OF ABSTRACT UNCLASSIFIED	20. LIMITATION OF ABSTRACT UL	

ACKNOWLEDGEMENTS

The author acknowledges the helpful guidance and encouragement of Drs. P. Varshney and D. Weiner. Special thanks to R. Vienneau and T. Robins for their skillful software engineering support leading to the results shown in section VII. Thanks also to D. Gentile for helpful suggestions in the document preparation. The author also wishes to express his appreciation to Mr. Frank Rehm and Mr. Fred Demma for their managerial support of this work.

Contents

I. INTRODUCTION	1
II. VECTOR PROCESS DEFINITION	3
III. THE COMPLEX CORRELATION FUNCTION AND SPECTRAL PROPERTIES	6
A. IN-PHASE AND QUADRATURE COMPONENT FORM	6
B. POLAR FORM	10
C. CORRELATION FUNCTION SHAPING APPROACH	13
1. GENERAL DEVELOPMENT	13
2. THE AUTOCORRELATION FUNCTION	17
a. THE GAUSSIAN SHAPED AUTOCORRELATION FUNCTION	17
b. THE EXPONENTIAL SHAPED AUTOCORRELATION FUNCTION	18
c. THE SINC SHAPED AUTOCORRELATION FUNTION	19
d. NORMALIZATION BY THE WHITE NOISE VARIANCE	19
e. POLAR FORM WITH A DOPPLER SHIFT	20
3. THE CROSS-CORRELATION FUNCTION	20
a. THE GAUSSIAN SHAPED CROSS-CORRELATION FUNCTION	21
b. THE EXPONENTIAL SHAPED CROSS-CORRELATION FUNCTION	25
c. THE SINC SHAPED CROSS-CORRELATION FUNCTION	26
d. MULTICHANNEL DOPPLER PROCESSES	26
4. CONSTRAINT CONDITIONS FOR CORRELATION FUNCTIONS	29
a. GENERAL. CONSTRAINT CONDITIONS	29
b. CONDITIONS FOR POSITIVE SEMI-DEFINITENESS	32
D. SPECTRA FOR COMPLEX CORRELATION FUNCTIONS	41
1. GENERAL RELATIONSHIPS	41
2. QUADRATIC COMPONENT FORM	44
3. SPECTRAL DISTRIBUTION USING FUNCTIONAL SHAPING	45
a. SPECTRUM OF THE GAUSSIAN SHAPED AUTOCORRELATION	45
b. SPECTRUM OF THE EXPONENTIAL SHAPED AUTOCORRELATION	49

E. SPECIAL PROPERTIES OF COMPLEX CORRELATION FUNCTIONS	51
1. EVEN AND ODD COMPONENTS	51
a. SINGLE CHANNEL CASE	51
b. MULTICHANNEL CASE	54
2. NARROWBAND BANDPASS PROCESSES	56
a. SINGLE CHANNEL CASE	56
b. MULTICHANNEL CASE	62
IV. ERGODICITY OF THE CORRELATION FUNCTIONS	70
A. ERGODICITY OF THE AUTOCORRELATION FUNCTION	70
B. ERGODICITY OF THE CROSS-CORRELATION FUNCTION	78
V. MULTICHANNEL AUTOREGRESSIVE PROCESS MODELS	83
A. DEFINITION OF THE AR PROCESS	83
B. THE YULE-WALKER EQUATION	85
VI. PROCESS SYNTHESIS	87
A. GENERAL PROCEDURE	87
B. ALTERNATE APPROACH	92
C. COMPLEX PROCESSES WITH JOINTLY GAUSSIAN QUADRATURE COMPONENTS	92
VII. SYNTHESIS RESULTS	98
A. SINGLE CHANNEL CASE	98
B. MULTICHANNEL CASE	109
C. THE AUTOCORRELATION FUNCTION ERGODICITY RESULTS	134
D. THE CROSS-CORRELATION FUNCTION ERGODICITY RESULTS	157
REFERENCES	171
APPENDIX A	173
APPENDIX B	175
APPENDIX C	181
APPENDIX D	185
APPENDIX E	190
APPENDIX F	192
APPENDIX G	194
APPENDIX H	197

I. INTRODUCTION

In this report, a method of synthesizing multichannel random processes with variable temporal and cross-correlation properties is developed. This synthesis method provides a capability to generate processes for the evaluation of multichannel detection and estimation algorithms currently being assessed [1]. In detection analyses, this program provides a means to assess performance capability in terms of a receiver operating characteristic (ROC) by allowing for parametric variations such as signal-to-noise (S/N) and clutter-to-noise (C/N) ratios, pulse-to-pulse correlation and cross-channel correlation properties.

In section II, the vector observation processes of interest are defined together with their associated correlation matrix. The complex auto- and cross-correlation functions are considered in section III. These functions are initially introduced in terms of their quadrature and polar forms. However, in section III.C, we propose a functional shaping approach which enables these functions to be considered directly in terms of their correlation parameters. This approach is the key feature which provides control of the process parameters in the synthesis procedure. These functional forms, however, do not necessarily satisfy the properties of correlation functions. In section III.C.4, we discuss important constraint conditions on the functional parameters which must be imposed to satisfy these properties. We note, however, that these conditions are necessary, but not in themselves sufficient, to ensure the proper functional form for correlation functions. Therefore, care must be used in the parameter selection process in order to synthesize physically realizable processes.

In section IV, the concept of ergodicity of the correlation functions is discussed in terms of the temporal and cross-correlation parameters. This relationship is of critical importance in detection and estimation schemes which utilize parameter estimation methods. Ergodicity is the condition under which time-averaged statistics of random processes approximate those obtained by ensemble averages. This condition is often assumed in estimation and other signal processing applications. In this section, the ergodicity condition for auto- and cross-channel correlation functions is derived in terms of fundamental process parameters. Specifically, analytic expressions are developed for the variance of the time-averaged correlation functions for discrete, complex processes. These expressions provide a performance measure which can be used to specify the

window size of the observation interval required to achieve a specific value of this variance. A unique aspect of this development is the determination of the functional dependence of these expressions in terms of the process temporal and ensemble correlation parameters. In addition, the analytic expressions are simplified for the general case of complex processes with jointly Gaussian quadrature components where the usual assumptions associated with a complex Gaussian process are relaxed.

In section V and VI, we define autoregressive (AR) vector processes and propose a method for their synthesis in terms of the correlation parameters. This method provides a generalization of the single channel approach proposed in [2] to the multivariate case. Finally, in section VII, we illustrate examples of the synthesized outputs as well as a validation of the ergodicity analysis discussed in section IV.

II. THE VECTOR PROCESS DEFINITION

In this report, we will consider the synthesis of vector processes under hypotheses H_0 and H_1 , such that

$$\begin{aligned} H_1: \quad \underline{x}(n) &= \underline{s}(n) + \underline{c}(n) + \underline{w}(n) & n &= 1, 2, \dots, N \\ H_0: \quad \underline{x}(n) &= \underline{c}(n) + \underline{w}(n) & n &= 1, 2, \dots, N \end{aligned} \quad (2.1)$$

where $\underline{x}(n)$ is a zero mean, wide-sense stationary $J \times 1$ received observation vector consisting of J channels and $\underline{s}(n)$, $\underline{c}(n)$ and $\underline{w}(n)$ are zero mean, complex Gaussian random $J \times 1$ vector processes describing the signals, non-white noise (clutter) and white noise, respectively. These vectors are treated here as uncorrelated with each other. However, methods to correlate $\underline{s}(n)$ and $\underline{c}(n)$ could be used to model physical conditions such as radar multi-path or reverberation. Furthermore, $\underline{w}(n)$ is uncorrelated with itself in time, but not across channels, so that

$$E[\underline{w}(n) \underline{w}^H(k)] = \begin{cases} [0] & n \neq k \\ R_{ww}(0) & n = k \end{cases} \quad (2.2)$$

where $R_{ww}(0)$ is the $J \times J$ correlation matrix of $\underline{w}(n)$. The vector processes $\underline{s}(n)$ and $\underline{c}(n)$, however, contain an arbitrary correlation in time and between channels. We will consider the condition where $\underline{s}(n)$, $\underline{c}(n)$ and $\underline{w}(n)$ are jointly wide-sense stationary processes. The correlation matrix for the observation data expressed in index ordered form [3] is

$$R_{\underline{x}\underline{x}} = E[\underline{x}_{1,N}^H \underline{x}_{1,N}] \quad (2.3)$$

where

$$\underline{x}_{1,N}^T = [\underline{x}^T(1) \quad \underline{x}^T(2) \dots \underline{x}^T(N)] \quad (2.4a)$$

$$\underline{x}^T(k) = [x_1(k) \quad x_2(k) \dots x_J(k)]. \quad (2.4b)$$

Under the condition of wide-sense stationarity, $R_{\underline{X}\underline{X}}$ is a Hermitian, positive semi-definite matrix. We will prove this below. Furthermore, this matrix can be written in block form as

$$R_{\underline{X}\underline{X}}^B = \begin{bmatrix} R_{\underline{X}\underline{X}}(0) & R_{\underline{X}\underline{X}}(-1) & \dots & R_{\underline{X}\underline{X}}(-N+1) \\ R_{\underline{X}\underline{X}}(1) & R_{\underline{X}\underline{X}}(0) & \dots & R_{\underline{X}\underline{X}}(-N+2) \\ \dots & \dots & \dots & \dots \\ R_{\underline{X}\underline{X}}(N-1) & R_{\underline{X}\underline{X}}(N-2) & \dots & R_{\underline{X}\underline{X}}(0) \end{bmatrix} = \begin{bmatrix} R_{\underline{X}\underline{X}}^H(0) & R_{\underline{X}\underline{X}}^H(1) & \dots & R_{\underline{X}\underline{X}}^H(N-1) \\ R_{\underline{X}\underline{X}}^H(-1) & R_{\underline{X}\underline{X}}^H(0) & \dots & R_{\underline{X}\underline{X}}^H(N-2) \\ \dots & \dots & \dots & \dots \\ R_{\underline{X}\underline{X}}^H(-N+1) & R_{\underline{X}\underline{X}}^H(-N+2) & \dots & R_{\underline{X}\underline{X}}^H(0) \end{bmatrix} \quad (2.5)$$

where

$$R_{\underline{X}\underline{X}}(l) = E[\underline{X}(k) \underline{X}^H(k-l)] \quad \begin{matrix} k = 1, 2, \dots, N \\ l = 0, \pm 1, \dots, \pm(N-1) \end{matrix} \quad (2.6)$$

and the last expression in eq (2.5) results because $R_{\underline{X}\underline{X}}(l) = R_{\underline{X}\underline{X}}^H(-l)$. It is noted, however, that each block matrix of $R_{\underline{X}\underline{X}}$ is not Hermitian; i.e., $R_{\underline{X}\underline{X}}(l) \neq R_{\underline{X}\underline{X}}^H(l)$ for $l \neq 0$. We also note that $R_{\underline{X}\underline{X}}$ is block Toeplitz. The superscript B denotes that $R_{\underline{X}\underline{X}}$ is written in block form where each block as defined in eq(2.6) is a $J \times J$ correlation matrix over the J channels.

We now show that the matrix expressed in eqs(2.3) and (2.5) is positive semi-definite[4]. Using eq(2.4a) in (2.3), we can express the correlation matrix as

$$R_{\underline{X}\underline{X}} = E \left\{ \begin{bmatrix} \underline{X}(1) \\ \underline{X}(2) \\ \vdots \\ \underline{X}(N) \end{bmatrix} [\underline{X}^H(1) \underline{X}^H(2) \dots \underline{X}^H(N)] \right\} \quad (2.7)$$

where we note the dyadic form of the observation vector process. We now let ξ be an arbitrary (non-zero) $JN \times 1$ complex valued vector. Define the scalar random variable y as the inner product of ξ and $\underline{X}_{1,N}$ so that

$$y = \xi^H \underline{x}_{1,N} \quad (2.8)$$

Taking the Hermitian transpose of both sides of eq(2.8) and recognizing that y is a scalar, we obtain

$$y^* = \underline{x}_{1,N}^H \xi \quad (2.9)$$

Eqs (2.8) and (2.9) can now be used to obtain

$$E[|y|^2] = E[yy^*] \quad (2.10a)$$

$$= E[\xi^H \underline{x}_{1,N} \underline{x}_{1,N}^H \xi] \quad (2.10b)$$

$$= \xi^H E[\underline{x}_{1,N} \underline{x}_{1,N}^H] \xi \quad (2.10c)$$

$$= \xi^H R_{\underline{xx}} \xi \quad (2.10d)$$

where $R_{\underline{xx}}$ is the correlation matrix defined in eqs(2.3), (2.5), and (2.7). Since

$$E[|y|^2] \geq 0 \quad (2.11)$$

then

$$\xi^H R_{\underline{xx}} \xi \geq 0 \quad (2.12)$$

so that $R_{\underline{xx}}$ is positive semi-definite. We note, however, that the correlation matrix

$$R_{\underline{xx}}(l) = E[\underline{x}(k) \underline{x}^H(k-l)] \quad (2.13)$$

is not Hermitian for $l \neq 0$. Thus eq(2.10d) does not hold for $R_{\underline{xx}}(l)$. It is the property that the correlation matrix is expressed in the dyadic form of eq(2.7) that provides the non-negative quadratic expression noted in eq(2.12). This very specific structure of the correlation matrix imposes restrictions on the functional form of the auto- and cross-correlation functions and must be considered in the functional shaping method described in this report.

III. COMPLEX CORRELATION FUNCTION AND SPECTRAL PROPERTIES

In this chapter, we consider the complex auto- and cross-correlation functions. In section III.A, these functions are presented in terms of the in-phase(I) and quadrature(Q) form. This form will be helpful in developing some interesting properties of complex auto- and cross-correlation functions not often addressed in the literature. The polar form of these functions is considered in section III.B. This form will enable us to consider correlation functions (and thus spectra through the Fourier transform) with general shapes, subject to constraint conditions imposed on correlation functions. Furthermore, these general functions will be expressed in terms of various correlation parameters. These considerations are discussed in section III.C. In chapter V, these forms of the correlation function are then used in a method to synthesize Gaussian autoregressive processes with various spectral shape. In section III.D, the spectral properties associated with complex autocorrelation functions are considered. Finally, in section III.E, several properties associated with the even and odd components of the correlation functions are presented; in addition, some important properties of narrowband, stationary, bandpass processes are reviewed.

A. In-Phase and Quadrature Component Form

In this section, we consider the form of the complex auto- and cross correlation functions in terms of an in-phase(I) and quadrature(Q) form. Consider the wide-sense stationary, zero-mean, complex Gaussian baseband process $\{x_i(n)\}$ for channel i expressed in terms of its in-phase and quadrature components such that

$$x_i(n) = x_{iI}(n) + jx_{iQ}(n). \quad (3.A.1)$$

For jointly stationary processes, the cross-correlation ($i \neq j$)¹ and autocorrelation ($i=j$) function is expressed as

$$R_{ij}(l) = E[x_i(n)x_j^*(n-l)] \quad (3.A.2a)$$

$$= E\{[x_{iI}(n) + jx_{iQ}(n)][x_{jI}(n-l) - jx_{jQ}(n-l)]\} \quad (3.A.2b)$$

$$= \{E[x_{iI}(n)x_{jI}(n-l)] + E[x_{iQ}(n)x_{jQ}(n-l)]\} \\ + j\{E[x_{iQ}(n)x_{jI}(n-l)] - E[x_{iI}(n)x_{jQ}(n-l)]\} \quad (3.A.2c)$$

$$= \{R_{ij}^{II}(l) + R_{ij}^{QQ}(l)\} + j\{R_{ij}^{QI}(l) - R_{ij}^{IQ}(l)\} \quad (3.A.2d)$$

$$= R_{Aij}(l) + jR_{Bij}(l) \quad (3.A.2e)$$

where

$$R_{Aij}(l) = R_{ij}^{II}(l) + R_{ij}^{QQ}(l) \quad (3.A.3a)$$

$$R_{Bij}(l) = R_{ij}^{QI}(l) - R_{ij}^{IQ}(l) \quad (3.A.3b)$$

and

$$R_{ij}^{II}(l) = E[x_{iI}(n)x_{jI}(n-l)] \quad (3.A.3c)$$

$$R_{ij}^{QQ}(l) = E[x_{iQ}(n)x_{jQ}(n-l)] \quad (3.A.3d)$$

$$R_{ij}^{IQ}(l) = E[x_{iI}(n)x_{jQ}(n-l)] \quad (3.A.3e)$$

$$R_{ij}^{QI}(l) = E[x_{iQ}(n)x_{jI}(n-l)] \quad (3.A.3f)$$

¹The subscript j for channel j should not be confused with $\sqrt{-1}$.

We note that the correlation functions in eqs(3.A.3) are real. In section III.E, we will discuss some interesting properties regarding the evenness and oddness of these functions. For stationary processes, we have the property

$$R_{ij}(l) = R_{ji}^*(-l). \quad (3.A.4)$$

PROOF

Consider

$$R_{ij}(n, n-l) = R_{ij}(l) = E[x_i(n)x_j^*(n-l)] \quad (3.A.5)$$

and

$$R_{ji}(n-l, n) = R_{ji}(-l) = E[x_j(n-l)x_i^*(n)] \quad (3.A.6)$$

From eq.(3.A.6)

$$R_{ji}^*(-l) = E[x_i(n)x_j^*(n-l)]. \quad (3.A.7)$$

The proof follows from the equivalence of the RHS of eqs(3.A.5) and (3.A.7).

The autocorrelation property follows when $i=j$ so that

$$R_{ii}(l) = R_{ii}^*(-l). \quad (3.A.8)$$

We now consider the complex process $x_i(n)$ to consist of a signal $s_i(n)$ plus an additive disturbance such that

$$x_i(n) = s_i(n) + c_i(n) + w_i(n) \quad (3.A.9)$$

where $c_i(n)$ and $w_i(n)$ are additive non-white and white noise processes on channel i , respectively. In section III.C, we develop functional forms of the correlation functions for the signal and disturbance processes which will allow considerable flexibility in modeling these processes. In quadrature component form $s_i(n)$ is expressed as

$$s_i(n) = s_{iI}(n) + js_{iQ}(n). \quad (3.A.10)$$

For stationary processes, the correlation function for the signal process can be written using eq(3.A.2e) as

$$R_{sij}(l) = R_{Aij}^s(l) + jR_{Bij}^s(l) \quad (3.A.11)$$

where

$$R_{Aij}^s(l) = R_{sij}^{II}(l) + R_{sij}^{QQ}(l) \quad (3.A.12a)$$

and

$$R_{Bij}^s(l) = R_{sij}^{QI}(l) - R_{sij}^{IQ}(l). \quad (3.A.12b)$$

The corresponding disturbance correlation function is expressed as

$$R_{dij}(l) = R_{cij}(l) + R_{wij}(l) \quad (3.A.13a)$$

$$= [R_{Aij}^c(l) + jR_{Bij}^c(l)] + [R_{Aij}^w(l) + jR_{Bij}^w(l)]. \quad (3.A.13b)$$

At $l = 0$, from eq(3.A.2e)

$$R_{gij}(0) = R_{Aij}^g(0) + jR_{Bij}^g(0) \quad g = s, c, w \quad (3.A.14)$$

where g is used to denote s, c and w ; ie., the signal, non-white and white noise processes, respectively. However, we also have the definition

$$\rho_{gij} = \frac{R_{gij}(0)}{\sigma_{gii}\sigma_{gjj}} \quad g = s, c, w \quad (3.A.15)$$

where ρ_{gij} is the complex cross-correlation coefficient for processes $\{g_i\}$ and $\{g_j\}$, σ_{gii} and σ_{gjj} are the standard deviations associated with each channel process i and j , respectively, with corresponding variances

$$\sigma_{gii}^2 = R_{gii}(0) \quad g = s, c, w \quad (3.A.16a)$$

and

$$\sigma_{gjj}^2 = R_{gjj}(0) \quad g = s, c, w. \quad (3.A.16b)$$

From eqs.(3.A.14) and (3.A.15), we see that

$$R_{Aij}^g(0) = \text{Re}[\rho_{gij}] \sigma_{gii} \sigma_{jj} \quad (3.A.17a)$$

and

$$R_{Bij}^g(0) = \text{Im}[\rho_{gij}] \sigma_{gii} \sigma_{jj} \quad (3.A.17b)$$

Eqs.(3.A.17a) and (3.A.17b) relate the constants $R_{Aij}^g(0)$ and $R_{Bij}^g(0)$ to the cross correlation coefficient and the channel standard deviations.

Finally, for the autocorrelation function ($i=j$), $R_{gii}(l)$ peaks at $l=0$. The cross-correlation function $R_{gij}(l)$, however, does not, in general, peak at lag zero. We designate its peak value as lag l_{gij} .

B. Polar Form

In polar form, the cross-correlation functions introduced in the previous section are expressed as

$$R_{gij}(l) = \left\{ [R_{Aij}^g(l)]^2 + [R_{Bij}^g(l)]^2 \right\}^{1/2} \exp[j\theta_{gij}(l)] \quad (3.B.1a)$$

$$= |R_{gij}(l)| \exp[j\theta_{gij}(l)] \quad g = s, c, w \quad (3.B.1b)$$

where

$$\theta_{gij}(l) = \tan^{-1}[R_{Bij}^g(l)/R_{Aij}^g(l)]. \quad (3.B.2)$$

For the autocorrelation function ($i=j$), the imaginary part $R_{Bii}^g(l)$ is an odd function of l (see section III.E) so that at $l=0$, $\theta_{gii}(0) = 0$. Therefore, $R_{gii}(0)$ is real. It is the variance of the zero mean process and represents a measure of the total power in the corresponding power spectrum. We have designated this quantity for the channel i processes as σ_{gii}^2 [see eq(3.A.16a)].

For the cross-correlation function ($i \neq j$), $R_{Bij}^g(l)$ is not in general odd. Thus $\theta_{gij}(0)$ is not necessarily zero. And so, in general, the quantity $R_{gij}(0)$ is complex. We will designate this quantity as the complex constant G_{ij} such that

$$R_{gij}(0) = G_{ij} = (G_A)_{ij} + j(G_B)_{ij} \quad (3.B.3)$$

where $G = S, C, W$ for signal, non-white, and white noise processes, respectively. Using eqs(3.A.14), (3.A.17) and (3.B.3), we have

$$R_{Aij}^g(0) = (G_A)_{ij} = \text{Re}[\rho_{gij}] \sigma_{gii} \sigma_{gjj} \quad (3.B.4a)$$

and

$$R_{Bij}^g(0) = (G_B)_{ij} = \text{Im}[\rho_{gij}] \sigma_{gii} \sigma_{gjj} \quad (3.B.4b)$$

In addition, we also have from eq.(3.A.15) and (3.B.3)

$$R_{gij}(0) = G_{ij} = (\rho_{gij}) \sigma_{gii} \sigma_{gjj} \quad (3.B.5)$$

From eqs(3.B.1), (3.B.4a) and (3.B.4b), at $l=0$

$$R_{gij}(0) = \left\{ [R_{Aij}^g(0)]^2 + [R_{Bij}^g(0)]^2 \right\}^{1/2} \exp[j\theta_{gij}(0)] \quad (3.B.6a)$$

$$= |\rho_{gij}| \sigma_{gii} \sigma_{gjj} \exp[j\theta_{gij}(0)]. \quad (3.B.6b)$$

From eqs(3.B.5) and (3.B.6b), we have

$$\rho_{g_{ij}} = |\rho_{g_{ij}}| \exp[j\theta_{g_{ij}}(0)] \quad (3.B.7a)$$

or

$$|\rho_{g_{ij}}| = \rho_{g_{ij}} \exp\{-j\theta_{g_{ij}}(0)\}. \quad (3.B.7b)$$

We can also develop additional relationships involving the phase and amplitude between $R_{g_{ij}}(l)$ and $R_{g_{ji}}(l)$. Using the same form as eq.(3.B.1) for $R_{g_{ji}}(l)$,

we have

$$R_{g_{ji}}(l) = \left\{ [R_{A_{ji}}^g(l)]^2 + [R_{B_{ji}}^g(l)]^2 \right\}^{1/2} \exp[j\theta_{g_{ji}}(l)] \quad (3.B.8a)$$

$$= |R_{g_{ji}}(l)| \exp[j\theta_{g_{ji}}(l)]. \quad (3.B.8b)$$

From eq.(3.A.4), we have

$$R_{g_{ij}}(l) = [R_{g_{ji}}(-l)]^* \quad (3.B.9a)$$

Using the conjugate property, we have

$$|R_{g_{ij}}(l)| = |R_{g_{ji}}(-l)|. \quad (3.B.10)$$

and

$$\theta_{g_{ij}}(l) = -\theta_{g_{ji}}(-l). \quad (3.B.11)$$

Eq (3.B.11) implies an odd relationship between $\theta_{g_{ij}}(l)$ and $\theta_{g_{ji}}(l)$; however, we emphasize that these phase terms are not in themselves odd functions; ie., $\theta_{g_{ij}}(l)$ does not in general equal $-\theta_{g_{ij}}(-l)$. In particular, we note that $\theta_{g_{ij}}(0)$ is not

necessarily equal to zero. For $i=j$, however, the relationship $R_{g_{ii}}(-l) = [R_{g_{ii}}(l)]^*$ provides us with the expression (see section III.E.1.a)

$$\theta_{g_{ii}}(-l) = -\theta_{g_{ii}}(l) \quad (3.B.12)$$

indicating that the phase function for the autocorrelation function is odd.

C. Correlation Function Shaping Approach

1.) General Development

We now consider modeling the cross-correlation function $R_{g_{ij}}(l)$ with functional forms that will enable us to obtain generalized distributions for these functions as well as the autocorrelation function. We express these equations as

$$R_{g_{ij}}(l) = K_{g_{ij}} f_g(\lambda_{g_{ij}}, l - l_{g_{ij}}) \exp\{j\theta_{g_{ij}}(l)\} \quad l \geq 0, \quad g=s,c \quad (3.C.1)$$

where $\lambda_{g_{ij}}$ is defined as the temporal cross-correlation coefficient for $i \neq j$ and the temporal autocorrelation coefficient for $i=j$. It provides a measure of the correlation between successive pulses on a given channel ($i=j$) or between channels ($i \neq j$), and is discussed further in section III.D; $K_{g_{ij}}$ is a real, constant, normalizing coefficient which will be derived presently; $l_{g_{ij}}$ is the lag value at which the corresponding real function $f_g(\bullet)$ has a peak value of unity. We note that the cross-correlation function does not necessarily peak at lag zero as the autocorrelation function does; ie. for $i=j$, $l_{g_{ii}} = 0$. The functions $f(\bullet)$ are selected to specify the shape of the correlation function magnitude and will be considered

below. Using $l = 0$ in eq(3.C.1) together with the definition used in eq(3.B.3), we have

$$R_{gij}(0) = G_{ij} = K_{gij} f_g(\lambda_{gij}, |l_{gij}|) \Big|_{l=0} \exp\{j\theta_{gij}(0)\}. \quad (3.C.2)$$

Solving eq(3.C.2) for the normalizing coefficient

$$K_{gij} = \frac{G_{ij}}{f_g(\lambda_{gij}, |l_{gij}|) \Big|_{l=0}} \exp\{-j\theta_{gij}(0)\} \quad (3.C.3)$$

so that eq(3.C.1) becomes

$$R_{gij}(l) = \frac{G_{ij} f_g(\lambda_{gij}, |l_{gij}|)}{f_g(\lambda_{gij}, |l_{gij}|) \Big|_{l=0}} \exp\{j[\theta_{gij}(l) - \theta_{gij}(0)]\}. \quad (3.C.4a)$$

Also, eq(3.A.4) enables us to obtain

$$\begin{aligned} R_{gji}(l) &= [R_{gij}(-l)]^* \\ &= \frac{G_{ij}^* f_g^*(\lambda_{gij}, |-l_{gij}|)}{f_g^*(\lambda_{gij}, |-l_{gij}|) \Big|_{l=0}} \exp\{-j[\theta_{gij}(-l) - \theta_{gij}(0)]\}. \end{aligned} \quad (3.C.4b)$$

The normalizing procedure presented above was utilized so that at $l=0$, we have $R_{gij}(0) = G_{ij} = (\rho_{gij})\sigma_{gii}\sigma_{gjj}$ as noted in eq.(3.B.5). When the equality in eq.(3.B.5) is used in the above equations, we obtain

$$R_{gij}(l) = \frac{(\rho_{gij})\sigma_{gii}\sigma_{gjj} f_g(\lambda_{gij}, |l_{gij}|)}{f_g(\lambda_{gij}, |l_{gij}|) \Big|_{l=0}} \exp\{j[\theta_{gij}(l) - \theta_{gij}(0)]\} \quad (3.C.5a)$$

$g = s, c$

or from eq(3.B.7b)

$$R_{gij}(l) = \frac{|\rho_{gij}| \sigma_{gii} \sigma_{gjj} f_g(\lambda_{gij}, l - l_{gij})}{f_g(\lambda_{gij}, l - l_{gij})|_{l=0}} \exp\{j[\theta_{gij}(l)]\} \quad g = s, c. \quad (3.C.5b)$$

Also,

$$R_{gji}(l) = \frac{(\rho_{gij})^* \sigma_{gii} \sigma_{gjj} f_g(\lambda_{gij}, -l - l_{gij})}{f_g(\lambda_{gij}, l - l_{gij})|_{l=0}} \exp\{-j[\theta_{gij}(-l) - \theta_{gij}(0)]\} \quad g = s, c \quad (3.C.5c)$$

or

$$R_{gji}(l) = \frac{|\rho_{gij}| \sigma_{gii} \sigma_{gjj} f_g(\lambda_{gij}, -l - l_{gij})}{f_g(\lambda_{gij}, l - l_{gij})|_{l=0}} \exp\{-j[\theta_{gij}(-l)]\} \quad g = s, c. \quad (3.C.5d)$$

The last four equations provide us with a useful description of the cross-correlation function in terms of the cross-correlation coefficient ρ_{gij} , the standard deviations σ_{ii} and σ_{jj} of the channel i and j processes, respectively, and the temporal cross-correlation coefficient, λ_{gij} .

For the autocorrelation function ($i=j$), we have

$$|\rho_{gii}| = 1 \quad (3.C.6a)$$

since any given channel process is totally correlated with itself at zero lag. Also,

$$\theta_{gii}(0) = 0 \quad (3.C.6b)$$

since $\theta_{gij}(l)$ is an odd function of l (see section III.E.1.a). Eq(3.C.5b) for the autocorrelation function now becomes

$$R_{gii}(l) = \frac{\sigma_{gii}^2 f_g(\lambda_{gii}, l)}{f_g(\lambda_{gii}, l)|_{l=0}} \exp\{j[\theta_{gii}(l)]\} \quad (3.C.7)$$

where we again note that $l_{gij}=0$ for $i=j$ since the autocorrelation function peaks at lag zero. Furthermore, since the function $f_g(\bullet)$ for the autocorrelation function has a peak value of unity at $l=0$, eq.(3.C.7) reduces to

$$R_{gii}(l) = \sigma_{gii}^2 f_g(\lambda_{gii}, l) \exp\{j\theta_{gii}(l)\} \quad g=s,c. \quad (3.C.8)$$

At $l = 0$, eq.(3.C.8) becomes

$$R_{gii}(0) = \sigma_{gii}^2 \quad g=s,c \quad (3.C.9)$$

which is, as expected, the variance of the zero mean, channel i process. Finally, we also point out that since K_{gij} in eq(3.C.3) is a real constant, then, defining

K_{gij} as

$$K_{gij} = K_{gij} f_g(\lambda_{gij}, l - l_{gij})|_{l=0} \quad (3.C.10a)$$

eq(3.C.3) enables us to obtain

$$K_{gij} = G_{ij} \exp\{-j\theta_{gij}(0)\} \quad (3.C.10b)$$

$$= (\rho_{gij}) \sigma_{gii} \sigma_{gjj} \exp\{-j\theta_{gij}(0)\}. \quad (3.C.10c)$$

$$= |\rho_{gij}| \sigma_{gii} \sigma_{gjj} \quad (3.C.10d)$$

where eqs(3.C.10c) and (3.C.10d) result from eqs(3.B.5) and (3.B.7b), respectively. We note that K_{gij} is also real, although G_{ij} and ρ_{gij} are in general complex.

In the above discussion, we have proposed using functional forms to characterize the magnitude and phase of the correlation functions. The motivation for this approach is that it allows us flexibility in modeling random processes with various correlation and spectral shape. We caution, however that at this point we have not constrained these functions to meet all the criteria that are

necessary and sufficient to characterize correlation functions. In fact, determining all of these conditions in a general formulation is a difficult task. In section III.C.4, we consider several constraint conditions including the important condition of positive semi-definiteness of the correlation matrix. In that section, we show that even for correlation matrices of small dimension, determination of an analytic solution of the constraint conditions is tedious. However, empirical methods to control the parameters can be utilized.

2. The Autocorrelation Function

In this section, we consider the special cases of the Gaussian, exponential and sinc shaped autocorrelation functions using the form denoted in eq(3.C.8).

a. The Gaussian Shaped Autocorrelation Function

In this special case, we consider autocorrelation functions with Gaussian shaped magnitudes for the signal and clutter processes such that (dropping the subscript i notation for convenience)

$$f_s(\lambda_s, l) = (\lambda_s)^{l^2} = \exp[-2\pi^2 \mu_s^2 T^2 l^2] \quad (3.C.11a)$$

and

$$f_c(\lambda_c, l) = (\lambda_c)^{l^2} = \exp[-2\pi^2 \mu_c^2 T^2 l^2] \quad (3.C.11b)$$

where

$$\lambda_g = \exp[-2\pi^2 \mu_g^2 T^2] \quad g = s, c \quad (3.C.12)$$

and λ_g is a real constant such that $0 \leq \lambda_g \leq 1$ and T is the sample period. In section III.D, we show that μ_g^2 with $g=s, c$ is the variance of the Gaussian spectra

associated with the signal($g=s$) or non-white noise($g=c$). Using these equations in eq(3.C.8) provides

$$R_s(l) = \sigma_s^2 f(\lambda_s, l) \exp[j\theta_s(l)] = \sigma_s^2 (\lambda_s)^{|l|} \exp[j\theta_s(l)] \quad l \geq 0 \quad (3.C.13a)$$

and

$$R_c(l) = \sigma_c^2 f(\lambda_c, l) \exp[j\theta_c(l)] = \sigma_c^2 (\lambda_c)^{|l|} \exp[j\theta_c(l)] \quad l \geq 0. \quad (3.C.13b)$$

Using eq(3.C.13b) in (3.A.13a) for $i=j$, we obtain

$$R_d(l) = \sigma_c^2 (\lambda_c)^{|l|} \exp[j\theta_c(l)] + \sigma_w^2 \delta(l) \quad l \geq 0 \quad (3.C.13c)$$

where d denotes the entire disturbance process consisting of non-white plus white noise and the white noise autocorrelation function has been expressed in terms of the Kronecker delta function, $\delta(l)$. Eqs(3.C.13a) and (3.C.13b) indicate that λ_g is a measure of the correlation magnitude between consecutive samples [2] of the process on channel i . This is determined by considering that the magnitude of $R_g(l)$ at $l = 1$ is decreased by the factor λ_g as compared to the magnitude at $l = 0$; ie.

$$|R_g(1)| = \lambda_g R_g(0). \quad (3.C.14)$$

The relationship $R_g(-l) = [R_g(l)]^*$ where $g=s,c$ provides the appropriate value of the autocorrelation function at negative lag values.

b. The Exponential Shaped Autocorrelation Function

In the case of the exponential shaped autocorrelation function, we have

$$f_s(\lambda_s, l) = (\lambda_s)^{|l|} \quad (3.C.15a)$$

and

$$f_c(\lambda_c, l) = (\lambda_c)^{|l|} \quad (3.C.15b)$$

And so, eqs(3.C.8) and (3.A.13a) enable us to obtain

$$R_s(l) = \sigma_s^2 (\lambda_s)^{|l|} \exp[j\theta_s(l)] \quad (3.C.16a)$$

and

$$R_d(l) = \sigma_c^2 (\lambda_c)^{|l|} \exp[j\theta_c(l)] + \sigma_w^2 \delta(l). \quad (3.C.16b)$$

c. The Sinc Shaped Autocorrelation Function

In this case, the shaping function for the autocorrelation function is expressed as

$$f_s(\lambda_s, l) = \frac{\sin[2\pi(1-\lambda_s)l]}{[2\pi(1-\lambda_s)l]} \quad (3.C.16c)$$

so that

$$R_s(l) = \sigma_s^2 \frac{\sin[2\pi(1-\lambda_s)l]}{[2\pi(1-\lambda_s)l]} \exp[j\theta_s(l)]. \quad (3.C.16d)$$

d. Normalization by the White Noise Variance

If the expressions in the first equality of eqs(3.C.13a) and (3.C.13c) are normalized by the white noise variance σ_w^2 , we have

$$r_s(l) = \frac{R_s(l)}{\sigma_w^2} = (\text{SNR}) f_s(\lambda_s, l) \exp[j\theta_s(l)] \quad (3.C.17a)$$

and

$$r_d(l) = \frac{R_d(l)}{\sigma_w^2} = (\text{CNR}) f_c(\lambda_c, l) \exp[j\theta_c(l)] + \delta(l) \quad (3.C.17b)$$

where

$$\text{SNR} = \sigma_s^2 / \sigma_w^2 \quad (3.C.18a)$$

and

$$\text{CNR} = \sigma_c^2 / \sigma_w^2. \quad (3.C.18b)$$

Eqs.(3.C.17a) and (3.C.17b) are equivalent to those suggested in [2].

e. Polar Form with a Doppler Shift

The expression for the correlation functions can be modified using a linear phase shift term to explicitly account for a Doppler center frequency. In this case, eqs.(3.C.13a) and (3.C.13c) can be expressed as

$$R_s(l) = \sigma_s^2 f_s(\lambda_s, l) \exp[j\theta_s(l)] \exp[j2\pi f_s l T] \quad (3.C.19a)$$

and

$$R_d(l) = \sigma_c^2 f_c(\lambda_c, l) \exp[j\theta_c(l)] \exp[j2\pi f_c l T] + \sigma_w^2 \delta(l) \quad (3.C.19b)$$

where f_s and f_c are the signal and clutter Doppler center frequencies, respectively.

3. The Cross-Correlation Function

We will now consider the special cases of Gaussian, exponential and sinc shaped cross-correlation functions. In section III.C.4, constraint equations will be developed in order to control the positive semi-definiteness of the appropriate correlation matrices.

a. Gaussian Shaped Cross-Correlation Function

In this special case, we consider cross-correlation functions with Gaussian shaped magnitudes for the signal and non-white noise processes using eqs(3.C.5a).

Consider the functional form

$$f_g(\lambda_{gij}, |l|_{gij}) = (\lambda_{gij})^{|l|_{gij}^2} \quad g=s,c \quad (3.C.20)$$

where (see section III.D)

$$\lambda_{gij} = \exp[-2\pi^2 \mu_{gij}^2 T^2] \quad (3.C.21)$$

and $0 \leq \lambda_{gij} \leq 1$. Using eq(3.C.20), the normalizing terms in the denominators of eqs(3.C.5) become

$$f_g(\lambda_{gij}, |l|_{gij})|_{l=0} = (\lambda_{gij})^{|l|_{gij}^2} \quad g=s,c. \quad (3.C.22)$$

Using eqs(3.C.20) and (3.C.22) in eqs(3.C.5a) and (3.C.5b), we obtain

$$R_{gij}(l) = \frac{(\rho_{gij})\sigma_{gii}\sigma_{gjj}(\lambda_{gij})^{|l|_{gij}^2}}{(\lambda_{gij})^{|l|_{gij}^2}} \exp\{j[\theta_{gij}(l)-\theta_{gij}(0)]\} \quad g = s,c \quad (3.C.23a)$$

$$= \frac{|\rho_{gij}|\sigma_{gii}\sigma_{gjj}(\lambda_{gij})^{|l|_{gij}^2}}{(\lambda_{gij})^{|l|_{gij}^2}} \exp\{j\theta_{gij}(l)\} \quad g = s,c. \quad (3.C.23b)$$

Also

$$R_{gji}(l) = \frac{(\rho_{gji})\sigma_{gii}\sigma_{gjj}(\lambda_{gji})^{|l|_{gji}^2}}{(\lambda_{gji})^{|l|_{gji}^2}} \exp\{j[\theta_{gji}(l)-\theta_{gji}(0)]\} \quad g = s,c \quad (3.C.23c)$$

$$= \frac{|\rho_{gji}| \sigma_{gii} \sigma_{gjj} (\lambda_{gji})^{(l-l_{gji})^2}}{(\lambda_{gji})^{l_{gji}^2}} \exp\{j\theta_{gji}(l)\}$$

$$g = s, c. \quad (3.C.23d)$$

Eq(3.C.23a) implies that λ_{gij} is a measure of the correlation magnitude between consecutive samples (but delayed by lag l_{gij}) across channels i and j . This is determined by noting that $|R_{gij}(l)|$ decreases by the factor λ_{gij} at $l = l_{gij} \pm 1$ as compared to the magnitude value at $l = l_{gij}$; ie.

$$|R_{gij}(l_{gij} \pm 1)| = \lambda_{gij} |R_{gij}(l_{gij})|. \quad (3.C.24)$$

Examination of eq(3.C.23a) indicates that at $l = 0$, we obtain the desired result that $R_{gij}(0) = (\rho_{gij}) \sigma_{gii} \sigma_{gjj}$. We also note that at $l = l_{gij}$

$$R_{gij}(l_{gij}) = \frac{(\rho_{gij}) \sigma_{gii} \sigma_{gjj}}{(\lambda_{gij})^{l_{gij}^2}} \exp\{j[\theta_{gij}(l_{gij}) - \theta_{gij}(0)]\} \quad (3.C.25a)$$

$$= \frac{|\rho_{gij}| \sigma_{gii} \sigma_{gjj}}{(\lambda_{gij})^{l_{gij}^2}} \exp\{j\theta_{gij}(l_{gij})\} \quad (3.C.25b)$$

Eq(3.C.25b) indicates that as λ_{gij} approaches zero, the correlation function would increase significantly if $|\rho_{gij}|$ were not controlled. In section III.C.4, we will show that we must at least restrict $|\rho_{gij}|$ such that $|\rho_{gij}| \leq (\lambda_{gij})^{l_{gij}^2}$ in order to satisfy one condition of cross-correlation functions. However, we will also show that this condition is necessary, but not sufficient, to properly shape the cross-correlation function.

We now consider that from eqs(3.A.4) and (3.C.23a)

$$R_{gji}(l) = [R_{gij}(-l)]^* \quad (3.C.26a)$$

$$= \frac{(\rho_{gij})^* \sigma_{gii} \sigma_{gjj} (\lambda_{gij})^{(l+l_{gij})^2}}{(\lambda_{gij})^{l_{gij}^2}} \exp\{-j[\theta_{gij}(-l) - \theta_{gij}(0)]\}$$

$$g=s,c. \quad (3.C.26b)$$

We can now show that

$$\rho_{gij} = \rho_{gji}^* \quad (3.C.27a)$$

$$l_{gij} = -l_{gji} \quad (3.C.27b)$$

$$\lambda_{gij} = \lambda_{gji} \quad (3.C.27c)$$

$$\theta_{gij}(l) = -\theta_{gji}(-l) \quad g = s,c. \quad (3.C.27d)$$

Proof

Eq.(3.C.27d) was proven in eq.(3.B.11). From eq.(3.A.4), we have at $l=0$,

$$R_{gij}(0) = [R_{gji}(0)]^*. \quad (3.C.28)$$

Using eqs.(3.C.23a) and (3.C.23c) in eq(3.C.28), the equality in eq(3.C.27a) follows directly. We now consider the absolute values

$$|R_{gij}(l)|^2 = \frac{|\rho_{gij}|^2 \sigma_{gii}^2 \sigma_{gjj}^2 (\lambda_{gij})^{2(l+l_{gij})^2}}{(\lambda_{gij})^{2l_{gij}^2}} \quad (3.C.29a)$$

and

$$|R_{gji}(-l)|^2 = \frac{|\rho_{gij}|^2 \sigma_{gii}^2 \sigma_{gjj}^2 (\lambda_{gji})^{2(l+l_{gji})^2}}{(\lambda_{gji})^{2(l_{gji})^2}} \quad (3.C.29b)$$

where we have used the equality, $|\rho_{gij}|^2 = |\rho_{gji}|^2$. Using the equality expressed in eq(3.B.10), we now obtain

$$\frac{(\lambda_{gij})^{2(l-l_{gij})^2}}{(\lambda_{gij})^{2l_{gij}^2}} = \frac{(\lambda_{gji})^{2(l+l_{gji})^2}}{(\lambda_{gji})^{2l_{gji}^2}}. \quad (3.C.30)$$

Eq.(3.C.30) must be satisfied at all values of l . At $l = l_{gij}$,

$$(\lambda_{gji})^{2(l_{gij}+l_{gji})^2} = \frac{(\lambda_{gji})^{2l_{gji}^2}}{(\lambda_{gij})^{2l_{gij}^2}} \quad g=s,c \quad (3.C.31a)$$

while at $l = -l_{gji}$

$$(\lambda_{gij})^{2(l_{gij}+l_{gji})^2} = \frac{(\lambda_{gij})^{2l_{gij}^2}}{(\lambda_{gji})^{2l_{gji}^2}} \quad g=s,c. \quad (3.C.31b)$$

Noting the inverse relationship expressed by the RHS of eqs.(3.C.31a) and (3.C.31b), we have

$$(\lambda_{gij})^{2(l_{gij}+l_{gji})^2} = (\lambda_{gji})^{-2(l_{gij}+l_{gji})^2}. \quad (3.C.32)$$

Since $0 \leq \lambda_{gij}, \lambda_{gji} \leq 1$, eq.(3.C.32) can only be satisfied if

$$l_{gij} = -l_{gji} \quad g=s,c. \quad (3.C.33)$$

Using eq.(3.C.33) in eq.(3.C.30), it follows that

$$\lambda_{gij} = \lambda_{gji} \quad g=s,c. \quad (3.C.34)$$

b. Exponential Shaped Cross-Correlation Function

In the case of cross-correlation functions with an exponentially shaped magnitude, we have

$$f_g(\lambda_{gij}, l_{gij}) = (\lambda_{gij})^{|l_{gij}|} \quad g=s,c \quad (3.C.35)$$

where $0 \leq \lambda_{gij} \leq 1$. At $l=0$, we have

$$f_g(\lambda_{gij}, l_{gij})|_{l=0} = (\lambda_{gij})^{|l_{gij}|} \quad g=s,c. \quad (3.C.36)$$

Using these results in eq.(3.C.5a), we have

$$R_{gij}(l) = \frac{(\rho_{gij}) \sigma_{gii} \sigma_{gij} (\lambda_{gij})^{|l_{gij}|}}{(\lambda_{gij})^{|l_{gij}|}} \exp\{j[\theta_{gij}(l) - \theta_{gij}(0)]\} \quad g = s,c. \quad (3.C.37a)$$

Again, using eq(3.A.4)

$$R_{gji}(l) = \frac{(\rho_{gij})^* \sigma_{gii} \sigma_{gij} (\lambda_{gij})^{|l_{gij}|}}{(\lambda_{gij})^{|l_{gij}|}} \exp\{-j[\theta_{gij}(-l) - \theta_{gij}(0)]\} \quad g = s,c. \quad (3.C.37b)$$

c. The Sinc Shaped Cross-Correlation Function

In this case, the shaping function for the cross-correlation function is expressed as

$$f_g[\lambda_{g_{ij}}, (l-l_{g_{ij}})] = \frac{\sin[2\pi(1-\lambda_{g_{ij}})|l-l_{g_{ij}}|]}{[2\pi(1-\lambda_{g_{ij}})|l-l_{g_{ij}}|]} \quad g = s, c. \quad (3.C.38)$$

At $l = 0$, we have

$$f_g[\lambda_{g_{ij}}, (l-l_{g_{ij}})]|_{l=0} = \frac{\sin[2\pi(1-\lambda_{g_{ij}})l_{g_{ij}}]}{[2\pi(1-\lambda_{g_{ij}})l_{g_{ij}}]} \quad g = s, c. \quad (3.C.39)$$

so that

$$R_{g_{ij}}(l) = \frac{\rho_{g_{ij}} \sigma_{g_{ii}} \sigma_{g_{jj}} \left[\frac{\sin[2\pi(1-\lambda_{g_{ij}})|l-l_{g_{ij}}|]}{[2\pi(1-\lambda_{g_{ij}})|l-l_{g_{ij}}|]} \right]}{\left[\frac{\sin[2\pi(1-\lambda_{g_{ij}})l_{g_{ij}}]}{[2\pi(1-\lambda_{g_{ij}})l_{g_{ij}}]} \right]} \exp[j\theta_{g_{ij}}(l)] \quad g = s, c. \quad (3.C.40)$$

d. Multichannel Doppler Processes

If a baseband signal $g_i(n)$ on channel i is considered to have a Doppler center frequency f_{g_i} , we can express this process as

$$g_i(n) = \{g_{iI}(n) + jg_{iQ}(n)\} \exp[j2\pi f_{g_i} nT] \quad (3.C.41)$$

where T is the pulse repetition period. The cross-correlation function is therefore

$$R_{g_{ij}}(n, n-l) = E[g_i(n)g_j^*(n-l)] \quad (3.C.42a)$$

$$= E\{[g_{iI}(n) + jg_{iQ}(n)][g_{jI}(n-l) - jg_{jQ}(n-l)]\} \\ \cdot \exp[j2\pi f_{g_i} nT] \exp[-j2\pi f_{g_j}(n-l)T] \quad (3.C.42b)$$

$$\begin{aligned}
&= E \{ [g_{iI}(n)g_{jI}(n-l)] + [g_{iQ}(n)g_{jQ}(n-l)] \\
&\quad + j[g_{iQ}(n)g_{jI}(n-l)] - g_{iI}(n)g_{jQ}(n-l)] \} \\
&\quad \cdot \exp[j2\pi f_{g_i}nT] \exp[-j2\pi f_{g_j}(n-l)T].
\end{aligned} \tag{3.C.42c}$$

For joint-stationary conditions on the random processes contained in the expectation operation,

$$R_{g_{ij}}(n, n-l) = [R_{A_{ij}}^g(l) + jR_{B_{ij}}^g(l)] \exp\{j2\pi[(f_{g_i} - f_{g_j})nT + f_{g_j}lT]\}. \tag{3.C.43}$$

We note that this cross-correlation function is not time independent for $f_{g_i} \neq f_{g_j}$ due to the term involving the frequency difference in the exponential. Thus, the processes are not jointly stationary. This situation would result, for example, when processing data from two or more radar systems operating at different center frequencies. However, since the time dependent term is deterministic, it can be removed in the pre-processing. This is achieved by selection of a reference channel and frequency multiplying the other channel signals so that the resulting Dopplers are all equal to that of the reference. The proper mixing terms are obtained as follows. First, consider the Doppler frequency on channel i expressed as

$$f_{g_i} = \frac{2vf_{oi}}{c} \tag{3.C.44}$$

where v is the object velocity, f_{oi} is the channel i carrier frequency and c is the velocity of light. We therefore have the relation between channels i and j , such that

$$\frac{f_{g_i}}{f_{oi}} = \frac{f_{g_j}}{f_{oj}} = \frac{2v}{c} \tag{3.C.45}$$

If we select channel i as the reference channel so that $f_{gi} = f_{gR}$ and $f_{oi} = f_{oR}$ where f_{gR} is the Doppler on the reference channel and f_{oR} is the reference channel carrier frequency, we have

$$f_{gR} = \left[\frac{f_{oR}}{f_{oj}} \right] f_{gj} \quad j = 1, 2, \dots, J. \quad (3.C.46)$$

And so, if each channel j is frequency multiplied by its appropriate factor (f_{oR}/f_{oj}), all of the Dopplers will be equal and eq(3.C.43) reduces to

$$R_{gij}(l) = [R_{Aij}^g(l) + jR_{Bij}^g(l)] \exp[j2\pi f_{gR} l T]. \quad (3.C.47)$$

This result depends only on lag l and therefore satisfies the stationarity condition. The preprocessing proposed here, of course, would be performed subsequent to processing stages which might utilize the raw Doppler information contained on each channel.

The corresponding polar functional expression for eq(3.C.5a) is

$$R_{gij}(l) = \frac{|\rho_{gij}| \sigma_{gii} \sigma_{gjj} f_g(\lambda_{gij}, l - l_{gij})}{f_g(\lambda_{gij}, l - l_{gij})|_{l=0}} \exp\{j[\theta_{gij}(l)]\} \exp(j2\pi f_{gR} l T). \quad (3.C.48)$$

4.) Constraint Conditions For Correlation Functions

In this section, we discuss the constraints that must be imposed on the parameters of the functional forms discussed in the previous sections to ensure that these functions have the appropriate form for correlation functions. These conditions are discussed in the next two subsections. In III.4.a, we develop general constraint conditions while in III.4.b, the condition of positive semi-definite correlation matrices is considered. As noted in section II, the multichannel correlation matrix is Hermitian and positive semi-definite for stationary processes. The expressions, developed in eqs(3.C.5a) through (3.C.5d), are contained as the elements of the multichannel correlation matrix, R_{XX} . Therefore, we must ensure that this matrix, when using elements obtained from these equations, satisfies the condition of positive semi-definiteness; ie. a matrix for which all eigenvalues are non-negative or all subminor matrices of R_{XX} have a non-negative determinant [12,13]. These conditions will impose constraints on the terms ρ_{gij} , λ_{gij} , λ_{gii} , σ_{gii}^2 , and l_{gij} .

a. General Constraint Conditions

Several important constraints can be developed in a straightforward manner by generalizing a discussion noted in [5]; ie., with the real constant α , we consider

$$E[|x_i(n+l) + \alpha x_j(n)|^2] = E\{[x_i(n+l) + \alpha x_j(n)][x_i^*(n+l) + \alpha x_j^*(n)]\} \quad (3.C.49a)$$

$$\begin{aligned} &= E[x_i(n+l)x_i^*(n+l)] + \alpha E[x_j(n)x_i^*(n+l)] \\ &\quad + \alpha E[x_i(n+l)x_j^*(n)] + \alpha^2 E[x_j(n)x_j^*(n)] \end{aligned} \quad (3.C.49b)$$

$$= R_{ii}(0) + \alpha[R_{ji}(-l) + R_{ij}(l)] + \alpha^2 R_{jj}(0) \quad (3.C.49c)$$

$$= R_{ii}(0) + \alpha[R_{ij}^*(l) + R_{ij}(l)] + \alpha^2 R_{jj}(0) \quad (3.C.49d)$$

so that

$$E[|x_i(n+l) + \alpha x_j(n)|^2] = R_{ii}(0) + 2\alpha \text{Re}\{R_{ij}(l)\} + \alpha^2 R_{jj}(0). \quad (3.C.49e)$$

The above quadratic is nonnegative for any α ; therefore, its discriminant is nonpositive so that from eq.(3.C.49e)

$$[\text{Re}\{R_{ij}(l)\}]^2 \leq R_{ii}(0)R_{jj}(0). \quad (3.C.50a)$$

Likewise, interchanging i and j in eq. (3.C.49a), we obtain

$$[\text{Re}\{R_{ji}(l)\}]^2 \leq R_{ii}(0)R_{jj}(0). \quad (3.C.50b)$$

Since the geometric mean of two numbers does not exceed their arithmetic mean, we also have

$$2|\text{Re}\{R_{ij}(l)\}| \leq R_{ii}(0) + R_{jj}(0) \quad (3.C.51a)$$

and

$$2|\text{Re}\{R_{ji}(l)\}| \leq R_{ii}(0) + R_{jj}(0). \quad (3.C.51b)$$

Alternative expressions can be obtained from eq.(3.C.49c) such that

$$[R_{ij}(l) + R_{ji}(-l)]^2 \leq 4R_{ii}(0)R_{jj}(0) \quad (3.C.52a)$$

and

$$[R_{ji}(l) + R_{ij}(-l)]^2 \leq 4R_{ii}(0)R_{jj}(0). \quad (3.C.52b)$$

We will now consider the specific example of the Gaussian cross-correlation function and demonstrate how the above equations are utilized to constrain the function parameters. Using the real constant defined by eq.(3.C.10c) in eqs.(3.C.23a) and (3.C.26b), we obtain

$$R_{gij}(l) = \frac{K_{gij}(\lambda_{gij})^{(l-l_{gij})^2}}{(\lambda_{gij})^{l_{gij}^2}} \exp[j\theta_{gij}(l)] \quad (3.C.53a)$$

and

$$R_{gji}(l) = \frac{K_{gij}(\lambda_{gij})^{(l+l_{gij})^2}}{(\lambda_{gij})^{l_{gij}^2}} \exp[-j\theta_{gij}(-l)]. \quad (3.C.53b)$$

Inserting eqs(3.C.53a) and (3.C.53b) in constraint eq(3.C.52a)

$$\left[\frac{K_{gij}(\lambda_{gij})^{(l-l_{gij})^2}}{(\lambda_{gij})^{l_{gij}^2}} \exp[j\theta_{gij}(l)] + \frac{K_{gij}(\lambda_{gij})^{(-l+l_{gij})^2}}{(\lambda_{gij})^{l_{gij}^2}} \exp[-j\theta_{gij}(l)] \right]^2 \leq 4\sigma_{gii}^2 \sigma_{gjj}^2. \quad (3.C.54)$$

Noting that $(-l + l_{gij})^2 = (l - l_{gij})^2$, we have

$$\frac{4(K_{gij})^2(\lambda_{gij})^{2(l-l_{gij})^2}}{(\lambda_{gij})^{2l_{gij}^2}} \cos^2[\theta_{gij}(l)] \leq 4\sigma_{gii}^2 \sigma_{gjj}^2 \quad (3.C.55a)$$

so that from eq(3.C.10d),

$$\frac{|p_{gij}|^2(\lambda_{gij})^{2(l-l_{gij})^2}}{(\lambda_{gij})^{2l_{gij}^2}} \cos^2[\theta_{gij}(l)] \leq 1. \quad (3.C.55b)$$

The most stringent condition for this constraint equation occurs when $l = l_{gij}$, so that

$$|p_{gij}|^2 \leq \frac{(\lambda_{gij})^{2l_{gij}^2}}{\cos^2[\theta_{gij}(l_{gij})]}. \quad (3.C.56a)$$

Taking the positive square root of both sides of this equation, we have the constraint

$$|\rho_{gij}| \leq \frac{(\lambda_{gij})^2 l_{gij}}{|\cos[\theta_{gij}(l_{gij})]|} \quad (3.C.56b)$$

The result expressed by eq(3.C.56b) provides a constraint for $|\rho_{gij}|$ which is upper bound. It represents one of several conditions that must be satisfied by complex correlation functions.

Although the constraint procedure presented above is utilized in order to bound the constant parameters to those values which will provide the proper form of correlation matrices, it should be noted that they are necessary, but not sufficient conditions. In the next section, we will discuss the constraint of positive semi-definite correlation matrices and show that they lead to additional constraint conditions which are also not in themselves sufficient.

b. Conditions for Positive Semi-Definiteness

In this section, we consider conditions for positive semi-definiteness of the correlation matrix described in eq(2.5). By considering a specific example of this correlation matrix, it is shown that additional relationships exist among the parameters leading to further constraint equations. However, as we will show, with appropriate adjustment of the parameters, positive semi-definiteness can be achieved. The principal motivation for satisfying this constraint is two-fold. First, we are further restricting these arbitrary functional forms to conform to the proper shapes of correlation functions. Second, we are satisfying a condition for physical realizability. In section V, we discuss a method for the synthesis of multichannel AR processes which insures that the positive semi-definiteness

constraint is maintained. The most direct method, however, would be a determination of the eigenvalues through a singular value decomposition (SVD).

EXAMPLE

In this example, a 4x4 correlation matrix R_{XX} for a two channel process will be considered. The Gaussian shaped distribution will be used for both the auto- and cross- correlation functions so that (dropping the g=s,c notation)

$$R_{kk}(l) = \sigma_{kk}^2 (\lambda_{kk})^{l^2} \exp[j\theta_{kk}(l)] \quad k = i, j \quad (3.C.57a)$$

$$R_{ij}(l) = \frac{|\rho_{ij}| \sigma_{ii} \sigma_{jj} (\lambda_{ij})^{(l-l_{ij})^2}}{(\lambda_{ij})^{l_{ij}^2}} \exp[j\theta_{ij}(l)] \quad (3.C.57b)$$

$$R_{ji}(l) = \frac{|\rho_{ij}| \sigma_{ii} \sigma_{jj} (\lambda_{ij})^{(l+l_{ij})^2}}{(\lambda_{ij})^{l_{ij}^2}} \exp[-j\theta_{ij}(-l)]. \quad (3.C.57c)$$

Using these relations in the 4x4 correlation matrix and simplifying for real correlation functions, we have

$$R_{XX} = \begin{bmatrix} R_{11}(0) & R_{12}(0) & R_{11}(1) & R_{12}(1) \\ R_{21}(0) & R_{22}(0) & R_{21}(1) & R_{22}(1) \\ R_{11}(-1) & R_{12}(-1) & R_{11}(0) & R_{12}(0) \\ R_{21}(-1) & R_{22}(-1) & R_{21}(0) & R_{22}(0) \end{bmatrix} \quad (3.C.58a)$$

$$= \begin{bmatrix} \sigma_{11}^2 & |\rho_{12}| \sigma_{11} \sigma_{22} & \sigma_{11}^2 \lambda_{11} & |\rho_{12}| \sigma_{11} \sigma_{22} (\lambda_{12})^{1-2l_{12}} \\ |\rho_{12}| \sigma_{11} \sigma_{22} & \sigma_{22}^2 & |\rho_{12}| \sigma_{11} \sigma_{22} (\lambda_{12})^{1+2l_{12}} & \sigma_{22}^2 \lambda_{22} \\ \sigma_{11}^2 \lambda_{11} & |\rho_{12}| \sigma_{11} \sigma_{22} (\lambda_{12})^{1+2l_{12}} & \sigma_{11}^2 & |\rho_{12}| \sigma_{11} \sigma_{22} \\ |\rho_{12}| \sigma_{11} \sigma_{22} (\lambda_{12})^{1-2l_{12}} & \sigma_{22}^2 \lambda_{22} & |\rho_{12}| \sigma_{11} \sigma_{22} & \sigma_{22}^2 \end{bmatrix} \quad (3.C.58b)$$

As noted above, all subminor matrices must be non-negative for positive semi-definiteness. In this section, we will consider a few of the required constraint equations by requiring the determinants of the four principal minors in eq(3.C.58b) to be positive. After considerable algebraic manipulation of these determinants, we obtain the inequalities

$$\sigma_{11}^2 \geq 0 \quad (3.C.59a)$$

$$\sigma_{11}^2 \sigma_{22}^2 [1 - |\rho_{12}|^2] \geq 0 \quad (3.C.59b)$$

$$\sigma_{22}^4 \sigma_{22}^2 \{1 - (\lambda_{11})^2 - A_1 |\rho_{12}|^2\} \geq 0 \quad (3.C.59c)$$

$$\sigma_{11}^4 \sigma_{22}^2 \{1 - C - A_2 |\rho_{12}|^2 + B |\rho_{12}|^4\} \geq 0 \quad (3.C.59d)$$

where

$$A_1 = 1 + K_1^2 - 2(\lambda_{11})K_1 \quad (3.C.60a)$$

$$K_1 = \frac{(\lambda_{12})^{(1-2l_{12})^2}}{(\lambda_{12})^{l_{12}^2}} = (\lambda_{12})^{1-2l_{12}} \quad (3.C.60b)$$

$$A_2 = 2 + [K_1^2 + K_2^2] - 2(\lambda_{11} + \lambda_{22})[K_1 + K_2] + 2(\lambda_{11})(\lambda_{22})[1 + (\lambda_{12})^2] \quad (3.C.60c)$$

$$K_2 = \frac{(\lambda_{12})^{(1+2l_{12})^2}}{(\lambda_{12})^{l_{12}^2}} = (\lambda_{12})^{1+2l_{12}} \quad (3.C.60d)$$

$$B = 1 - 2(\lambda_{12})^2 + (\lambda_{12})^4 \quad (3.C.60e)$$

$$C = (\lambda_{11})^2 + (\lambda_{22})^2 - (\lambda_{11})^2(\lambda_{22})^2. \quad (3.C.60f)$$

Eqs(3.C.59a) and (3.C.59b) are always satisfied since σ_{11}^2 is positive and $|\rho_{12}|^2 \leq 1$. In Appendix E, we show that

$$A_1 \geq 1 - (\lambda_{11})^2 \geq 0 \quad (3.C.61a)$$

$$0 \leq B \leq 1 \quad (3.C.61b)$$

$$0 \leq C \leq 1. \quad (3.C.61c)$$

Since σ_{11} and σ_{22} are also positive, then eq(3.C.59c) is satisfied when

$$|\rho_{12}|^2 \leq \frac{1 - (\lambda_{11})^2}{A_1}. \quad (3.C.62)$$

Using eq(3.C.61a) in eq(3.C.62), we note that the condition $|\rho_{12}|^2 \leq 1$ is maintained. Eq(3.C.56d) is satisfied when

$$A_2 |\rho_{12}|^2 - B |\rho_{12}|^4 \leq 1 - C \quad (3.C.64a)$$

or

$$|\rho_{12}|^2 [A_2 - B |\rho_{12}|^2] \leq 1 - C. \quad (3.C.64b)$$

Eq(3.C.64a) can also be expressed as

$$B |\rho_{12}|^4 - A_2 |\rho_{12}|^2 + (1 - C) \geq 0. \quad (3.C.64c)$$

Since this quadratic is non-negative for any $|\rho_{12}|^2$, its discriminant is non-positive so that

$$(A_2)^2 \leq 4B(1-C). \quad (3.C.64d)$$

The inequalities in eqs(3.C.62) and (3.C.64a) through (3.C.64c) can always be achieved for sufficiently small values of $|\rho_{12}|$. This will be an important control parameter in the process synthesis procedure. We now consider several examples using the above constraints.

CASE 1

In this case, we consider the parameters $\lambda_{12} = \lambda_{11} = \lambda_{22}$ and $l_{12}=0$ so that from eqs(3.C.60a) through (3.C.60f)

$$K_1 = K_2 = \lambda_{12} = \lambda_{11} \quad (3.C.65a)$$

$$A_1 = 1 - (\lambda_{11})^2 \quad (3.C.65b)$$

$$B = 1 - 2(\lambda_{11})^2 + (\lambda_{11})^4 \quad (3.C.65c)$$

$$\begin{aligned} A_2 &= 2 + 2(\lambda_{11})^2 - 8(\lambda_{11})^2 + 2(\lambda_{11})^2[1 + (\lambda_{11})^2] \\ &= 2[1 - 2(\lambda_{11})^2 + (\lambda_{11})^4] \\ &= 2B \end{aligned} \quad (3.C.65d)$$

$$C = 2(\lambda_{11})^2 - (\lambda_{11})^4. \quad (3.C.65e)$$

In this case, eq(3.C.62) is always satisfied since it reduces to

$$|\rho_{12}| \leq 1 \quad (3.C.66)$$

while eq(3.C.64a) becomes

$$2B|\rho_{12}|^2 - B|\rho_{12}|^4 \leq 1 - 2(\lambda_{11})^2 + (\lambda_{11})^4 = B \quad (3.C.67)$$

so that

$$2|\rho_{12}|^2 - |\rho_{12}|^4 \leq 1. \quad (3.C.68)$$

This equation is also satisfied for $|\rho_{12}| \leq 1$ so that the constraint equations dicussed here are satisfied for all values of $|\rho_{12}|$. This condition is observed in Table 3.1 which shows the values of the 4x4, 3x3 and 2x2 principal minor determinants of eq(3.C.58b), respectively. In the special case where $|\rho_{12}|=1$ and $\sigma_{11}=\sigma_{22}$, both processes become identical. In particular, when $\lambda_{12}=\lambda_{11}=\lambda_{22} = 0$, we have the case of two identical white noise processes.

CASE 2

We first note in [2] of Table 3.1 that when $\lambda_{11}=\lambda_{22}=1$, but $\lambda_{12} \leq 1$, even the small value of $|\rho_{12}|=0.0001$ causes the determinant D_4 to go negative. In this case, we make a small reduction in the temporal correlation coefficients from unity and observe the effect on the range of permissable values of λ_{12} . Consider $\lambda_{11} = \lambda_{22} = 0.95$, $|\rho_{12}| = 0.0001$ and $l_{12} = 2$. From eq(3.C.60f), $C = 0.99049$ so that eqs(3.C.62) and (3.C.64a) become, respectively

$$|\rho_{12}|^2 \leq 0.0975/A_1 \quad (3.C.69)$$

and

$$A_2|\rho_{12}|^2 - B|\rho_{12}|^4 \leq 9.506 \times 10^{-3}. \quad (3.C.70)$$

Using $|\rho_{12}|^2 = 1 \times 10^{-8}$ and eq(3.C.60a) in (3.C.69), we obtain

$$A_1 = 1 + K_1^2 - 2(.95)K_1 \leq \frac{.0975}{1 \times 10^{-8}} = 9.75 \times 10^6. \quad (3.C.71)$$

Since $K_1 = (\lambda_{12})^{-3}$, then, solving for λ_{12} yields

$$(\lambda_{12})^{-6} - 2(.95)(\lambda_{12})^{-3} \approx (\lambda_{12})^{-6} \leq 9.75 \times 10^6 \quad (3.C.72)$$

or

$$(\lambda_{12})^6 \geq 1.0256 \times 10^{-7} \quad (3.C.73)$$

so that

$$(\lambda_{12}) \geq 0.0685. \quad (3.C.74)$$

This result agrees with the 3x3 determinant D_3 of eq(3.C.58b) in [3] of Table 3.1; ie., D_3 goes negative for $\lambda_{12} \leq 0.0685$. The more stringent condition, however, is expressed by eq(3.C.70). For $\lambda_{12} \leq 0.3$, $A_2 \approx (\lambda_{12})^{-6}$ and $|\rho_{12}|^4 \approx 0$ so that eq(3.C.70) can be approximated as

$$(\lambda_{12})^{-6} |\rho_{12}|^2 \leq 9.506 \times 10^{-3} \quad (3.C.75a)$$

or

$$(\lambda_{12})^6 \geq 1.05196 \times 10^{-6} \quad (3.C.75b)$$

so that

$$\lambda_{12} \geq 0.1008479 \quad (3.C.75c)$$

which agrees with the value where D_4 in [3] goes negative.

The significant result of this case, however, is observed by first noting that from eq(3.C.75), we have

$$|p_{12}| \leq .0975(\lambda_{12})^3. \quad (3.C.76)$$

We note, however, that from the previously developed constraint eq(3.C.56b) with $l_{12} = 2$, we have the inequality

$$|p_{12}| \leq (\lambda_{12})^4. \quad (3.C.77)$$

Therefore, when $\lambda_{12} \leq .0975$, eq(3.C.77) is more restrictive than eq(3.C.76). However, when $\lambda_{12} > .0975$ eq (3.C.76) is the more stringent condition. This case illustrates that neither constraint is sufficient to guarantee that the functionals will have the proper form for correlation functions. In the absence of such a sufficient condition, the procedure will be to utilize the more stringent condition; ie., positive definiteness or eq(3.C.53b) recognizing, of course, that either of these two conditions may not be sufficient. As noted previously, an SVD method appears to be an efficient means to check positive semi-definiteness. A recent correspondence on this topic appears in [13].

This case also illustrates that as the individual channel processes each become more uncorrelated(ie., more whitened), they can also become less correlated with each other as noted by the small value of λ_{12} . It is significant to note that although λ_{11} and λ_{22} were lowered by a relatively small amount(ie., from unity to 0.95), the value of λ_{12} could be lowered significantly, provided $|p_{12}|$ is low. Examination of [3] and [5] in Table 3.1, however, also indicates that the lower bound on λ_{12} is highly dependent upon $|p_{12}|$.

	$ p_{12} $	λ_{11}	λ_{22}	λ_{12}	D_4	D_3	D_2	l_{12}
	0.0	1.0	1.0	1.0	0	0	36.0	2.0
	0.1				0	0	35.6	
[1]	0.5				0	0	27.0	
	0.9				0	0	6.8	
	1.0				0	0	0.0	
[2]	0.0	1.0	1.0	0.99	0	0	36.0	
	0.0001				-1.0×10^8	0	36.0	
	0.0001	0.95	0.95	0.90	12.32	31.59	36.0	
				0.20	12.12	31.54		
[3]				0.11	5.04	29.7		
				0.10	-0.59	28.35		
				0.070	-97.6	4.07		
				0.069	-107.6	1.59		
				0.068	-118.6	-1.16		
	0.0001	0.90	0.90	0.999	46.79	61.56		
				0.30	46.77	61.55		
[4]				0.10	33.87	58.33		
				0.09	22.46	55.47		
				0.08	-2.56	49.21		
				0.07	-64.24	34.04		
				0.06	-230.7	-7.85		

Table 3.1 Computed values for the principal minor determinants of the 4x4 correlation matrix R_{XX} .

	$ p_{12} $	λ_{11}	λ_{22}	λ_{12}	D_4	D_3	D_2	l_{12}
	0.9	0.95	0.95	0.990	1.59	4.30	6.83	2.0
				0.980	0.92	2.68		
[5]				0.970	0.083	0.43		
				0.969	0.0003	0.169		
				0.968	-0.082	-0.10		
	0.9	0.9	0.9	0.970	1.149	1.647		
[6]				0.966	0.135	0.943		
				0.965	-0.131	-0.188		
	0.001	0.1	0.1	1.0	1270.2	320.7		
[7]	0.50				220.4	174.9		
	0.54				45.7	150.6		
	0.55				-1.5×10^{-4}	144.3		
[8]		0.0	0.0	1.0				

Table 3.1 (contin.)

D. Spectra for Complex Correlation Functions

1. General Relationships

The power spectral density $P_{ii}(f)$ of the continuous random process $x_i(t)$ is defined as the Fourier transform of its autocorrelation function such that

$$P_{ii}(f) = \int_{-\infty}^{\infty} R_{ii}(\tau) \exp(-j2\pi f\tau) d\tau \quad (3.D.1)$$

while for the discrete processes $x(n)$, we use the discrete Fourier transform

$$P_{ii}(f) = T \sum_{l=-\infty}^{\infty} R_{ii}(l) \exp(-j2\pi f l T) \quad (3.D.2)$$

where $P_{ii}(f)$ is assumed to be bandlimited to $\pm \frac{1}{2} T$ Hz, and is periodic in frequency with period $\frac{1}{T}$ Hz.

The cross-power spectrum $P_{ij}(f)$ of two processes $x_i(\cdot)$ and $x_j(\cdot)$ is similarly expressed in terms of the cross-correlation functions such that for continuous processes

$$P_{ij}(f) = \int_{-\infty}^{\infty} R_{ij}(\tau) \exp(-j2\pi f\tau) d\tau \quad (3.D.3)$$

while for the discrete processes

$$P_{ij}(f) = T \sum_{l=-\infty}^{\infty} R_{ij}(l) \exp(-j2\pi f l T). \quad (3.D.4)$$

Using the continuous time version of eq (3.A.8); i.e.

$$R_{ii}(\tau) = R_{ii}^*(-\tau) \quad (3.D.5)$$

in eq (3.D.1), we have

$$P_{ii}(f) = \int_{-\infty}^{\infty} R_{ii}^*(-\tau) \exp(-j2\pi f\tau) d\tau \quad (3.D.6a)$$

$$= \int_{-\infty}^{\infty} R_{ii}^*(\tau) \exp(j2\pi f\tau) d\tau = [P_{ii}(f)]^* \quad (3.D.6b)$$

where the last equality results by changing the variable τ to $-\tau$ and appropriately changing the direction of the integration. Similarly, using eq (3.D.5) in eq (3.D.2) provides the discrete time version as

$$P_{ii}(f) = T \sum_{l=-\infty}^{\infty} R_{ii}^*(-l) \exp(-j2\pi f l T) \quad (3.D.7a)$$

$$= T \sum_{l=-\infty}^{\infty} R_{ii}^*(l) \exp(+j2\pi f l T) = [P_{ii}(f)]^*. \quad (3.D.7b)$$

Equations (3.D.6b) and (3.D.7b) indicate that the autospectra are real. Since, in general

$$R_{ij}(l) \neq R_{ij}^*(-l) \quad (3.D.8a)$$

and

$$R_{ij}(\tau) \neq R_{ij}^*(-\tau) \quad (3.D.8b)$$

the cross-spectra is, in general, complex. From the Fourier inversion formula, we have

$$R_{ii}(\tau) = \int_{-\infty}^{\infty} P_{ii}(f) \exp(j2\pi f\tau) df \quad (3.D.9a)$$

and

$$R_{ij}(\tau) = \int_{-\infty}^{\infty} P_{ij}(f) \exp(j2\pi f\tau) df \quad (3.D.9b)$$

for continuous time processes; the inverse discrete time Fourier transform yields

$$R_{ii}(l) = \int_{-\frac{1}{2T}}^{\frac{1}{2T}} P_{ii}(f) \exp(j2\pi f l T) df \quad (3.D.10a)$$

and

$$R_{ij}(l) = \int_{-\frac{1}{2T}}^{\frac{1}{2T}} P_{ij}(f) \exp(j2\pi f l T) df. \quad (3.D.10b)$$

At $\tau = 0$, eqs (3.D.9a) and (3.D.9b) become

$$R_{ii}(0) = \int_{-\infty}^{\infty} P_{ii}(f) df \quad (3.D.11a)$$

and

$$R_{ij}(0) = \int_{-\infty}^{\infty} P_{ij}(f) df \quad (3.D.11b)$$

for continuous time processes; for $l=0$, eqs (3.D.10a) and (3.D.10b) become

$$R_{ii}(0) = \int_{-\frac{1}{2T}}^{\frac{1}{2T}} P_{ii}(f) df \quad (3.D.12a)$$

and

$$R_{ij}(0) = \int_{-\frac{1}{2T}}^{\frac{1}{2T}} P_{ij}(f) df \quad (3.D.12b)$$

for discrete time processes.

2. Quadrature Component Form

We now consider the continuous complex autocorrelation function in terms of its quadrature components, such that

$$R_{ii}(\tau) = R_{A_{ii}}(\tau) + jR_{B_{ii}}(\tau). \quad (3.D.13)$$

Using eq (3.D.13) in eq (3.D.1), we have

$$P_{ii}(f) = \int_{-\infty}^{\infty} R_{A_{ii}}(\tau) \exp(-j2\pi f\tau) d\tau + j \int_{-\infty}^{\infty} R_{B_{ii}}(\tau) \exp(-j2\pi f\tau) d\tau. \quad (3.D.14)$$

But since $R_{A_{ii}}(\tau)$ is even and $R_{B_{ii}}(\tau)$ is odd (see section III.E.1.a), eq (3.D.14) becomes

$$P_{ii}(f) = \int_{-\infty}^{\infty} R_{A_{ii}}(\tau) \cos(2\pi f\tau) d\tau + \int_{-\infty}^{\infty} R_{B_{ii}}(\tau) \sin(2\pi f\tau) d\tau \quad (3.D.15a)$$

$$= P_{A_{ii}}(f) + P_{B_{ii}}(f) \quad (3.D.15b)$$

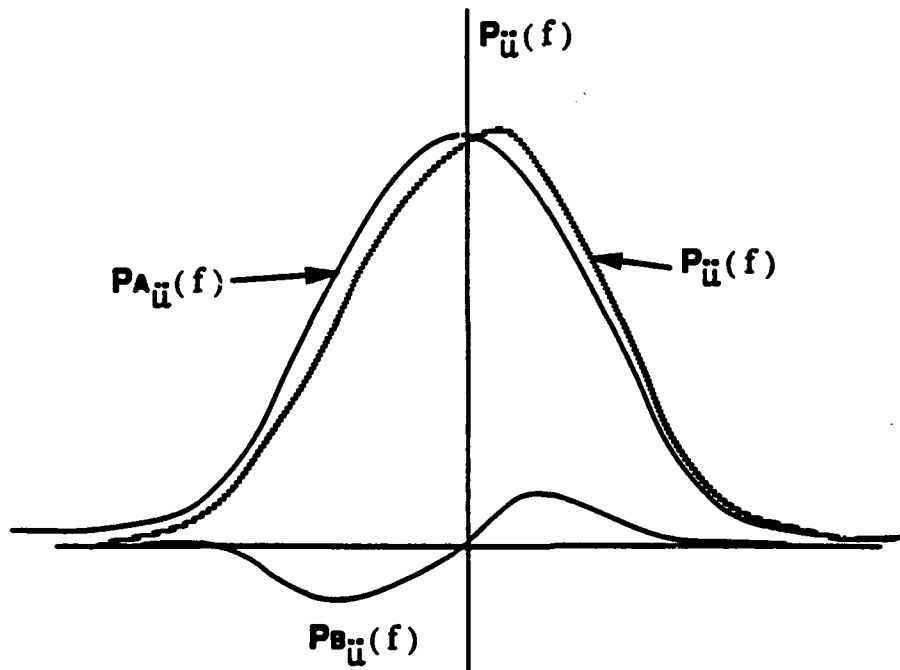


Fig. 3.D.1 Even and odd components of the power spectral density

Eq(3.D.15b) indicates that the autospectrum is real, as noted previously. Since the first integral is an even function and the second is odd, the resulting summation will, in general, distort the spectrum about $f=0$ as shown in Fig.(3.D.1). In the case where $P_{B_{ii}}(f) = 0$, the spectrum is even. This results when $R_{B_{ii}}(\tau)=0$, so that $R_{ii}(\tau)$ is real.

3. Spectral Distribution Using the Functional Shaping Method

We now present a discussion which will help to clarify the role of the temporal correlation coefficient λ_{ii} introduced in section III.C to shape the autocorrelation function.

a. Spectrum of the Gaussian Shaped Autocorrelation Function

In this case, we consider a real autocorrelation function for a continuous-time process on channel i. The form of equation (3.C.11a) together with that of eq(3.C.12) is used with the subscript notation g dropped. Specifically,

$$\theta_{ii}(\tau) = 0 \quad (3.D.16a)$$

and

$$f(\lambda_{ii}, \tau) = \lambda_{ii}^{\tau^2} = \exp(-2\pi^2 \mu_{ii}^2 \tau^2) \quad (3.D.16b)$$

where

$$\lambda_{ii} = \exp(-2\pi^2 \mu_{ii}^2). \quad (3.D.17)$$

With these expressions

$$R_{ii}(\tau) = \sigma_{s_{ii}}^2 \exp(-2\pi^2 \mu_{ii}^2 \tau^2) \quad (3.D.18)$$

is a real, Gaussian shaped autocorrelation function. Taking the derivative of eq(3.D.1) with respect to f and eq(3.D.9a) with respect to τ , we have

$$\dot{P}_{ii}(f) = \int_{-\infty}^{\infty} [-j2\pi\tau R_{ii}(\tau)] \exp(-j2\pi f\tau) d\tau \quad (3.D.19a)$$

and

$$\dot{R}_{ii}(\tau) = \int_{-\infty}^{\infty} [j2\pi f P_{ii}(f)] \exp(+j2\pi f\tau) df. \quad (3.D.19b)$$

Therefore,

$$\dot{P}_{ii}(f) \xleftrightarrow{\text{F.T}} -j2\pi\tau R_{ii}(\tau) \quad (3.D.20a)$$

and

$$\dot{R}_{ii}(\tau) \xleftrightarrow{\text{F.T}} j2\pi f P_{ii}(f) \quad (3.D.20b)$$

where $\xleftrightarrow{\text{F.T}}$ denotes the Fourier transform pair. Taking the derivative of eq(3.D.18) with respect to τ

$$\dot{R}_{ii}(\tau) = -4\pi^2 \mu_{ii}^2 \tau R_{ii}(\tau) \quad (3.D.21)$$

so that from eq. (3.D.20b)

$$j2\pi f P_{ii}(f) \xleftrightarrow{\text{F.T}} -4\pi^2 \mu_{ii}^2 \tau R_{ii}(\tau). \quad (3.D.22)$$

Dividing both sides of (3.D.22) by $-j2\pi\mu_{ii}^2$ yields

$$-\left[\frac{f}{\mu_{ii}^2}\right] P_{ii}(f) \xleftrightarrow{\text{F.T}} -j2\pi\tau R_{ii}(\tau). \quad (3.D.23)$$

Using eq. (3.D.20a) and eq.(3.D.23)

$$\dot{P}_{ii}(f) = - \left[\frac{f}{2} \right] P_{ii}(f). \quad (3.D.24)$$

Solving this equation for $P_{ii}(f)$, we obtain

$$P_{ii}(f) = P_{ii}(0) \exp(-f^2/2\mu_{ii}^2) \quad (3.D.25)$$

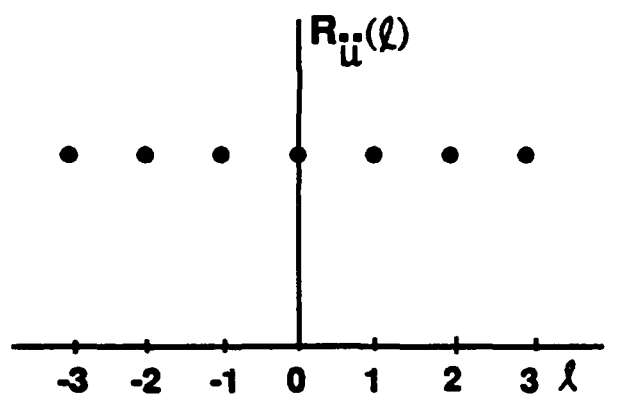
where it is now observed that μ_{ii}^2 is the variance of the Gaussian power spectral density function. Eq(3.D.25) indicates that the real, Gaussian autocorrelation function results in a symmetric, Gaussian power spectral density (PSD).

For the discrete time case, $\tau \rightarrow lT$ where T is the sample period, so that

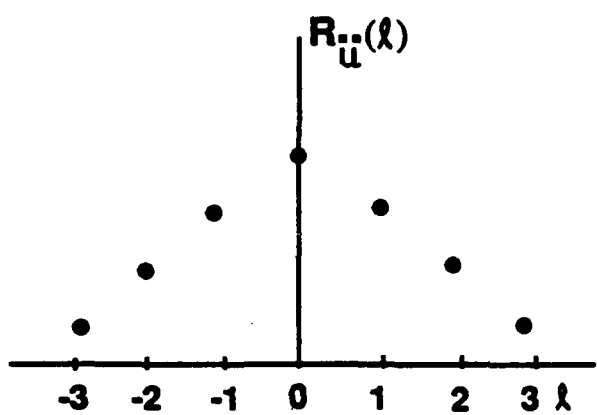
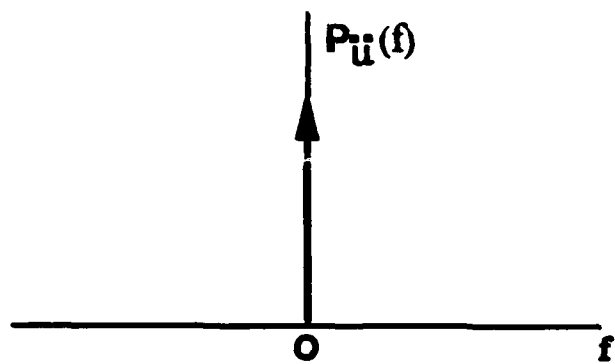
$$R_{ii}(l) = \sigma_{sii}^2 \exp(-2\pi^2 \mu_{ii}^2 T^2 l^2) \quad (3.D.26a)$$

$$= \sigma_{sii}^2 \lambda_{ii}^2 \quad (3.D.26b)$$

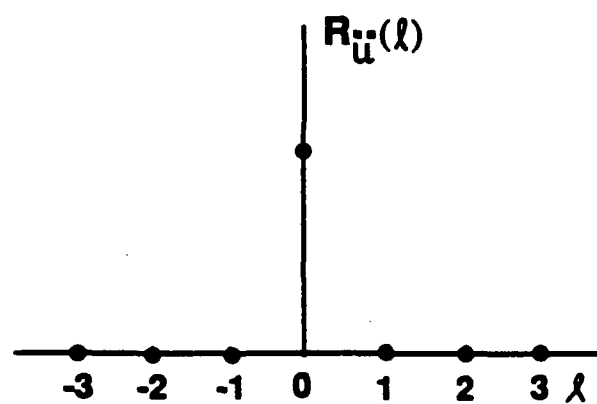
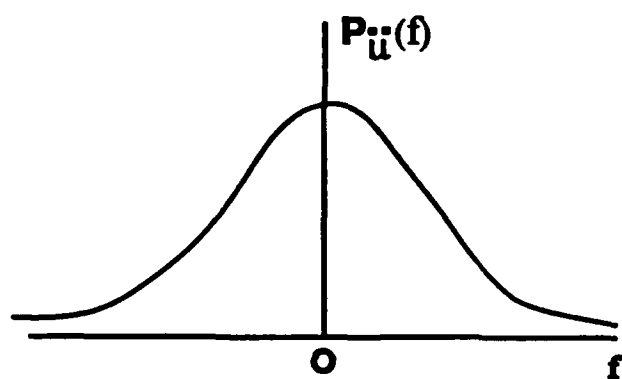
and the last equation results from eq(3.D.17). Also, from eq(3.D.17), we see that as the variance of the power spectrum μ_{ii}^2 ranges from zero to infinity, λ_{ii} goes from one to zero, respectively. Figure 3.D.2 shows the functional plot of $R_{ii}(l)$ and $P_{ii}(f)$ for $0 \leq \lambda_{ii} \leq 1$. For $\lambda_{ii} = 0$, $R_{ii}(l)$ is a delta function $\delta(l)$ and $P_{ii}(f)$ is a white noise spectrum. When $\lambda_{ii} = 1$, $R_{ii}(l)$ denotes the case of total temporal correlation with a line spectrum for $P_{ii}(f)$. For λ_{ii} ranging from zero to unity, all values of temporal correlation are obtained. Thus, λ_{ii} is a measure of the temporal correlation between consecutive samples of the random processes [2].



a.



b.



c.

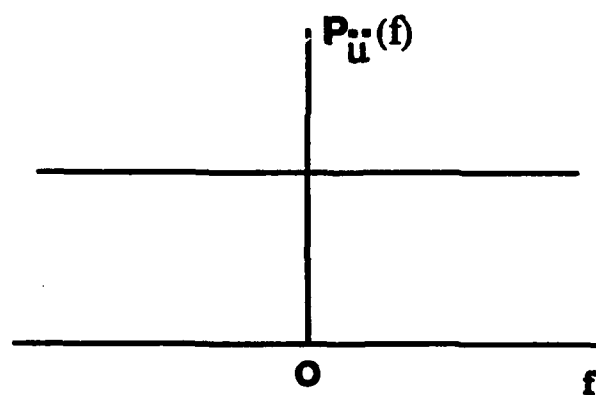


Fig 3.D.2 Functional plot of $R_{ii}(l)$ and $P_{ii}(l)$ for a.) $\lambda_{ii}=1$ b.) $0 \leq \lambda_{ii} \leq 1$ c.) $\lambda_{ii}=0$.

b. Spectrum of the Exponential Shaped Autocorrelation Function

In this section, we consider a real exponential autocorrelation function for a continuous time process on channel i. For this case, we have

$$\theta_{ii}(\tau) = 0 \quad (3.D.27a)$$

$$f(\lambda_{ii}, \tau) = \lambda_{ii}^{|\tau|} = \exp(-2\pi\gamma_{ii}|\tau|) \quad (3.D.27b)$$

where

$$\lambda_{ii} = \exp(-2\pi\gamma_{ii}). \quad (3.D.28)$$

With these expressions, we have

$$R_{ii}(\tau) = \sigma_{s ii}^2 \exp(-2\pi\gamma_{ii}|\tau|) \quad (3.D.29)$$

The power spectral density is determined by considering $R_{ii}(\tau)$ as the superposition of two functions such that

$$R_{ii}(\tau) = \sigma_{s ii}^2 \lambda_{ii}^{\tau} u(\tau) + \sigma_{s ii}^2 \lambda_{ii}^{-\tau} u(-\tau) \quad (3.D.30)$$

where $u(\tau)$ is the unit step function. And so, the power spectral density is expressed as

$$\begin{aligned} P_{ii}(f) &= \int_0^{\infty} \sigma_{s ii}^2 \exp(-2\pi\gamma_{ii}\tau) \exp(j2\pi f\tau) d\tau \\ &\quad + \int_{-\infty}^0 \sigma_{s ii}^2 \exp(-2\pi\gamma_{ii}\tau) \exp(j2\pi f\tau) d\tau \end{aligned} \quad (3.D.31a)$$

$$= \frac{\sigma_{s ii}^2}{(2\pi\gamma_{ii}) + j(2\pi f)} + \frac{\sigma_{s ii}^2}{(2\pi\gamma_{ii}) - j(2\pi f)} \quad (3.D.31b)$$

$$= \frac{2\sigma_{sii}^2(2\pi\gamma_{ii})}{(2\pi\gamma_{ii})^2 + (2\pi f)^2} \quad (3.D.31c)$$

The peak value of this function occurs at $f=0$ so that

$$P_{ii}(0) = \frac{\sigma_{sii}^2}{\pi\gamma_{ii}} \quad (3.D.32)$$

Also

$$P_{ii}(\gamma_{ii}) = \frac{\sigma_{sii}^2}{2\pi\gamma_{ii}} \quad (3.D.33)$$

so that the 3-dB down points occur at $f = \gamma_{ii}$ in the exponential case. The inflection point of $P_{ii}(f)$ occurs at $f = \gamma_{ii} \frac{\sqrt{3}}{3}$.

E. Special Properties of Complex Correlation Functions

1. Even and Odd Components

a. Single Channel Case

In this section we develop some interesting and useful properties of complex auto- and cross-correlation functions. We consider the complex, stationary, baseband random process

$$x(n) = x_I(n) + jx_Q(n) \quad (3.E.1.1)$$

where we have dropped the channel subscript notation for convenience. The complex autocorrelation function is obtained from eq. (3.A.2e) as

$$R(l) = R_A(l) + jR_B(l) \quad (3.E.1.2)$$

where

$$R_A(l) = R_{II}(l) + R_{QQ}(l) \quad (3.E.1.3a)$$

$$R_B(l) = R_{QI}(l) - R_{IQ}(l) \quad (3.E.1.3b)$$

and

$$R_{II}(l) = E[x_I(n)x_I(n-l)] \quad R_{QQ}(l) = E[x_Q(n)x_Q(n-l)] \quad (3.E.1.3c)$$

$$R_{IQ}(l) = E[x_I(n)x_Q(n-l)] \quad R_{QI}(l) = E[x_Q(n)x_I(n-l)] \quad (3.E.1.3d)$$

The prime intent of this section is to consider some conditions under which we may satisfy the special properties

$$\boxed{R_{IQ}(l) = -R_{QI}(l)} \quad (3.E.1.4)$$

and

$$\boxed{R_{II}(l) = R_{QQ}(l)} \quad (3.E.1.5)$$

These equations are satisfied when $x(n)$ is a wide-sense stationary narrowband process[see Section III.E.2a]. In this section, we show that eq(3.E.1.4) is satisfied in general, when $R_{IQ}(l)$ and $R_{QI}(l)$ are both odd functions.

For stationary processes, we have the following properties:

$$R_{ii}(l) = R_{ii}^*(-l) \quad (3.E.1.6)$$

and

$$R_{ij}(l) = R_{ji}^*(-l) . \quad (3.E.1.7)$$

Substituting eq(3.E.1.2) into (3.E.1.6), we have (dropping the subscript i)

$$R_A(l) + jR_B(l) = R_A(-l) - jR_B(-l). \quad (3.E.1.8)$$

Equating real and imaginary terms

$$R_A(l) = R_A(-l) \quad (3.E.1.9)$$

and

$$R_B(l) = -R_B(-l) \quad (3.E.1.10)$$

indicating that $R_A(l)$ and $R_B(l)$ are even and odd, respectively. Also, applying eq(3.E.1.6) to $R_{II}(l)$ and $R_{QQ}(l)$, we have

$$R_{II}(l) = R_{II}^*(-l) = R_{II}(-l) \quad (3.E.1.11a)$$

and

$$R_{QQ}(l) = R_{QQ}^*(-l) = R_{QQ}(-l) \quad (3.E.1.11b)$$

where the last equality results because these functions are real. Thus, $R_{II}(l)$ and $R_{QQ}(l)$ are even functions of l . Applying eq(3.E.1.7) to $R_{IQ}(l)$ and $R_{QI}(l)$, we have

$$R_{IQ}(l) = R_{QI}^*(-l) = R_{QI}(-l) \quad (3.E.1.12)$$

where again, $R_{QI}(l)$ is real.

We note at this point that although $R_{II}(l)$ and $R_{QQ}(l)$ have been shown to be even functions, no similar conclusion can be made at this point about $R_{IQ}(l)$ and $R_{QI}(l)$. However, expressing $R_{QI}(l)$ in terms of its even and odd components, we obtain

$$R_{QI}(l) = R_{QI}^e(l) + R_{QI}^o(l). \quad (3.E.1.13)$$

Eq.(3.E.1.12) can now be written as

$$R_{IQ}(l) = R_{QI}(-l) = R_{QI}^e(-l) + R_{QI}^o(-l). \quad (3.E.1.14)$$

From the property of even and odd functions

$$R_{IQ}(l) = R_{QI}^e(l) - R_{QI}^o(l). \quad (3.E.1.15)$$

Solving for $R_{QI}^o(l)$ in eq.(3.E.1.13) and substituting into eq(3.E.1.15), we have

$$R_{IQ}(l) = R_{QI}^e(l) - [R_{QI}(l) - R_{QI}^e(l)] \quad (3.E.1.16a)$$

$$= -R_{QI}(l) + 2R_{QI}^e(l). \quad (3.E.1.16b)$$

A similar equation is obtained by solving for $R_{QI}^e(l)$ in eq.(3.E.1.13) so that eq.(3.E.1.15) becomes

$$R_{IQ}(l) = R_{QI}(l) - 2R_{QI}^o(l). \quad (3.E.1.17)$$

These last two equations show the explicit dependence of $R_{IQ}(l)$ on the evenness and oddness of $R_{QI}(l)$. These equations indicate that when $R_{QI}(l)$ has no even component (ie., when it is an odd function),

$$R_{IQ}(l) = -R_{QI}(l) \quad \text{for } R_{QI}(l) = R_{QI}^o(l). \quad (3.E.1.18)$$

On the other hand, when $R_{QI}(l)$ has no odd component (ie. when it is an even function),

$$R_{IQ}(l) = +R_{QI}(l) \quad \text{for } R_{QI}(l) = R_{QI}^e(l). \quad (3.E.1.19)$$

These last two equations can be substituted into eq.(3.E.1.3b) to obtain the extreme values of $R_B(l)$; ie.,

$$R_B(l) = \begin{cases} 2R_{QI}(l) & R_{QI}(l) = R_{QI}^0(l) \\ 0 & R_{QI}(l) = R_{QI}^e(l). \end{cases} \quad (3.E.1.20)$$

Thus, the degree of evenness or oddness of $R_{QI}(l)$ [or $R_{IQ}(l)$] controls the imaginary part of the correlation function, $R_B(l)$. For $R_{QI}(l)$ totally even, $R_B(l) = 0$, so that $R(l)$ is real. In this case, the spectrum is even. As $R_{QI}(l)$ becomes progressively odd, the $R_B(l)$ term increases with the result that the spectrum becomes distorted about the carrier frequency.

At this point, we note that eqs.(3.E.1.16b) and (3.E.1.17) were developed without imposing any restrictions on the process $\{x(n)\}$ other than wide-sense stationarity. It can be shown, however, that for narrowband, wide-sense stationary bandpass processes, eq.(3.E.1.18) results. This is discussed in section III.E.2.a. Apparently, the narrowband restriction is a special case which yields an odd $R_{QI}(l)$ function.

b. Multichannel Case

In this section, we consider several properties of the complex cross-correlation function between the two processes $x_i(n)$ and $x_j(n)$ where

$$x_i(n) = x_{iI}(n) + jx_{iQ}(n) \quad (3.E.1.21a)$$

and

$$x_j(n) = x_{jI}(n) + jx_{jQ}(n). \quad (3.E.1.21b)$$

Assuming wide-sense joint stationarity, the complex cross-correlation function is obtained from eq(3.A.2e) as

$$R_{ij}(l) = R_{A_{ij}}(l) + jR_{B_{ij}}(l) \quad (3.E.1.22)$$

where

$$R_{Aij}(l) = R_{ij}^{\Pi}(l) + R_{ij}^{QQ}(l) \quad (3.E.1.23a)$$

$$R_{Bij}(l) = R_{ij}^{QI}(l) - R_{ij}^{IQ}(l) \quad (3.E.1.23b)$$

and

$$R_{ij}^{\Pi}(l) = E[x_{iI}(n)x_{jI}(n-l)] \quad (3.E.1.24a)$$

$$R_{ij}^{QQ}(l) = E[x_{iQ}(n)x_{jQ}(n-l)] \quad (3.E.1.24b)$$

$$R_{ij}^{IQ}(l) = E[x_{iI}(n)x_{jQ}(n-l)] \quad (3.E.1.24c)$$

$$R_{ij}^{QI}(l) = E[x_{iQ}(n)x_{jI}(n-l)] \quad (3.E.1.24d)$$

Under the stationarity conditions assumed here, we have the relation

$$R_{ij}(l) = R_{ji}^*(-l). \quad (3.E.1.25)$$

Substituting eq(3.E.1.22) into eq(3.E.1.25) enables us to obtain

$$R_{Aij}(l) = R_{Aji}(-l) \quad (3.E.1.26a)$$

and

$$R_{Bij}(l) = -R_{Bji}(-l). \quad (3.E.1.26b)$$

Applying eq(3.E.1.25) to the real functions in eqs(3.E.1.24), we have

$$R_{ij}^{\Pi}(l) = R_{ji}^{\Pi}(-l) \quad (3.E.1.27a)$$

$$R_{ij}^{QQ}(l) = R_{ji}^{QQ}(-l) \quad (3.E.1.27b)$$

$$R_{ij}^{IQ}(l) = R_{ji}^{QI}(-l) \quad (3.E.1.27c)$$

$$R_{ij}^{QI}(l) = R_{ji}^{IQ}(-l). \quad (3.E.1.27d)$$

2. Narrowband Bandpass Processes

a. Single Channel Case

We now consider a real, narrowband, bandpass process $n_i(t)$ such that

$$n_i(t) = \text{Re}[x_i(t)\exp(j2\pi f_{c_i}t)] \quad (3.E.2.1)$$

where $x_i(t)$ is the complex baseband process previously defined in eq(3.A.1) as

$$x_i(t) = x_{iI}(t) + jx_{iQ}(t). \quad (3.E.2.2)$$

The quantities $x_{iI}(t)$ and $x_{iQ}(t)$ are the real-valued low pass quadrature components. Using eq(3.E.2.2) in (3.E.2.1), the process $n_i(t)$ can be expressed in canonical form as

$$n_i(t) = x_{iI}(t)\cos(2\pi f_{c_i}t) - x_{iQ}(t)\sin(2\pi f_{c_i}t). \quad (3.E.2.3)$$

Taking the Hilbert transform of eq(3.E.2.3) and recognizing that the quadrature components are low pass, we obtain

$$\hat{n}_i(t) = x_{iI}(t)\sin(2\pi f_{c_i}t) + x_{iQ}(t)\cos(2\pi f_{c_i}t). \quad (3.E.2.4)$$

Eqs(3.E.2.3) and (3.E.2.4) can now be used to solve for the quadrature components resulting in

$$x_{iI}(t) = n_i(t)\cos(2\pi f_{c_i}t) + \hat{n}_i(t)\sin(2\pi f_{c_i}t) \quad (3.E.2.5a)$$

and

$$x_{iQ}(t) = \hat{n}_i(t)\cos(2\pi f_{c_i}t) - n_i(t)\sin(2\pi f_{c_i}t). \quad (3.E.2.5b)$$

In this section, we will determine relationships between the auto- and cross-correlation functions of the quadrature components of the process $x_i(t)$ under the

assumption that $n_i(t)$ is stationary. In this case the correlation function of $n_i(t)$ is $R_{n_i n_i}(\tau)$ while the power spectral density is $S_{n_i n_i}(f)$ centered about $\pm f_{c_i}$.

Dropping the redundant subscript i notation, we consider the Hilbert transform of $n(t)$ as

$$\hat{n}(t) = \frac{1}{\pi} \int_{-\infty}^{\infty} \frac{n(\lambda)}{t-\lambda} d\lambda. \quad (3.E.2.6)$$

The cross-correlation function $R_{n\hat{n}}(\tau)$ is expressed as

$$R_{n\hat{n}}(\tau) = E[n(t)\hat{n}(t-\tau)]. \quad (3.E.2.7)$$

Substituting eq (3.E.2.6) into (3.E.2.7)

$$R_{n\hat{n}}(\tau) = E \left[\frac{1}{\pi} \int_{-\infty}^{\infty} \frac{n(t)n(\lambda)}{t-\tau-\lambda} d\lambda \right] \quad (3.E.2.8)$$

Interchanging the expectation and integration

$$R_{n\hat{n}}(\tau) = \frac{1}{\pi} \int_{-\infty}^{\infty} \frac{E[n(t)n(\lambda)]}{t-\tau-\lambda} d\lambda. \quad (3.E.2.9)$$

Assuming wide-sense stationarity on the bandpass process,

$$R_{nn}(t-\lambda) = E[n(t)n(\lambda)] \quad (3.E.2.10)$$

so that

$$R_{n\hat{n}}(\tau) = \frac{1}{\pi} \int_{-\infty}^{\infty} \frac{R_{nn}(t-\lambda)}{t-\tau-\lambda} d\lambda. \quad (3.E.2.11)$$

Now let $\alpha = t - \lambda$ so that $d\lambda = -d\alpha$ and

$$R_{n\hat{n}}(\tau) = \frac{1}{\pi} \int_{\infty}^{-\infty} \frac{R_{nn}(\alpha)}{\alpha-\tau} (-d\alpha) \quad (3.E.2.12a)$$

$$= \frac{1}{\pi} \int_{-\infty}^{\infty} \frac{R_{nn}(\alpha)}{\alpha - \tau} d\alpha \quad (3.E.2.12b)$$

$$= -\frac{1}{\pi} \int_{-\infty}^{\infty} \frac{R_{nn}(\alpha)}{\tau - \alpha} d\alpha = -\hat{R}_{nn}(\tau) \quad (3.E.2.12c)$$

Similarly,

$$R_{nn}^{\wedge}(\tau) = E[\hat{n}(t)n(t-\tau)] \quad (3.E.2.13a)$$

$$= E \left[\frac{1}{\pi} \int_{-\infty}^{\infty} \frac{n(\lambda)n(t-\tau)}{t-\lambda} d\lambda \right] \quad (3.E.2.13b)$$

$$= \frac{1}{\pi} \int_{-\infty}^{\infty} \frac{E[n(\lambda)n(t-\tau)]}{t-\lambda} d\lambda \quad (3.E.2.13c)$$

$$= \frac{1}{\pi} \int_{-\infty}^{\infty} \frac{R_{nn}(\lambda-t+\tau)}{t-\lambda} d\lambda \quad (3.E.2.13d)$$

Let $\alpha = \lambda - t + \tau$ so that $d\lambda = d\alpha$ and

$$R_{nn}^{\wedge}(\tau) = \frac{1}{\pi} \int_{-\infty}^{\infty} \frac{R_{nn}(\alpha)}{\tau - \alpha} d\alpha = \hat{R}_{nn}(\tau) \quad (3.E.2.14)$$

and so noting the equality of eqs(3.E.2.12c) and (3.E.2.14)

$$R_{nn}^{\wedge}(\tau) = -R_{nn}^{\wedge}(\tau). \quad (3.E.2.15)$$

Also, at $\tau = 0$ the function $R_{nn}(\alpha)/\alpha$ is odd so that

$$R_{nn}^{\wedge}(0) = 0. \quad (3.E.2.16)$$

We now consider the correlation functions associated with the quadrature components defined in eq(3.E.2.5a) and (3.E.2.5b)

$$R_{ii}^{\Pi}(\tau) = E[x_{iI}(t)x_{iI}(t-\tau)] \quad (3.E.2.17a)$$

$$\begin{aligned} &= E[n(t)n(t-\tau)]\cos(2\pi f_c t)\cos[2\pi f_c(t-\tau)] \\ &\quad + E[n(t)\hat{n}(t-\tau)]\cos(2\pi f_c t)\sin[2\pi f_c(t-\tau)] \\ &\quad + E[\hat{n}(t)n(t-\tau)]\sin(2\pi f_c t)\cos[2\pi f_c(t-\tau)] \\ &\quad + E[\hat{n}(t)\hat{n}(t-\tau)]\sin(2\pi f_c t)\sin[2\pi f_c(t-\tau)]. \end{aligned} \quad (3.E.2.17b)$$

Let

$$A = 2\pi f_c t \quad (3.E.2.18a)$$

$$B = 2\pi f_c(t-\tau) \quad (3.E.2.18b)$$

Using the identities

$$\cos(A - B) = \cos A \cos B + \sin A \sin B \quad (3.E.2.18c)$$

$$\sin(A - B) = \sin A \cos B - \cos A \sin B \quad (3.E.2.18d)$$

we obtain

$$\cos(2\pi f_c t)\cos[2\pi f_c(t-\tau)] = \cos(2\pi f_c \tau) - \sin A \sin B \quad (3.E.2.18e)$$

$$\cos(2\pi f_c t)\sin[2\pi f_c(t-\tau)] = \cos A \sin B \quad (3.E.2.18f)$$

$$\sin(2\pi f_c t)\cos[2\pi f_c(t-\tau)] = \sin A \cos B \quad (3.E.2.18g)$$

$$\sin(2\pi f_c t)\sin[2\pi f_c(t-\tau)] = \sin A \sin B \quad (3.E.2.18h)$$

Using these relations and eqs(3.E.2.14) and (3.E.2.15) in (3.E.2.18b)

$$\begin{aligned} R_{ii}^{\Pi}(\tau) &= R_{nn}(\tau)[\cos(2\pi f_c \tau) - \sin A \sin B] \\ &\quad - \hat{R}_{nn}(\tau)\cos A \sin B + \hat{R}_{nn}(\tau)\sin A \cos B \\ &\quad + R_{nn}^{\wedge\wedge}(\tau)\sin A \sin B \\ &= R_{nn}(\tau)[\cos(2\pi f_c \tau) - \sin A \sin B] \\ &\quad + \hat{R}_{nn}(\tau)[\sin A \cos B - \cos A \sin B] \end{aligned} \quad (3.E.2.19a)$$

$$\begin{aligned}
& + R_{nn}^{\wedge\wedge}(\tau)\sin A\sin B \\
& = R_{nn}(\tau)[\cos(2\pi f_c\tau) - \sin A\sin B]
\end{aligned}
\tag{3.E.2.19b}$$

$$\begin{aligned}
& + \hat{R}_{nn}(\tau)\sin(2\pi f_c\tau) \\
& + R_{nn}^{\wedge\wedge}(\tau)[\sin A\sin B]
\end{aligned}
\tag{3.E.2.19c}$$

In Appendix B, we show that

$$R_{nn}^{\wedge\wedge}(\tau) = + R_{nn}(\tau) \tag{3.E.2.20}$$

so that

$$\begin{aligned}
R_{ii}^{\Pi}(\tau) &= R_{nn}(\tau)\cos(2\pi f_c\tau) \\
&+ \hat{R}_{nn}(\tau)\sin(2\pi f_c\tau)
\end{aligned}
\tag{3.E.2.21}$$

Similarly,

$$\begin{aligned}
R_{ii}^{QQ}(\tau) &= R_{nn}(\tau)\cos(2\pi f_c\tau) \\
&+ \hat{R}_{nn}(\tau)\sin(2\pi f_c\tau)
\end{aligned}
\tag{3.E.2.22}$$

so that

$$\boxed{R_{ii}^{\Pi}(\tau) = R_{ii}^{QQ}(\tau).} \tag{3.E.2.23}$$

We now consider

$$R_{ii}^{IQ}(\tau) = E[n_I(t)n_Q(t-\tau)] \tag{3.E.2.24a}$$

$$\begin{aligned}
&= E[n(t)\hat{n}(t-\tau)]\cos(2\pi f_c t)\cos[2\pi f_c(t-\tau)] \\
&\quad + E[\hat{n}(t)\hat{n}(t-\tau)]\sin(2\pi f_c t)\cos[2\pi f_c(t-\tau)] \\
&\quad - E[n(t)n(t-\tau)]\cos(2\pi f_c t)\sin[2\pi f_c(t-\tau)] \\
&\quad - E[\hat{n}(t)n(t-\tau)]\sin(2\pi f_c t)\sin[2\pi f_c(t-\tau)]
\end{aligned} \tag{3.E.2.24b}$$

$$\begin{aligned}
&= R_{nn}^{\wedge}(\tau)\cos A\cos B + R_{nn}^{\wedge\wedge}(\tau)\sin A\cos B \\
&\quad - R_{nn}(\tau)\cos A\sin B - R_{nn}^{\wedge}(\tau)\sin A\sin B
\end{aligned} \tag{3.E.2.24c}$$

$$\begin{aligned}
&= R_{nn}^{\wedge}(\tau)\cos A\cos B + R_{nn}(\tau)\sin A\cos B \\
&\quad - R_{nn}(\tau)\cos A\sin B - R_{nn}^{\wedge}(\tau)\sin A\sin B
\end{aligned} \tag{3.E.2.24d}$$

where eq(3.E.2.20) was used to in the second term above. From eqs.(3.E.2.12c) and (3.E.2.14)

$$R_{nn}^{\wedge}(\tau) = -\hat{R}_{nn}(\tau) \tag{3.E.2.25a}$$

$$R_{nn}^{\wedge\wedge}(\tau) = \hat{R}_{nn}(\tau) \tag{3.E.2.25b}$$

so that

$$\begin{aligned}
R_{ii}^{IQ}(\tau) &= R_{nn}(\tau)[\sin A\cos B - \cos A\sin B] \\
&\quad - \hat{R}_{nn}(\tau)[\cos A\cos B + \sin A\sin B]
\end{aligned} \tag{3.E.2.26a}$$

$$= R_{nn}(\tau)\sin(A - B) - \hat{R}_{nn}(\tau)\cos(A - B) \tag{3.E.2.26b}$$

$$= R_{nn}(\tau)\sin(2\pi f_c \tau) - \hat{R}_{nn}(\tau)\cos(2\pi f_c \tau). \tag{3.E.2.26c}$$

Similarly,

$$- R_{ii}^{QI}(\tau) = R_{nn}(\tau)\sin(2\pi f_c \tau) - \hat{R}_{nn}(\tau)\cos(2\pi f_c \tau) \tag{3.E.2.27d}$$

so that

$$\boxed{R_{ii}^{IQ}(\tau) = - R_{ii}^{QI}(\tau).} \tag{3.E.2.27e}$$

We also note that since $R_{nn}(\tau)$ is even and $\hat{R}_{nn}(\tau)$ is odd, then eq(3.E.2.26c) indicates that $R_{ii}^{IQ}(\tau)$ is odd. It was noted at the end of section III.E.1.a, that the narrowband process is a special case which results in odd cross-correlation quadrature components $R_{ii}^{IQ}(\tau)$ and $R_{ii}^{QI}(\tau)$.

b. Multichannel Case

We now consider two real, narrowband, bandpass processes $n_i(t)$ and $n_j(t)$ defined in eq(3.E.2.1) and develop properties similar to those developed in the previous section. Specifically, we will determine relationships between the cross-correlation functions of the quadrature components involving $x_i(t)$ and $x_j(t)$; ie., $R_{ij}^{II}(\tau)$, $R_{ij}^{QQ}(\tau)$, $R_{ij}^{QI}(\tau)$ and $R_{ij}^{IQ}(\tau)$. The bandpass processes are expressed as

$$n_i(t) = \text{Re}[x_i(t)\exp(j2\pi f_{c_i}t)] \quad (3.E.2.28a)$$

and

$$n_j(t) = \text{Re}[x_j(t)\exp(j2\pi f_{c_j}t)]. \quad (3.E.2.28b)$$

In section III.C.3.c, however, we suggested that each channel process can be translated to a common reference frequency f_{c_R} . And so, f_{c_i} and f_{c_j} in (3.E.2.41) can be replaced with f_{c_R} . Eqs(3.E.2.28) can then be expressed as

$$n_i(t) = \text{Re}[x_i(t)\exp(j2\pi f_{c_R}t)] \quad (3.E.2.28c)$$

and

$$n_j(t) = \text{Re}[x_j(t)\exp(j2\pi f_{c_R}t)]. \quad (3.E.2.28d)$$

Using the quadrature form for $x_i(t)$ and $x_j(t)$ expressed in eq(3.A.1), we obtain the canonical forms for the above equations as

$$n_i(t) = x_{iI}(t)\cos(2\pi f_{c_R}t) - x_{iQ}(t)\sin(2\pi f_{c_R}t) \quad (3.E.2.28e)$$

and

$$n_j(t) = x_{jI}(t)\cos(2\pi f_{c_R}t) - x_{jQ}(t)\sin(2\pi f_{c_R}t). \quad (3.E.2.28f)$$

The Hilbert transform of $n_j(t)$ is expressed as

$$\hat{n}_j(t) = \frac{1}{\pi} \int_{-\infty}^{\infty} \frac{n_j(\lambda)}{t-\lambda} d\lambda. \quad (3.E.2.29)$$

Assuming wide-sense joint stationarity between the two bandpass processes, the cross-correlation function $R_{n_i \hat{n}_j}(\tau)$ is expressed as

$$R_{n_i \hat{n}_j}(\tau) = E[n_i(t) \hat{n}_j(t-\tau)]. \quad (3.E.2.30)$$

Substituting eq (3.E.2.29) into (3.E.2.30)

$$R_{n_i \hat{n}_j}(\tau) = E \left[\frac{1}{\pi} \int_{-\infty}^{\infty} \frac{n_i(t) n_j(\lambda)}{t-\tau-\lambda} d\lambda \right] \quad (3.E.2.31)$$

Interchanging the expectation and integration

$$R_{n_i \hat{n}_j}(\tau) = \frac{1}{\pi} \int_{-\infty}^{\infty} \frac{E[n_i(t) n_j(\lambda)]}{t-\tau-\lambda} d\lambda. \quad (3.E.2.32)$$

We now consider,

$$R_{n_i n_j}(t-\lambda) = E[n_i(t) n_j(\lambda)] \quad (3.E.2.33)$$

so that

$$R_{n_i \hat{n}_j}(\tau) = \frac{1}{\pi} \int_{-\infty}^{\infty} \frac{R_{n_i n_j}(t-\lambda)}{t-\tau-\lambda} d\lambda. \quad (3.E.2.34)$$

Now let $\alpha = t - \lambda$ so that $d\lambda = -d\alpha$ and

$$R_{n_i \hat{n}_j}(\tau) = \frac{1}{\pi} \int_{-\infty}^{\infty} \frac{R_{n_i n_j}(\alpha)}{\alpha - \tau} (-d\alpha) \quad (3.E.2.35a)$$

$$= \frac{1}{\pi} \int_{-\infty}^{\infty} \frac{R_{n_i n_j}(\alpha)}{\alpha - \tau} d\alpha \quad (3.E.2.35b)$$

$$= -\frac{1}{\pi} \int_{-\infty}^{\infty} \frac{R_{n_i n_j}(\alpha)}{\tau - \alpha} d\alpha \quad (3.E.2.35c)$$

$$= -\hat{R}_{n_i n_j}(\tau). \quad (3.E.2.35d)$$

Similarly,

$$R_{\hat{n}_i n_j}^A(\tau) = E[\hat{n}_i(t) n_j(t-\tau)] \quad (3.E.2.36a)$$

$$= E \left[\frac{1}{\pi} \int_{-\infty}^{\infty} \frac{n_i(\lambda) n_j(t-\tau)}{t-\lambda} d\lambda \right] \quad (3.E.2.36b)$$

$$= \frac{1}{\pi} \int_{-\infty}^{\infty} \frac{E[n_i(\lambda) n_j(t-\tau)]}{t-\lambda} d\lambda \quad (3.E.2.36c)$$

$$= \frac{1}{\pi} \int_{-\infty}^{\infty} \frac{R_{n_i n_j}(\lambda - t + \tau)}{t - \lambda} d\lambda \quad (3.E.2.36d)$$

Let $\alpha = \lambda - t + \tau$ so that $d\lambda = d\alpha$ and eq(3.E.2.36d) becomes

$$R_{\hat{n}_i n_j}^A(\tau) = \frac{1}{\pi} \int_{-\infty}^{\infty} \frac{R_{n_i n_j}(\alpha)}{\tau - \alpha} d\alpha \quad (3.E.2.37a)$$

$$= \hat{R}_{n_i n_j}(\tau). \quad (3.E.2.37b)$$

From eqs(3.E.2.35d) and (3.E.2.37b), we have

$$R_{n_i \hat{n}_j}(\tau) = -R_{\hat{n}_i n_j}(\tau). \quad (3.E.2.38)$$

We now consider the cross-correlation functions associated with the quadrature components of the $x_i(t)$ and $x_j(t)$ processes defined in eqs(3.E.2.5a) and (3.E.2.5b). First, consider

$$R_{ij}^{\Pi}(\tau) = E[x_{iI}(t)x_{jI}(t-\tau)]. \quad (3.E.2.39)$$

Using eqs(3.E.2.28e) and (3.E.2.28f) and the corresponding Hilbert transforms, we solve for

$$x_{iI}(t) = n_i(t)\cos(2\pi f_{c_R}t) + \hat{n}_i(t)\sin(2\pi f_{c_R}t) \quad (3.E.2.40a)$$

and

$$x_{iQ}(t) = \hat{n}_i(t)\cos(2\pi f_{c_R}t) - n_i(t)\sin(2\pi f_{c_R}t). \quad (3.E.2.40b)$$

Using eq(3.E.2.40a) and the corresponding equation for $x_{jI}(t)$ in eq(3.E.2.39), we obtain

$$\begin{aligned} R_{ij}^{\Pi}(\tau) = & E[n_i(t)n_j(t-\tau)]\cos(2\pi f_{c_R}t)\cos[2\pi f_{c_R}(t-\tau)] \\ & + E[n_i(t)\hat{n}_j(t-\tau)]\cos(2\pi f_{c_R}t)\sin[2\pi f_{c_R}(t-\tau)] \\ & + E[\hat{n}_i(t)n_j(t-\tau)]\sin(2\pi f_{c_R}t)\cos[2\pi f_{c_R}(t-\tau)] \\ & + E[\hat{n}_i(t)\hat{n}_j(t-\tau)]\sin(2\pi f_{c_R}t)\sin[2\pi f_{c_R}(t-\tau)]. \end{aligned} \quad (3.E.2.41)$$

We now define

$$A = 2\pi f_{c_R}t \quad (3.E.2.42a)$$

and

$$B = 2\pi f_{cR}(t-\tau). \quad (3.E.2.42b)$$

Let us recall the identities

$$\cos(A - B) = \cos A \cos B + \sin A \sin B \quad (3.E.2.42c)$$

$$\sin(A - B) = \sin A \cos B - \cos A \sin B. \quad (3.E.2.42d)$$

Using eq(3.E.2.42C), we have

$$\cos(2\pi f_{cR}t) \cos[2\pi f_{cR}(t-\tau)] = \cos(2\pi f_{cR}\tau) - \sin A \sin B. \quad (3.E.2.42e)$$

From the identities defined above,

$$\cos(2\pi f_{cR}t) \sin[2\pi f_{cR}(t-\tau)] = \cos A \sin B \quad (3.E.2.42f)$$

$$\sin(2\pi f_{cR}t) \cos[2\pi f_{cR}(t-\tau)] = \sin A \cos B \quad (3.E.2.42g)$$

$$\sin(2\pi f_{cR}t) \sin[2\pi f_{cR}(t-\tau)] = \sin A \sin B. \quad (3.E.2.42h)$$

Eq(3.E.2.41) can now be written

$$\begin{aligned} R_{ij}^{\Pi}(\tau) = & R_{n_i n_j}(\tau) [\cos(2\pi f_{cR}\tau) - \sin A \sin B] \\ & + R_{n_i \hat{n}_j}^{\Lambda}(\tau) \cos A \sin B \\ & + R_{\hat{n}_i n_j}^{\Lambda}(\tau) \sin A \cos B \\ & + R_{\hat{n}_i \hat{n}_j}^{\Lambda}(\tau) \sin A \sin B \end{aligned} \quad (3.E.2.43a)$$

$$\begin{aligned}
&= R_{n_i n_j}(\tau) [\cos(2\pi f_{c_r} \tau) - \sin A \sin B] \\
&\quad + \hat{R}_{n_i n_j}(\tau) [\sin A \cos B - \cos A \sin B] \\
&\quad + R_{\hat{n}_i \hat{n}_j}(\tau) \sin A \sin B
\end{aligned} \tag{3.E.2.43b}$$

where we have used eqs(3.E.2.35d) and (3.E.2.37b) to obtain (3.E.2.43b). In Appendix A, we show that

$$R_{\hat{n}_i \hat{n}_j}(\tau) = R_{n_i n_j}(\tau) . \tag{3.E.2.44}$$

Using this equation and the identity expressed in eq(3.E.2.42d),

$$R_{ij}^{\Pi}(\tau) = R_{n_i n_j}(\tau) \cos(2\pi f_{c_R} \tau) + \hat{R}_{n_i n_j}(\tau) \sin(2\pi f_{c_R} \tau). \tag{3.E.2.45}$$

Similarly, using the relation $\sin(A-B) = -\sin(B-A)$, we obtain

$$R_{ij}^{QQ}(\tau) = R_{n_i n_j}(\tau) \cos(2\pi f_{c_R} \tau) + \hat{R}_{n_i n_j}(\tau) \sin(2\pi f_{c_R} \tau) \tag{3.E.2.46}$$

so that

$$\boxed{R_{ij}^{\Pi}(\tau) = R_{ij}^{QQ}(\tau).} \tag{3.E.2.47}$$

Next, we consider

$$R_{ij}^{IQ}(\tau) = E[x_{iI}(t)x_{jQ}(t-\tau)]. \tag{3.E.2.48}$$

Using eqs(3.E.2.40a) and the j channel equivalent of eq(3.E.2.40b) in (3.E.2.48), we obtain

$$\begin{aligned}
R_{ij}^{IQ}(\tau) &= E[n_i(t)\hat{n}_j(t-\tau)]\cos(2\pi f_{c_R}t)\cos[2\pi f_{c_R}(t-\tau)] \\
&\quad + E[\hat{n}_i(t)\hat{n}_j(t-\tau)]\sin(2\pi f_{c_R}t)\cos[2\pi f_{c_R}(t-\tau)] \\
&\quad - E[n_i(t)n_j(t-\tau)]\cos(2\pi f_{c_R}t)\sin[2\pi f_{c_R}(t-\tau)] \\
&\quad - E[\hat{n}_i(t)n_j(t-\tau)]\sin(2\pi f_{c_R}t)\sin[2\pi f_{c_R}(t-\tau)]
\end{aligned}
\tag{3.E.2.49a}$$

$$\begin{aligned}
&= R_{n_i\hat{n}_j}(\tau)\cos A\cos B + R_{\hat{n}_i\hat{n}_j}(\tau)\sin A\cos B \\
&\quad - R_{n_in_j}(\tau)\cos A\sin B - R_{\hat{n}_in_j}(\tau)\sin A\sin B
\end{aligned}
\tag{3.E.2.49b}$$

$$\begin{aligned}
&= R_{n_i\hat{n}_j}(\tau)\cos A\cos B + R_{n_in_j}(\tau)\sin A\cos B \\
&\quad - R_{n_in_j}(\tau)\cos A\sin B - R_{\hat{n}_in_j}(\tau)\sin A\sin B
\end{aligned}
\tag{3.E.2.49c}$$

where eq(3.E.2.44) was used in the second term above. Using eqs.(3.E.2.35d) and (3.E.2.37b) in (3.E.2.49c)

$$\begin{aligned}
R_{ij}^{QI}(\tau) &= R_{n_in_j}(\tau)[\sin A\cos B - \cos A\sin B] \\
&\quad - \hat{R}_{n_in_j}(\tau)[\cos A\cos B + \sin A\sin B]
\end{aligned}
\tag{3.E.2.50a}$$

$$= R_{n_in_j}(\tau)\sin(A - B) - \hat{R}_{n_in_j}(\tau)\cos(A - B)
\tag{3.E.2.50b}$$

$$= R_{n_in_j}(\tau)\sin(2\pi f_{c_R}\tau) - \hat{R}_{n_in_j}(\tau)\cos(2\pi f_{c_R}\tau).
\tag{3.E.2.50c}$$

Similarly,

$$R_{ij}^{IQ}(\tau) = E[x_{iQ}(t)x_{jI}(t-\tau)]
\tag{3.E.2.51a}$$

$$\begin{aligned}
&= E[\hat{n}_i(t)n_j(t-\tau)]\cos(2\pi f_{c_R}t)\cos[2\pi f_{c_R}(t-\tau)] \\
&\quad + E[\hat{n}_i(t)\hat{n}_j(t-\tau)]\cos(2\pi f_{c_R}t)\sin[2\pi f_{c_R}(t-\tau)] \\
&\quad - E[n_i(t)n_j(t-\tau)]\sin(2\pi f_{c_R}t)\cos[2\pi f_{c_R}(t-\tau)] \\
&\quad - E[n_i(t)n_j(t-\tau)]\sin(2\pi f_{c_R}t)\sin[2\pi f_{c_R}(t-\tau)]
\end{aligned}
\tag{3.E.2.51b}$$

$$\begin{aligned}
&= R_{\hat{n}_i \hat{n}_j}^{\hat{n}_i \hat{n}_j}(\tau) \cos A \cos B + R_{\hat{n}_i \hat{n}_j}^{\hat{n}_i \hat{n}_j}(\tau) \cos A \sin B \\
&\quad - R_{\hat{n}_i \hat{n}_j}^{\hat{n}_i \hat{n}_j}(\tau) \sin A \cos B - R_{\hat{n}_i \hat{n}_j}^{\hat{n}_i \hat{n}_j}(\tau) \sin A \sin B
\end{aligned} \tag{3.E.2.51c}$$

$$\begin{aligned}
&= R_{\hat{n}_i \hat{n}_j}^{\hat{n}_i \hat{n}_j}(\tau) \cos A \cos B + R_{\hat{n}_i \hat{n}_j}^{\hat{n}_i \hat{n}_j}(\tau) \cos A \sin B \\
&\quad - R_{\hat{n}_i \hat{n}_j}^{\hat{n}_i \hat{n}_j}(\tau) \sin A \cos B - R_{\hat{n}_i \hat{n}_j}^{\hat{n}_i \hat{n}_j}(\tau) \sin A \sin B
\end{aligned} \tag{3.E.2.51d}$$

$$\begin{aligned}
&= \hat{R}_{\hat{n}_i \hat{n}_j}(\tau) [\cos A \cos B + \sin A \sin B] \\
&\quad - R_{\hat{n}_i \hat{n}_j}(\tau) [\sin A \cos B - \cos A \sin B]
\end{aligned} \tag{3.E.2.51e}$$

$$= \hat{R}_{\hat{n}_i \hat{n}_j}(\tau) \cos(2\pi f_{c_R} t) - R_{\hat{n}_i \hat{n}_j}(\tau) \sin(2\pi f_{c_R} \tau) \tag{3.E.2.51f}$$

so that

$$\boxed{R_{ij}^{IQ}(\tau) = -R_{ij}^{QI}(\tau).} \tag{3.E.2.52}$$

IV. ERGODICITY OF THE CORRELATION FUNCTIONS

A. Ergodicity of the Autocorrelation Function

Ergodicity is the condition which enables time-averaged statistics of random processes to approximate those obtained by ensemble averages. This condition is often assumed in estimation and other signal processing applications. The ensemble autocorrelation function is defined as the expectation of lagged products of a given process when averaged over an ensemble of realizations. If the time-averaged autocorrelation function obtained from a single realization approximates this function, the process is called autocorrelation ergodic. In this section, we derive the functional dependence of ergodicity on the correlation parameters defined in section III.C. Consider the time-averaged estimate of the autocorrelation function expressed as[†]

$$\hat{R}_{iiT}(l, N) = \frac{1}{2N+1} \sum_{n=-N}^N x_i(n) x_i^*(n-l). \quad (4.A.1)$$

The variance of $\hat{R}_{iiT}(l, N)$ at each lag l is expressed as

$$V_{ii}(l, N) = E \left\{ [\hat{R}_{iiT}(l, N) - E[\hat{R}_{iiT}(l, N)]] [\hat{R}_{iiT}^*(l, N) - E[\hat{R}_{iiT}^*(l, N)]] \right\} \quad (4.A.2a)$$

$$= E[\hat{R}_{iiT}(l, N) \hat{R}_{iiT}^*(l, N)] - E[\hat{R}_{iiT}(l, N)] E[\hat{R}_{iiT}^*(l, N)]. \quad (4.A.2b)$$

In Appendix B, it is shown that

[†] In section VII.C, we will consider alternate forms of the estimator which are used in practice. These forms will involve the biased and unbiased time-averaged correlation function estimators using limited data samples. The final expressions for the variance of the correlation function differ [7] as will be noted (Appendix B). The motivation for using the definition of eq(4.A.1) is that it will provide mathematical convenience in the discussion to follow. In addition, we will develop expressions which will reduce to those expressed in the literature for the special case of real processes [6].

$$V_{ii}(l, N) = \frac{1}{2N+1} \sum_{k=-2N}^{2N} \left[1 - \frac{|k|}{2N+1} \right] C_{\phi\phi}(k, l) \quad (4.A.3a)$$

and for ergodicity of the autocorrelation function, we must maintain the condition

$$\lim_{N \rightarrow \infty} V_{ii}(l, N) = \lim_{N \rightarrow \infty} \frac{1}{2N+1} \sum_{k=-2N}^{2N} \left[1 - \frac{|k|}{2N+1} \right] C_{\phi\phi}(k, l) = 0 \quad (4.A.3b)$$

where

$$C_{\phi\phi}(k, l) = E \left[\{ \phi(n, l) - E[\phi(n, l)] \} \{ \phi^*(n-k, l) - E[\phi^*(n-k, l)] \} \right] \quad (4.A.4a)$$

$$= E[\phi(n, l) \phi^*(n-k, l)] - E[\phi(n, l)] E[\phi^*(n-k, l)] \\ - E[\phi(n, l)] E[\phi^*(n-k, l)] + E[\phi(n, l)] E[\phi^*(n-k, l)] \quad (4.A.4b)$$

$$= R_{\phi\phi}(k, l) - E[\phi(n, l)] E[\phi^*(n-k, l)] \quad (4.A.4c)$$

with

$$\phi(n, l) = x_i(n) x_i^*(n - l) \quad (4.A.5a)$$

and

$$R_{\phi\phi}(k, l) = E[\phi(n, l) \phi^*(n - k, l)]. \quad (4.A.5b)$$

From eq(4.A.5a)

$$E[\phi(n, l)] = R_{ii}(l) \quad (4.A.6a)$$

and

$$E[\phi^*(n-k, l)] = R_{ii}^*(l) \quad (4.A.6b)$$

so that from eq(4.A.4c)

$$C_{\phi\phi}(k, l) = R_{\phi\phi}(k, l) - |R_{ii}(l)|^2. \quad (4.A.7)$$

And so, eq(4.A.3a) becomes

$$V_{ii}(l, N) = \frac{1}{2N+1} \sum_{k=-2N}^{2N} \left[1 - \frac{|k|}{2N+1} \right] [R_{\phi\phi}(k, l) - |R_{ii}(l)|^2] \quad (4.A.8)$$

We now consider,

$$R_{\phi\phi}(k,l) = E[\phi(n,l)\phi^*(n-k,l)] \quad (4.A.9a)$$

$$= E[x_i(n)x_i^*(n-l)x_i^*(n-k)x_i(n-l-k)]. \quad (4.A.9b)$$

For processes with zero-mean, jointly stationary Gaussian quadrature components $x_{iI}(n)$ and $x_{iQ}(n)$, eq(4.A.9b) can be expressed as [see Appendix H]

$$\begin{aligned} R_{\phi\phi}(k,l) &= E[x_i(n)x_i^*(n-l)]E[x_i^*(n-k)x_i(n-l-k)] \\ &\quad + E[x_i(n)x_i^*(n-k)]E[x_i^*(n-l)x_i(n-l-k)] \\ &\quad + E[x_i(n)x_i(n-l-k)]E[x_i^*(n-l)x_i^*(n-k)]. \end{aligned} \quad (4.A.10a)$$

$$= R_{ii}(l)R_{ii}^*(l) + R_{ii}(k)R_{ii}^*(k) + F_{ii}(l,k) \quad (4.A.10b)$$

$$= |R_{ii}(l)|^2 + |R_{ii}(k)|^2 + F_{ii}(l,k) \quad (4.A.10c)$$

where

$$F_{ii}(l,k) = E[x_i(n)x_i(n-l-k)]E[x_i^*(n-l)x_i^*(n-k)]. \quad (4.A.11)$$

Using eq(4.A.10c) in (4.A.8), we have

$$V_{ii}(l,N) = \frac{1}{2N+1} \sum_{k=-2N}^{2N} \left[1 - \frac{|k|}{2N+1} \right] [|R_{ii}(k)|^2 + F_{ii}(l,k)]. \quad (4.A.12)$$

We note that the functional dependence of $V_{ii}(l,N)$ on l is due to the function $F_{ii}(l,k)$. In Appendix C, we show that only the real part of $F_{ii}(l,k)$ contributes to the summation in eq(4.A.12), so that

$$V_{ii}(l, N) = \frac{1}{2N+1} \sum_{k=-2N}^{2N} \left[1 - \frac{|k|}{2N+1} \right] [|R_{ii}(k)|^2 + \text{Re}\{F_{ii}(l, k)\}] \quad (4.A.13a)$$

and the ergodicity condition becomes

$$\lim_{N \rightarrow \infty} V_{ii}(l, N) = \lim_{N \rightarrow \infty} \frac{1}{2N+1} \sum_{k=-2N}^{2N} \left[1 - \frac{|k|}{2N+1} \right] [|R_{ii}(k)|^2 + \text{Re}\{F_{ii}(l, k)\}] = 0. \quad (4.A.13b)$$

For real processes

$$F_{ii}(l, k) = E[x_i(n)x_i(n-l-k)]E[x_i(n-l)x_i(n-k)] \quad (4.A.14a)$$

$$= R_{ii}(k+l)R_{ii}(k-l) \quad (4.A.14b)$$

$$= R_{ii}(l+k)R_{ii}(l-k) \quad (4.A.14c)$$

and eq(4.A.13b) reduces to the discrete time form of eq(11-54) in [6]. For a specific value of N , the variance expressed by the LHS of eq(4.A.13a) can now be written as

$$V_{ii}(l, N) = E_{ii}(N) + L_{ii}(l, N) \quad (4.A.15)$$

where

$$E_{ii}(N) = \frac{1}{2N+1} \sum_{k=-2N}^{2N} \left[1 - \frac{|k|}{2N+1} \right] |R_{ii}(k)|^2. \quad (4.A.16a)$$

and

$$L_{ii}(l, N) = \frac{1}{2N+1} \sum_{k=-2N}^{2N} \left[1 - \frac{|k|}{2N+1} \right] \text{Re}\{F_{ii}(l, k)\}. \quad (4.A.16b)$$

In Appendix C, it is also shown that

$$\text{Re}\{F_{ii}(l, k)\} = [R_{C_{ii}}(l+k)R_{C_{ii}}(l-k) + R_{D_{ii}}(l+k)R_{D_{ii}}(l-k)] \quad (4.A.17)$$

where

$$R_{C_{ii}}(\alpha) = R_{ii}^{\Pi}(\alpha) - R_{ii}^{QQ}(\alpha) \quad (4.A.18a)$$

and

$$R_{D_{ii}}(\alpha) = R_{ii}^{QI}(\alpha) + R_{ii}^{IQ}(\alpha). \quad (4.A.18b)$$

It is also noted that if the associated bandpass process for this baseband process is stationary and narrowband, then eqs(3.E.2.23) and (3.E.2.28) of section III.E.2.a hold, and $F_{ii}(l,k)$ is zero. And so, the expression for $V_{ii}(l,N)$ becomes independent of l and reduces to

$$V_{ii}(l,N) = E_{ii}(N) = \frac{1}{2N+1} \sum_{k=-2N}^{2N} \left[1 - \frac{|k|}{2N+1} \right] |R_{ii}(k)|^2. \quad (4.A.19)$$

Using the functional form for the exponential shaped autocorrelation function, we have

$$R_{ii}(k) = \sigma_{ii}^2 (\lambda_{ii})^{|k|} \exp[j\theta_{ii}(k)] \quad (4.A.20)$$

so that

$$|R_{ii}(k)|^2 = \sigma_{ii}^4 (\lambda_{ii})^{2|k|}. \quad (4.A.21)$$

Using eq(4.A.21) in (4.A.19), the autocorrelation ergodic property holds provided

$$\lim_{N \rightarrow \infty} E_{ii}(N) = \lim_{N \rightarrow \infty} \frac{1}{2N+1} \sum_{k=-2N}^{2N} \left[1 - \frac{|k|}{2N+1} \right] \sigma_{ii}^4 (\lambda_{ii})^{2|k|} = 0 \quad (4.A.22)$$

is true where $0 \leq \lambda_{ii} < 1$. Thus, the form of eq(4.A.20) enables us to express the variance as a function of λ_{ii} and σ_{ii}^2 . We now consider two limiting values for λ_{ii} using eq(4.A.22).

CASE 1 High Temporal Correlation and Negligable $F_{ij}(l,k)$

When $\lambda_{ij} = 1$, the LHS of eq(4.A.22) reduces to

$$\lim_{N \rightarrow \infty} E_{ij}(N) = \lim_{N \rightarrow \infty} \frac{1}{2N+1} \sum_{k=-2N}^{2N} \left[1 - \frac{|k|}{2N+1} \right] \sigma_{ij}^4 \quad (4.A.23a)$$

$$= \lim_{N \rightarrow \infty} \frac{\sigma_{ij}^4}{2N+1} \sum_{k=-2N}^{2N} (1) - \lim_{N \rightarrow \infty} \frac{\sigma_{ij}^4}{2N+1} \sum_{k=-2N}^{2N} \frac{|k|}{2N+1} \quad (4.A.23b)$$

$$= \lim_{N \rightarrow \infty} \left[\frac{4N+1}{2N+1} \right] \sigma_{ij}^4 - \lim_{N \rightarrow \infty} \frac{\sigma_{ij}^4}{(2N+1)^2} \sum_{k=-2N}^{2N} |k| \quad (4.A.23c)$$

$$= 2 \sigma_{ij}^4 - \lim_{N \rightarrow \infty} \frac{2N(2N+1)}{(2N+1)^2} \sigma_{ij}^4 = \sigma_{ij}^4 \neq 0. \quad (4.A.23d)$$

Eq(4.A.23d) indicates that for total temporal correlation (ie., $\lambda_{ij}=1$), the process is not ergodic.

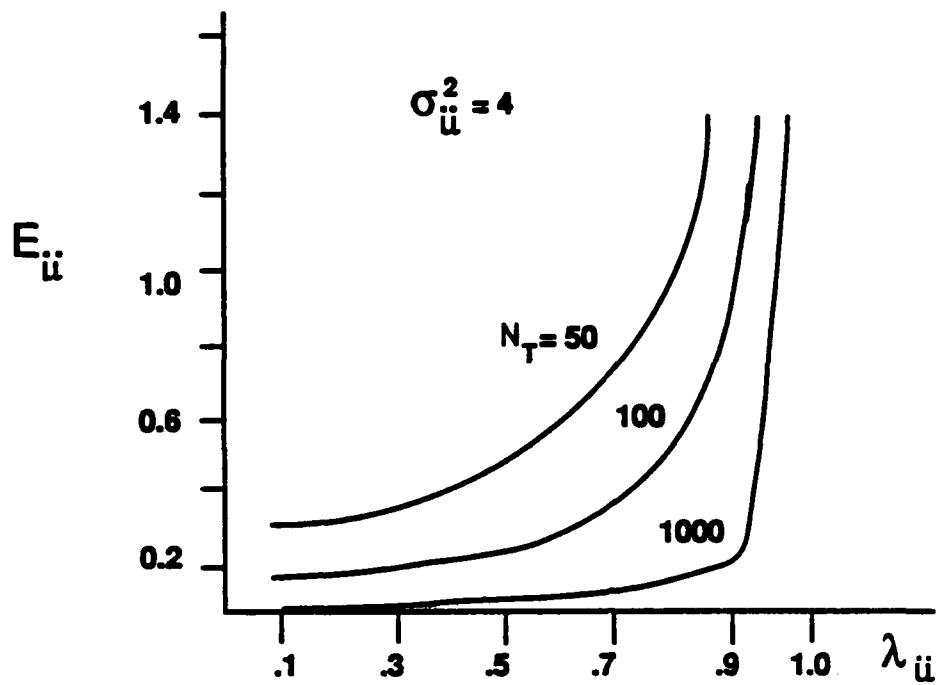
CASE 2 Low Temporal Correlation and Negligable $F_{ij}(l,k)$

When $\lambda_{ij} \approx 0$, non-negligeable terms occur only at $k = 0$, so that eq(4.A.19) reduces to

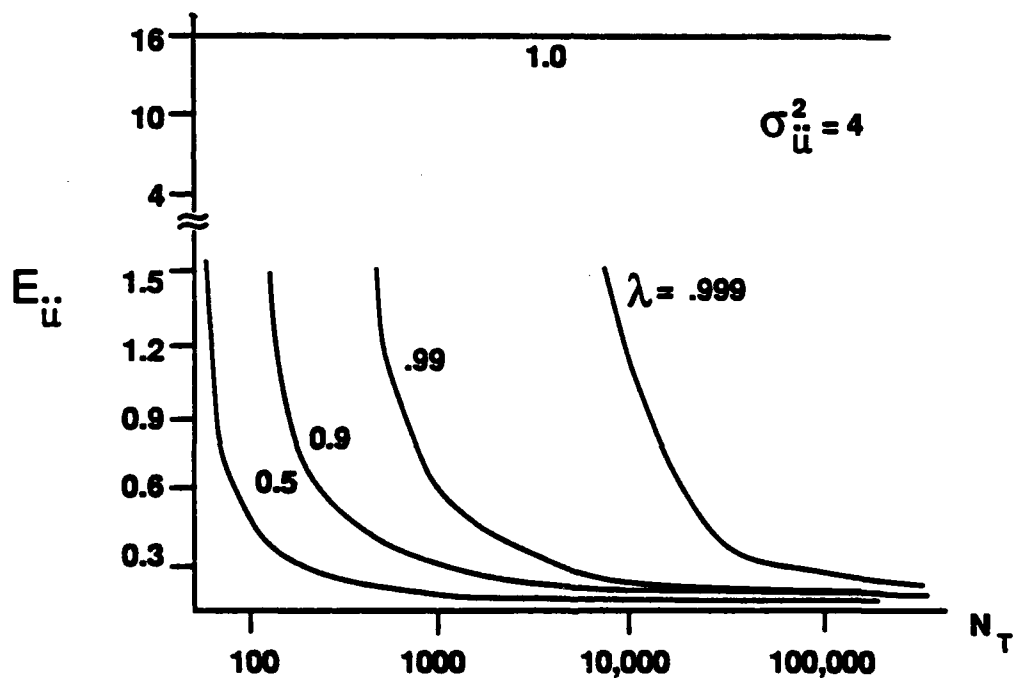
$$\lim_{N \rightarrow \infty} E_{ij}(N) = \lim_{N \rightarrow \infty} \left[\frac{1}{2N+1} \right] \sigma_{ij}^4 = 0. \quad (4.A.24)$$

Thus, ergodicity holds and time averages may provide good results for sufficiently high values of N .

In Fig 4.A.1a, we plot $E_{ij}(N_T)$ expressed in eq(4.A.22) as a function of λ_{ij} where $0 \leq \lambda_{ij} \leq 1$ for the total number of sample observations $N_T=2N+1$ ranging



a.



b.

Fig 4.A.1 Variance of the time-averaged exponentially shaped autocorrelation function plotted versus a.) λ_{ij} and b.) N_T for the case where $F_{ij}(l,k) \approx 0$.

from 100 to 10,000. In Fig 4.A.1b, we plot $E_{ij}(N_T)$ as a function of N_T for specific values of λ_{ij} . We again emphasize that in these cases, that $F_{ij}(l,k)$ is negligible. For $F_{ij}(l,k) \neq 0$, $V_{ij}(\bullet)$ is a function of l . The l dependence also occurs when estimating with limited data (see Section VII). Fig.4.A.1 provides a measure of the variance of the time-averaged autocorrelation function in terms of the temporal correlation for specific sample integration sizes. Specifically, Fig 4.A.1b provides two important features. First, it reveals the convergence limit of $E_{ij}(N)$ as N approaches large values. Second, it provides a performance measure which indicates the required sample size to obtain a specific value for the variance of the autocorrelation function. As this figure shows, as λ_{ij} approaches unity (ie., high temporal correlation), the sample size requirement increases significantly. In section VII.C, we will consider $E_{ij}(N)$ using autoregressive processes. For these processes, we utilize the autocorrelation function for AR processes in eq(4.A.19).

Finally, we note that for stationary processes with $\lambda_{ij} \neq 1$, there exists a value of $N_0(\lambda_{ij})$ such that for $N_T > N_0(\lambda_{ij})$ ergodicity of the autocorrelation function approximately holds; ie., for $\lambda_{ij} < 1$, there is a number of required sample observations $N_0(\lambda_{ij})$ such that for

$$N_T > N_0(\lambda_{ij}) \quad (4.A.25a)$$

there is an ϵ such that

$$V_{ij}(l) < \epsilon \quad (4.A.25b)$$

where N_T is the total number of sample observations and ϵ is arbitrarily small. The ergodicity condition results since $V_{ij}(l)$ is monotonically decreasing. However, as noted above, for values of λ_{ij} close to unity, N_T may be extremely large in order to reduce the variance to a required value. Finally, for $\lambda_{ij}=1$, ergodicity no longer holds.

B. Ergodicity of the Cross-Correlation Function

For the cross-correlation function, lagged products between two processes are averaged over an ensemble of realizations. In this case, we consider wide-sense jointly stationary processes $x_i(n)$ and $x_j(n)$ such that

$$\beta(n,l) = x_i(n) x_j^*(n-l). \quad (4.B.1)$$

The autocorrelation function for $\beta(n)$ is expressed as

$$R_{\beta\beta}(k,l) = E[\beta(n)\beta^*(n-k)]. \quad (4.B.2)$$

From eq(4.B.1)

$$E[\beta(n,l)] = R_{ij}(l) \quad (4.B.3a)$$

$$E[\beta^*(n-k,l)] = R_{ij}^*(l). \quad (4.B.3b)$$

Using the same form as eq(4.A.4c)

$$C_{\beta\beta}(k,l) = R_{\beta\beta}(k,l) - E[\beta(n,l)] E[\beta^*(n-k,l)] \quad (4.B.4a)$$

$$= R_{\beta\beta}(k,l) - |R_{ij}(l)|^2. \quad (4.B.4b)$$

The variance of the time-averaged cross-correlation function is therefore expressed as

$$V_{ij}(l,N) = \frac{1}{2N+1} \sum_{k=-2N}^{2N} \left[1 - \frac{|k|}{2N+1} \right] C_{\beta\beta}(k,l). \quad (4.B.5)$$

For ergodicity of the cross-correlation function, we must maintain the condition

$$\lim_{N \rightarrow \infty} V_{ij}(l,N) = \lim_{N \rightarrow \infty} \frac{1}{2N+1} \sum_{k=-2N}^{2N} \left[1 - \frac{|k|}{2N+1} \right] C_{\beta\beta}(k,l) = 0. \quad (4.B.6)$$

Using eq(4.B.4b) in (4.B.5), we have

$$V_{ij}(l, N) = \frac{1}{2N+1} \sum_{k=-2N}^{2N} \left[1 - \frac{|k|}{2N+1} \right] [R_{\beta\beta}(k, l) - |R_{ij}(l)|^2]. \quad (4.B.7)$$

We now consider

$$R_{\beta\beta}(k, l) = E[\beta(n, l) \beta^*(n - k, l)] \quad (4.B.8a)$$

$$= E[x_i(n) x_j^*(n - l) x_i^*(n - k) x_j(n - l - k)] \quad (4.B.8b)$$

so that eq(4.B.5) becomes

$$V_{ij}(l, N) = \frac{1}{2N+1} \sum_{k=-2N}^{2N} \left[1 - \frac{|k|}{2N+1} \right] \cdot \{ E[x_i(n) x_j^*(n - l) x_i^*(n - k) x_j(n - l - k)] - |R_{ij}(l)|^2 \}. \quad (4.B.9)$$

For processes with zero-mean, jointly stationary, Gaussian quadrature components, eq(4.B.8b) can be expressed as (see Appendix H)

$$\begin{aligned} R_{\beta\beta}(k, l) &= E[x_i(n) x_j^*(n - l)] E[x_i^*(n - k) x_j(n - l - k)] \\ &\quad + E[x_i(n) x_i^*(n - k)] E[x_j^*(n - l) x_j(n - l - k)] \\ &\quad + E[x_i(n) x_j(n - l - k)] E[x_j^*(n - l) x_i^*(n - k)] \end{aligned} \quad (4.B.10a)$$

$$= R_{ij}(l) R_{ij}^*(l) + R_{ii}(k) R_{jj}^*(k) + F_{ij}(l, k) \quad (4.B.10b)$$

$$= |R_{ij}(l)|^2 + R_{ii}(k) R_{jj}^*(k) + F_{ij}(l, k) \quad (4.B.10c)$$

where

$$F_{ij}(l,k) = E[x_i(n)x_j(n-l-k)]E[x_j^*(n-l)x_i^*(n-k)]. \quad (4.B.11)$$

Using eq(4.B.10c) in (4.B.7), we obtain

$$V_{ij}(l,N) = \frac{1}{2N+1} \sum_{k=-2N}^{2N} \left[1 - \frac{|k|}{2N+1} \right] [R_{ii}(k)R_{jj}^*(k) + F_{ij}(l,k)]. \quad (4.B.12)$$

In Appendix D, we show that the summation in eq(4.B.12) over positive and negative values cancels the imaginary terms in $R_{ii}(k)R_{jj}^*(k)$ and $F_{ij}(l,k)$, so

$$V_{ij}(l,N) = \frac{1}{2N+1} \sum_{k=-2N}^{2N} \left[1 - \frac{|k|}{2N+1} \right] \text{Re}[R_{ii}(k)R_{jj}^*(k) + F_{ij}(l,k)]. \quad (4.B.13)$$

We note that the term $\text{Re}[F_{ij}(l,k)]$ will contribute a dependence of $V_{ij}(l,N)$ upon cross-correlation terms such as $|p_{ij}|$. The ergodicity condition expressed by eq(4.B.6) now reduces to

$$\lim_{N \rightarrow \infty} V_{ij}(l,N) = \lim_{N \rightarrow \infty} \frac{1}{2N+1} \sum_{k=-2N}^{2N} \left[1 - \frac{|k|}{2N+1} \right] \text{Re}[R_{ii}(k)R_{jj}^*(k) + F_{ij}(l,k)] = 0. \quad (4.B.14)$$

In Appendix D, it is also noted that for each of these real terms, their values at positive k equals those at negative k , so that

$$V_{ij}(l,N) = \frac{1}{2N+1} \sum_{k=0}^{2N} \left[1 - \frac{|k|}{2N+1} \right] \{ 2\text{Re}[R_{ii}(k)R_{jj}^*(k) + F_{ij}(l,k)] - [R_{ii}(0)R_{jj}(0) + F_{ij}(l,0)] \}. \quad (4.B.15)$$

The term at $k=0$ is subtracted so that it is not counted twice. Finally, it is also shown (see Appendix D) that if the corresponding bandpass processes are jointly stationary and narrowband, then $F_{ij}(l,k)=0$ so that

$$V_{ij}(l,N) = E_{ij}(N) \quad (4.B.16a)$$

where

$$E_{ij}(N) = \frac{1}{2N+1} \sum_{k=-2N}^{2N} \left[1 - \frac{|k|}{2N+1} \right] \text{Re}[R_{ii}(k)R_{jj}^*(k)]. \quad (4.B.16b)$$

We now consider the functional dependence of eq(4.B.16) on the correlation parameters.

CASE 1 High Temporal Correlation and Negligable $F_{ij}(l,k)$

Using the Gaussian shaped functional form of eq(3.C.13a) for the autocorrelation functions, eq(4.B.16b) becomes

$$V_{ij}(l,N) = E_{ij}(N) = \frac{\sigma_{ii}^2 \sigma_{jj}^2}{2N+1} \sum_{k=-2N}^{2N} \left[1 - \frac{|k|}{2N+1} \right] (\lambda_{ii})^{k^2} (\lambda_{jj})^{k^2} \cdot \cos [\theta_{ii}(k) - \theta_{jj}(k)] \quad (4.B.17)$$

For high temporal correlation on the i and j processes, $\lambda_{ii} \approx \lambda_{jj} \approx 1$. In this case, large values of N are required to reduce $V_{ij}(l,N)$. For total temporal correlation on both channels (ie., $\lambda_{ii}=\lambda_{jj}=1$) and real correlation functions [so that $\theta_{ii}(k)=\theta_{jj}(k)=0$ and the spectra are even], the LHS of eq(4.B.14) simplifies to

$$\lim_{N \rightarrow \infty} E_{ij}(N) = \lim_{N \rightarrow \infty} \frac{\sigma_{ii}^2 \sigma_{jj}^2}{2N+1} \sum_{k=-2N}^{2N} \left[1 - \frac{|k|}{2N+1} \right] (\lambda_{ii})^{k^2} (\lambda_{jj})^{k^2} \quad (4.B.18a)$$

$$= \lim_{N \rightarrow \infty} \frac{\sigma_{ii}^2 \sigma_{jj}^2}{2N+1} \sum_{k=-2N}^{2N} (1) - \lim_{N \rightarrow \infty} \frac{\sigma_{ii}^2 \sigma_{jj}^2}{2N+1} \sum_{k=-2N}^{2N} \frac{|k|}{2N+1} \quad (4.B.18b)$$

$$= \lim_{N \rightarrow \infty} \left[\frac{4N+1}{2N+1} \right] \sigma_{ii}^2 \sigma_{jj}^2 - \lim_{N \rightarrow \infty} \left[\frac{2N(2N+1)}{(2N+1)^2} \right] \sigma_{ii}^2 \sigma_{jj}^2 \quad (4.B.18c)$$

$$= 2\sigma_{ii}^2 \sigma_{jj}^2 - \sigma_{ii}^2 \sigma_{jj}^2 = \sigma_{ii}^2 \sigma_{jj}^2 \neq 0. \quad (4.B.18d)$$

Eq(4.B.18d) indicates that in the case of total temporal correlation, the cross-correlation function does not maintain the ergodicity condition.

CASE 2 Low Temporal Correlation and Negligable $F_{ij}(l,k)$

In this case, we consider processes i and j with low temporal correlation so that $\lambda_{ii} = \lambda_{jj} \approx 0$. If $F_{ij}(l,k) \approx 0$, eq(4.B.16b) applies. Again, considering real, Gaussian correlation functions, we have

$$\lim_{N \rightarrow \infty} E_{ij}(N) = \lim_{N \rightarrow \infty} \frac{\sigma_{ii}^2 \sigma_{jj}^2}{2N+1} \sum_{k=-2N}^{2N} \left[1 - \frac{|k|}{2N+1} \right] (\lambda_{ii})^{k^2} (\lambda_{jj})^{k^2}. \quad (4.B.19)$$

For small λ_{ii} and λ_{jj} , only the $k = 0$ term is significant so that

$$\lim_{N \rightarrow \infty} E_{ij}(N) = \lim_{N \rightarrow \infty} \frac{\sigma_{ii}^2 \sigma_{jj}^2}{2N+1} = 0. \quad (4.B.20)$$

Ergodicity holds for this case so that time averages may provide good results for sufficiently high values of N. This condition will also be maintained provided either λ_{ii} or λ_{jj} is sufficiently small. However, larger values of N will be required to reduce $E_{ij}(N)$ to a specified value.

CASE 3 Non-Negligable $F_{ij}(l,k)$

In this case, $\text{Re}[F_{ij}(l,k)]$ contributes to $V_{ij}(l,N)$ in eq(4.B.13). Eq(D.8b) in Appendix D expresses this function in terms of the correlation functions of the quadrature terms. In general, these terms describe the dependence of $V_{ij}(\bullet)$ upon lag l as well as the cross-correlation between the ith and jth processes.

V. MULTICHANNEL AUTOREGRESSIVE PROCESS MODELS

A. DEFINITION OF THE AR PROCESS

In this analysis, the multichannel observation processes obtained under hypotheses H_i with $i = 0, 1$ are assumed to be generated by multichannel autoregressive processes. The multichannel $J \times 1$ vector process $\underline{x}(n|H_i)$ with $i=0,1$ is expressed as

$$\underline{x}(n|H_i) = - \sum_{k=1}^{M_i} A_{M_i}^H(k|H_i) \underline{x}(n-k) + \underline{u}(n|H_i) \quad i = 0,1 \quad (5.1)$$

where $A_{M_i}^H(k|H_i)$ is the k th $J \times J$ matrix coefficient for an AR process of model order M_i . We note that it is expressed in terms of the Hermitian operation for notational convenience, but is not treated here as a Hermitian matrix. The vector $\underline{u}(n)$ is a $J \times 1$ white noise driving vector which, in general, has an arbitrary correlation across the J channels so that

$$E[\underline{u}(n)\underline{u}^H(n-l)] = \begin{cases} [0] & l \neq 0 \\ R_{uu}(0) \equiv [\Sigma_f] & l = 0. \end{cases} \quad (5.2)$$

$R_{uu}(0) \equiv [\Sigma_f]$ is the $J \times J$ covariance matrix of the vector process $\underline{u}(n)$ and may have off-diagonal components. Since $\underline{u}(n)$ is uncorrelated in time, but retains an arbitrary correlation across channels, then with wide-sense joint stationarity of the channel processes assumed, we can consider

$$\underline{u}(n) = C \underline{v}(n) \quad (5.3)$$

where the $J \times J$ matrix C is a constant matrix. This matrix gives rise to the channel correlation on $\underline{u}(n)$. The vector $\underline{v}(n)$ is a Gaussian white noise vector uncorrelated in time and across channels such that

$$E[\underline{v}(n)\underline{v}^H(n-l)] = \begin{cases} [0] & l \neq 0 \\ D_v & l = 0. \end{cases} \quad (5.4)$$

The elements of the diagonal matrix D_v are the variance terms associated with the white noise driving term on each channel. And so, from eq (5.3) we can obtain the zero-lag correlation matrix (assuming wide-sense stationarity)

$$R_{uu}(0) = E [\underline{u}(n) \underline{u}^H(n)] \equiv [\Sigma_f] \quad (5.5a)$$

$$= E [C_Y(n) \underline{y}^H(n) C^H] \quad (5.5b)$$

$$= CD_v C^H \quad (5.5c)$$

We could assume unit variance on all elements of D_v without loss of generality so that $D_v = I$. The significance of this discussion is that the correlation matrix $R_{uu}(0)$ is a constant matrix associated with the white noise driving term $\underline{u}(n)$. The correlation between the channel elements of $\underline{u}(n)$ gives rise to the off-diagonal terms in $R_{uu}(0)$. Since $R_{uu}(0)$ expressed in eq (5.5) is Hermitian†, positive semi-definite, we could also perform an LDL^H decomposition such that

$$R_{uu}(0) = L_u D_u L_u^H \quad (5.6)$$

where L_u is unit diagonal lower triangular. Solving for D_u , we obtain

$$D_u = L_u^{-1} R_{uu}(0) (L_u^{-1})^H \quad (5.7a)$$

$$= E [L_u^{-1} \underline{u}(n) \underline{u}^H(n) (L_u^{-1})^H] \quad (5.7b)$$

$$= E [\underline{z}(n) \underline{z}^H(n)] \quad (5.7c)$$

where

$$\underline{z}(n) = L_u^{-1} \underline{u}(n) \quad (5.8)$$

so that $\underline{z}(n)$ is a $J \times 1$ vector containing uncorrelated elements. It represents an underlying process of the multichannel AR process which can be viewed as a "spatially-causal" white noise driving term. Since L_u^{-1} is also lower triangular unit diagonal, it is invertible so that from eq (5.8)

† It is noted that in general the correlation matrix $R_{uu}(l)$ is not Hermitian for $l \neq 0$.

$$\underline{u}(n) = L_u \underline{z}(n) \quad (5.9)$$

Eq (5.9) indicates that $\underline{u}(n)$, originally defined in eq (5.3), could identically be generated by the $\underline{z}(n)$ process through the transformation matrix L_u ; i.e. eq (5.1) can be written in the equivalent form

$$\underline{x}(n|H_i) = - \sum_{k=1}^{M_i} A_{M_i}^H(k|H_i) \underline{x}(n-k) + L_u(H_i) \underline{z}(n|H_i) \quad i = 0,1 \quad (5.10)$$

where $L_u(H_i)$ denotes the specific matrix L_u under hypothesis H_i . In [1], a two stage multichannel prediction error filter is considered which uses estimates of the $A_{M_i}^H(k|H_i)$ coefficients to obtain an approximation of $\underline{u}(n)$ in the first stage and an estimate of L_u^{-1} to obtain an approximation of the temporally and spatially uncorrelated process $\underline{z}(n|H_i)$.

B. THE YULE-WALKER EQUATION

The relationship between the matrix coefficients $A_M^H(k)$, the covariance matrix $[\Sigma_f]$ of the forward AR driving noise vector and the known correlation matrix R_{xx} from eq(2.3) can be expressed [2] as

$$\Delta_M^H[\tilde{R}_{xx}] = \{[\Sigma_f] [0] \dots [0]\} \quad (5.11)$$

where

$$\Delta_M^H = [I \ A_M^H(1) \ A_M^H(2) \ \dots \ A_M^H(M)]. \quad (5.12a)$$

and

$$[\Sigma_f] = E[\underline{u}(n)\underline{u}^H(n)] \quad (5.12b)$$

The matrix $[\tilde{R}_{xx}]$ is the reversed order correlation matrix of $[R_{xx}]$; i.e., the correlation matrix obtained with the time order of the vector $\underline{x}_{1,N}$ from eq(2.4b) reversed. The corresponding equations for the stationary, backward AR process is expressed as

$$B_M^H[\tilde{R}_{xx}] = \{[0] \dots [0] [\Sigma_b]^H\} \quad (5.13)$$

where

$$\mathbf{B}_M^H = [\mathbf{B}_M^H(M) \dots \mathbf{B}_M^H(1) \mathbf{I}] \quad (5.14)$$

and $[\Sigma_b]$ is the covariance matrix of the backward AR driving noise vector.

Eqs(5.11) and (5.13) are the augmented forms of the multichannel Yule-Walker equations.

VI. PROCESS SYNTHESIS

A. General Procedure

In this section, we discuss the synthesis procedure used to generate wide-sense stationary, multichannel autoregressive processes with Gaussian statistics. The $J \times 1$ vectors $\underline{s}(n)$ and $\underline{c}(n)$ defined in eq(2.1) are generated as distinct, multichannel AR processes for the signal and non-white noise, respectively, although each channel will be an ARMA process [16,17,10]. They are controlled individually using the scheme shown in Fig 6.A.1 which is similar to that suggested in [2] for scalar process synthesis. In this paper, the synthesis procedure is generalized to consider multichannel vector processes in which we are able to control the variance and temporal correlation on each channel, the cross-channel correlation as well as the signal-to-noise (S/N) and clutter-to-noise (C/N) ratios.

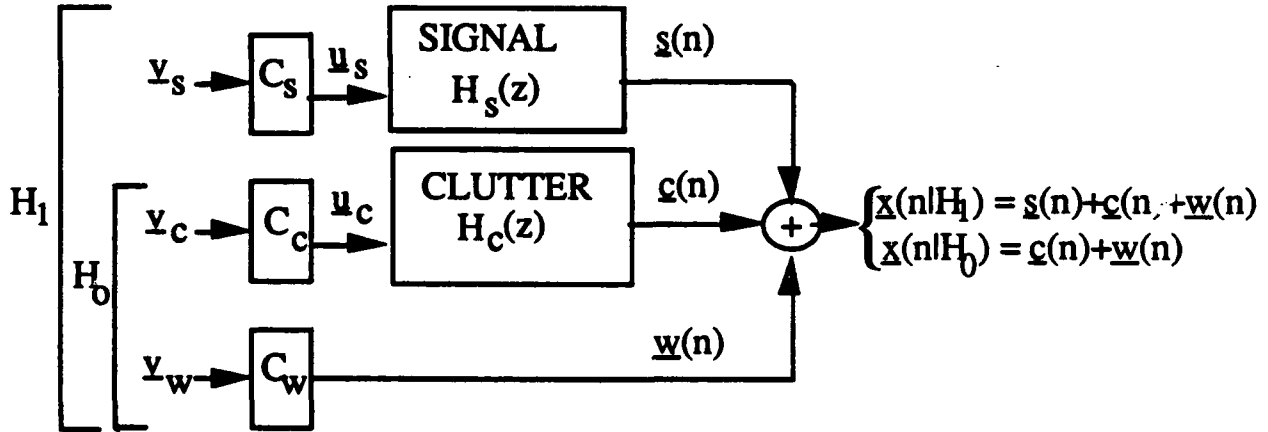


Figure 6.A.1

In section III.C, we discussed a method to shape the magnitude and phase of correlation functions with various functional forms. Once these correlation functions have been determined to obtain a desired spectral shape, the Yule-Walker equation presented in section IV can be used to determine the AR coefficients for the process with a model order chosen to fit the desired spectrum

within certain tolerance specifications. In the procedure used here, correlation functions for the signal and non-white noise are specified separately using $R_{s_{ij}}(l)$ and $R_{c_{ij}}(l)$, respectively. The autoregressive PSD which would result from these coefficients provides a fit to the desired spectrum. Alternatively, when these coefficients are used in the AR equation, we are able to generate processes which provide a fit to the desired spectrum in a MMSE sense. Specifically, the following procedure is used to generate the AR time sequenced values:

- (1) the desired shapes of the autocorrelation and cross-correlation values are obtained using the $f(\cdot)$ functions by the methods of section III.C.
- (2) the order of the AR process (for synthesis) is selected based upon a specified tolerance for fitting the desired spectrum.
- (3) the values of $R_{s_{ij}}(l)$ and $R_{c_{ij}}(l)$ form the signal and clutter correlation matrix elements designated as R_{ss} and R_{cc} , respectively.
- (4) the multichannel Yule-Walker equations are solved using the Levinson-Wiggins-Robinson recursion [15] to determine the matrix coefficients $A_g^H(k)$ and $[\Sigma_f]_g^H$ for $k = 1, 2, \dots, M_g$; i.e.,

$$\Delta_g^H [\tilde{R}_{gg}] = \{[\Sigma_f]_g^H [0] \dots [0]\} \quad g = s, c \quad (6.A.1)$$

where

$$\Delta_g^H = [I \ A_g^H(1) \ A_g^H(2) \dots A_g^H(M_g)] \quad g = s, c \quad (6.A.2)$$

$$\tilde{R}_{gg} = E[\underline{g}_{n, n-M_g}^H \underline{g}_{n, n-M_g}] \quad g = s, c \quad (6.A.3a)$$

$$\underline{g}_{n, n-M_g}^T = [g^T(n) \ g^T(n-1) \dots g^T(n-M_g)] \quad g = s, c \quad (6.A.3b)$$

$$[\Sigma_f]_g = E[\underline{u}_g(n) \underline{u}_g^H(n)] = [\Sigma_f]_g^H \quad g = s, c \quad (6.A.4)$$

$$\underline{u}_g^T(n) = [u_1^g(n) \ u_2^g(n) \dots u_J^g(n)] \quad g = s, c \quad (6.A.5)$$

(5) the values of $A_g^H(k)$ are now used in the generation of $\underline{g}(n)$ and $\underline{c}(n)$ via the equation

$$\underline{g}(n) = - \sum_{k=1}^{M_g} A_g^H(k) \underline{g}(n-k) + \underline{u}_g(n) \quad g = s, c \quad (6.A.6)$$

where M_g is the order of the signal model, $A_g^H(k)$ is the matrix coefficient of the process $\underline{g}(n)$ and $\underline{u}_g(n)$ is a white noise driving vector with covariance matrix $[\Sigma_f]_g$. The vectors $\underline{u}_g(n)$ and $\underline{w}(n)$ are generated using

$$\underline{u}_g(n) = C_g \underline{v}_g(n) \quad g = s, c \quad (6.A.7a)$$

and

$$\underline{w}(n) = C_w \underline{v}_w(n) \quad (6.A.7b)$$

where $\underline{v}_g(n)$ $g=s, c$ and $\underline{v}_w(n)$ are white noise vectors with unit variance on each channel. Using eqs(6.A.7), we obtain

$$[\Sigma_f]_g = E[\underline{u}_g(n) \underline{u}_g^H(n)] = E[C_g \underline{v}_g(n) \underline{v}_g^H(n) C_g^H] \quad g = s, c \quad (6.A.8a)$$

and

$$R_{ww}(0) = E[\underline{w}(n) \underline{w}^H(n)] = E[C_w \underline{v}_w(n) \underline{v}_w^H(n) C_w^H]. \quad (6.A.8b)$$

Using

$$E[\underline{v}_g(n) \underline{v}_g^H(n)] = E[\underline{v}_w(n) \underline{v}_w^H(n)] = I \quad (6.A.9)$$

where I is a $J \times J$ identity matrix, eqs(6.A.8) can be written as

$$[\Sigma_f]_g = C_g E[\underline{v}_g(n) \underline{v}_g^H(n)] C_g^H = C_g C_g^H \quad g = s, c \quad (6.A.10a)$$

and

$$R_{ww}(0) = C_w E[\underline{v}_w(n) \underline{v}_w^H(n)] C_w^H = C_w C_w^H \quad (6.A.10b)$$

Eqs(6.A.10) indicate that C_g and C_w can be obtained by the Cholesky decomposition of $[\Sigma_f]_g$ and $R_{ww}(0)$, respectively. The vectors $\underline{u}_s(n)$, $\underline{u}_c(n)$ and $\underline{w}(n)$ in Fig 6.A.1 are therefore controlled to be zero-mean, Gaussian white noise vectors uncorrelated in time but with an arbitrary correlation across channels; ie.,

$$E[\underline{u}_g(n)\underline{u}_g^H(n-l)] = \begin{cases} [0] & l \neq 0 \\ R_{uu}^g(0) \equiv [\Sigma_f]_g & l = 0 \end{cases} \quad g = s, c \quad (6.A.11)$$

$$E[\underline{w}(n)\underline{w}^H(n-l)] = \begin{cases} [0] & l \neq 0 \\ R_{ww}(0) & l = 0. \end{cases} \quad (6.A.12)$$

In general, the matrices $[\Sigma_f]_g$ and $R_{ww}(0)$ have off-diagonal components. The functions $H_s(z)$ and $H_c(z)$ are the model filter transfer functions for the synthesis of the signal and clutter processes, respectively.

EXAMPLE

In this example, we consider the synthesis of a real, single channel AR process of order two using real, Gaussian shaped correlation functions. The correlation function is therefore expressed as

$$R^s(l) = \sigma_s^2 (\lambda_s)^{|l|}. \quad (6.A.13)$$

The Yule-Walker equation for this case is

$$\begin{bmatrix} R(0) & R(1) & R(2) \\ R(-1) & R(0) & R(1) \\ R(-2) & R(-1) & R(0) \end{bmatrix} \begin{bmatrix} 1 \\ a(1) \\ a(2) \end{bmatrix} = \begin{bmatrix} \sigma_u^2 \\ 0 \\ 0 \end{bmatrix} \quad (6.A.14)$$

where σ_u^2 is the variance of the white noise driving term of the associated AR process. Using the functional form of eq(6.A.13) in (6.A.14) and solving for the coefficients, we have (dropping the script s notation)

$$a(1) = \frac{R(2)R(-1) - R(1)R(0)}{R(0)R(0) - R(1)R(-1)} = -\lambda_s(\lambda_s^2 + 1) \quad (6.A.15)$$

$$a(2) = \frac{R(1)R(1) - R(2)R(0)}{R(0)R(0) - R(1)R(-1)} = \lambda_s^2 \quad (6.A.16)$$

$$\sigma_u^2 = R(0) + a(1)R(+1) + a(2)R(+2) \quad (6.A.17a)$$

$$= \sigma_s^2 - \sigma_s^2 \lambda_s^2 (\lambda_s^2 + 1) + \sigma_s^2 \lambda_s^6 \quad (6.A.17b)$$

$$= \sigma_s^2 [1 - \lambda_s^2 - \lambda_s^4 + \lambda_s^6] \quad (6.A.17c)$$

We now consider the effect of these results when used in the AR equation (6.A.6); ie.,

$$s(n) = -a(1)s(n-1) - a(2)s(n-2) + u(n). \quad (6.A.18)$$

Using eqs(6.A.15) and (6.A.16) in (6.A.18), we have

$$s(n) = \lambda_s(\lambda_s^2 + 1)s(n-1) - \lambda_s^2 s(n-2) + u(n) \quad (6.A.19)$$

where the white noise driving term $u(n)$ has the variance σ_u^2 . We note from eq(6.A.13) that as λ_s approaches zero, the correlation function approaches a delta function with variance σ_s^2 . Therefore, $s(n)$ is expected to be an uncorrelated white noise process with variance σ_s^2 . Examination of eq(6.A.19) indicates that $s(n)$ is approaching the white noise process $u(n)$ for small λ_s since the AR coefficients are becoming vanishingly small. In addition, eq(6.A.17c) indicates that the variance of $u(n)$ is approximated by that of $s(n)$ as required. We therefore have a method for process synthesis that allows one to control the variance and temporal correlation over a wide range of values. Furthermore,

for a specific σ_s^2 , the variance of the synthesized processes will remain fixed independent of the choice of λ_s .

B. Alternate Approach

We could characterize the observation processes $\underline{x}(n|H_i)$ defined in eq(2.1) as multichannel AR processes under each hypothesis. We would then have

$$\underline{x}(n|H_i) = - \sum_{k=1}^{M_i} A_{M_i}^H(k|H_i) \underline{x}(n-k) + \underline{u}(n|H_i) \quad i = 0,1 \quad (6.B.1)$$

where M_i , $A_{M_i}^H(k|H_i)$ and $\underline{u}(n|H_i)$ denote the model order, the matrix coefficients and the white noise driving term under each hypothesis, respectively. Eq (6.B.1) could be utilized to generate the processes under each hypothesis using predetermined values for the coefficients. This approach is useful in the diagnostics of parameter estimation algorithms; i.e., one could validate that the estimates of the coefficients converge to the known preassigned model coefficients as well as assess the convergence rate and final error variance. This approach, however, does not allow control over the variations of the signal-to-noise (S/N) and/or signal-to-clutter (S/C) ratios for parametric performance evaluations.

C. Complex Processes with Jointly Gaussian Quadrature Components

In this section, we discuss the conditions which enable us to control the Gaussian statistics of the synthesized processes. We accomplish this through the white noise driving vectors, $\underline{u}_g(n)$ and $\underline{v}_g(n)$ in eq(6.A.7). Initially, we present the constraints on the quadrature correlation functions associated with $\underline{v}_g(n)$ in order to obtain conventional complex Gaussian processes. Next, we relax these constraints in order to synthesize the more general case of complex processes which contain correlated Gaussian quadrature components.

Let us now consider expressing $\underline{v}_g(n)$ and C_g in eq(6.A.7) using their quadrature components so that (dropping the g subscript)

$$\underline{y}(n) = \underline{y}_I(n) + j \underline{y}_Q(n) \quad (6.C.1a)$$

and

$$C = C_I + j C_Q. \quad (6.C.1b)$$

Using these expressions in (6.A.7), we obtain

$$\underline{u}(n) = C \underline{y}(n) \quad (6.C.2a)$$

$$= [C_I + j C_Q][\underline{y}_I(n) + j \underline{y}_Q(n)] \quad (6.C.2b)$$

$$= [C_I \underline{y}_I(n) - C_Q \underline{y}_Q(n)] + j [C_Q \underline{y}_I(n) + C_I \underline{y}_Q(n)] \quad (6.C.2c)$$

so that

$$\underline{u}_I(n) = C_I \underline{y}_I(n) - C_Q \underline{y}_Q(n) \quad (6.C.3a)$$

$$\underline{u}_Q(n) = C_Q \underline{y}_I(n) + C_I \underline{y}_Q(n). \quad (6.C.3b)$$

We now have

$$R_{uu}^{\Pi}(0) = E[\underline{u}_I(n) \underline{u}_I^T(n)] \quad (6.C.4a)$$

$$= E\{[C_I \underline{y}_I(n) - C_Q \underline{y}_Q(n)][\underline{y}_I^T(n) C_I^T - \underline{y}_Q^T(n) C_Q^T]\} \quad (6.C.4b)$$

$$= C_I R_{vv}^{\Pi}(0) C_I^T + C_Q R_{vv}^{QQ}(0) C_Q^T - C_Q R_{vv}^{QI}(0) C_I^T - C_I R_{vv}^{IQ}(0) C_Q^T \quad (6.C.4c)$$

Similarly,

$$R_{uu}^{QQ}(0) = E[\underline{u}_Q(n) \underline{u}_Q^T(n)] \quad (6.C.5a)$$

$$= E\{[C_Q \underline{y}_I(n) + C_I \underline{y}_Q(n)][\underline{y}_I^T(n) C_Q^T + \underline{y}_Q^T(n) C_I^T]\} \quad (6.C.5b)$$

$$= C_Q R_{vv}^{\Pi}(0) C_Q^T + C_I R_{vv}^{QI}(0) C_Q^T + C_Q R_{vv}^{IQ}(0) C_I^T + C_I R_{vv}^{QQ}(0) C_I^T \quad (6.C.5c)$$

$$R_{uu}^{IQ}(0) = E[\underline{u}_I(n) \underline{u}_Q^T(n)] \quad (6.C.6a)$$

$$= E \{ [C_I y_I(n) - C_Q y_Q(n)] [y_I^T(n) C_Q^T + y_Q^T(n) C_I^T] \} \quad (6.C.6b)$$

$$= C_I R_{vv}^{\Pi}(0) C_Q^T - C_Q R_{vv}^{QI}(0) C_Q^T + C_I R_{vv}^{IQ}(0) C_I^T - C_Q R_{vv}^{QQ}(0) C_I^T \quad (6.C.6c)$$

$$R_{uu}^{QI}(0) = E[u_Q(n) u_I^T(n)] \quad (6.C.7a)$$

$$= E \{ [C_Q y_I(n) + C_I y_Q(n)] [y_I^T(n) C_I^T - y_Q^T(n) C_Q^T] \} \quad (6.C.7b)$$

$$= C_Q R_{vv}^{\Pi}(0) C_I^T + C_I R_{vv}^{QI}(0) C_I^T - C_Q R_{vv}^{IQ}(0) C_Q^T - C_I R_{vv}^{QQ}(0) C_Q^T. \quad (6.C.7c)$$

In the special case where

$$R_{vv}^{\Pi}(0) = R_{vv}^{QQ}(0) = \frac{1}{2} I \quad (6.C.8a)$$

$$R_{vv}^{IQ}(0) = R_{vv}^{QI}(0) = 0 \quad (6.C.8b)$$

and I is the identity matrix, we have

$$R_{uu}^{\Pi}(0) = \frac{1}{2} C_I C_I^T + \frac{1}{2} C_Q C_Q^T \quad (6.C.9a)$$

$$R_{uu}^{QQ}(0) = \frac{1}{2} C_Q C_Q^T + \frac{1}{2} C_I C_I^T \quad (6.C.9b)$$

$$R_{uu}^{IQ}(0) = \frac{1}{2} C_I C_Q^T - \frac{1}{2} C_Q C_I^T \quad (6.C.9c)$$

$$R_{uu}^{QI}(0) = \frac{1}{2} C_Q C_I^T - \frac{1}{2} C_I C_Q^T \quad (6.C.9d)$$

so that

$$R_{uu}^{\Pi}(0) = R_{uu}^{QQ}(0) \quad (6.C.10a)$$

and

$$R_{uu}^{IQ}(0) = -R_{uu}^{QI}(0). \quad (6.C.10b)$$

In the further restricted case where $C_Q=0$ (which occurs when the correlation functions in the Yule-Walker equation are real)

$$R_{uu}^{IQ}(0) = -R_{uu}^{QI}(0) = [0]. \quad (6.C.11)$$

The conditions expressed by eqs(6.C.10a) and (6.C.10b) are those required to ensure that the magnitude of the complex process $\underline{u}(n)$ is Gaussian. We note that these conditions result when eqs(6.C.8a) and (6.C.8b) hold; ie., when the white noise driving vector $\underline{v}(n)$ has variances of $\sigma_v^2/2$ on each channel quadrature component and the quadrature components on each channel are uncorrelated. In this special case, eq(6.A.8b) is maintained; ie.,

$$E[\underline{v}(n)\underline{v}^H(n)] = D_v = I. \quad (6.C.12)$$

If we generalize this case so that $\underline{v}(n)$ has an arbitrary variance on each channel quadrature component as well as an arbitrary correlation between the Gaussian quadrature components on each channel, the resulting $\underline{u}(n)$ is a more generally distributed process. We also note that eq(6.C.12) can continue to be satisfied by maintaining the relations

$$R_{vv}^{IQ}(0) = R_{vv}^{QI}(0) \quad (6.C.13a)$$

and

$$R_{vv}^{II}(0) + R_{vv}^{QQ}(0) = I. \quad (6.C.13b)$$

This can be seen by noting that

$$E[\underline{y}(n)\underline{y}^H(n)] = E\{[\underline{y}_I(n) + j \underline{y}_Q(n)][\underline{y}_I^T(n) - j \underline{y}_Q^T(n)]\} \quad (6.C.14a)$$

$$= [R_{\underline{v}\underline{v}}^{\Pi}(0) + R_{\underline{v}\underline{v}}^{QQ}(0)] + j [R_{\underline{v}\underline{v}}^{QI}(0) - R_{\underline{v}\underline{v}}^{IQ}(0)]. \quad (6.C.14b)$$

Substituting eqs(6.C.13) into (6.C.14b) yields (6.C.12). We emphasize that eqs(6.C.13a) and (6.C.13b) provide a more general condition than eqs(6.C.8a) and (6.C.8b); ie., the quadrature components are now able to be implemented with an arbitrary cross-correlation.

The arbitrary correlation on the quadrature components of $\underline{y}(n)$ could be obtained using

$$\begin{bmatrix} \underline{y}_I(n) \\ \underline{y}_Q(n) \end{bmatrix} = G \begin{bmatrix} \underline{p}_I(n) \\ \underline{p}_Q(n) \end{bmatrix} \quad (6.C.15)$$

where

$$E[\underline{p}_I(n)\underline{p}_Q^T(n)] = [0] \quad (6.C.16a)$$

$$E[\underline{p}_I(n)\underline{p}_I^T(n)] = E[\underline{p}_Q(n)\underline{p}_Q^T(n)] = \frac{1}{2} I. \quad (6.C.16b)$$

We now consider

$$R_{\underline{y}_I \underline{y}_Q}(0) = E\left\{ \begin{bmatrix} \underline{y}_I \\ \underline{y}_Q \end{bmatrix} \begin{bmatrix} \underline{y}_I^T & \underline{y}_Q^T \end{bmatrix} \right\} \quad (6.C.17a)$$

$$= \begin{bmatrix} E[\underline{y}_I(n)\underline{y}_I^T(n)] & E[\underline{y}_I(n)\underline{y}_Q^T(n)] \\ E[\underline{y}_Q(n)\underline{y}_I^T(n)] & E[\underline{y}_Q(n)\underline{y}_Q^T(n)] \end{bmatrix} \quad (6.C.17b)$$

$$= \begin{bmatrix} R_{\underline{v}\underline{v}}^{\Pi}(0) & R_{\underline{v}\underline{v}}^{IQ}(0) \\ R_{\underline{v}\underline{v}}^{QI}(0) & R_{\underline{v}\underline{v}}^{QQ}(0) \end{bmatrix} \quad (6.C.17c)$$

where each element in eq(6.C.17c) is a $J \times J$ diagonal matrix. Using eqs(6.C.15) through (6.C.16b) in the RHS of (6.C.17a)

$$R_{\underline{y}_I \underline{y}_Q}(0) = G E \left\{ \begin{bmatrix} \underline{p}_I \\ \underline{p}_Q \end{bmatrix} \begin{bmatrix} \underline{p}_I^T & \underline{p}_Q^T \end{bmatrix} \right\} G^T \quad (6.C.18a)$$

$$= \frac{1}{2} G G^T \quad (6.C.18b)$$

so that

$$\begin{bmatrix} R_{\underline{v}\underline{v}}^{\Pi}(0) & R_{\underline{v}\underline{v}}^{IQ}(0) \\ R_{\underline{v}\underline{v}}^{QI}(0) & R_{\underline{v}\underline{v}}^{QQ}(0) \end{bmatrix} = \frac{1}{2} G G^T. \quad (6.C.19)$$

The matrices on the LHS of eq(6.C.19) can be constrained to satisfy eqs(6.C.13a) and (6.C.13b) without loss of generality. In addition, they could be specified using functional forms similar to eqs(3.C.5) and (3.C.8). The diagonal form of these matrices implies that correlation only exists between the quadrature components of $\underline{y}_g(n)$ $g=s,c$ on a given channel and not across channels.

Therefore, for channels $i=1,2,\dots,J$, we would use

$$R_{ii}^{IQ}(0) = R_{ii}^{QI}(0) = |\rho_{ii}^{IQ}| \sigma_{ii}^{\Pi} \sigma_{ii}^{QQ} \quad i = 1,2,\dots,J \quad (6.C.20)$$

where σ_{ii}^{Π} and σ_{ii}^{QQ} are the standard deviations of the quadrature components on

channel i . The variances on each channel are subject to the constraint

$$(\sigma_{ii}^2)_{\Pi} + (\sigma_{ii}^2)_{QQ} = 1 \quad i = 1,2,\dots,J. \quad (6.C.21)$$

Also,

$$R_{ii}^{\Pi}(0) = (\sigma_{ii}^2)_{\Pi} \quad i = 1,2,\dots,J \quad (6.C.22a)$$

and

$$R_{ii}^{QQ}(0) = (\sigma_{ii}^2)_{QQ} \quad i = 1,2,\dots,J. \quad (6.C.22b)$$

Finally, eq(6.C.19) can be solved via the Cholesky decomposition to obtain G and eq(6.C.15) implemented to generate $\underline{y}_I(n)$ and $\underline{y}_Q(n)$ with variable correlation.

VII. SYNTHESIS RESULTS

A. Single Channel Case

In this section, we utilize the AR process synthesis procedure described in section VI to generate single channel autoregressive processes of order two. Using the Yule-Walker equation, two AR coefficients are obtained which, when substituted into the scaler form of eq(6.A.6), provides the required signal processes. For the processes shown in Figs 7.A.1 through 7.A.8, the real, Gaussian autocorrelation function was used. We note that an AR(2) process has an exponential autocorrelation function. In this case, we are generating processes which provide a 'fit' to the Gaussian autocorrelation function in a MMSE sense. We also note that in this case, the AR coefficients will be real. However, the processes $s(n)$ generated by eq(6.A.6) are complex since $u(n)$ is complex. Also, the resulting spectra will be even.

In Fig 7.A.1, we show the amplitude of the real part of the signal process with order two using a temporal correlation coefficient of $\lambda_s=0.99$ and variances σ_s^2 ranging from 2.0 to 8.0. We note the variation in the amplitudes of each plot as the variance changes. In Fig 7.A.2, we show the amplitude of the real part of the signal using a variance $\sigma_s^2=4.0$. In this case, however, we demonstrate the effect of varying the temporal correlation coefficient λ_s from 0.1 to 0.9999. We note that Figs 7.A.2a through 7.A.2c are plotted for 100 samples, while Fig.7.A.2d uses 200 samples. These figures illustrate the effect of λ_s in controlling the sample-to-sample correlation. It is apparent that as λ_s approaches unity, we are approaching the case of total correlation sample-to-sample; however, as λ_s goes to zero, the process becomes white. It is worth noting, at this

time, that the imaginary component follows the same behavior. Recognizing that the signal phase is expressed as

$$\theta_s(n) = \tan^{-1} \left[\frac{s_Q(n)}{s_I(n)} \right] \quad (7.A.1)$$

then, as λ_s approaches unity, $\theta_s(n)$ approaches a constant since $s_I(n)$ and $s_Q(n)$ are approaching constant values within a single trial. On the other hand, as λ_s approaches zero, $\theta_s(n)$ is random in time since $s_I(n)$ and $s_Q(n)$ exhibit random behavior. The important point to be made here is that the parameter λ_s controls the amplitude correlation as well as the phase coherence of the process. This capability will be utilized to demonstrate coherent integration gain in detection performance evaluations.

In Fig 7A.3, we show results for three separate trials of the real part of the signal process for $\lambda_s = 0.9999$ and $\sigma_s^2 = 4.0$ over 200 time samples. The point to be noted here is the randomness associated with the initial amplitude (and phase via the previous discussion). As noted, however, after the initial amplitude is selected at random, the remaining samples are highly correlated within each trial as governed by the high value of the temporal correlation coefficient. This feature will enable us to model processes such as Swerling fluctuating signals[14] in radar applications, for example.

Fig 7.A.4 shows the results of the model fitting procedure. The dotted curves plot the correlation functions predetermined by the functional shaping method. The solid curves are plots of the correlation function calculated using 10,000 samples of the process over 40 lag values. Figs 7.A.4a, 7.A.4b and 7.A.4c are plots for $\lambda_s = 0.95, 0.8$, and 1.0 , respectively. We first note the effect of λ_s on the correlation function; ie. as λ_s transitions from unity to zero, the correlation function ranges from that of a slowly varying function of the lag

value to that of a delta function. Next, we note from Figs 7.A.4a and 7.A.4b that the plots of the AR process of order two provide a fit to the predetermined correlation function. This is a result of the fact that it would require an AR process of infinite order to model the Gaussian correlation process exactly. These plots illustrate that the processes generated here are an approximation to those of the predetermined correlation function. In fact, they are the processes that fit the known model in a MMSE sense. In Fig 7.A.5, we show the autoregressive power spectral density (ARPSD) which is obtained using the AR coefficients obtained from the Yule-Walker equation. Fig 7.A.6 is the corresponding power spectral density (PSD) determined using a zero-filled 64 point FFT of the calculated correlation functions plotted in Fig 7.A.4. The plots for Figs 7.A.6a and 7.A.6b, show even spectra; however, we also note the dual peaks associated with the poles of the AR(2) model. The obvious point to be noted here is the behavior of the spectra for various values of λ_s ; ie. as λ_s ranges from unity to zero, the spectra transitions from its peaked behavior to the broad distribution associated with white noise processes. It is also interesting to note that as λ_s decreases, the pronounced pole positions are diminished as shown in Fig 7.A.6c. This is a result of the fact that the AR coefficients are becoming vanishingly small as noted by eqs(6.A.9) and (6.A.10).

In Figs 7.A.7 and 7.A.8, we show plots of the autocorrelation function and power spectral density, respectively, again using 10,000 samples of the same signal process, but in the presence of unit variance additive white noise. We note that the correlation functions in Fig 7.A.7 overlay the corresponding functions shown in Fig 7.A.4 except that at lag zero, they have increased by a unit value due to the uncorrelated noise process. A comparison of Figs 7.A.6 and 7.A.8 shows the increased levels due to the additive noise.

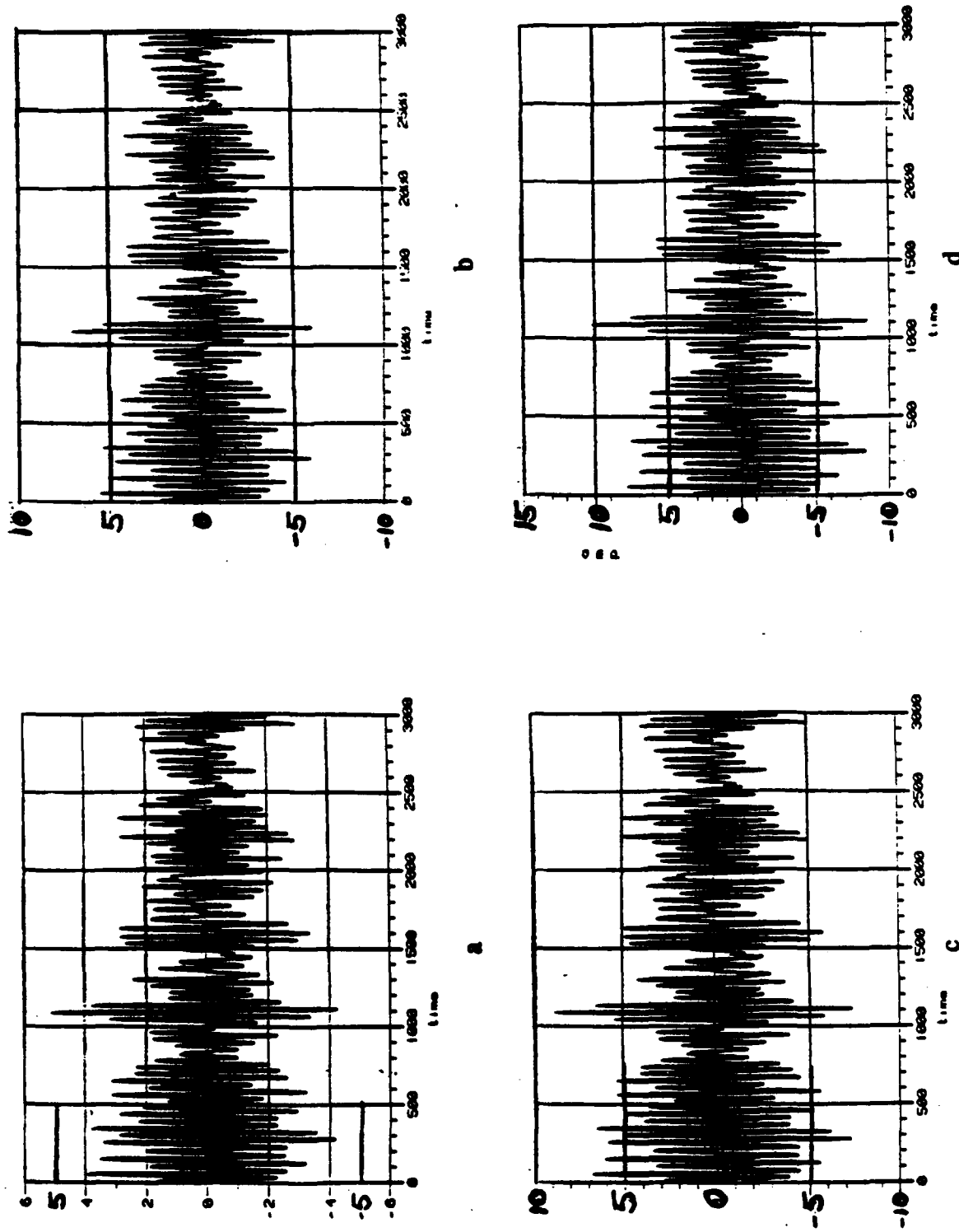
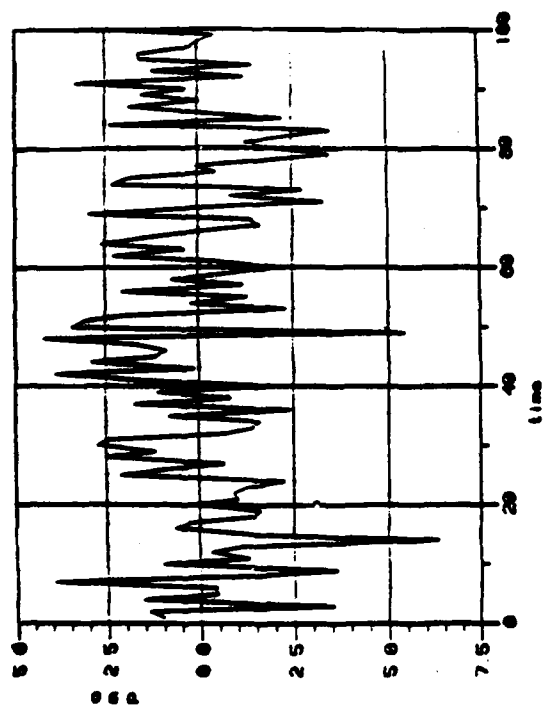
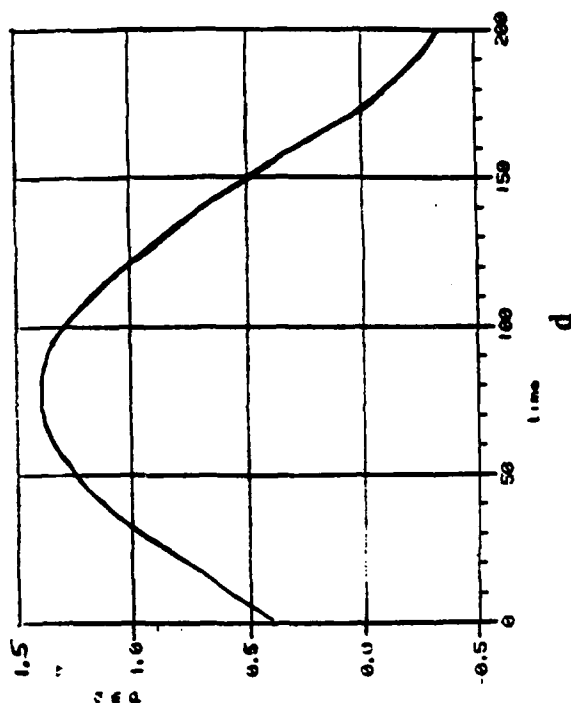


Fig. 7.A.1 Amplitude of the real part of an AR(2) signal process for $\lambda_s=0.99$ and 3000 sample observations a.) $\sigma_s^2=2.0$ b.) $\sigma_s^2=4.0$ c.) $\sigma_s^2=6.0$ d.) $\sigma_s^2=8.0$.



a

b



c

d

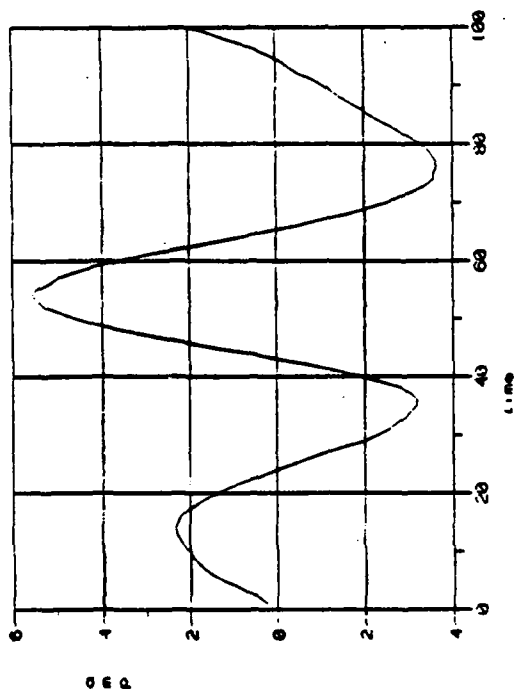


Fig. 7.A.2 Amplitude of the real part of the AR(2) signal process for $\sigma_s^2 = 4.0$ with a.) $\lambda_s = 0.1$ b.) $\lambda_s = 0.9$ c.) $\lambda_s = 0.99$ d.) $\lambda_s = 0.9999$.

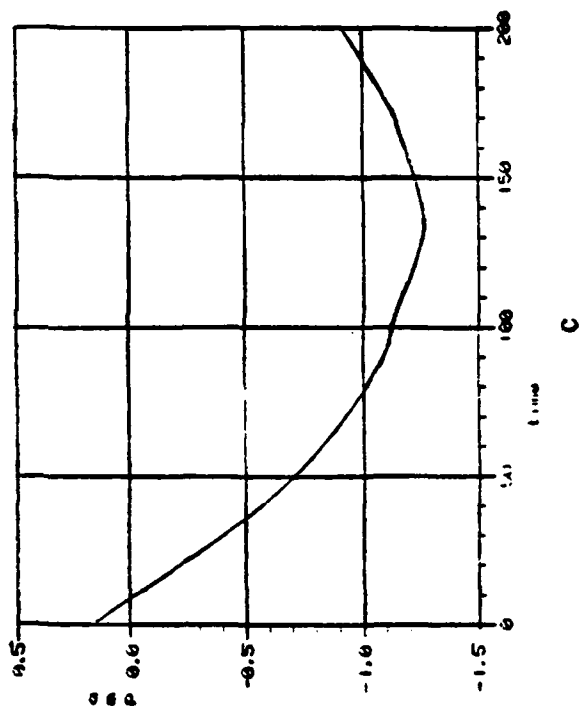
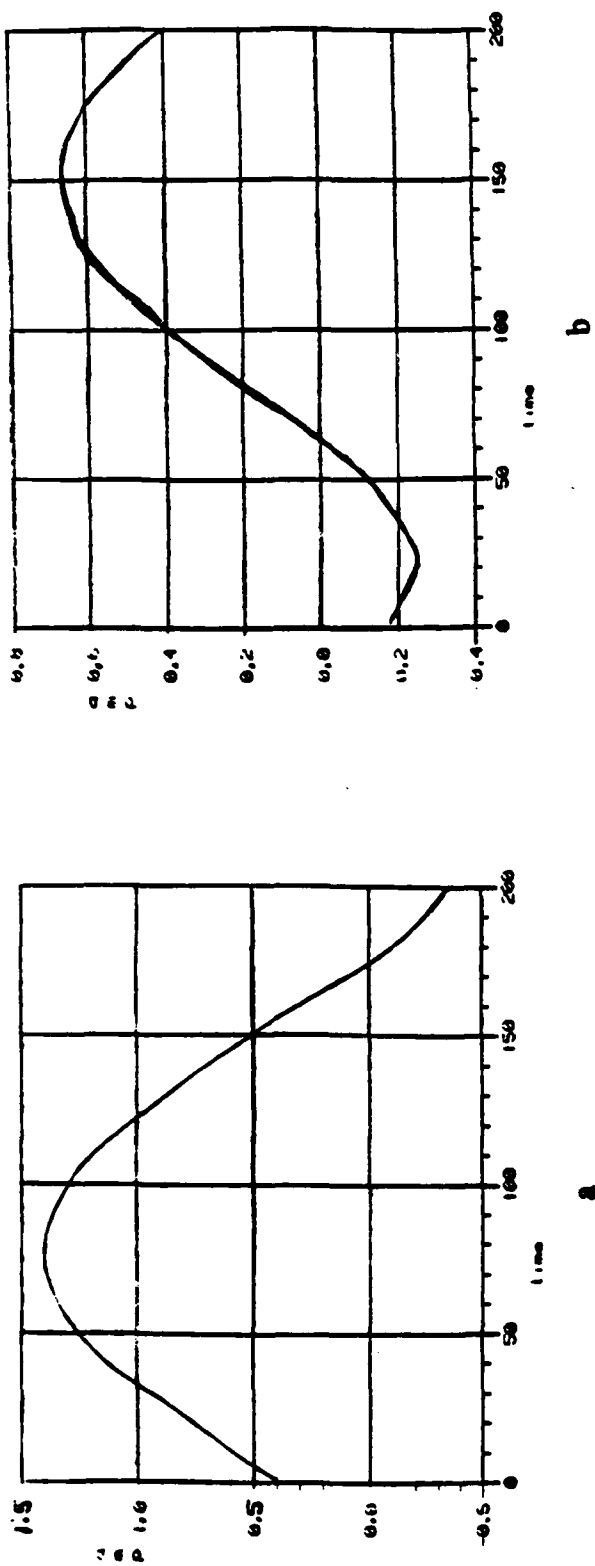


Fig. 7.A.3 Three independent trials of the real part of the AR(2) signal using $\sigma_s^2=4.0$ and $\lambda_s=0.9999$.

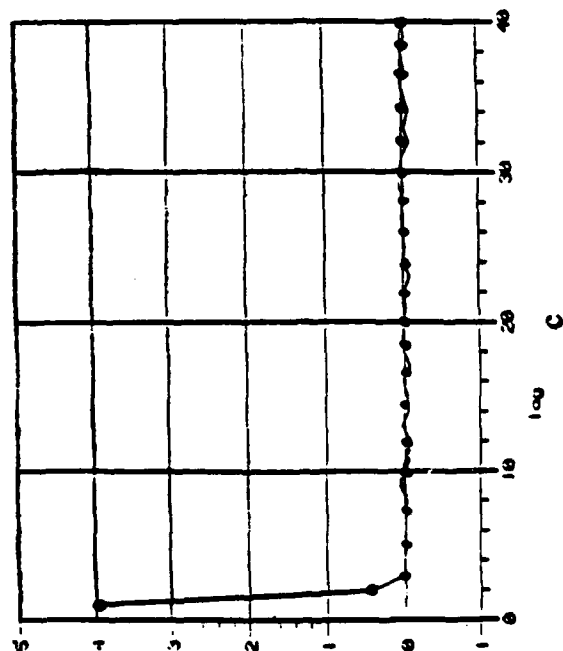
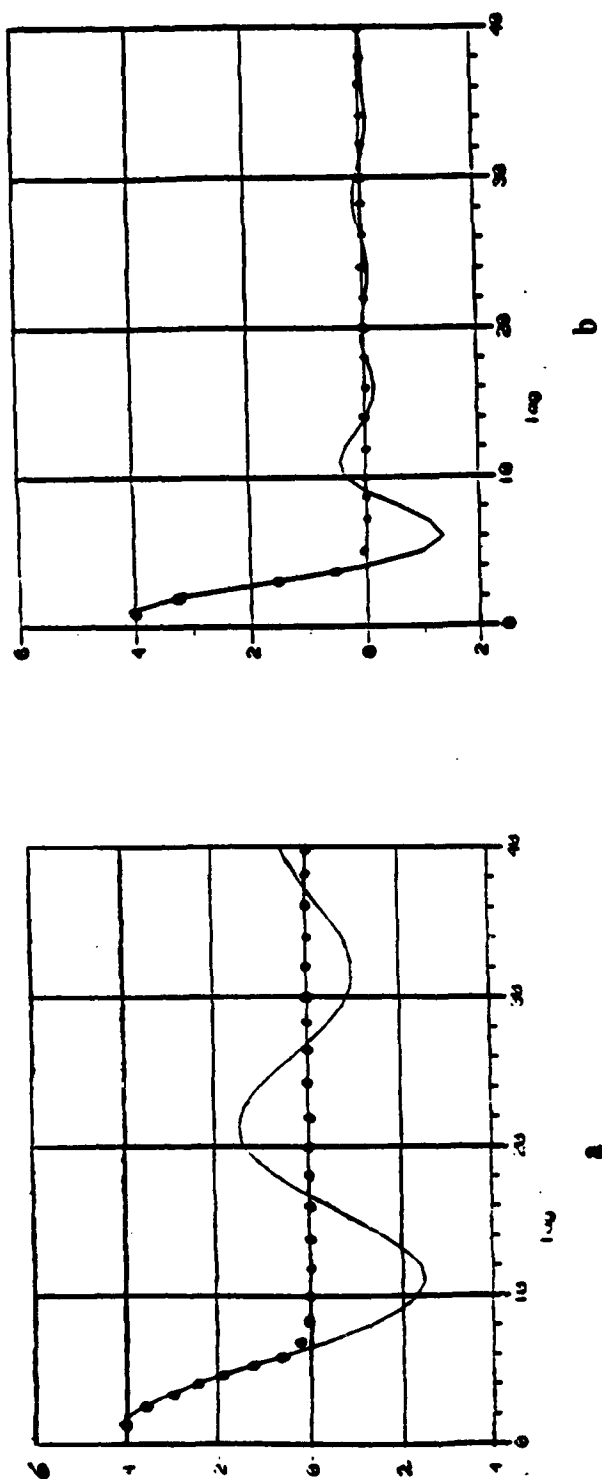


Fig. 7.A.4 Plots of the known(...) and estimated(—) correlation functions for the AR(2) process using 10,000 sample observations with a.) $\lambda_s=0.95$ b.) $\lambda_s=0.80$ c.) $\lambda_s=0.1$.

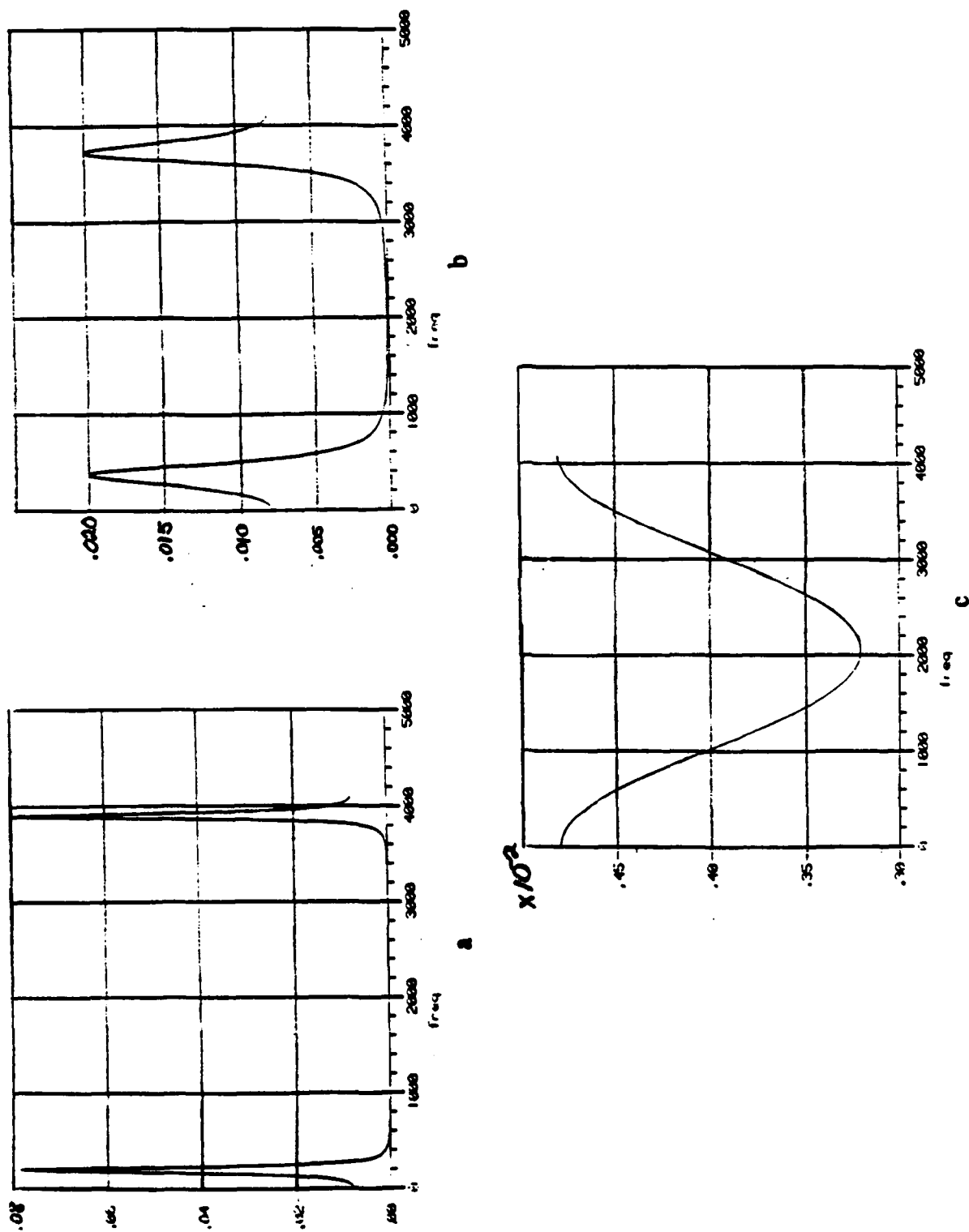


Fig. 7.A.5 Plots of the ARPSD computed using the AR(2) coefficients obtained from the Yule-Walker equation a.) $\lambda_s=0.95$ b.) $\lambda_s=0.80$ c.) $\lambda_s=0.1$.

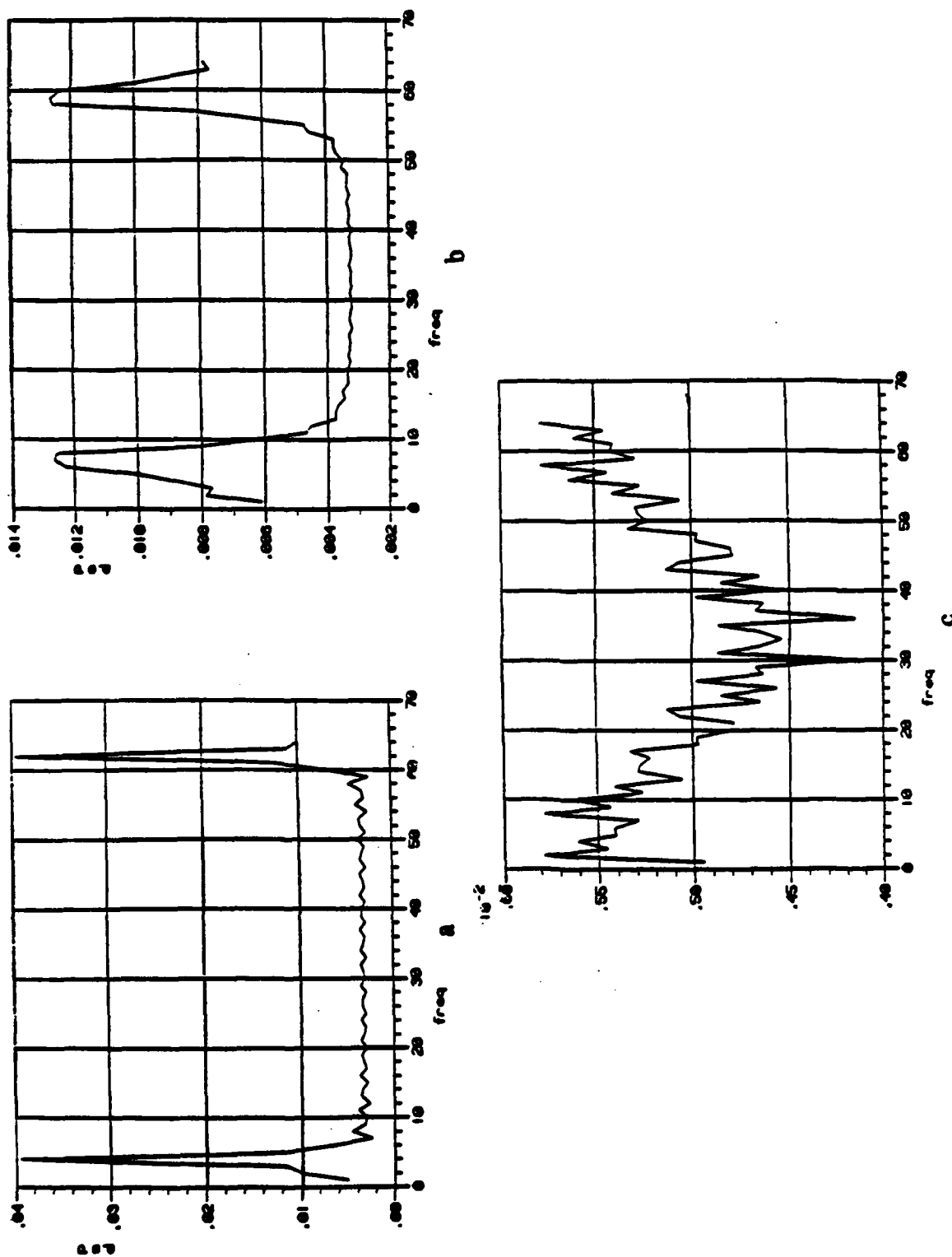
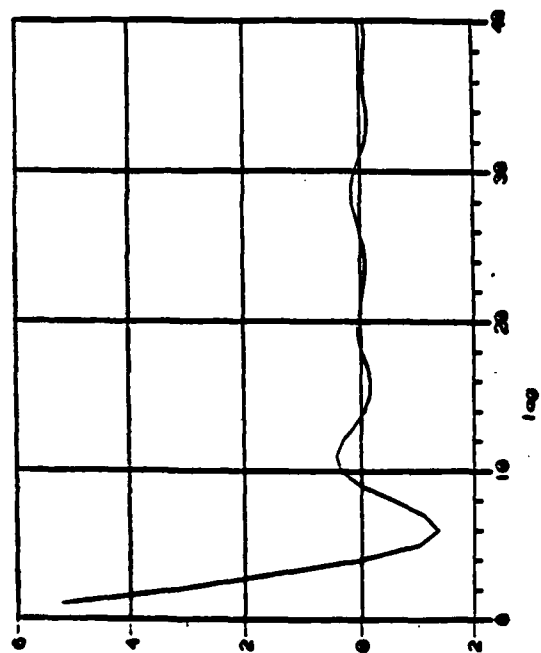


Fig. 7.A.6 PSD of the AR(2) process using a zero-filled 64-point FFT of the estimated correlation functions in Fig 7.A.4 with a.) $\lambda_s=0.95$ b.) $\lambda_s=0.80$ c.) $\lambda_s=0.1$.



b

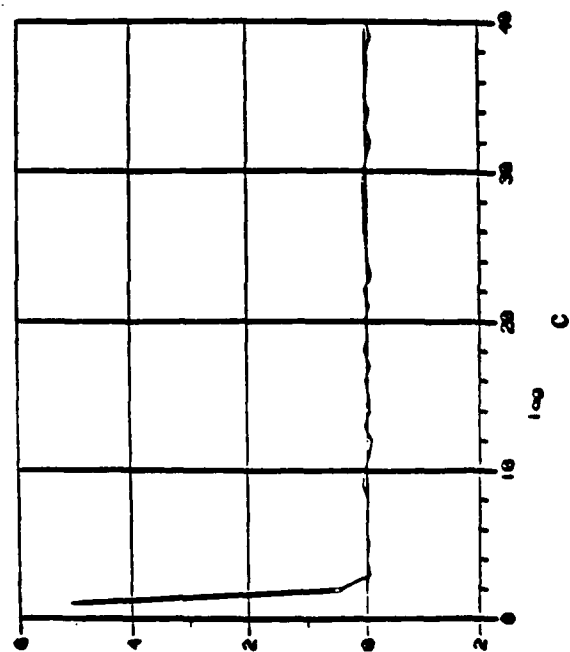
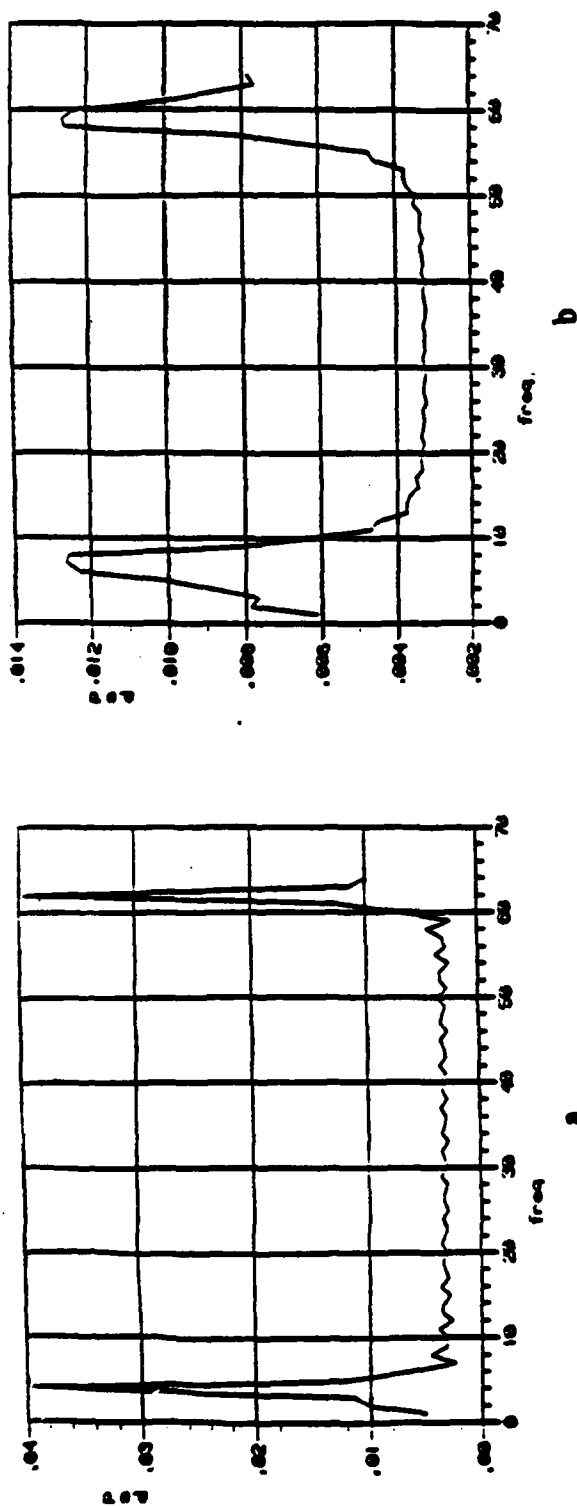
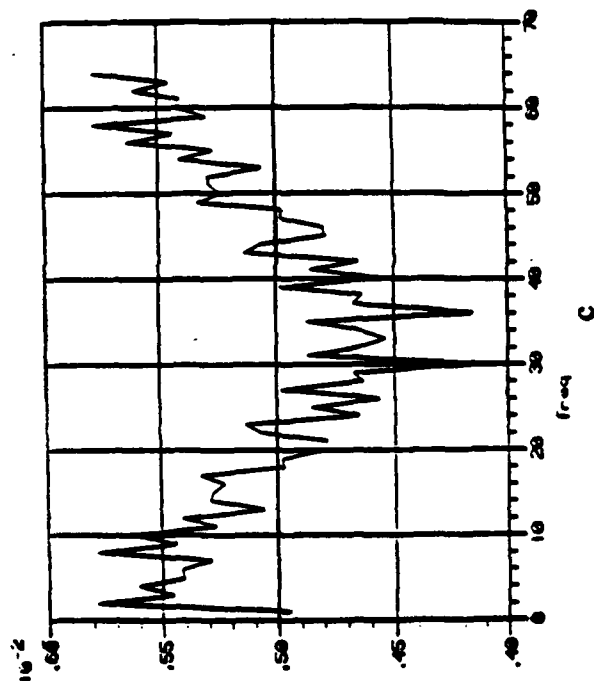


Fig. 7.A.7 Plots of the estimated correlation functions for the AR(2) process plus unit variance white noise using 10,000 sample observations with a.) $\lambda_s=0.95$ b.) $\lambda_s=0.80$ c.) $\lambda_s=0.1$.



b



c

Fig. 7.A.8 PSD of the AR(2) process plus unit variance white noise using a zero-filled 64-point FFT of the estimated correlation functions in Fig. 7.A.7 with a.) $\lambda_s=0.95$ b.) $\lambda_s=0.80$ c.) $\lambda_s=0.1$.

B. Multichannel Case

In this section, we consider the generation of a two channel vector process using the AR synthesis approach described in section VI. In this case, the multichannel Yule-Walker equation is solved for the forward AR matrix coefficients and the forward driving white noise covariance matrix. These matrices are used in eq(6.A.6) and (6.A.7) for process generation. We limit the results shown here to the case of real, Gaussian correlation functions. In sections VII.C and VII.D, we will quantitatively assess the ergodicity considerations developed in section IV. In this section, however, we will note several qualitative indications of the dependence of ergodicity on the correlation parameters.

Table 7.B.1 contains the parameters used in the auto- and cross-correlation functions described in eqs(3.C.13a) and (3.C.23b). The resulting values are then used in the correlation matrix of the multichannel Yule-Walker equation to solve for the coefficients C and $A(k)$ $k = 1, 2$. The resulting AR coefficient matrices are listed in Table 7.B.2. We will discuss these quantities later to gain further insight into the process generation procedure.

Figs 7.B.1 through 7.B.4 contain the results for processes with high temporal correlation on each channel. In Fig 7.B.1, $\lambda_{ii} = 0.9999$ on both channels with $|\rho_{12}| = 0.95$. In Figs 7.B.2 through 7.B.4, $\lambda_{ii} = 0.95$ on both channels, while the cross-correlation coefficient $|\rho_{12}|$ ranges from 0.99 to 0.0. Figs 7.B.1a and 7.B.1b show 200 sample observations of the synthesized processes for channels 1 and 2, respectively, for one realization. A second realization is shown in Figs 7.B.1c and 7.B.1d. A visual inspection of these two trials reveals the relatively high degree of cross-correlation between the two channels controlled by $|\rho_{12}| = 0.95$. Figs 7.B.1e and 7.B.1f show the corresponding ensemble averaged autocorrelation functions calculated using

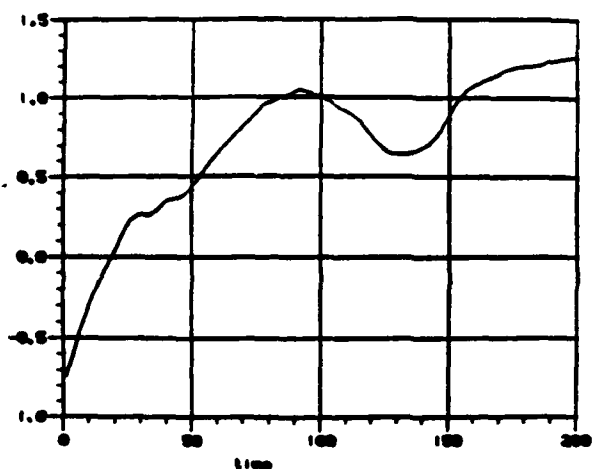
Fig.	order	σ_{11}^2	σ_{22}^2	$ \rho_{12} $	λ_{11}	λ_{22}	λ_{12}	l_{12}	$R_{12}(0)$
7.B.1	AR(2)	4	4	0.95	0.9999	0.9999	0.9999	0	3.8
7.B.2	AR(2)	4	4	0.99	0.95	0.95	0.95	0	3.96
7.B.3	AR(2)	4	4	0.5	0.95	0.95	0.95	0	2.0
7.B.4	AR(2)	4	4	0.0	0.95	0.95	arbitrary*	0	0.0
7.B.5	AR(2)	4	4	0.0	0.80	0.80	arbitrary*	0	0.0
7.B.6	AR(2)	4	4	0.0	0.40	0.40	arbitrary*	0	0.0
7.B.7	AR(2)	4	4	0.99	0.10	0.10	0.10	0	3.96
7.B.8	AR(2)	4	4	0.30	0.10	0.10	0.97	0	1.2
7.B.9	AR(2)	4	4	0.10	0.10	0.10	0.20	0	0.4
7.B.10	AR(2)	4	4	0.50	0.95	0.10	0.97	0	2.0
7.B.11	AR(2)	4	1	0.40	0.95	0.10	0.97	4	0.8
7.B.12	AR(4)	4	1	0.30	0.95	0.10	0.97	4	0.6

Table 7.B.1

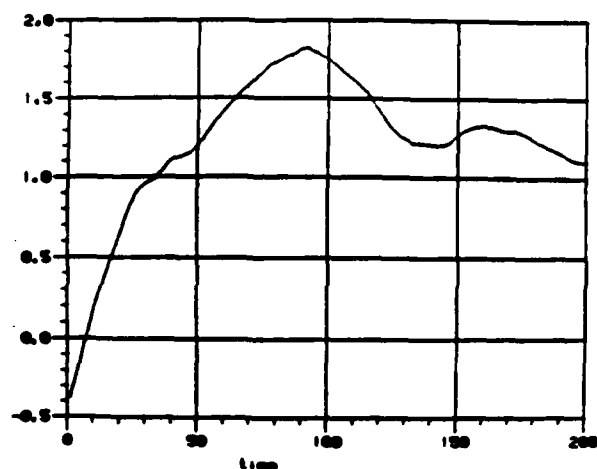
* Examination of eq(3.C.23b) indicates that for $|\rho_{12}| = 0$, the value of λ_{12} is arbitrary.

1,000 trials. We note that in Fig 7.B.1f, the experimentally obtained cross-correlation function evaluated for lag zero fell somewhat below the process variance of 4. The reason for this will be explained below. An overlay of six realizations of the corresponding time-averaged, biased, autocorrelation function for each channel is shown in Figs 7.B.1g and 7.B.1h, respectively. In these plots 10,000 time sample observations were used to estimate the functions over 64 lag values. Figs 7.B.1i and 7.B.1j show the temporal- averaged and ensemble averaged cross-correlation functions, respectively. Inspection of plots g and h indicates that the six realizations of the estimated time-averaged autocorrelation functions, each based on 10,000 time observations, vary considerably from trial-to-trial. This implies that the variance of the time-averaged autocorrelation functions is large. Likewise, this same behavior is noted for the time averaged cross-correlation function in plot i. These results provide an indication that ergodicity cannot be assumed to hold in this case even though the number of observations N_T is as high as 10,000; ie., the estimates of the auto- and cross-correlation functions obtained by time averaging over a single realization will, in general, differ considerably from the ensemble averaged value when the temporal correlation coefficients λ_{ij} are high.

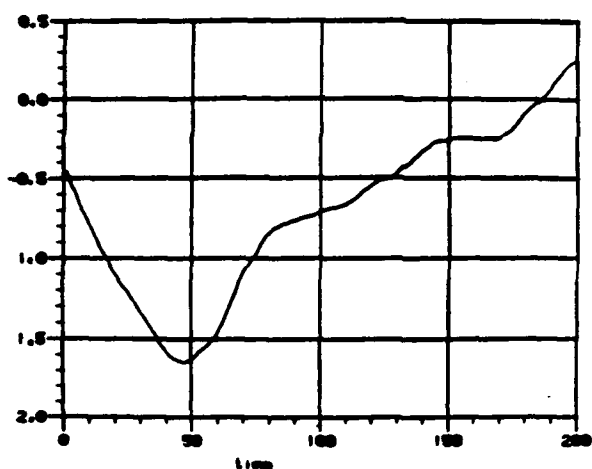
In Fig 7.B.2, the cross-correlation coefficient is increased slightly to 0.99 while the temporal correlation coefficients are reduced to 0.95 on both channels. Fig 7.B.2 shows the same data displays as Fig 7.B.1. We note in plots a and b, that both channel processes have become more uncorrelated in time as evidenced by their more rapid temporal fluctuation. However, we also note the high cross-correlation between the channel processes; ie., both waveforms are nearly identical (note the scale change on the plots a and b). This high correlation results from the high value of $|\rho_{12}|=0.99$. Again, plots e and f show the



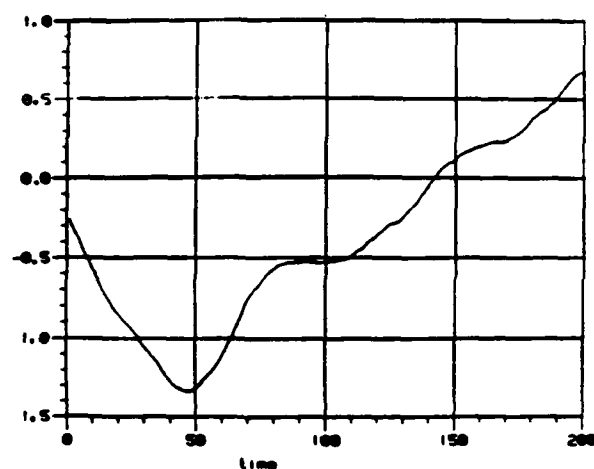
a



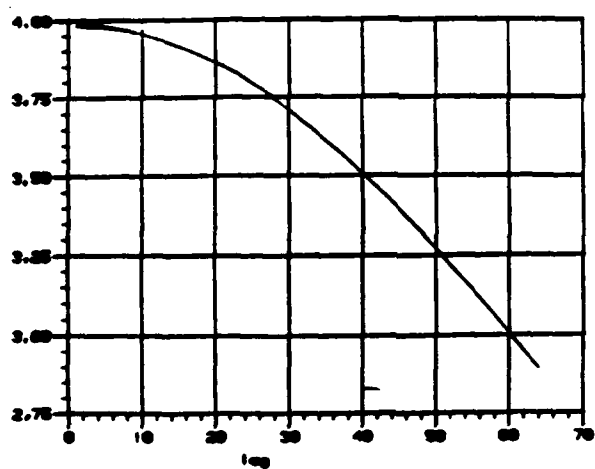
b



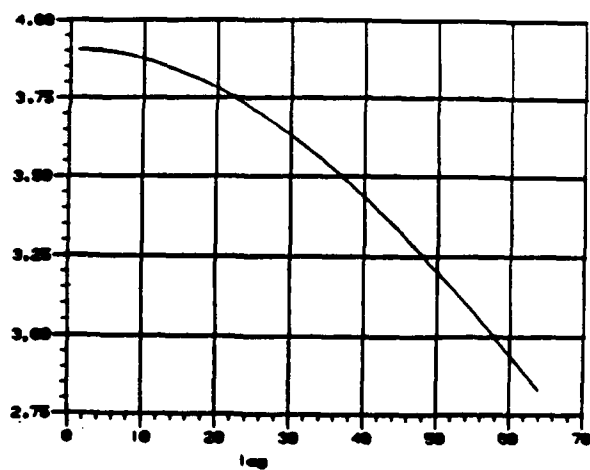
c



d

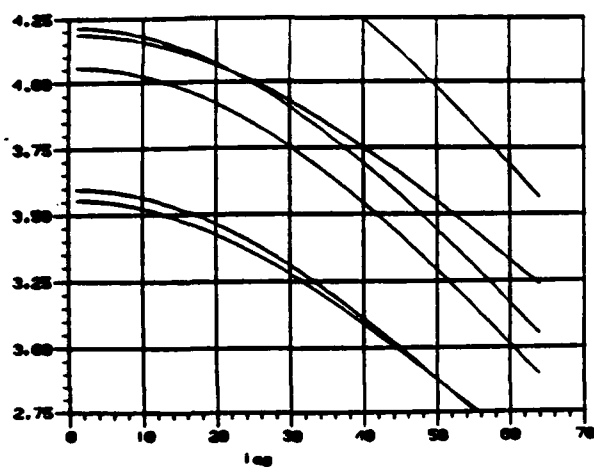


e

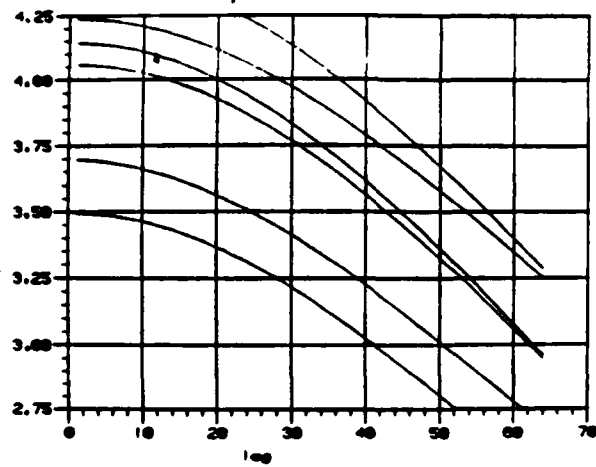


f

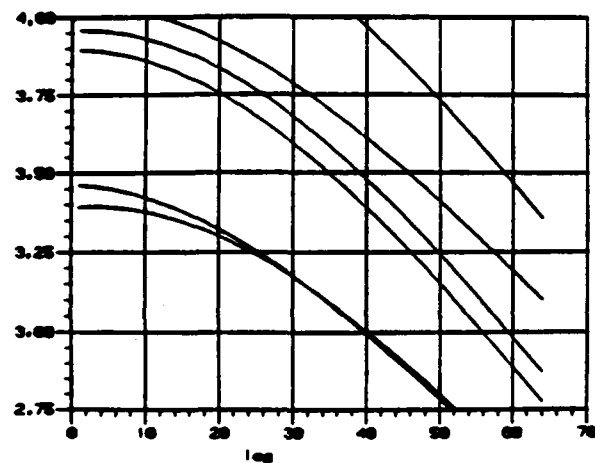
Fig. 7.B.1 Two channel AR(2) processes a.) channel 1 data (trial 1) b.) channel 2 data (trial 1) c.) channel 1 data (trial 2) d.) channel 2 data (trial 2) e.) ensemble averaged channel 1 autocorrelation (1,000 realizations) f.) ensemble averaged channel 2 autocorrelation (1,000 realizations).



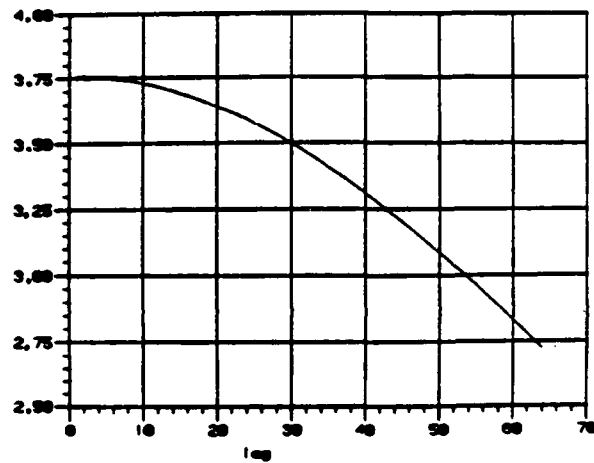
g



h

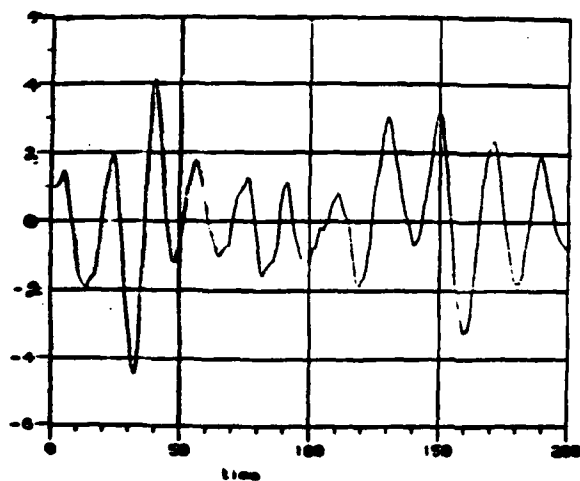


i

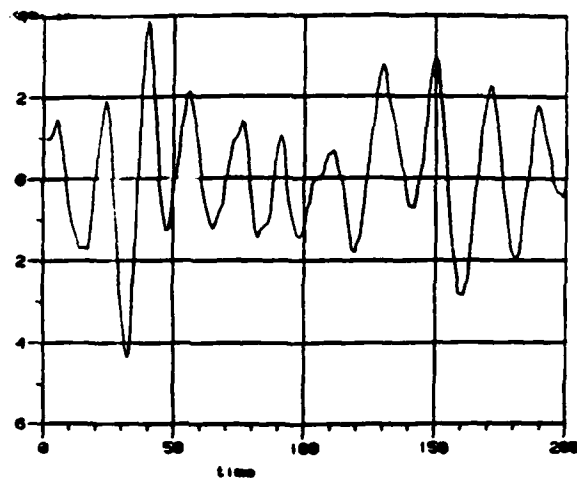


j

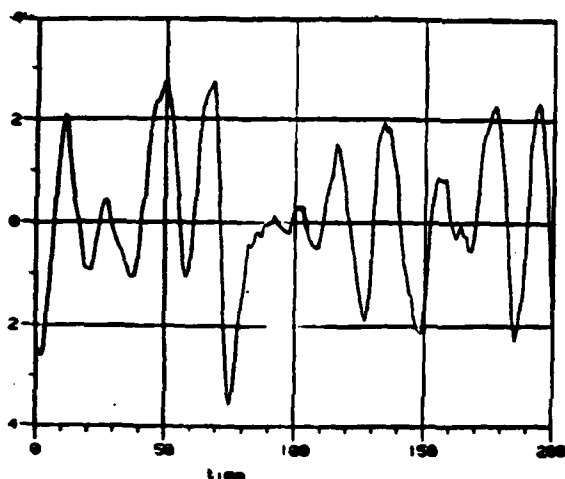
Fig. 7.B.1 (contin.) g.) time-averaged channel 1 autocorrelation (6 trials) h.) time averaged channel 2 autocorrelation (6 trials) i.) time-averaged cross-correlation (6 trials) j.) ensemble averaged cross-correlation (1,000 realizations).



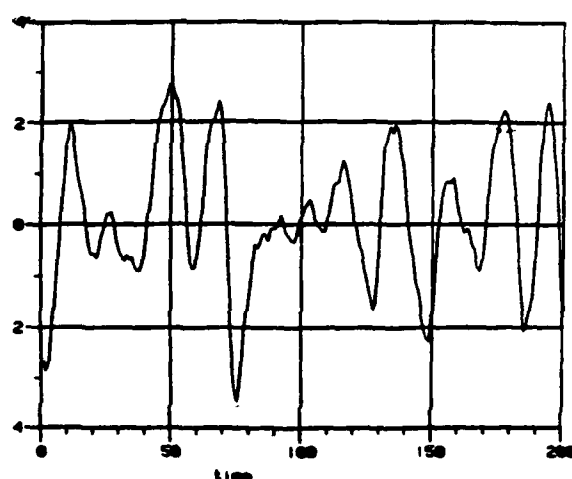
a



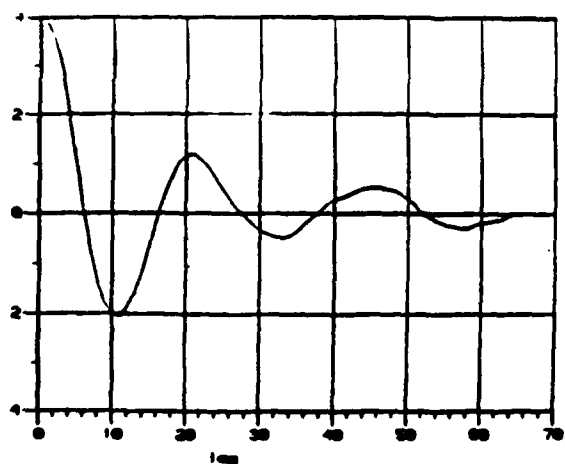
b



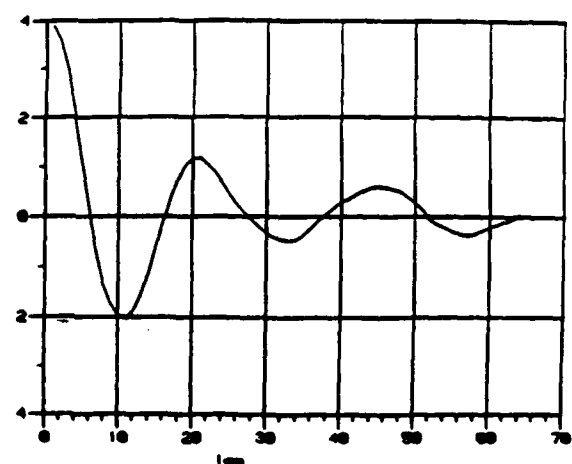
c



d

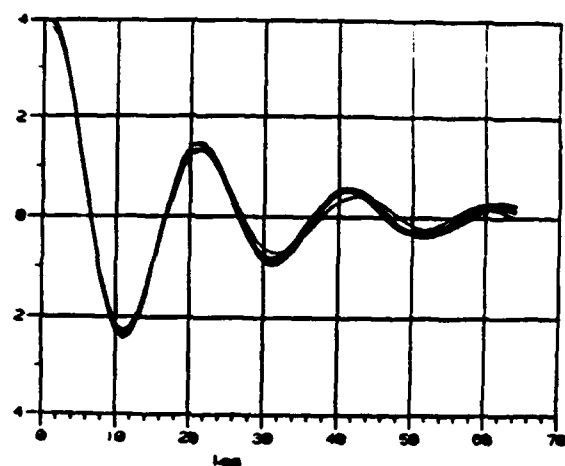


e

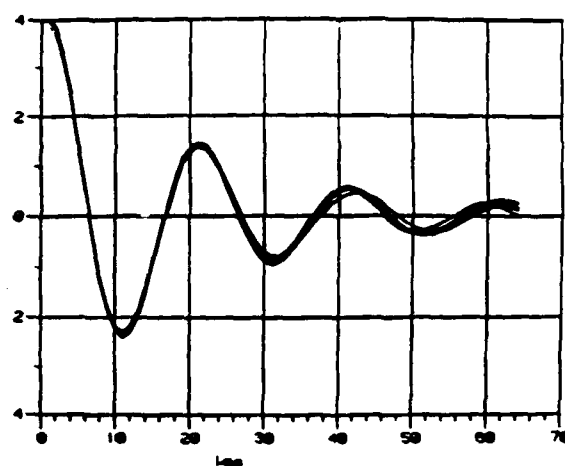


f

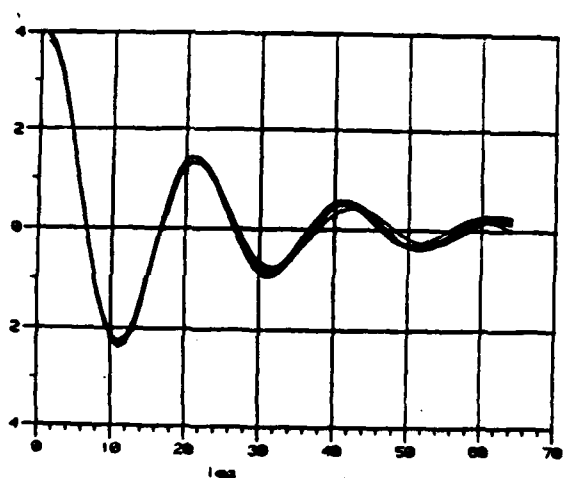
Fig. 7.B.2 Two channel AR(2) processes a.) channel 1 data (trial 1) b.) channel 2 data (trial 1) c.) channel 1 data (trial 2) d.) channel 2 data (trial 2) e.) ensemble averaged channel 1 autocorrelation (1,000 realizations) f.) ensemble averaged channel 2 autocorrelation (1,000 realizations).



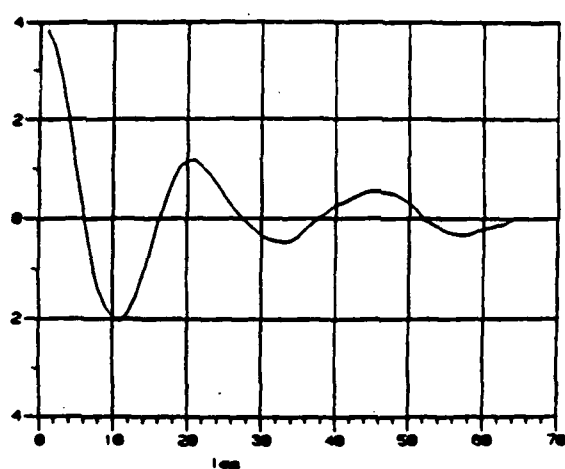
g



h



i



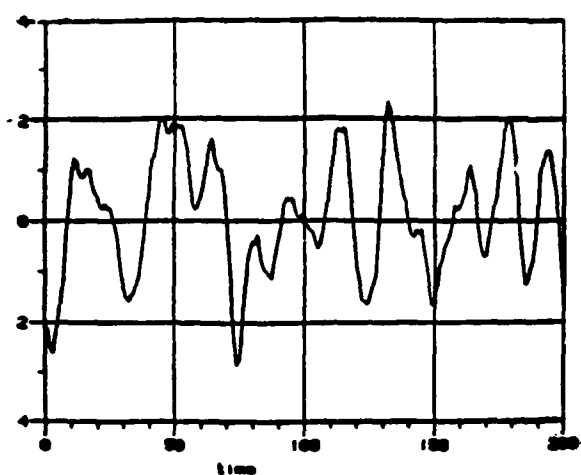
j

Fig. 7.B.2 (contin.) g.) time-averaged channel 1 autocorrelation (6 trials) h.)time averaged channel 2 autocorrelation (6 trials) i.) time-averaged cross-correlation (6 trials) j.) ensemble averaged cross-correlation (10,000 realizations).

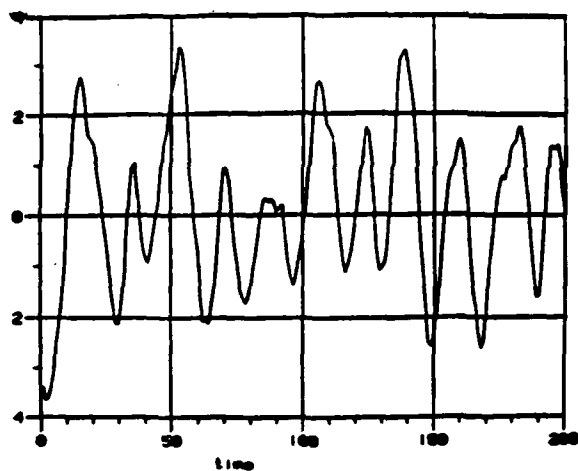
ensemble averaged autocorrelation functions for each channel. Six realizations of the corresponding time-averaged autocorrelation functions shown in plots g and h show a significant decrease in the variance of these functions as compared to the previous figure. Likewise the six realizations of the time-averaged cross-correlation function in plot i also show a reduction in their variance.

In Fig 7.B.3 and 7.B.4, the temporal correlation coefficients are held at 0.95 as in 7.B.2; however, the cross-correlation coefficient is reduced to 0.5 and 0.0, respectively. In each of these figures, plots a and b show a single realization of 200 sample observations. An overlay of six corresponding temporally-averaged autocorrelation functions, based on 10,000 time sample observations each, is shown in plots c and d. Six trials of the temporal-averaged cross-correlation function are shown in plot e, while the corresponding ensemble averaged result, based on 10,000 realizations, is shown in plot f. A visual comparison of the temporally-averaged autocorrelation functions in Figs 7.B.2g,h, 7.B.3c,d and 7.B.4c,d indicates that the variance associated with these plots appears to remain constant. Again, we note that λ_{11} and λ_{22} have remained constant, although $|\rho_{12}|$ has changed significantly. Close examination of the scale levels for the temporally averaged cross-correlation functions among these figures indicates that the variance of this function has not changed. We will discuss this point further in section VII.D.

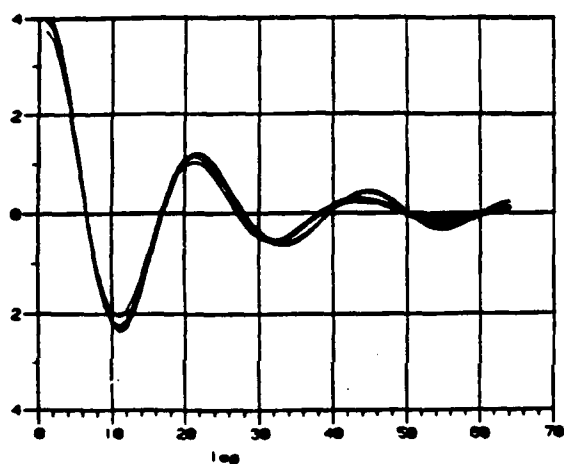
The cross-correlation coefficient is held at zero in Figs 7.B.5 and 7.B.6, while the temporal correlation coefficients are decreased to 0.8 and 0.4, respectively. Plots a and b for Figs 7.B.4, 7.B.5 and 7.B.6 show the effect of the decreasing temporal correlation; ie., the processes are becoming more whitened as λ_{ii} decreases. The resulting autocorrelation functions shown in plots c and d for these cases also reflect this trend by approaching a delta function as λ_{ii}



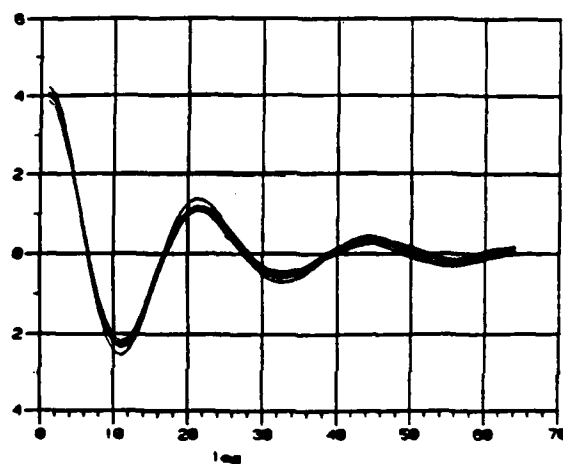
a



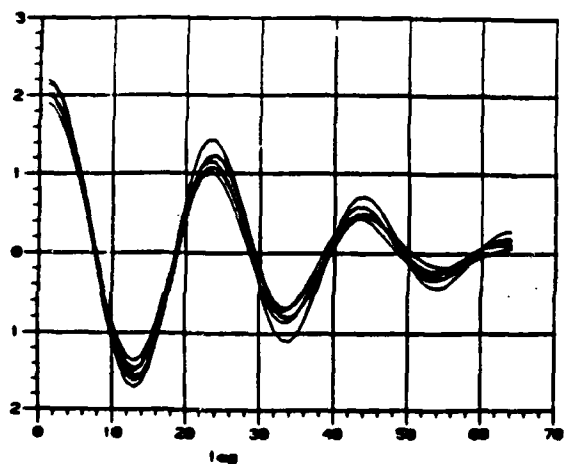
b



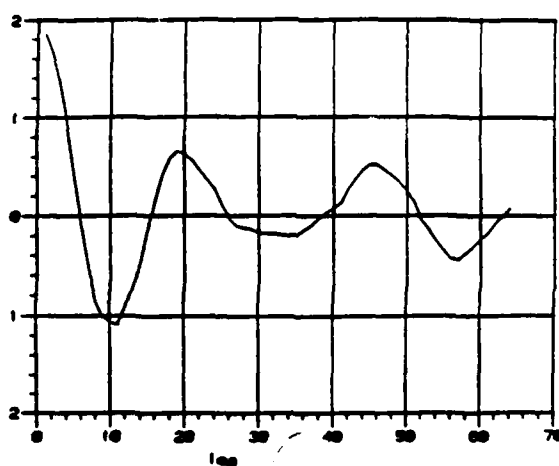
c



d



e



f

Fig. 7.B.3 Two channel AR(2) processes a.) channel 1 data b.) channel 2 data c.) time-averaged channel 1 autocorrelation (6 trials) d.) time-averaged channel 2 autocorrelation (6 trials) e.) time-averaged cross-correlation (6 trials) f.) ensemble averaged cross-correlation (10,000 realizations).

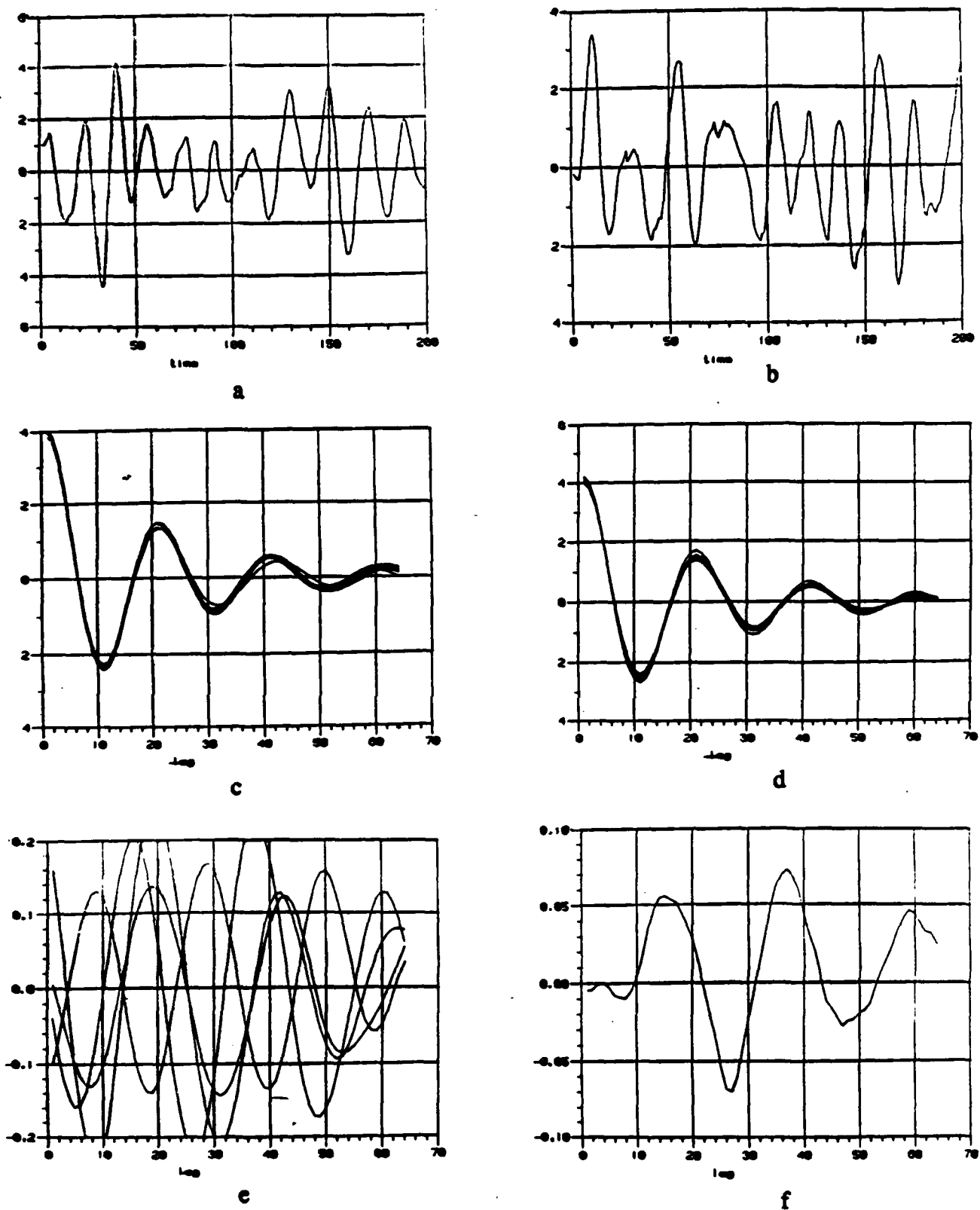


Fig. 7.B.4 Two channel AR(2) processes a.) channel 1 data b.) channel 2 data c.) time-averaged channel 1 autocorrelation (6 trials) d.) time-averaged channel 2 autocorrelation (6 trials) e.) time-averaged cross-correlation (4 trials) f.) ensemble averaged cross-correlation (10,000 realizations).

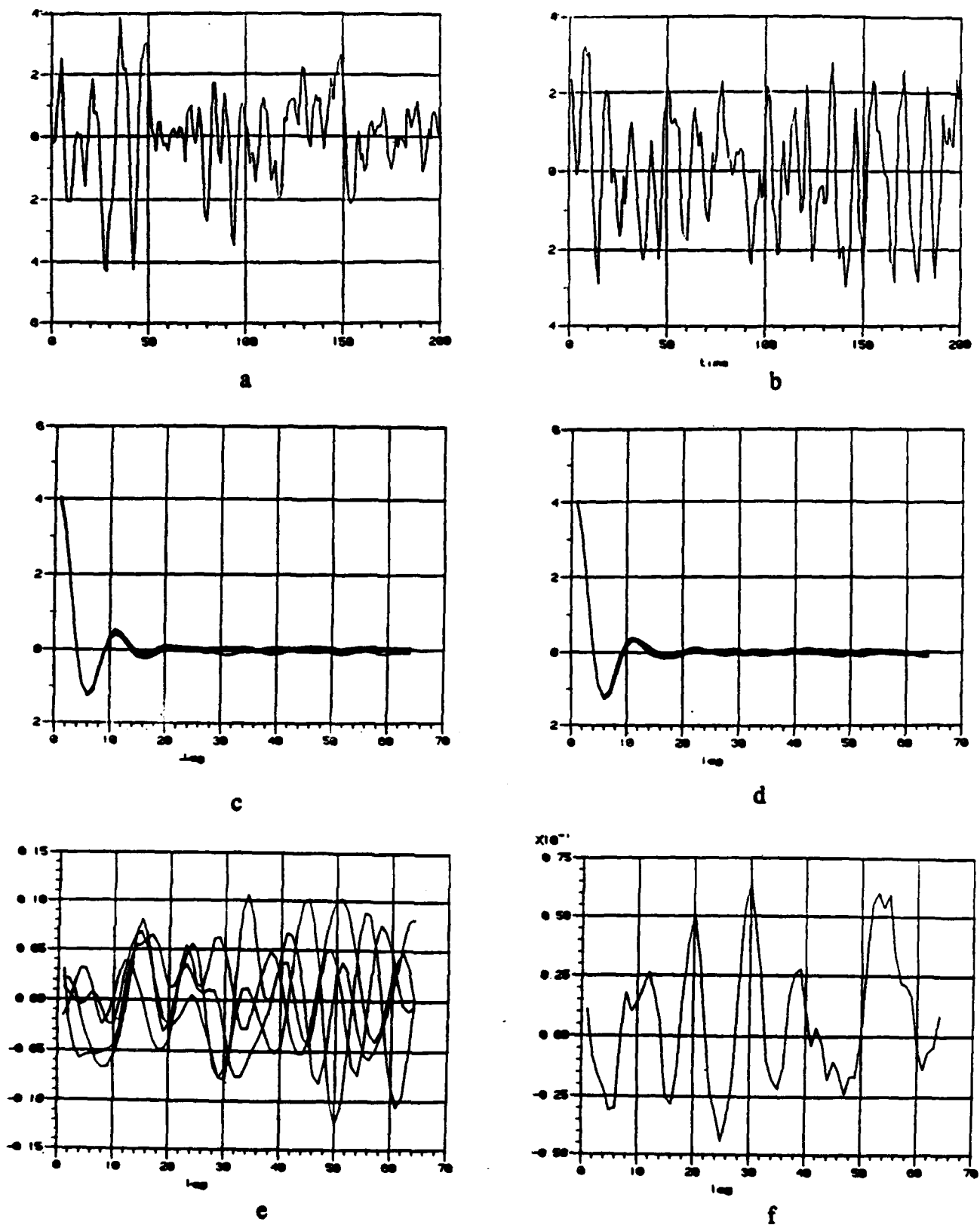
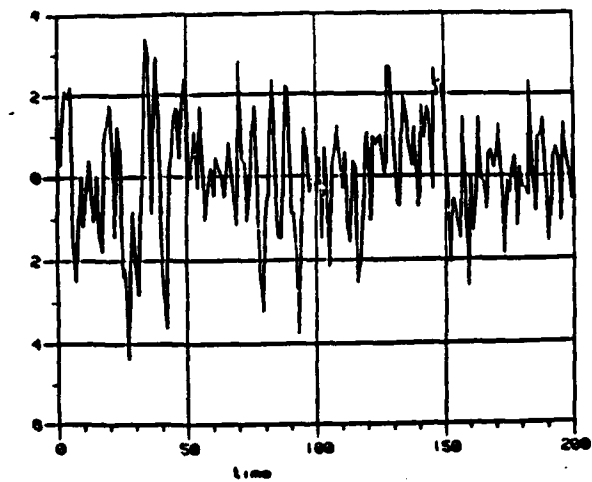
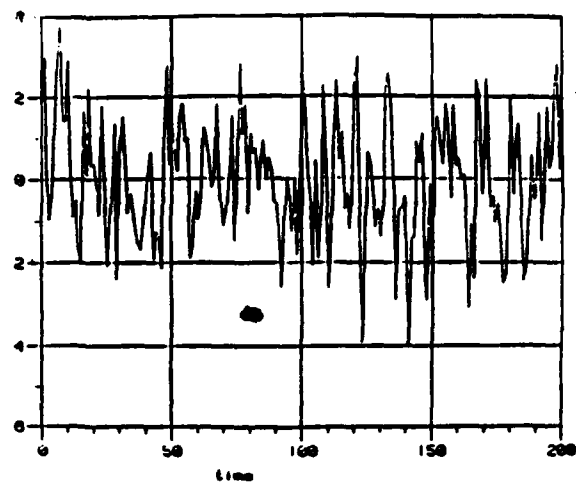


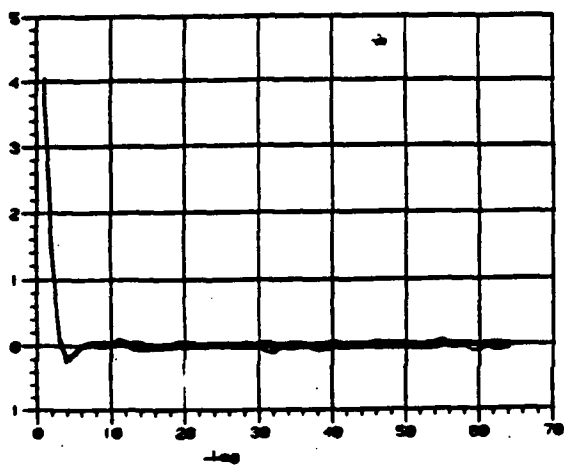
Fig. 7.B.5 Two channel AR(2) processes a.) channel 1 data b.) channel 2 data c.) time-averaged channel 1 autocorrelation (6 trials) d.) time-averaged channel 2 autocorrelation (6 trials) e.) time-averaged cross-correlation (6 trials) f.) ensemble averaged cross-correlation (10,000 realizations).



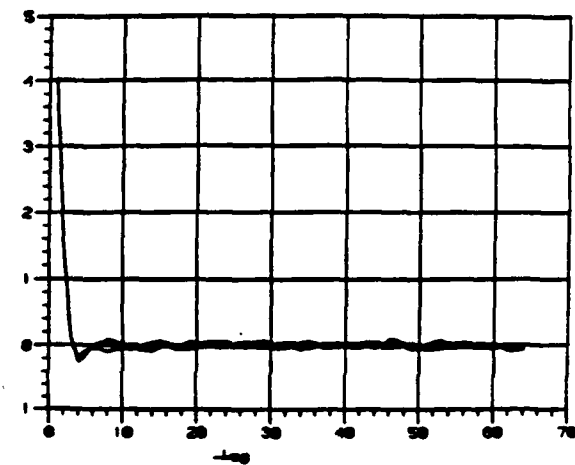
a



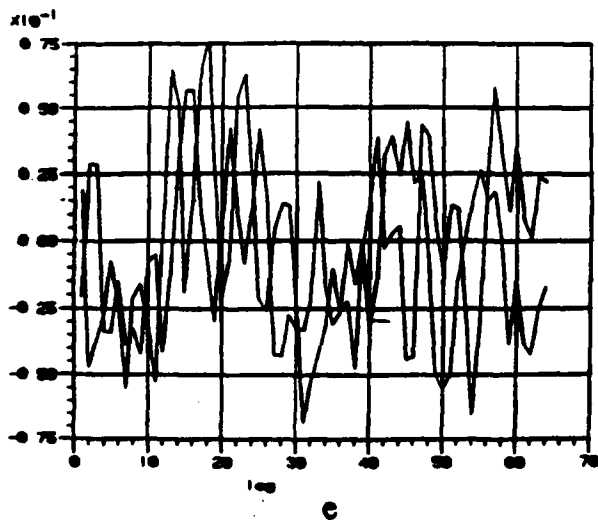
b



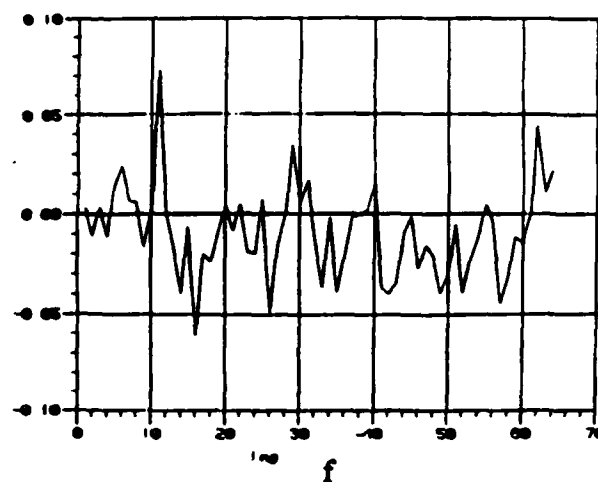
c



d



e



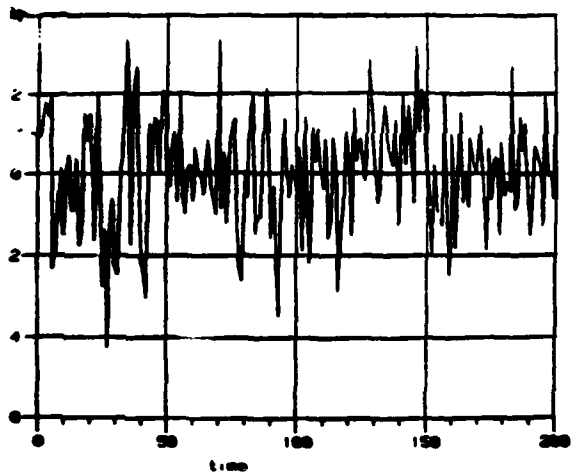
f

Fig. 7.B.6 Two channel AR(2) processes a.) channel 1 data b.) channel 2 data c.) time-averaged channel 1 autocorrelation (6 trials) d.) time-averaged channel 2 autocorrelation (6 trials) e.) time-averaged cross-correlation (6 trials) f.) ensemble averaged cross-correlation (10,000 realizations).

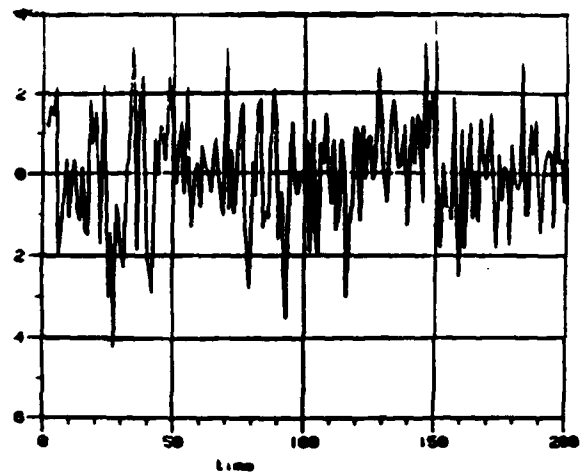
decreases. Close examination of plot e in each of these figures provides some indication that the variance of the cross-correlation function decreases as λ_{11} and λ_{22} decrease.

In Figs 7.B.7 through 7.B.12, similar plots are shown. Fig 7.B.7 shows the case of two noisy processes which are highly correlated. In Fig 7.B.8, the temporal cross-correlation coefficient λ_{12} is raised to 0.97. The value of $|\rho_{12}|$ was lowered to 0.3 in order to satisfy the positive semi-definiteness constraint condition. We note that in the expanded view of the cross-correlation function displayed in Fig 7.B.8f, the resulting estimated values at these lags remain high out to the lag value of 2. Beyond $l = 2$, however, the cross-correlation function drops significantly. This result will be discussed later. Fig 7.B.10 shows the interesting result obtained when the noisy signal on channel 2 is required to be correlated with the high temporally correlated channel 1 process. Fig 7.B.10c shows an overlay of the two distributions shown in plots a and b. As this figure indicates, the noisy channel 2 process appears as a modulation on the channel 1 process. It is also noted that the autocorrelation functions for each channel have maxima and minima which occur at the same lag values. In addition, an interesting peak occurs at the third lag value in plot e. We will consider this later.

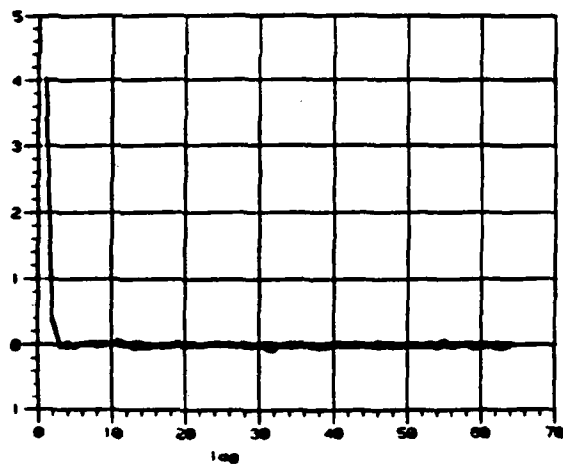
Finally, we consider the results shown in Figs 7.B.11 and 7.B.12, where l_{12} is specified to be 4. In these figures, we use AR(2) and AR(4) processes, respectively. Plots a and b in each figure show 200 samples of the processes. As in the previous case, the difference in temporal correlation on each channel is noted. The overlay in Fig 7.B.11c shows the effect of the distinct variances on each channel as well as the moderate amount of cross-correlation. Six realizations of the corresponding autocorrelation functions are shown in plots d



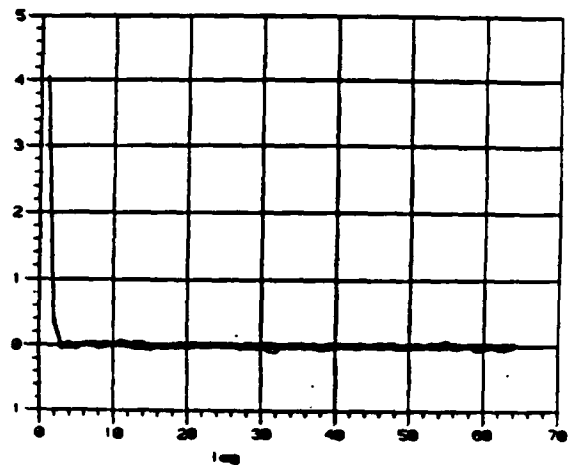
a



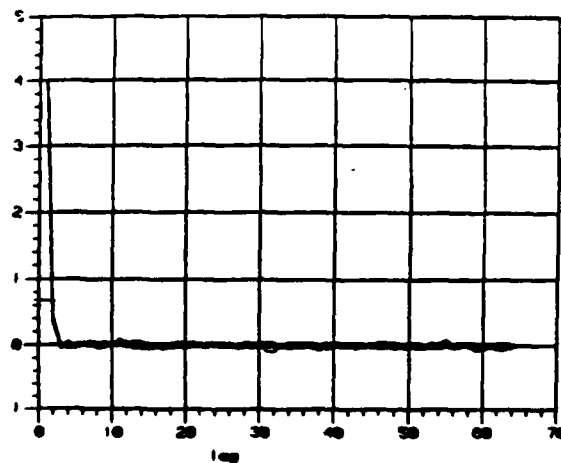
b



c



d



e

Fig. 7.B.7 Two channel AR(2) processes a.) channel 1 data b.) channel 2 data c.) time-averaged channel 1 autocorrelation (6 trials) d.) time-averaged channel 2 autocorrelation (6 trials) e.) time-averaged cross-correlation (6 trials).

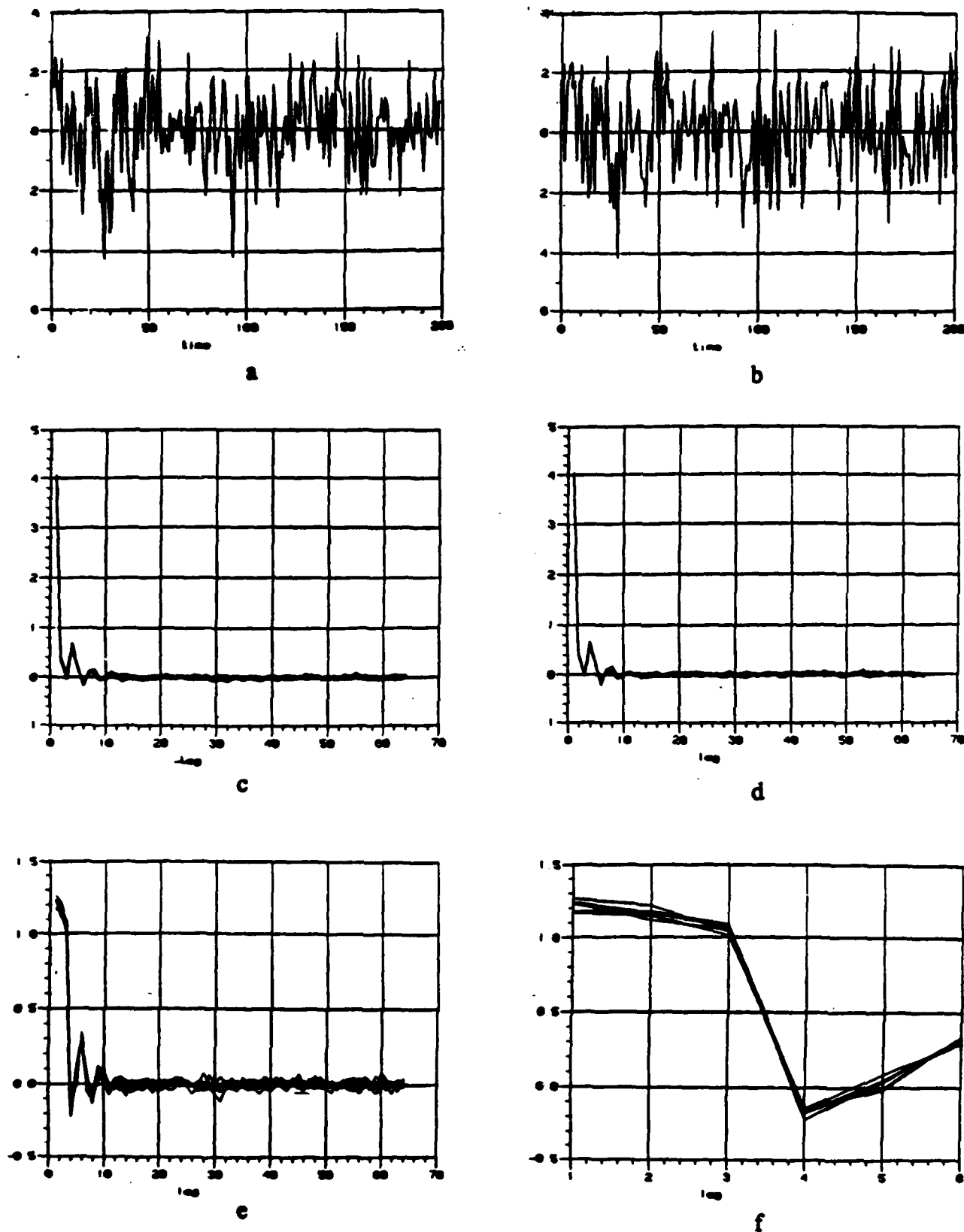


Fig. 7.B.8 Two channel AR(2) processes a.) channel 1 data b.) channel 2 data c.) time-averaged channel 1 autocorrelation (6 trials) d.) time-averaged channel 2 autocorrelation (6 trials) e.) time-averaged cross-correlation (64 lags-6 trials) f.) time-averaged cross-correlation (6 lags-6 trials).

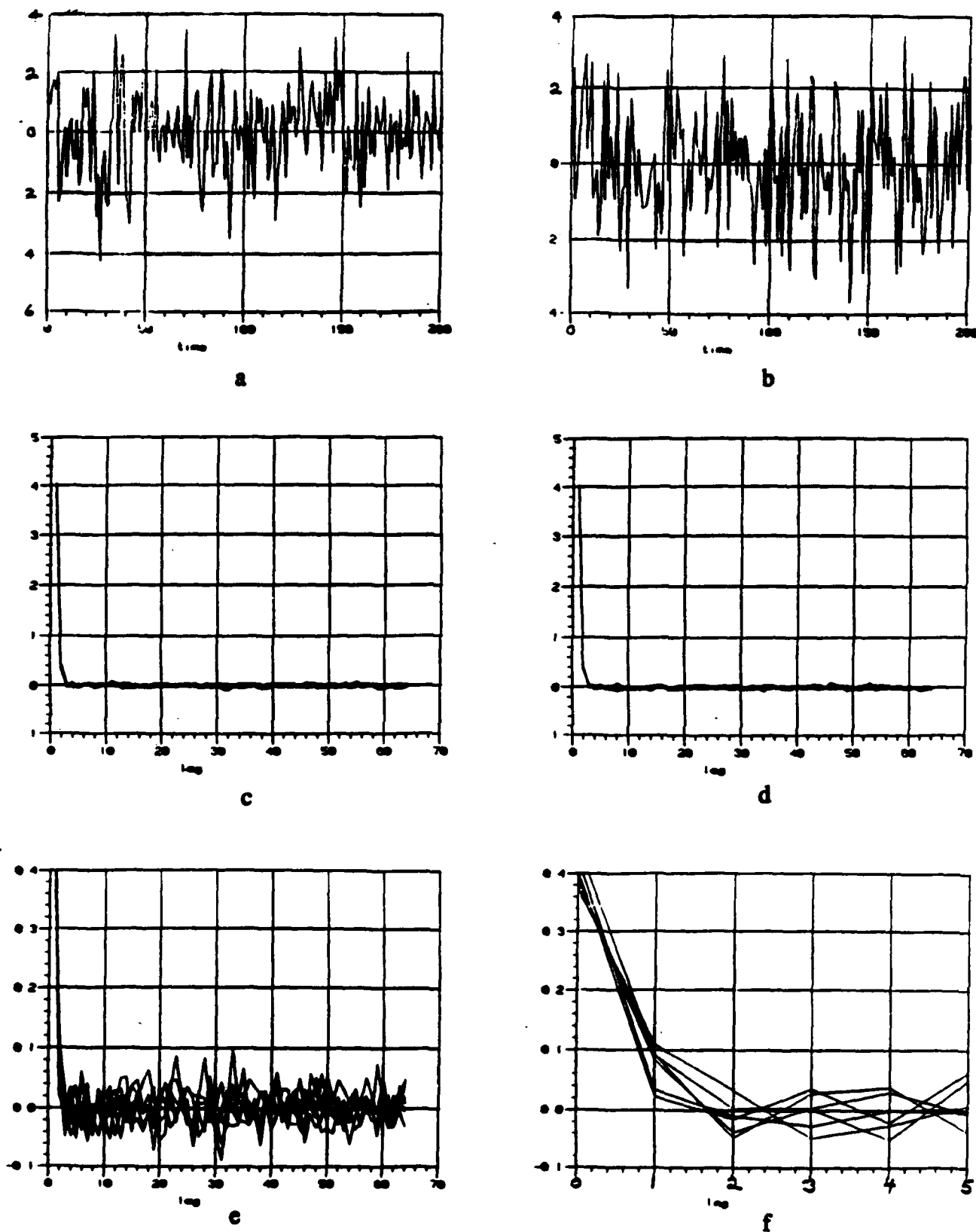
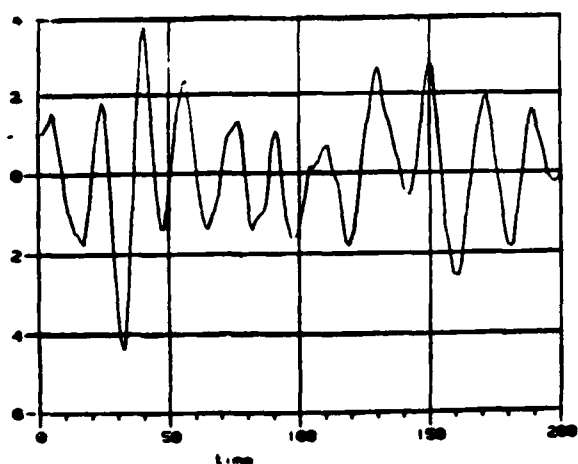
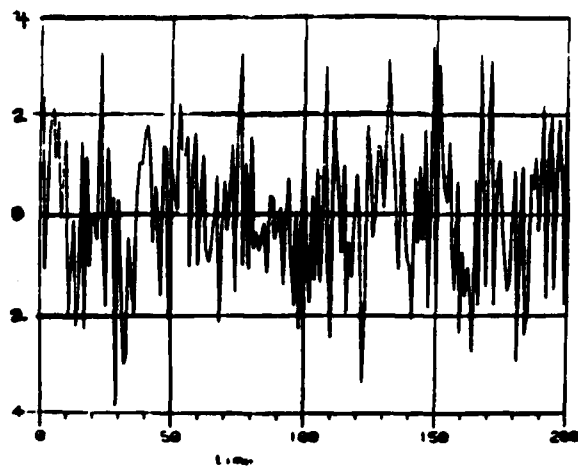


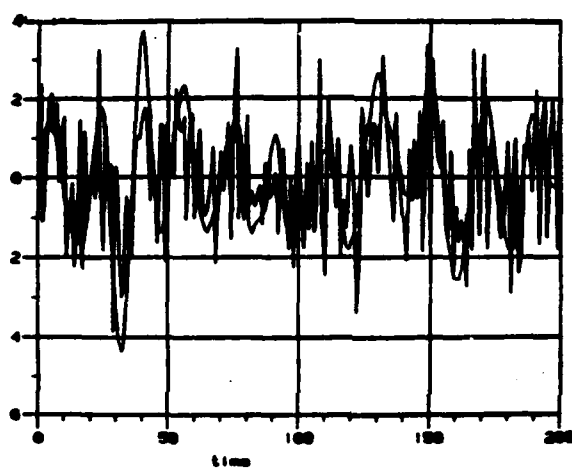
Fig. 7.B.9 Two channel AR(2) processes a.) channel 1 data b.) channel 2 data c.) time-averaged channel 1 autocorrelation (6 trials) d.) time-averaged channel 2 autocorrelation (6 trials) e.) time-averaged cross-correlation (64 lags-6 trials) f.) time-averaged cross-correlation (6 lags-6 trials).



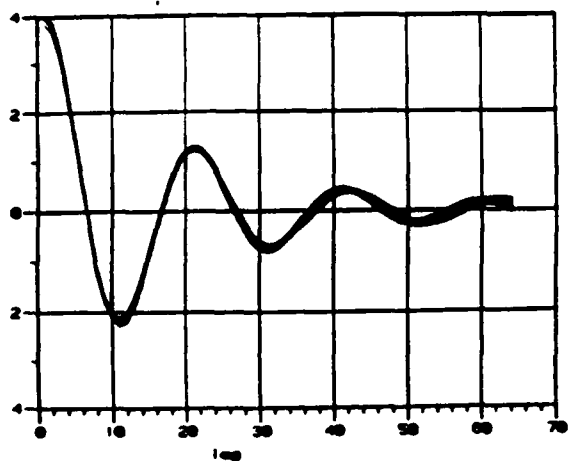
a



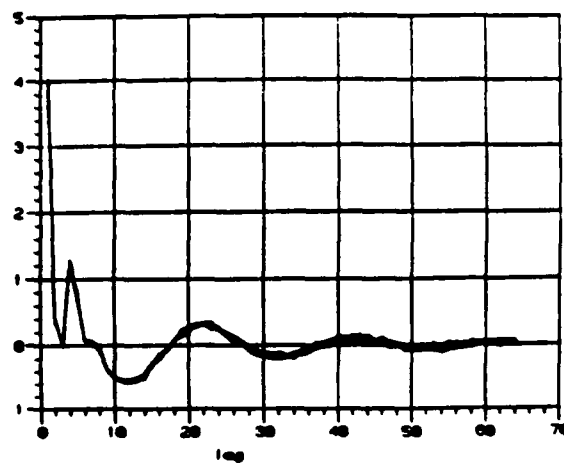
b



c



d



e

Fig. 7.B.10 Two channel AR(2) processes a.) channel 1 data b.) channel 2 data c.) overlay of channels 1 and 2 d.) time-averaged channel 1 auto- correlation (6 trials) e.) time-averaged channel 2 autocorrelation (6 trials).

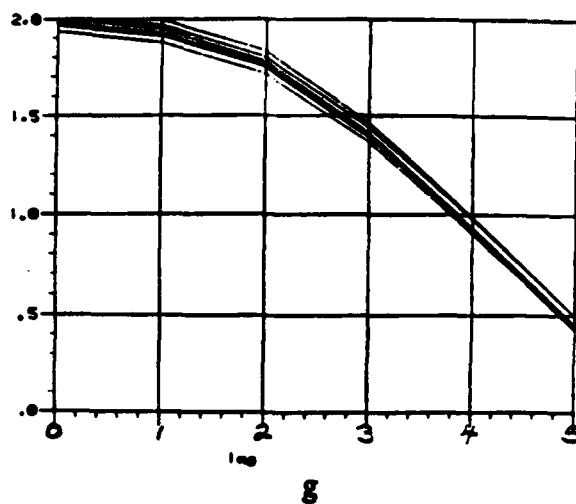
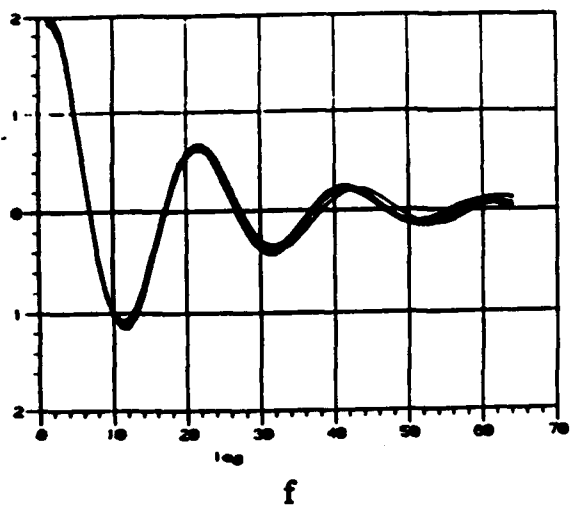
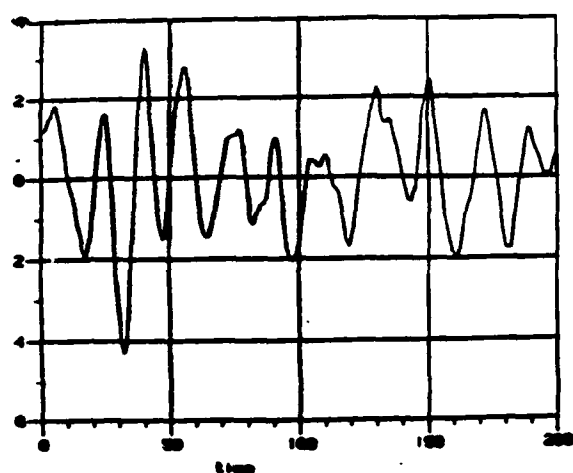
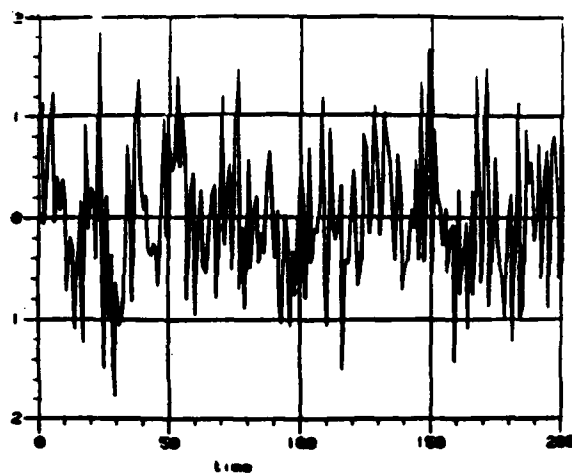


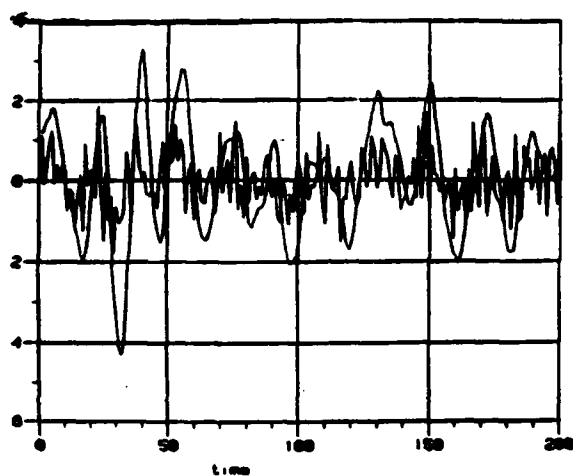
Fig 7.B.10 (contin.) f.) time-averaged cross-correlation (64 lags-6 trials) g.) time-averaged cross-correlation (6 lags-6 trials).



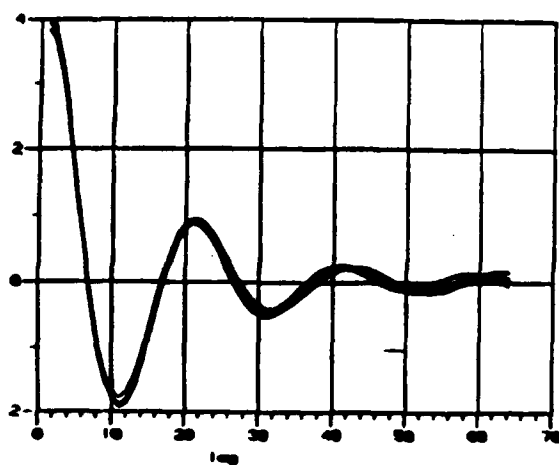
a



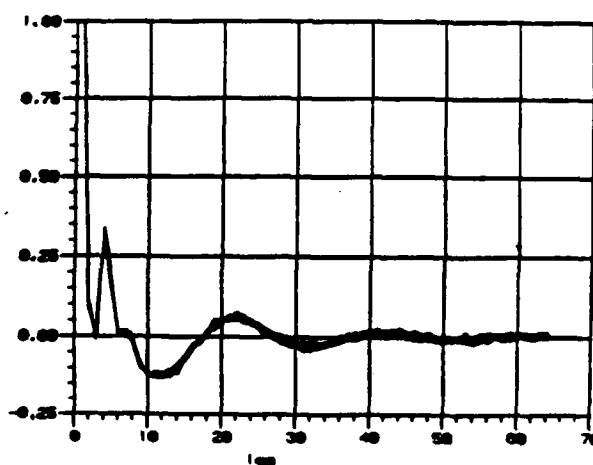
b



c



d



e

Fig. 7.B.11 Two channel AR(2) processes a.) channel 1 data b.) channel 2 data c.) overlay of channels 1 and 2 d.) time-averaged channel 1 auto- correlation (6 trials) e.) time-averaged channel 2 autocorrelation (6 trials).

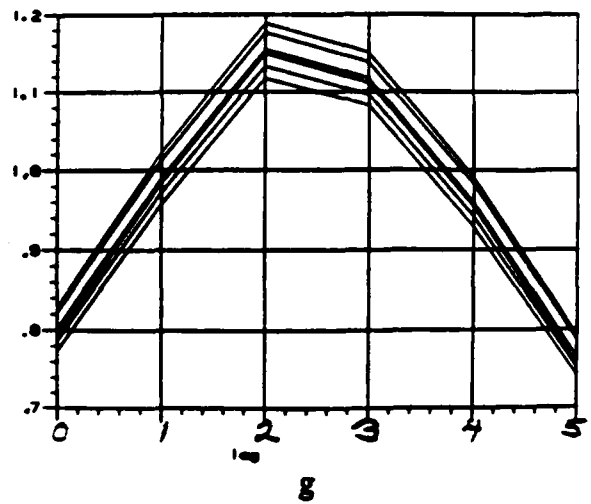
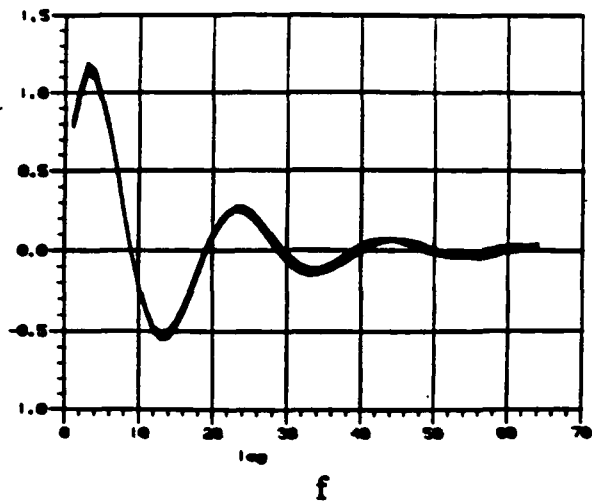
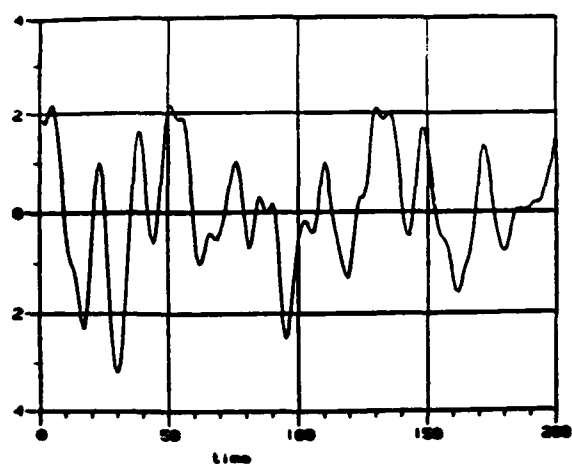
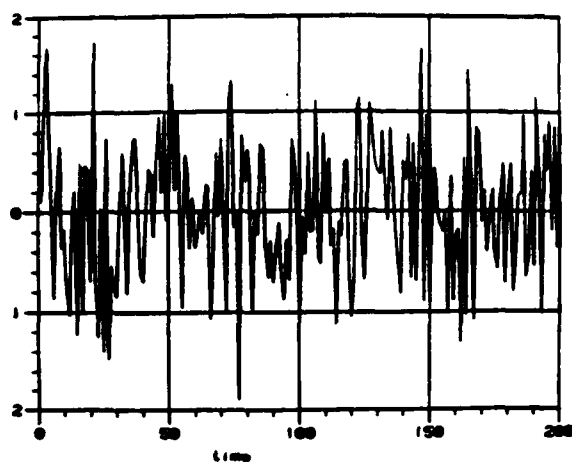


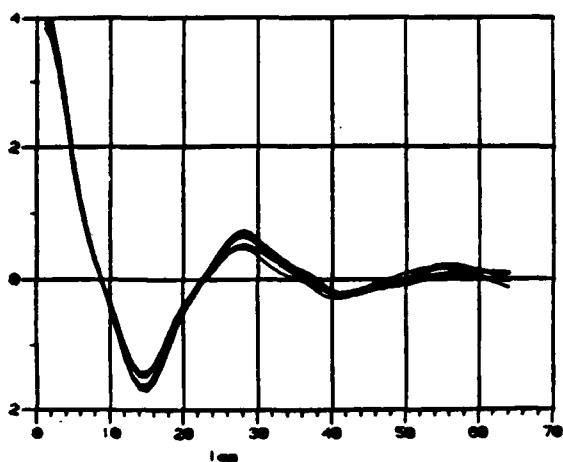
Fig 7.B.11 (contin.) f.) time-averaged cross-correlation (64 lags-6 trials) g.) time-averaged cross-correlation (6 lags-6 trials).



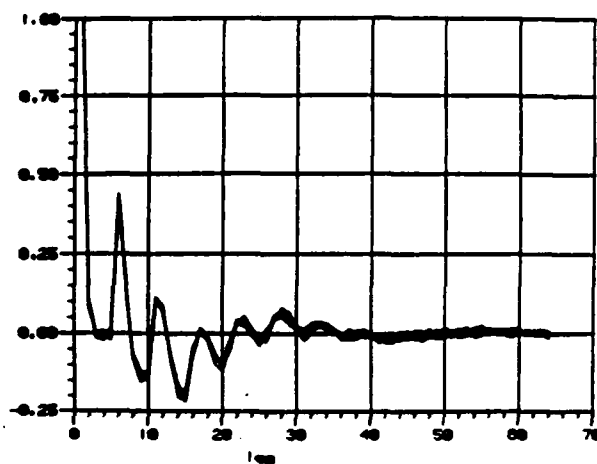
a



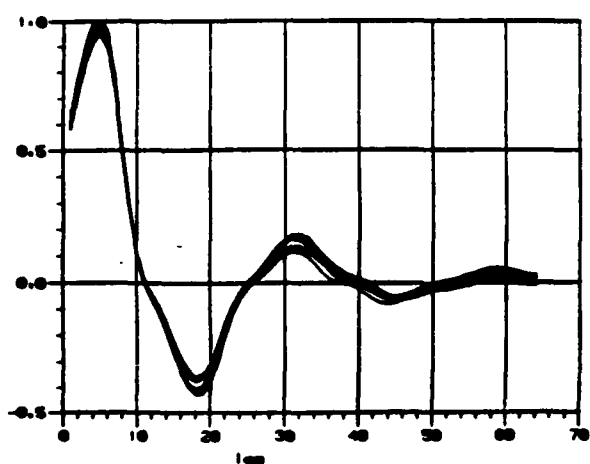
b



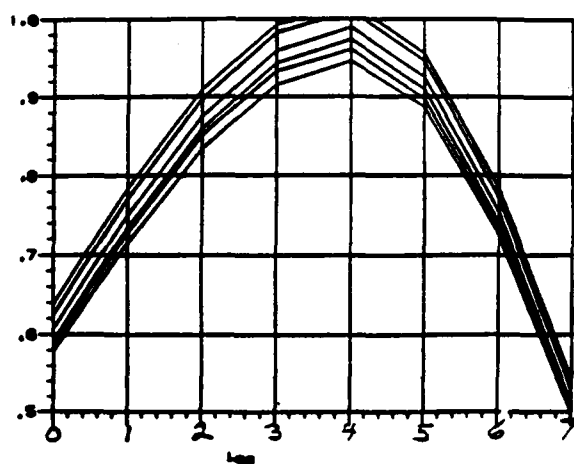
c



d



e



f

Fig. 7.B.12 Two channel AR(4) processes a.) channel 1 data b.) channel 2 data c.) time-averaged channel 1 autocorrelation (6 trials) d.) time- averaged channel 2 autocorrelation (6 trials) e.) time-averaged cross- correlation (64 lags-6 trials) f.) time-averaged cross-correlation (8 lags-6 trials).

and e for Fig 7.B.11 and plots c and d for Fig 7.B.12. The cross-correlation functions (six realizations) are displayed in the last two plots in each figure for 64 and 8 lag values, respectively. We note that in Fig 7.B.11g, the cross-correlation function peaks at a lag value of $l_{12} = 2$ rather than $l_{12} = 4$. In Fig 7.B.12f, however, we note that for the AR(4) process, the cross-correlation function does peak at $l_{12} = 4$. We also mention that in the case of the AR(4) process described in Fig 7.B.12, the parameter $|p_{12}|$ had to be lowered to the value of 0.3. This was necessary to maintain the positive semi-definiteness requirement. Finally, in plots c and d for Fig 7.B.12, we again note that the maxima and minima occur at the same lag values. In addition, we note that for this AR(4) process, the peak values of the channel 2 autocorrelation function follow the shape of the channel 1 autocorrelation function. The rapid decrease in this function between the peak values is a measure of the 'noisy' channel 2 process. The periodic peak values, however, are a measure of the correlation on this channel resulting from its moderate degree of cross-correlation (ie., $|p_{12}|=0.3$) with the high temporally correlated channel 1 process.

Considerable insight into the process generation scheme can be obtained by examining the coefficients in Table 7.B.2 which were determined from a solution of the Yule-Walker equation. For Fig 7.B.1, we first note that the white noise driving covariance matrix C has very low values compared to those in the $A(1)$ and $A(2)$ matrices. This will cause the resulting processes to be highly dependent upon the past data samples with minimal dependence upon the driving white noise vector. This increases the temporal correlation on the channel processes. In addition, the c_{11} and c_{21} elements of this matrix are approximately equal, while c_{44} is much smaller. This will cause the elements of the vector $\underline{u}(n)$ in eq(7.A.7) to be nearly identical, thus contributing to the high cross-correlation. We again

point out that in this case of high temporal correlation, the C matrix has small values. This will cause the variance of the white noise driving term to be small. If the overall variance of the process is required to be large, the synthesis process must be operated over a long initial transient period to allow the processes to reach sufficient magnitude. For this case, only 2,000 initial samples were generated before saving. This quantity was not sufficient and thus the low values shown in Fig 7.B.1f resulted.

In Fig 7.B.2, the c_{11} and c_{21} elements are again nearly equal and much greater than c_{44} so that the very high cross-correlation is obtained. We note, however, that all the C matrix elements have increased as compared to the previous case. This will cause the additive white noise driving variance to have a more significant effect on the resulting process. As a result, temporal correlation on each channel will decrease as expected since the λ_{11} and λ_{22} values have been decreased.

In Figs 7.B.4, we note that only c_{11} and c_{44} are non-zero. This will cause the vector $\underline{u}(n)$ to have totally uncorrelated elements, thus providing no cross-correlation as required since $|\rho_{12}|=0$. Examination of these elements for Figs 7.B.4 through 7.B.8 shows the increasing significance of the white noise driving term relative to the past values; ie., the C matrix eventually begins to weight the white noise vector $\underline{y}(n)$ higher than the $A(k)$ $k=1,2$ matrices weight the past samples. Thus, the temporal correlation decreases.

Fig.	A(1)	A(2)	C
7.B.1	$\begin{bmatrix} -1.98 & 4.54 \times 10^{-4} \\ 4.54 \times 10^{-4} & -1.98 \end{bmatrix}$	$\begin{bmatrix} 0.984 & -4.54 \times 10^{-4} \\ -4.54 \times 10^{-4} & -0.984 \end{bmatrix}$	$\begin{bmatrix} 0.0051 & 0.0 \\ 0.0049 & 0.0015 \end{bmatrix}$
7.B.2	$\begin{bmatrix} -1.81 & -3.6 \times 10^{-6} \\ 0.0 & -1.81 \end{bmatrix}$	$\begin{bmatrix} 0.903 & -3.8 \times 10^{-6} \\ 0.0 & 0.903 \end{bmatrix}$	$\begin{bmatrix} 0.269 & 0.0 \\ 0.266 & 0.038 \end{bmatrix}$
7.B.3	$\begin{bmatrix} -1.795 & -0.0313 \\ -0.0313 & -1.795 \end{bmatrix}$	$\begin{bmatrix} 0.903 & -6.23 \times 10^{-3} \\ -6.23 \times 10^{-3} & 0.903 \end{bmatrix}$	$\begin{bmatrix} 0.265 & 0.0 \\ 0.066 & 0.257 \end{bmatrix}$
7.B.4	$\begin{bmatrix} -1.81 & 0.0 \\ 0.0 & -1.81 \end{bmatrix}$	$\begin{bmatrix} 0.903 & 0.0 \\ 0.0 & 0.903 \end{bmatrix}$	$\begin{bmatrix} 0.269 & 0.0 \\ 0.0 & 0.269 \end{bmatrix}$
7.B.5	$\begin{bmatrix} -1.31 & 0.0 \\ 0.0 & -1.31 \end{bmatrix}$	$\begin{bmatrix} 0.64 & 0.0 \\ 0.0 & 0.64 \end{bmatrix}$	$\begin{bmatrix} 0.922 & 0.0 \\ 0.0 & 0.922 \end{bmatrix}$
7.B.6	$\begin{bmatrix} -0.464 & 0.0 \\ 0.0 & -0.464 \end{bmatrix}$	$\begin{bmatrix} 0.16 & 0.0 \\ 0.0 & 0.16 \end{bmatrix}$	$\begin{bmatrix} 1.81 & 0.0 \\ 0.0 & 1.81 \end{bmatrix}$
7.B.7	$\begin{bmatrix} -0.101 & 4.84 \times 10^{-7} \\ 4.78 \times 10^{-7} & -0.101 \end{bmatrix}$	$\begin{bmatrix} -0.01 & -2.9 \times 10^{-8} \\ -2.9 \times 10^{-8} & -0.01 \end{bmatrix}$	$\begin{bmatrix} 1.99 & 0.0 \\ 1.97 & 0.281 \end{bmatrix}$
7.B.8	$\begin{bmatrix} 0.072 & -0.334 \\ -0.334 & 0.072 \end{bmatrix}$	$\begin{bmatrix} 0.183 & -0.31 \\ -0.31 & 0.184 \end{bmatrix}$	$\begin{bmatrix} 1.82 & 0.0 \\ 0.74 & 0.166 \end{bmatrix}$
7.B.9	$\begin{bmatrix} -0.099 & -0.010 \\ -0.010 & -0.099 \end{bmatrix}$	$\begin{bmatrix} 0.099 & -0.019 \\ -0.019 & 0.099 \end{bmatrix}$	$\begin{bmatrix} 1.989 & 0.0 \\ 0.195 & 1.980 \end{bmatrix}$
7.B.10	$\begin{bmatrix} -1.792 & -0.0311 \\ -0.801 & 0.257 \end{bmatrix}$	$\begin{bmatrix} 0.9174 & -0.0292 \\ 0.0166 & 0.3545 \end{bmatrix}$	$\begin{bmatrix} 0.261 & 0.0 \\ 0.521 & 1.519 \end{bmatrix}$
7.B.11	$\begin{bmatrix} -1.632 & -0.149 \\ -0.782 & 0.162 \end{bmatrix}$	$\begin{bmatrix} 0.789 & -0.154 \\ 0.545 & 0.321 \end{bmatrix}$	$\begin{bmatrix} 0.213 & 0.0 \\ 0.639 & 0.608 \end{bmatrix}$
7.B.12	$\begin{bmatrix} -3.093 & -0.0418 \\ -4.053 & 0.283 \end{bmatrix}$	$\begin{bmatrix} 3.974 & -0.0386 \\ -8.2604 & 0.4039 \end{bmatrix}$	$\begin{bmatrix} 0.0665 & 0.0 \\ 0.5798 & 0.5834 \end{bmatrix}$
	A(3)	A(4)	
	$\begin{bmatrix} -2.573 & -0.0375 \\ -6.797 & 0.4123 \end{bmatrix}$	$\begin{bmatrix} 0.698 & -0.0384 \\ 2.085 & 0.452 \end{bmatrix}$	

Table 7.B.2

For the matrix elements corresponding to the Fig 7.B.8 results, we make the following observations. First, the relatively high values of the C matrix elements compared to the A(k) matrices again provides emphasis on the white noise driving term. Second, the relatively high and equal off-diagonal elements of the two A(k) matrices provides high cross-correlation with respect to the two past sample values. This result is controlled by the high value of $\lambda_{12}=0.97$. Third, the value $|\rho_{12}|=0.3$ has a significant effect on the c_{21} element. It is near the uppermost value for the cross-correlation coefficient that can be obtained under the constraint condition of positive semi-definiteness. The result is that the white noise vector is provided a moderately high cross-correlation. This case can be contrasted with the coefficients for Fig 7.B.9. In this case, the low value of $\lambda_{12}=0.2$ and $|\rho_{12}|=0.1$ causes the off-diagonal elements in the A(k) matrices and the c_{21} to decrease significantly.

C. The Autocorrelation Function Ergodicity Results

In this section, we will evaluate the ergodicity of the autocorrelation function. This will be accomplished by evaluating the variance of the time-averaged autocorrelation function as determined by its ergodic series. In section IV.A, we developed the expression described by eq(4.A.15). In that case, the time-averaged autocorrelation function $R_{iiT}(l)$ was estimated using eq(4.A.1). In practice, however, we use expressions such as the estimator

$$\hat{R}_{iiT}(l, N_T) = \begin{cases} \frac{1}{M} \sum_{n=0}^{N_T-l-1} x_i(n) x_i^*(n-l) & 0 \leq l \leq N_T-1 \\ \frac{1}{M} \sum_{n=0}^{N_T-||l|-1} x_i^*(n) x_i(n-||l|) & -(N_T-1) \leq l \leq 0. \end{cases} \quad (7.C.1)$$

For $M = N_T$, we obtain the biased estimator while for $M = N_T - l$, we have the unbiased estimator. In Appendix B, we derive the expression for the variance of the biased estimator and obtain

$$V_{B_{ii}}(l, N_T) = \frac{1}{N_T} \sum_{k=-(N_T-||l|-1)}^{N_T-||l|-1} \left[1 - \frac{||l|+|k|}{N_T} \right] C_{\phi\phi}(k, l) \quad (7.C.2a)$$

$$= \frac{1}{N_T} \sum_{k=-(N_T-||l|-1)}^{N_T-||l|-1} \left[1 - \frac{||l|+|k|}{N_T} \right] \left[|R_{ii}(k)|^2 + \text{Re}\{F_{ii}(l, k)\} \right] \quad (7.C.2b)$$

In the case where $F_{ii}(l, k)=0$, the form of eq(7.C.2b) indicates that $V_{B_{ii}}(l)$ decreases as a function of lag l . This results from the decreasing number of positive terms in the summation as well as the decrease in the first bracketed term

as lag l increases. This is to be contrasted with the form of eq(4.A.18) where the variance at each lag value was determined using the same number of sample values. As a result, eq(4.A.18) provided a constant variance independent of l when $F_{ij}(l,k)=0$. Finally, in [7] it is noted that the variance of the unbiased estimator may increase as a function of l since this variance expression has the term $\frac{1}{N_T - ||l||}$ before the summation.

In this section, we will consider the special case of the real, exponentially shaped autocorrelation function, and synthesize an AR(1) process. The real AR(1) process also has an exponential autocorrelation function expressed as

$$R_{AR}(k) = R_{AR}(0) [-a(1)]^{|k|} \quad (7.C.3a)$$

$$= \sigma_{AR}^2 [-a(1)]^{|k|}. \quad (7.C.3b)$$

where

$$R_{AR}(0) = \frac{\sigma_u^2}{1 - a^2(1)} = \sigma_{AR}^2 \quad (7.C.4)$$

and σ_u^2 , $a(1)$ and σ_{AR}^2 are the white noise driving variance, the AR(1) parameter, and the variance of the AR(1) process, respectively. Eq(7.C.4) follows from the Yule-Walker equation where

$$\sigma_u^2 = R_{AR}(0) + a(1)R_{AR}(-1) \quad (7.C.5a)$$

$$= \sigma_{AR}^2 - a^2(1) \sigma_{AR}^2 \quad (7.C.5b)$$

$$= \sigma_{AR}^2 [1 - a^2(1)]. \quad (7.C.5c)$$

With

$$-a(1) = \lambda_{AR} \quad (7.C.6)$$

we have

$$R_{AR}(k) = \sigma_{AR}^2 [\lambda_{AR}]^{|k|}. \quad (7.C.7)$$

Therefore, in this special case, the AR(1) autocorrelation function is equivalent to the autocorrelation function used in the correlation matrix of the Yule-Walker eq(6.A.1). In section IV, the functional form of the autocorrelation function expressed by eq(4.A.19) was used in eq(4.A.18). We note that this autocorrelation function is the function to which the synthesized processes are providing a best 'fit'. If, however, we are attempting to validate an analytic expression for eq(4.A.18) or eq(7.C.2b) using the synthesized AR processes, we must use the form for the AR autocorrelation function in this expression rather than the functional form which we are attempting to 'fit'. In general, the AR autocorrelation functions are a rather complicated function of the AR parameters[11]. In the case of the AR(1) process, however, we use eq(7.C.7) in (7.C.2b). We also note that in the case where $R_{ii}(\alpha)$ is real, the in-phase and quadrature components of the synthesized outputs are uncorrelated (see Appendix F) so that

$$R_{ii}^{QI}(\alpha) = R_{ii}^{IQ}(\alpha) = 0 \quad \text{all } \alpha. \quad (7.C.8)$$

In Appendix F, we also show that in this case

$$R_{ii}^{II}(\alpha) = R_{ii}^{QQ}(\alpha) \quad \text{all } \alpha \quad (7.C.9a)$$

and at $\alpha = 0$

$$R_{ii}^{\Pi}(0) = R_{ii}^{QQ}(0) = \sigma_{ii}^2 / 2. \quad (7.C.9b)$$

Using these equations in eqs(4.A.17a) and (4.A.17b), we have

$$\text{Re}\{F_{ii}(l,k)\} = 0 \quad \text{all } l,k. \quad (7.C.10)$$

From eq(7.C.7), eq(7.C.2b) becomes

$$V_{B_{ii}}(l, N_T) = \frac{1}{N_T} \sum_{k=-(N_T-|l|-1)}^{N_T-|l|-1} \left[1 - \frac{|l|+|k|}{N_T} \right] |R_{ii}(k)|^2 \quad (7.C.11a)$$

$$= \frac{1}{N_T} \sum_{k=-(N_T-|l|-1)}^{N_T-|l|-1} \left[1 - \frac{|l|+|k|}{N_T} \right] \sigma_{AR}^4 (\lambda_{AR})^{2|k|}. \quad (7.C.11b)$$

Eq(7.C.11b) is an analytic expression for the variance of the time-averaged autocorrelation function of the AR(1) process considered in this case. We now consider the expression used to calculate this variance with the synthesized data. Consider N_R realizations of the random process $x_i(n)$. Let each realization be indexed by the integer α ; $\alpha=1,2,\dots,N_R$. Corresponding to the realization with index α , let $\hat{R}_{iiT_b}(l, N_T|\alpha)$ be the biased, time-averaged cross-correlation function estimate using N_T observation samples. The sample variance of the time-averaged cross-correlation function estimates is computed from N_R realizations using the expression

$$\text{Var}[\hat{R}_{iiT_b}(l, N_T):N_R] = \frac{1}{N_R-1} \sum_{\alpha=1}^{N_R} |\hat{R}_{iiT_b}(l, N_T|\alpha) - \bar{\hat{R}}_{iiT_b}(l, N_R|\alpha)|^2 \quad (7.C.12)$$

where

$$\bar{\hat{R}}_{iiT_b}(l, N_R|\alpha) = \frac{1}{N_R} \sum_{\alpha=1}^{N_R} \hat{R}_{iiT_b}(l, N_T|\alpha). \quad (7.C.13)$$

In Fig 7.C.1, the maximum value of $V_{B_{ii}}(l, N_T)$, which occurs at $l=0$, is plotted (solid curves) as a function of $\lambda_{ii}=\lambda_{AR}$ for $N_T=100$ and $N_T=1000$ using the analytic expression of eq(7.C.11b). The corresponding sample variances of the time-averaged autocorrelation function estimates computed by eq(7.C.12) at lag zero using the synthesized data processes are also plotted (\bullet) on this curve. These values were computed using N_R realizations of the autocorrelation function estimates. For $N_T=100$, $N_R=10,000$ was used while for $N_T=1000$, the number of realizations was reduced to $N_R=1,000$.

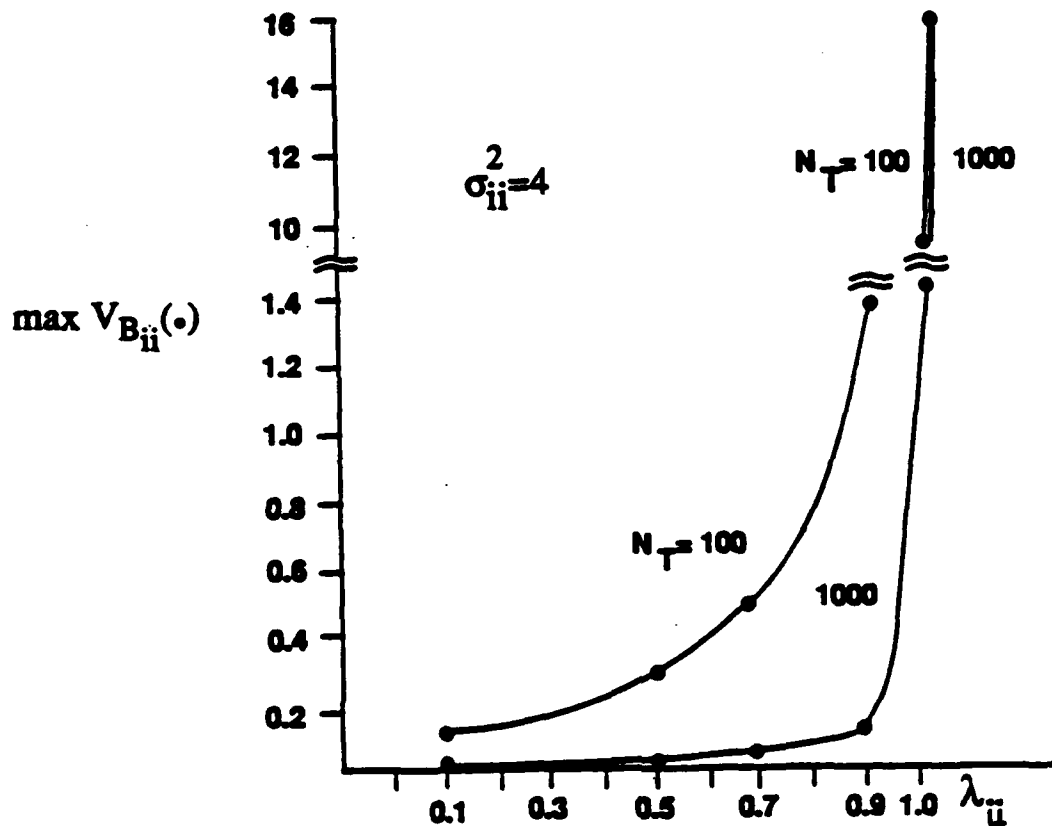


Fig 7.C.1 Maximum variance of the time-averaged exponentially shaped autocorrelation function versus λ_{ii} with $\sigma_{ii}^2=4$; analytical(-) and computed(\bullet).

Table 7.C.1 contains the parameters used in the process synthesis procedure as well as the values of N_T and N_R for the sample variance calculation. In these cases, the variance of the process σ_{ii}^2 was held fixed at 4 while λ_{ii} was varied from 0.1 to 0.99.

Figs 7.C.2 through 7.C.11 show the results for these variances based on the computed values of eq(7.C.12) and the analytic expression of eq(7.C.11b). In plot a of Fig 7.C.2, we show six realizations of the biased, time-averaged autocorrelation function plotted over 64 lag values using $N_T=100$ time samples. The corresponding ensemble averaged result is shown in plot b using $N_R=10,000$. The sample variance of the biased time-averaged autocorrelation function plotted in a is displayed in c. These values were computed using eq(7.C.12) with $N_R=10,000$. The corresponding analytic calculation using eq(7.C.11b) is shown in plot d. In plot e, we show the corresponding sample variance using the unbiased estimate of the autocorrelation function. As noted previously, the variance of the biased autocorrelation function decreases with l while that for the unbiased function may increase. This behavior is illustrated in plots c, d and e and is also noted in Fig 5.12 of ref [7]. In plots f, g, h and i, we show the ensemble averaged quadrature correlation functions estimated from the synthesized process using $N_R=10,000$. Examination of these plots validates eqs(7.C.8), (7.C.9a) and (7.C.9b) recognizing that a finite number of realizations were used in the computations.

In Figs 7.C.3 through 7.C.6, we show results similar to those described in Fig 7.C.2 (although the unbiased variance is no longer considered). In Fig 7.C.7

Fig.	σ_{ii}^2	λ_{ii}	N_T	N_R
7.C.2	4.0	0.1	100	10,000
7.C.3		0.5		
7.C.4		0.7		
7.C.5		0.9		
7.C.6		0.99		
7.C.7		0.1	1000	1000
7.C.8		0.5		
7.C.9		0.7		
7.C.10		0.9		
7.C.11		0.99		

Table 7.C.1

through 7.C.11, we show the results corresponding to plots a, b, c and d in the previous figures using $N_T=1000$ and $N_R=1000$.

A comparison of plot a in each of these figures graphically illustrates the increase in the variance of the time-averaged autocorrelation function as λ_{ij} approaches unity. In addition, a comparison of the figures corresponding to a specific value of λ_{ij} shows the decrease in this variance as N_T increases. The plots shown in Fig 7.C.1 summarize the results shown in these figures.

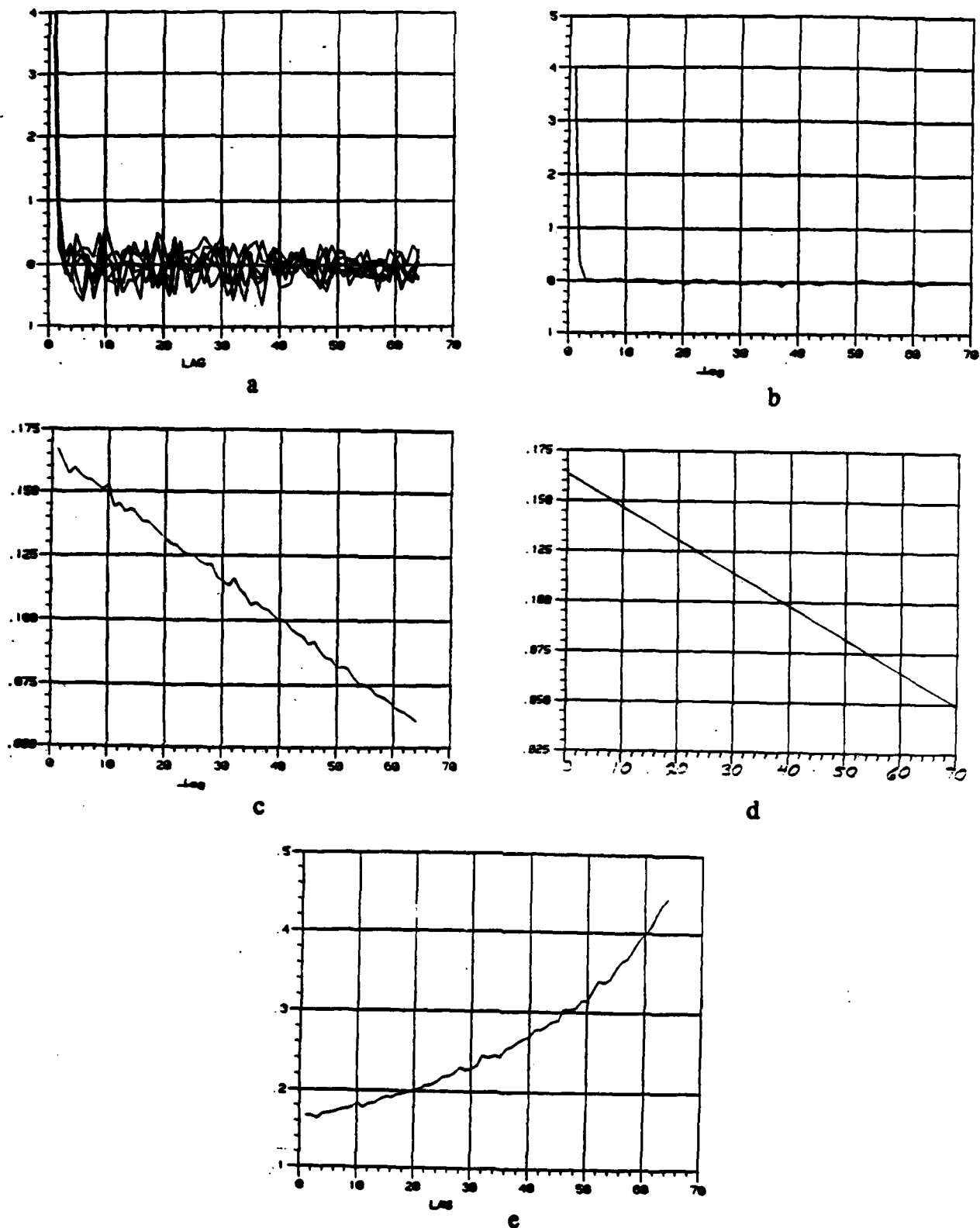


Fig 7.C.2 Time-averaged autocorrelation function and its variance for $\lambda=0.1$ and $\sigma_s^2=4$ a.) biased $R_T(l)$ (6 trials) using $N_T=100$ b.) ensemble averaged $R_E(l)$ using 10,000 realizations c.) sample variance of the biased $R_T(l)$ d.) analytical variance of biased $R_T(l)$ e.) sample variance of the unbiased $R_T(l)$.

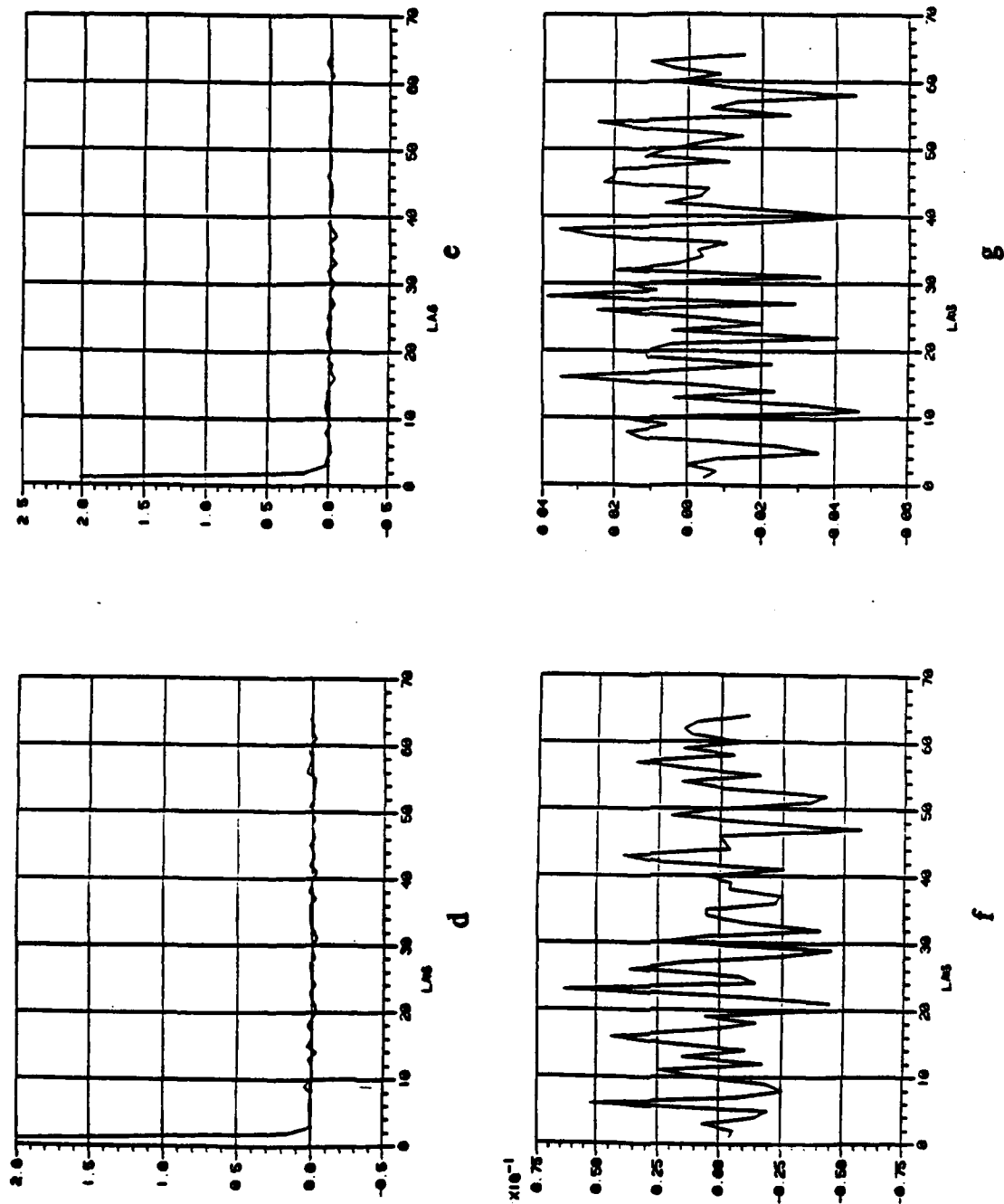


Fig 7.C.2 (contin.) Ensemble averaged quadrature correlation function for $\lambda=0.1$, $N_T=100$ and 10,000 realizations d.) $R_E^{II}(l)$ e.) $R_E^c(l)$ f.) $R_E^{IQ}(l)$ g.) $R_E^{QI}(l)$.

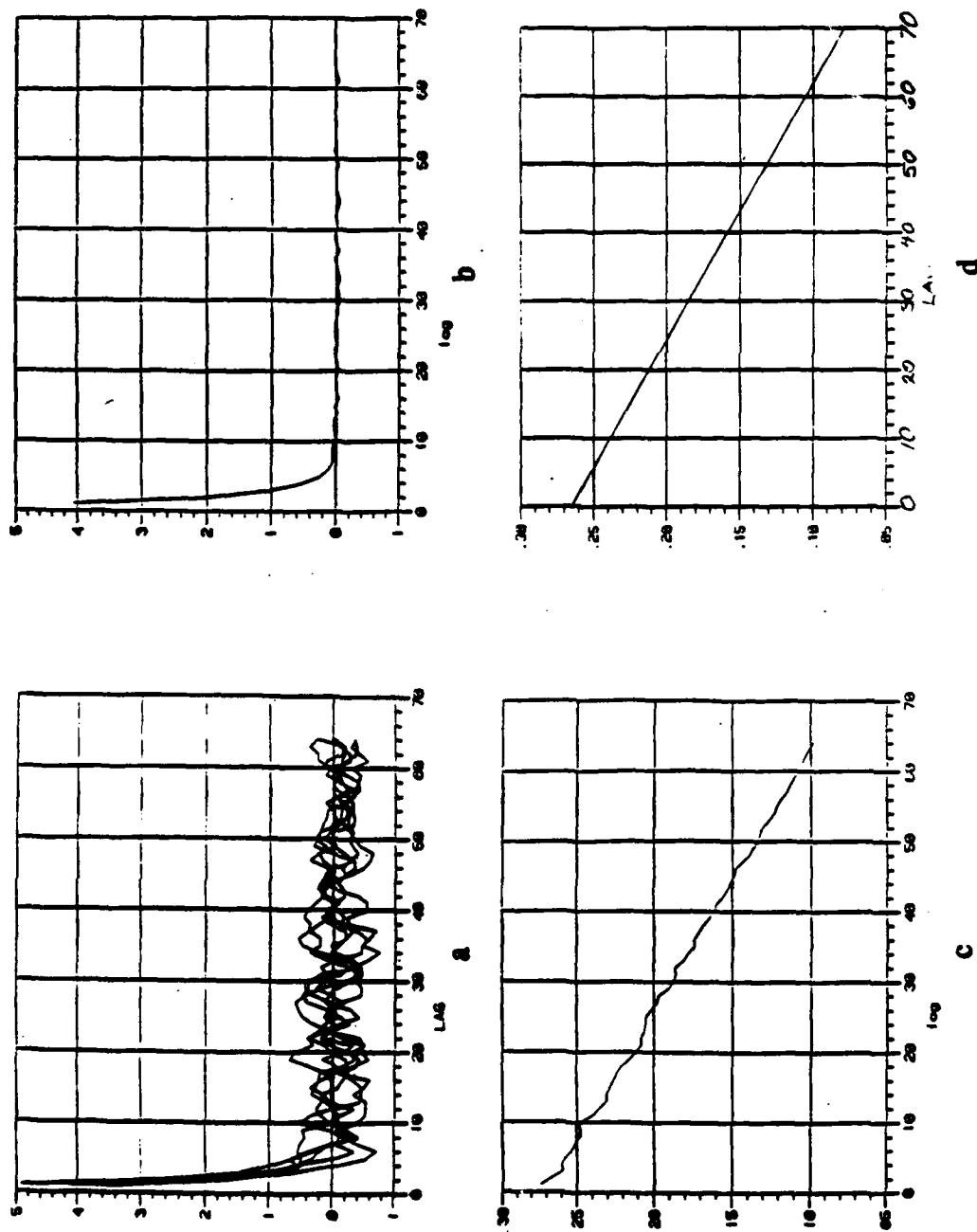


Fig 7.C.3 Time-averaged autocorrelation function and its variance for $\lambda=0.5$ and $\sigma_s^2=4$ a.) biased $R_T(l)$ (6 trials) using $N_T=100$ b.) ensemble averaged $R_E(l)$ using 10,000 realizations c.) sample variance of the biased $R_T(l)$ d.) analytical variance of biased $R_T(l)$.

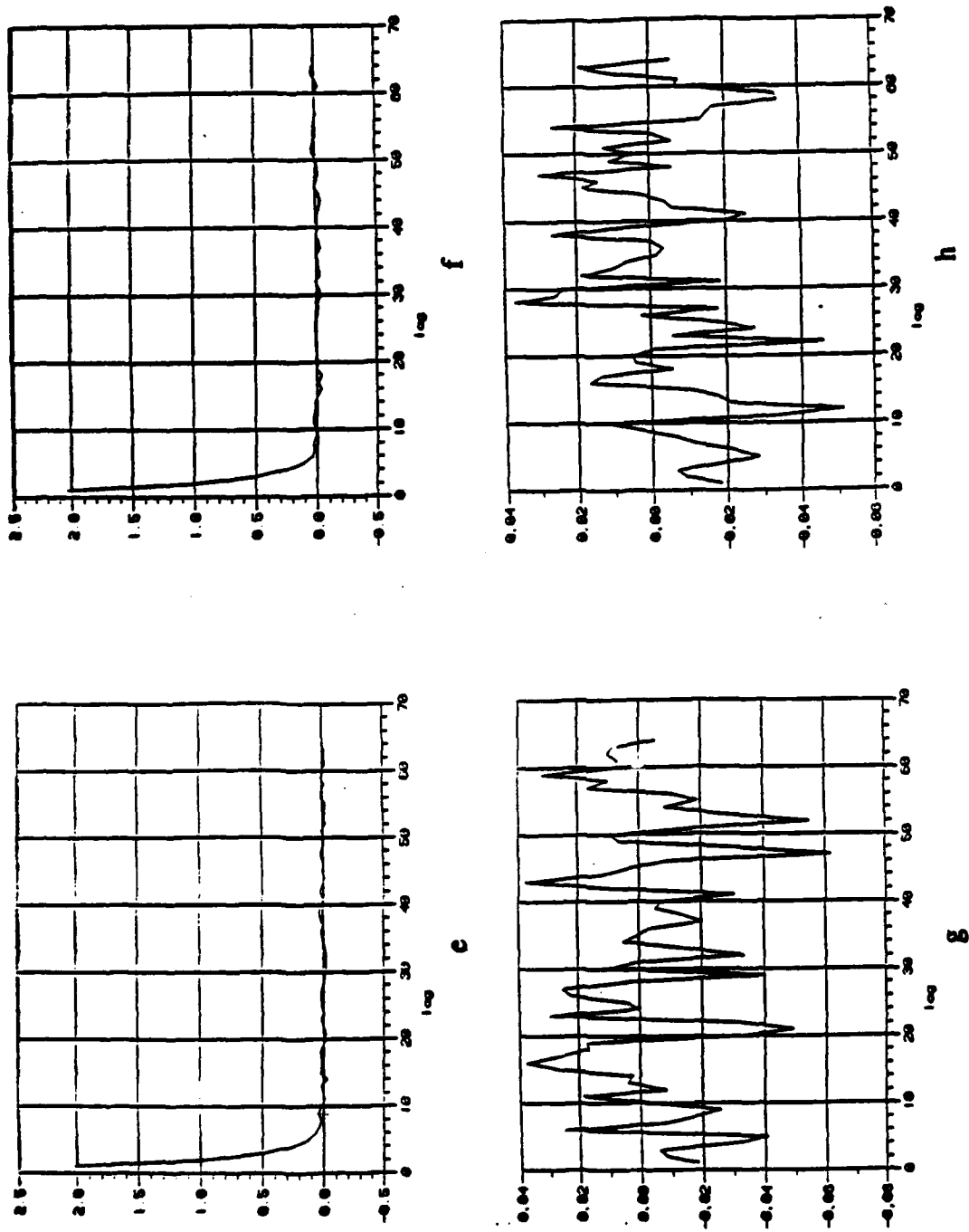


Fig 7.C.3 (contin.) Ensemble-averaged quadrature correlation function for $\lambda=0.5$, $N_T=100$ and 10,000 realizations c.) $R_E^{\text{II}}(0)$ f.) $R_E^{\text{QQ}}(0)$ g.) $R_E^{\text{IQ}}(0)$ h.) $R_E^{\text{QI}}(0)$.

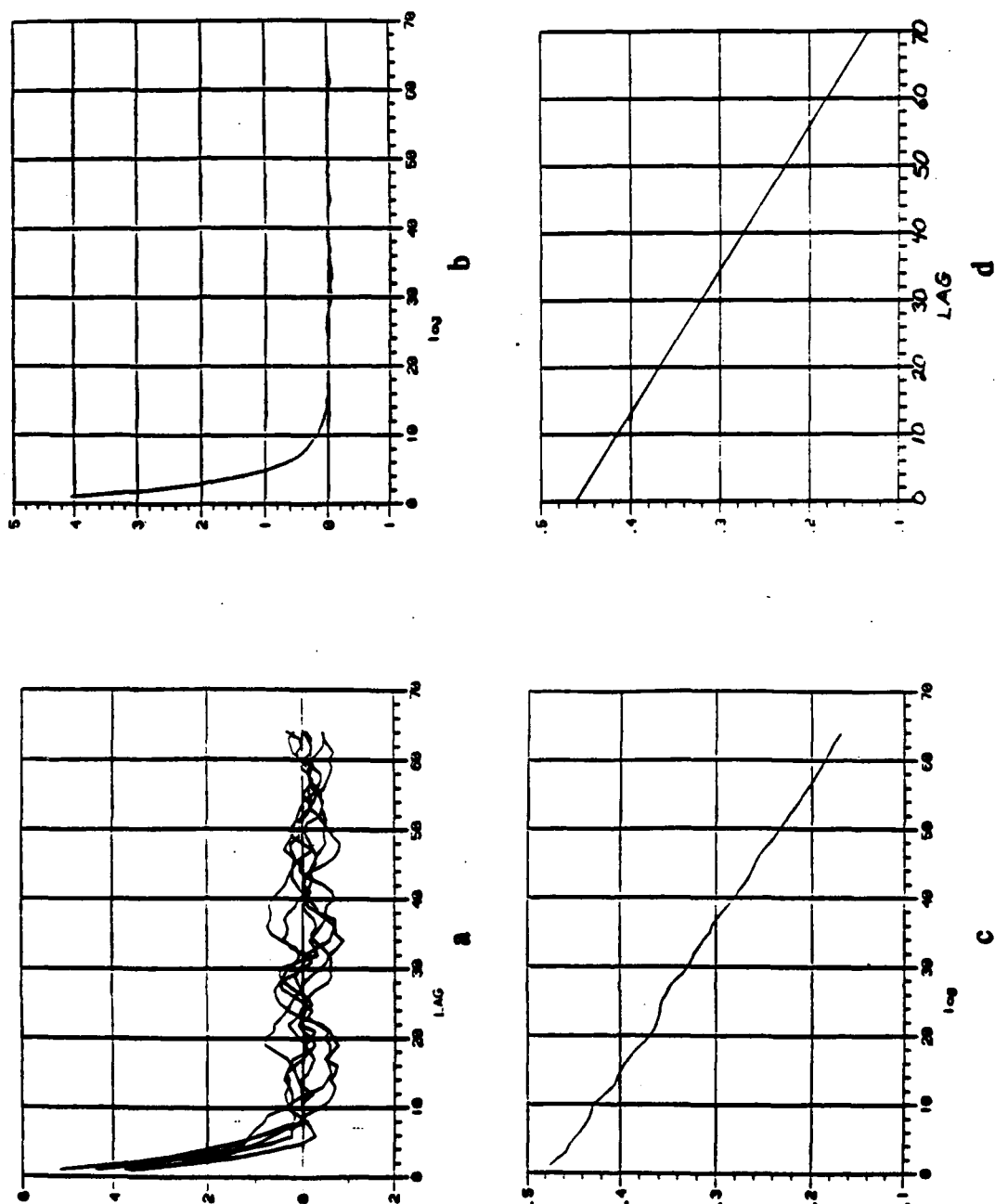


Fig 7.C.4 Time-averaged autocorrelation function and its variance for $\lambda=0.7$ and $\sigma_s^2=4$ a.) biased $R_T(l)$ (6 trials) using $N_T=100$ b.) ensemble averaged $R_T(l)$ using 10,000 realizations c.) sample variance of the biased $R_T(l)$ d.) analytical variance of biased $R_T(l)$.

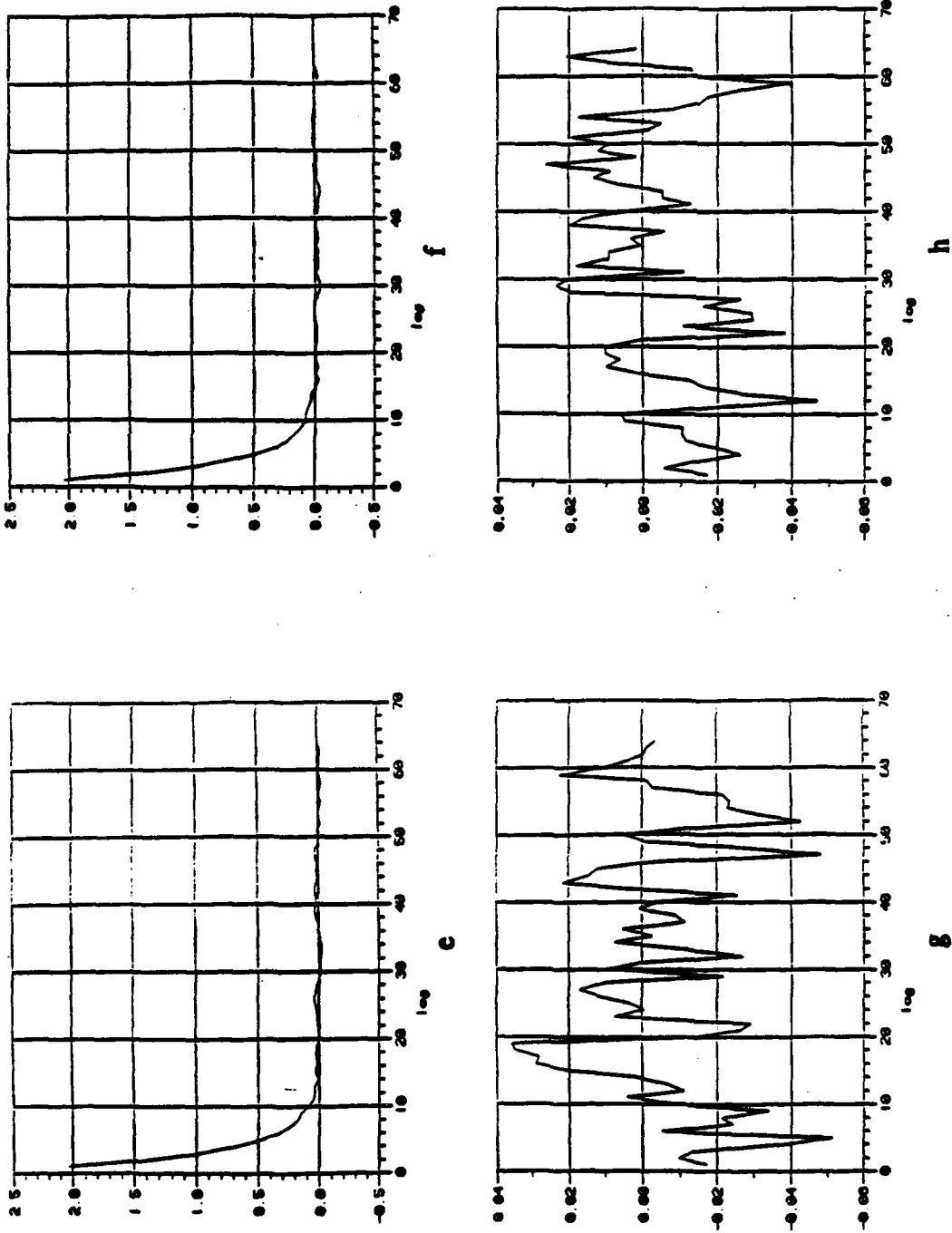


Fig 7.C.4 (contin.) Ensemble-averaged quadrature correlation function for $\lambda=0.7$, $N_T=100$ and 10,000 realizations c.) $R_E^{II}(l)$ f.) $R_E^{QQ}(l)$ g.) $I_Q(l)$ h.) $R_E^{QI}(l)$.

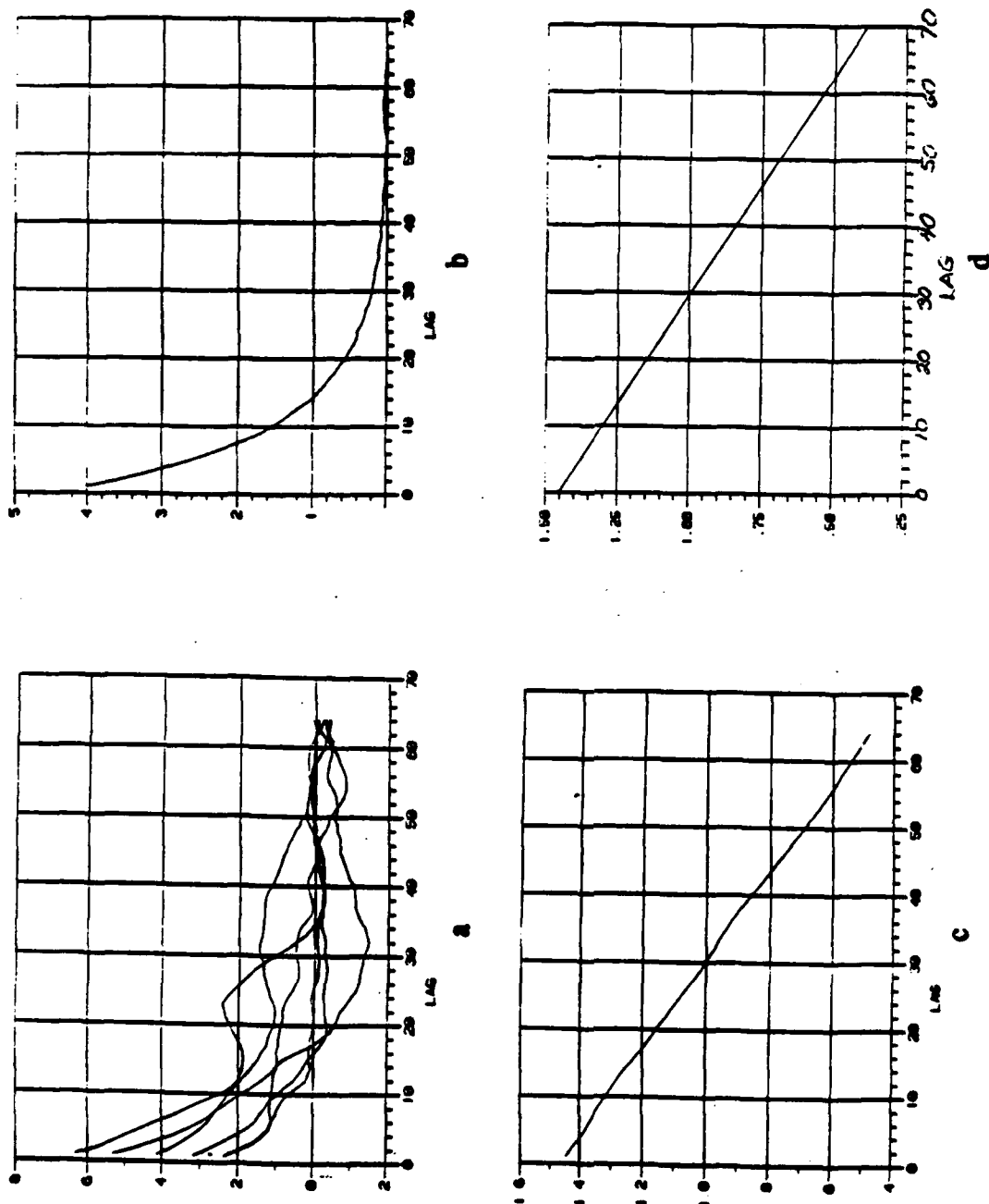


Fig 7.C.5 Time-averaged autocorrelation function and its variance for $\lambda=0.9$ and $\sigma_s^2=4$ a.) biased $R_T(l)$ (6 trials) using $N_T=100$ b.) ensemble averaged $R_E(l)$ using 10,000 realizations c.) sample variance of the biased $R_T(l)$ d.) analytical variance of biased $R_T(l)$.

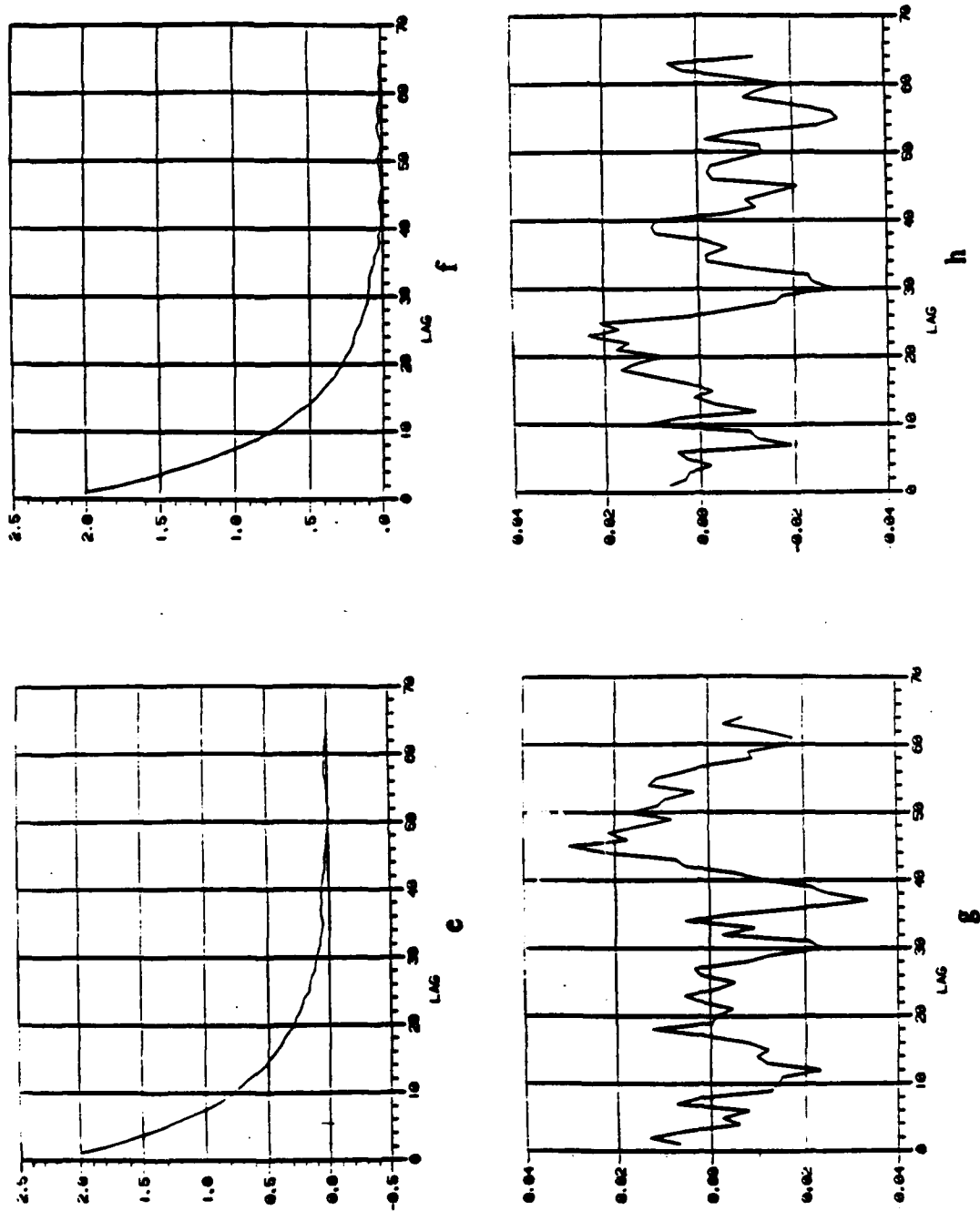


Fig 7.C.5 (contin.) Ensemble-averaged quadrature correlation function for $\lambda=0.9$, $N_T=100$ and 10,000 realizations c.) $R_E^{II}(l)$ f.) $R_E^f(l)$ g.) $R_E^{IQ}(l)$ h.) $R_E^{QI}(l)$.

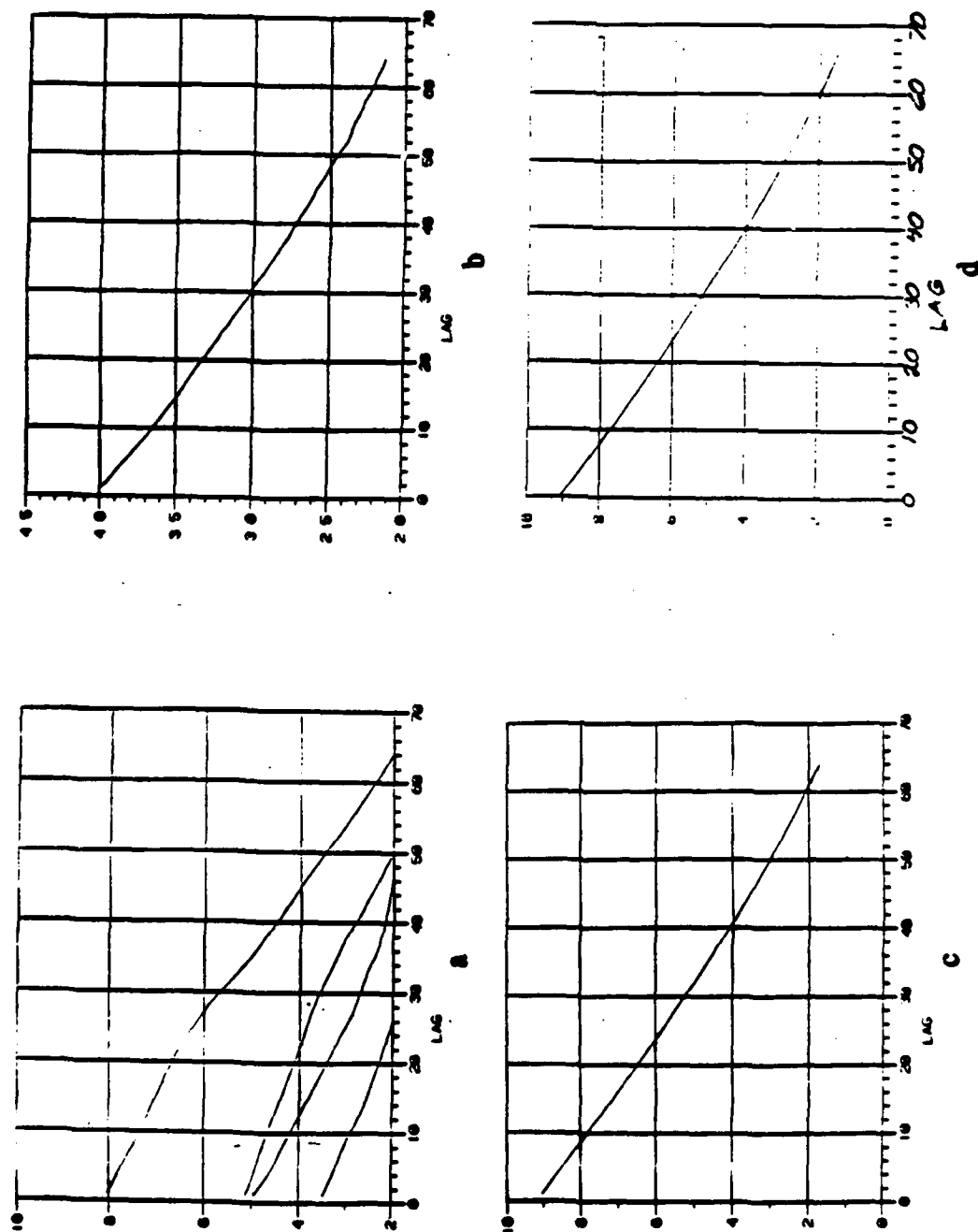


Fig 7.C.6 Time-averaged autocorrelation function and its variance for $\lambda=0.99$ and $\sigma_s^2=4$ a.) biased $R_T(l)$ (4 trials) using $N_T=100$ b.) ensemble averaged $R_E(l)$ using 10,000 realizations c.) sample variance of the biased $R_T(l)$ d.) analytical variance of biased $R_T(l)$.

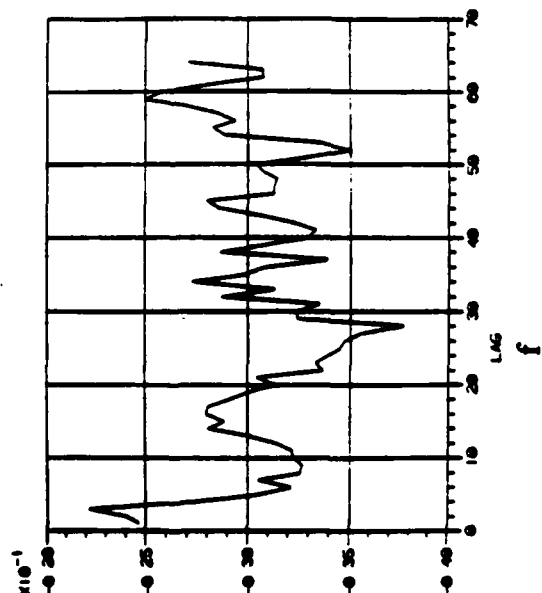
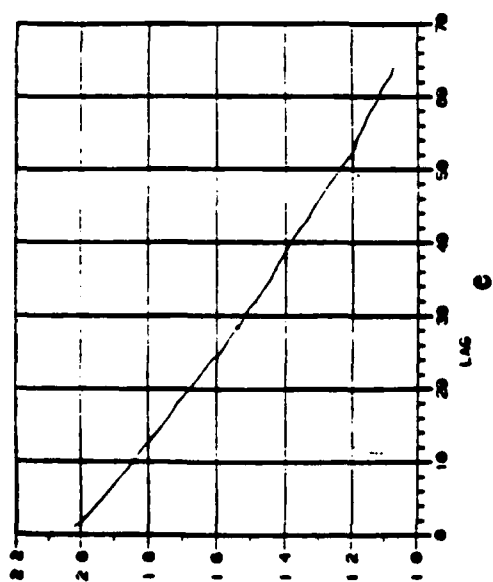
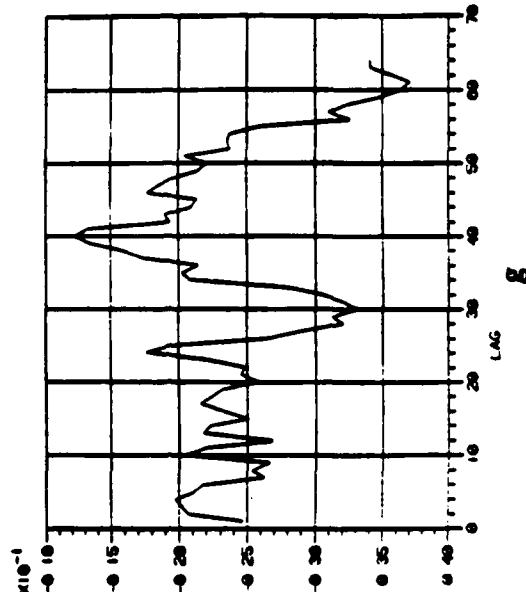
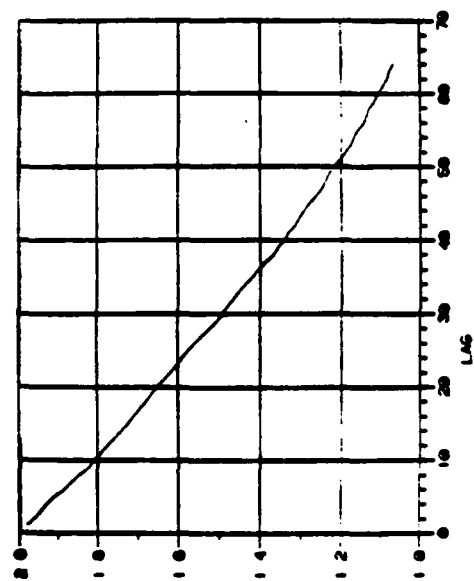


Fig 7.C.6 (contin.) Ensemble-averaged quadrature correlation function for $\lambda=0.99$, $N_T=100$ and 10,000 realizations e.) $R_E^{II}(l)$ f.) $R_E^{QQ}(l)$ g.) $R_E^{IQ}(l)$ h.) $R_E^{QI}(l)$.

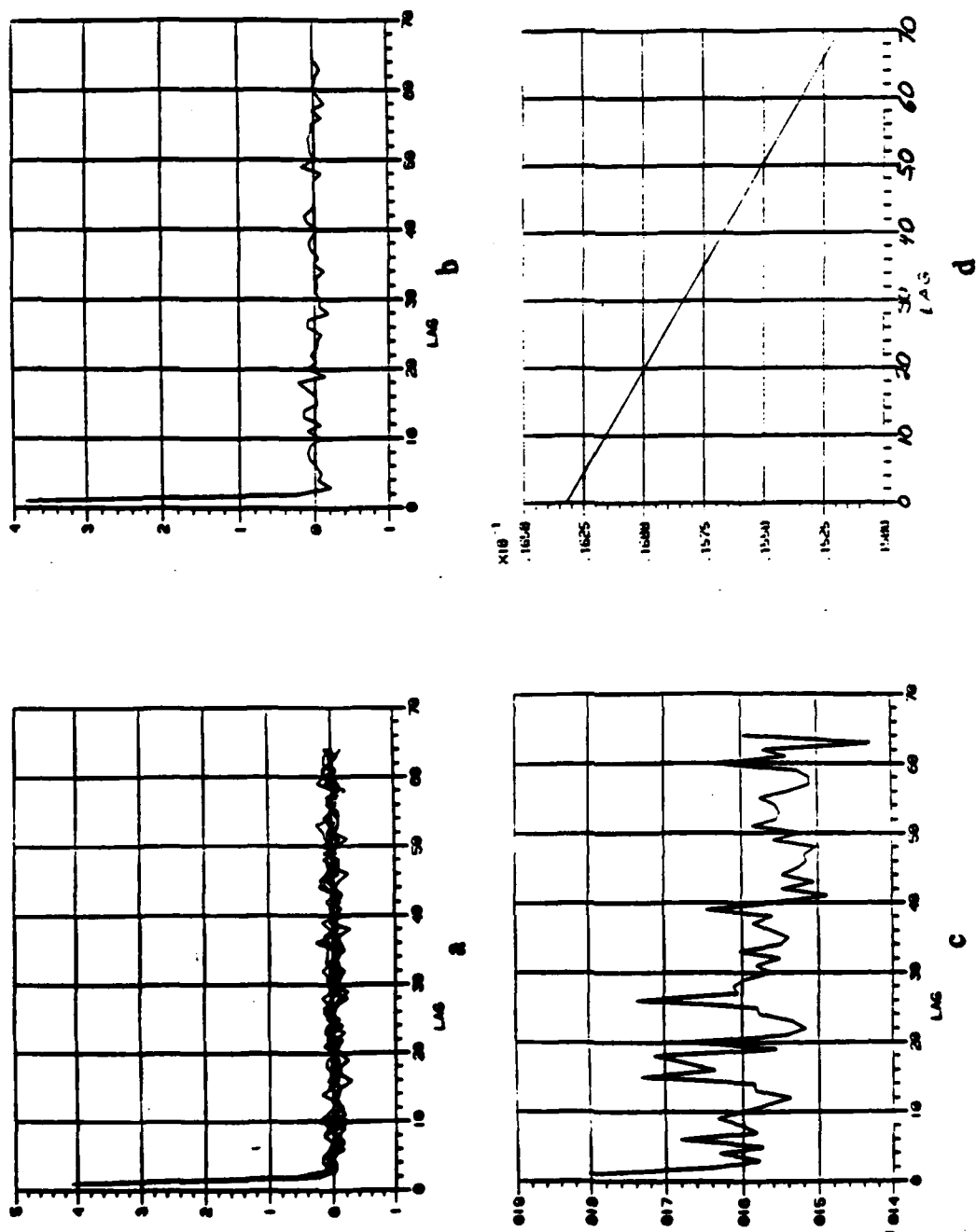


Fig 7.C.7 Time-averaged autocorrelation function and its variance for $\lambda=0.1$ and $\sigma_s^2=4$ a.) biased $R_T(l)$ (6 trials) using $N_T=1,000$ b.) ensemble averaged $R_E(l)$ using 10,000 realizations c.) sample variance of the biased $R_T(l)$ d.) analytical variance of biased $R_T(l)$.

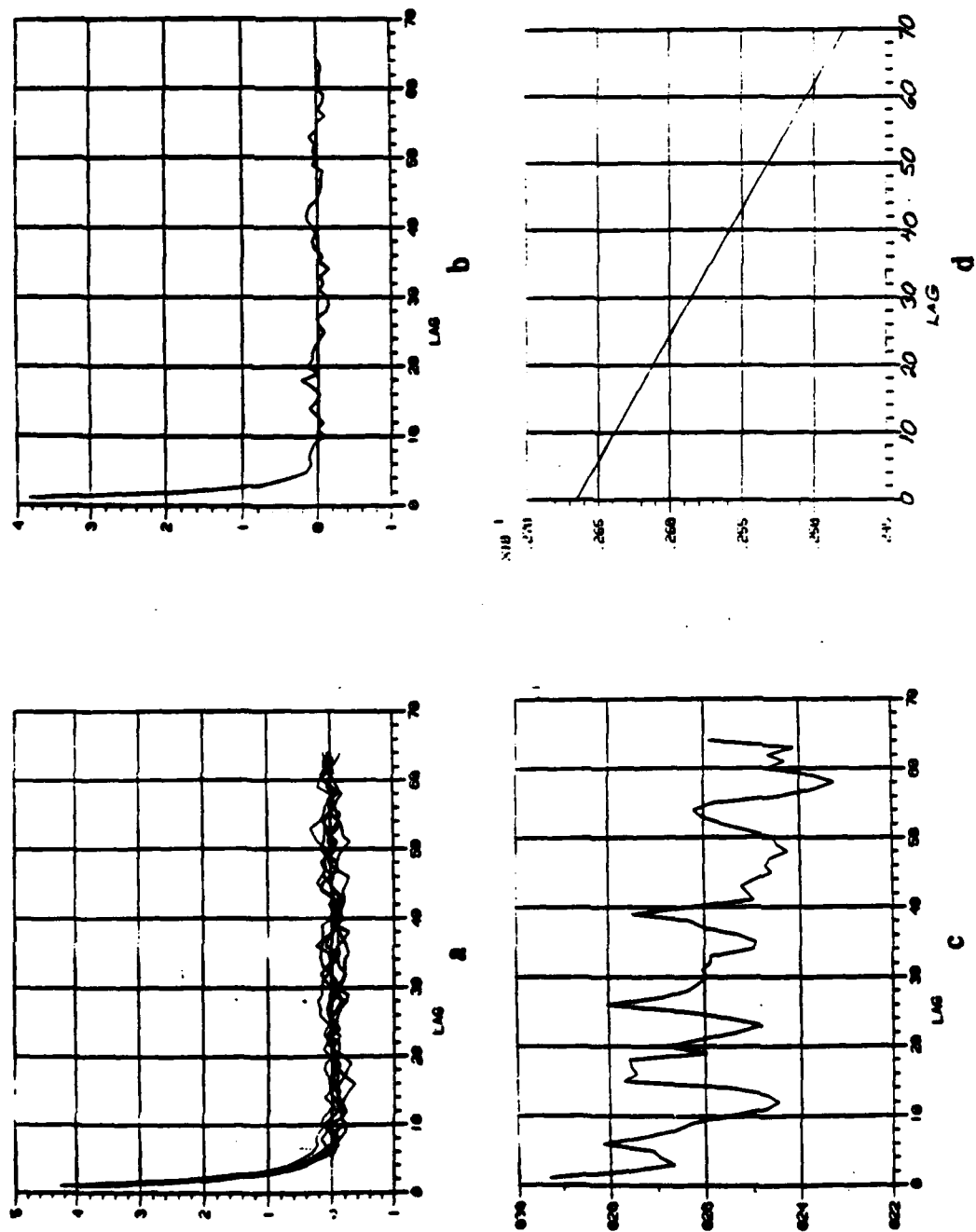


Fig 7.C.8 Time-averaged autocorrelation function and its variance for $\lambda=0.5$ and $\sigma_s^2=4$ a.) biased $R_T(l)$ (6 trials) using $N_T=1,000$ b.) ensemble averaged $R_E(l)$ using 10,000 realizations c.) sample variance of the biased $R_T(l)$ d.) analytical variance of biased $R_T(l)$.

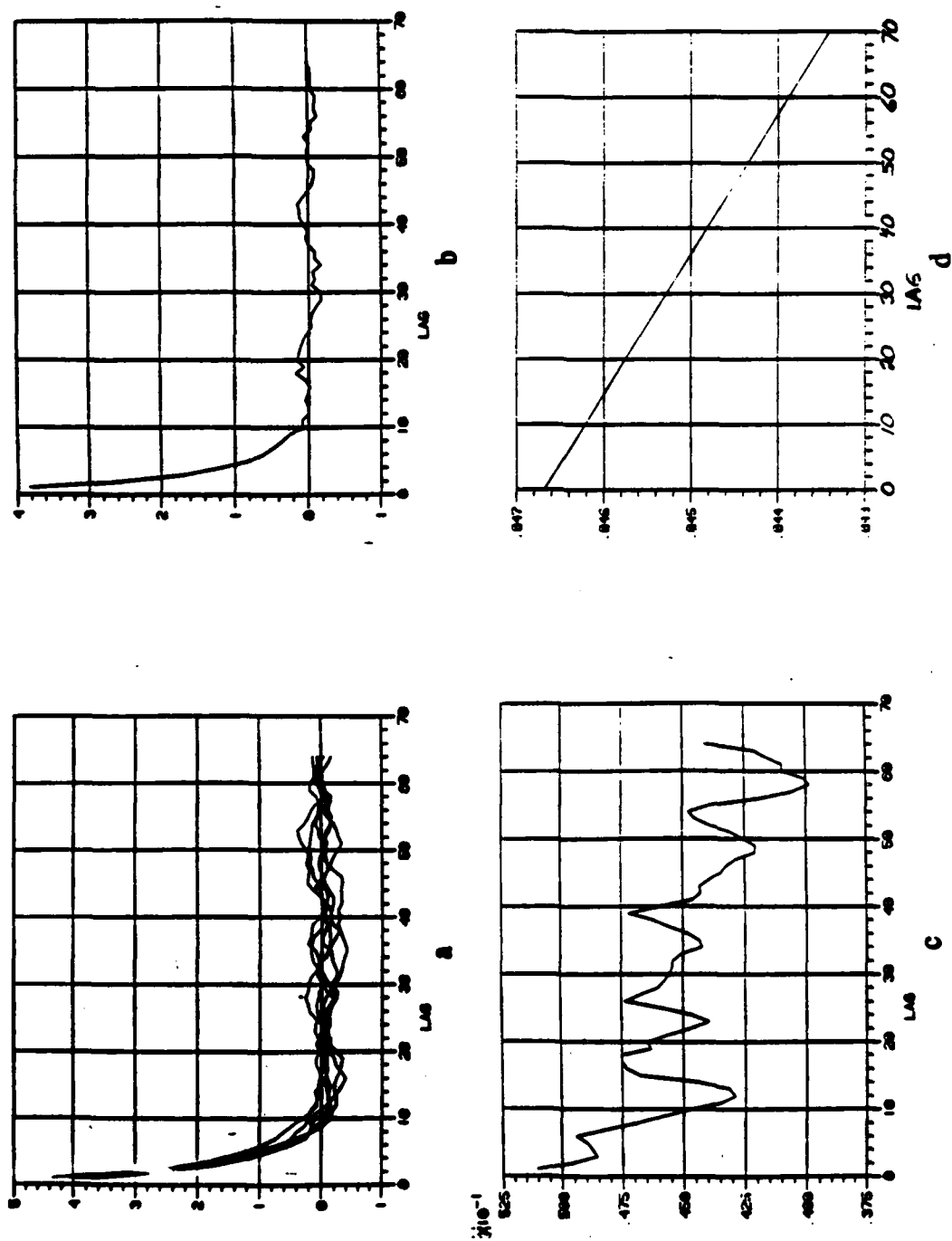


Fig 7.C.9 Time-averaged autocorrelation function and its variance for $\lambda=0.7$ and $\sigma_s^2=4$ a.) biased $R_T(l)$ (6 trials) using $N_T=1,000$ b.) ensemble averaged $R_T(l)$ using 10,000 realizations c.) sample variance of the biased $R_T(l)$ d.) analytical variance of biased $R_T(l)$.

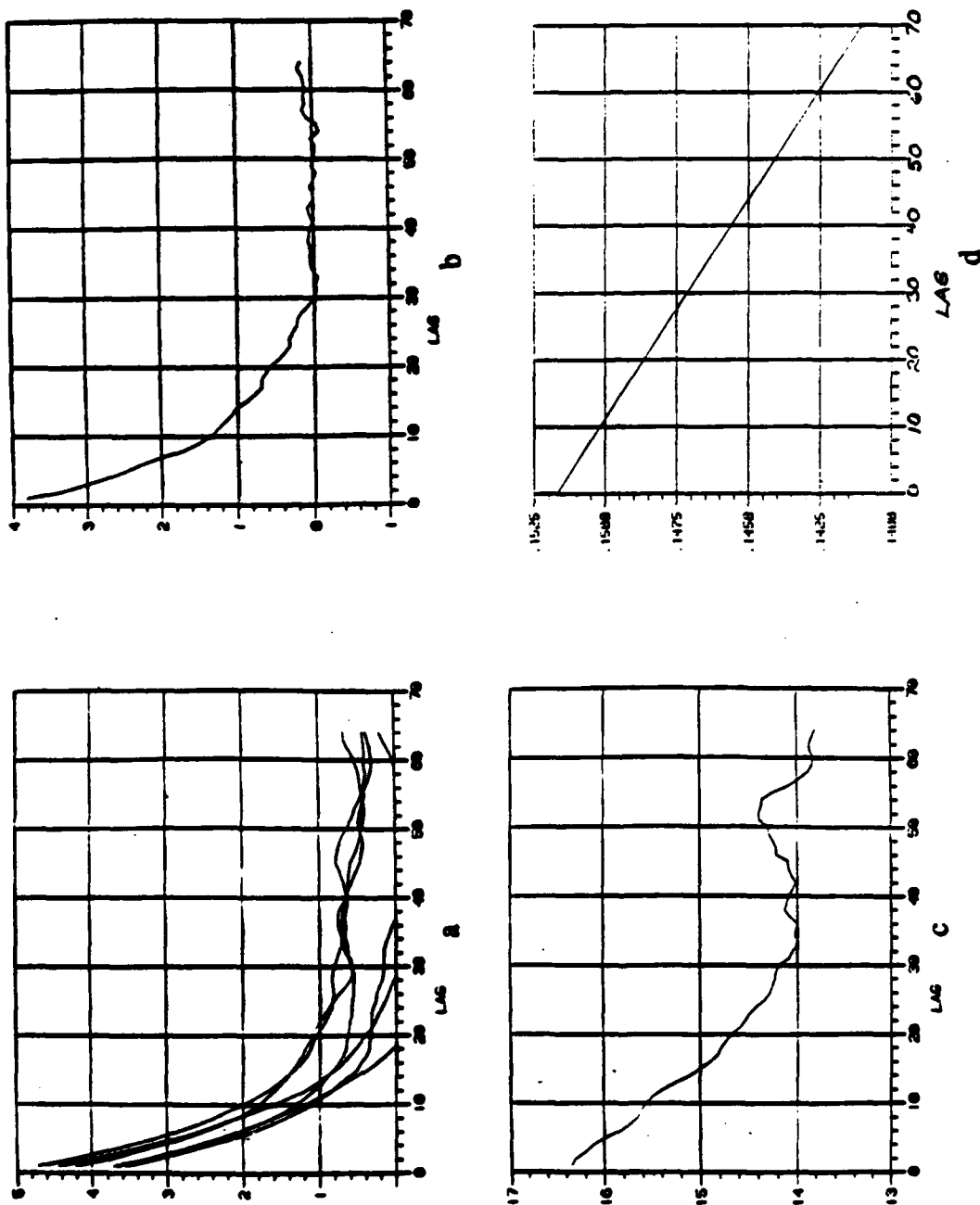


Fig 7.C.10 Time-averaged autocorrelation function and its variance for $\lambda=0.9$ and $\sigma_g^2=4$ a.) biased $R_T(l)$ (6 trials) using $N_T=1,000$ b.) ensemble averaged $R_T(l)$ using 10,000 realizations c.) sample variance of the biased $R_T(l)$ d.) analytical variance of biased $R_T(l)$.

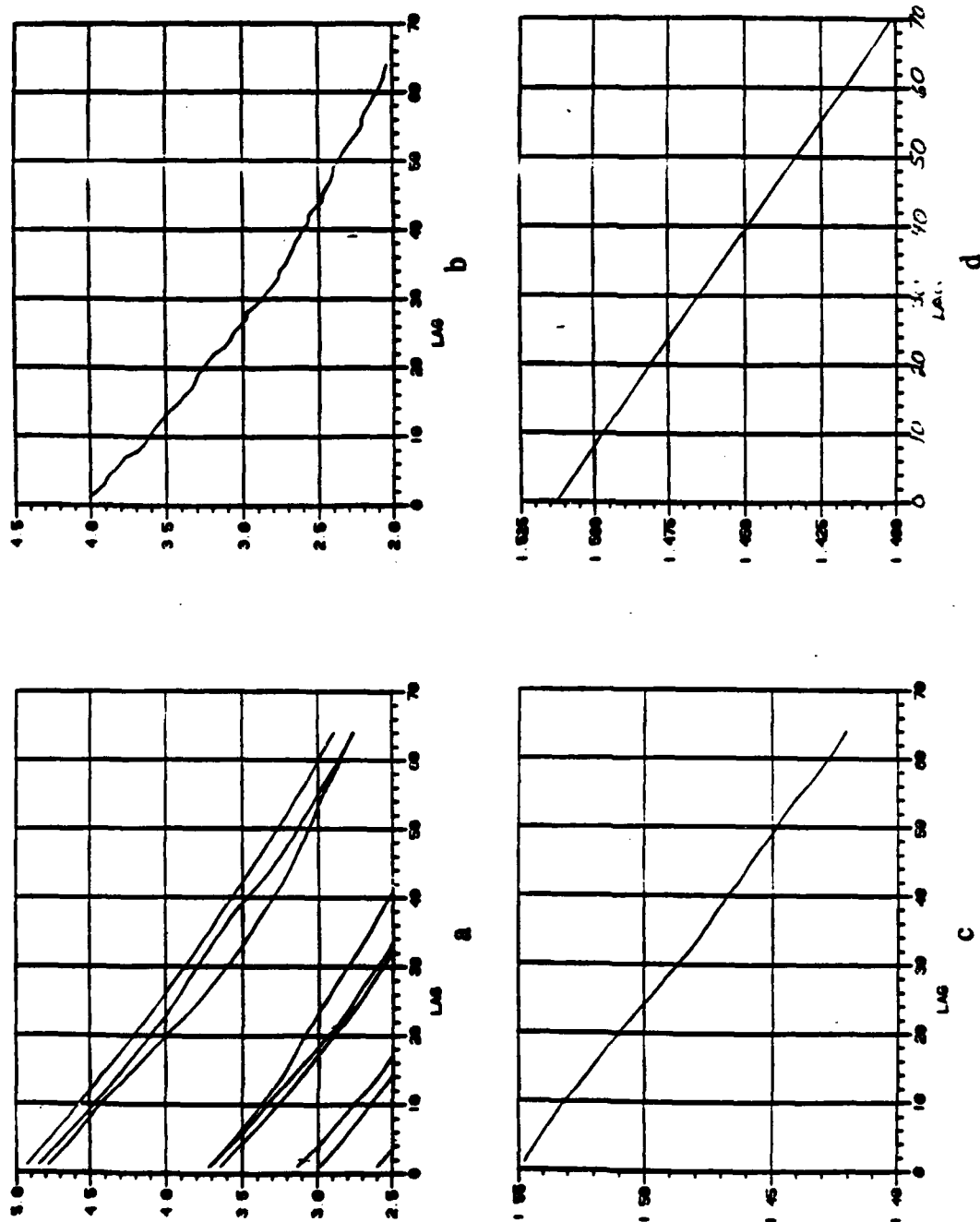


Fig 7.C.11 Time-averaged autocorrelation function and its variance for $\lambda=0.99$ and $\sigma_s^2=4$ a.) biased $R_T(l)$ (9 trials) using $N_T=1,000$ b.) ensemble averaged $R_E(l)$ using 10,000 realizations c.) sample variance of the biased $R_T(l)$ d.) analytical variance of biased $R_T(l)$.

D. The Cross-Correlation Function Ergodicity Results

In this section, we will evaluate the ergodicity of the cross-correlation function. This will be accomplished by evaluating the variance of the time-averaged cross-correlation function as determined by its ergodic series. In Section IV.B, we developed the expression for the variance described by eq(4.B.13). In this section, we will consider an expression for the variance of the biased, time-averaged cross-correlation function estimator using limited data. Following a similar discussion as presented in Section VII.C, eq(4.B.13) is modified for the biased estimator such that

$$V_{Bij}(l, N) = \frac{1}{N_T} \sum_{k=-(N_T-||l|-1)}^{N_T-||l|-1} \left[1 - \frac{||l|+|k|}{N_T} \right] \text{Re}[R_{ii}(k)R_{jj}^*(k) + F_{ij}(l, k)]. \quad (7.D.1)$$

We will now consider the case of a two channel AR(1) process with real correlation functions. Table 7.D.1 lists the parameters used in the synthesis procedure of section VI. Table 7.D.2 lists the A(1) and C matrices used in the AR process synthesis equation expressed by eqs(6.B.5) and (6.B.6). We note that in each of the A(1) matrices

$$-a_{11} = \lambda_{11} \quad (7.D.2a)$$

and

$$-a_{22} = \lambda_{22} \quad (7.D.2b)$$

while

$$a_{12} \approx a_{21} \approx 0. \quad (7.D.2c)$$

We also note that the cross-correlation between the process is controlled by the elements of the C matrices; ie., for high correlation, the c_{11} and c_{21} elements become nearly equal while c_{22} diminishes. For low correlation, the c_{21} element diminishes. From eqs(7.D.2), each channel process is an AR(1) process such that

$$R_{11}(k) = \sigma_{11}^2 (\lambda_{11})^{|k|} \quad (7.D.3a)$$

and

$$R_{22}(k) = \sigma_{22}^2 (\lambda_{22})^{|k|}. \quad (7.D.3b)$$

As in the previous section, we can show (see Section VI.C and Appendix G) that when $R_{ij}(k)$ is real, the in-phase and quadrature components of the synthesized outputs are uncorrelated so that

$$R_{ij}^{OI}(\alpha) = R_{ij}^{IQ}(\alpha) = 0. \quad (7.D.4)$$

We also show that in the case where

$$R_{ij}^{II}(\alpha) = R_{ij}^{QQ}(\alpha) \quad (7.D.5)$$

so that $F_{ij}(l,k)=0$, eq(7.D.1) can be written as

$$V_{Bij}(l,N) = \frac{1}{N_T} \sum_{k=-(N_T-|l|-1)}^{N_T-|l|-1} \left[1 - \frac{|l|+|k|}{N_T} \right] \sigma_{11}^2 (\lambda_{11})^{|k|} \sigma_{22}^2 (\lambda_{22})^{|k|} \quad (7.D.6)$$

In Fig 7.D.1, the peak value of $V_{Bij}(l)$ which occurs at $l=0$ is plotted (solid curves) as a function of $\lambda_{AR}=\lambda_{11}=\lambda_{22}$ for $N_T = 100$ and $N_T = 1000$ using the analytic expression of eq(7.D.6) and $\sigma_{11}^2 = \sigma_{22}^2 = 4$. The corresponding peak

values of the sample variances of the time-averaged cross-correlation function estimates computed using the synthesized data processes are also plotted (x) on this curve. These values were computed using N_R realizations of the functions. For $N_T = 100$, $N_R = 10,000$ was used while for $N_T = 1000$, the number of realizations was reduced to $N_R = 1,000$. The sample variances based on N_R realizations of the time-averaged cross-correlation function estimates are computed using the expression

$$\text{Var}[\hat{R}_{ijT_b}(l, N_T; N_R)] = \frac{1}{N_R - 1} \sum_{\alpha=1}^{N_R} |\hat{R}_{ijT_b}(l, N_T | \alpha) - \bar{\hat{R}}_{ijT_b}(l, N_R | \alpha)|^2 \quad (7.D.7)$$

where

$$\bar{\hat{R}}_{ijT_b}(l, N_R | \alpha) = \frac{1}{N_R} \sum_{\alpha=1}^{N_R} \hat{R}_{ijT_b}(l, N_T | \alpha). \quad (7.D.8)$$

and $\hat{R}_{ijT_b}(l, N_R | \alpha)$ is the biased, time-averaged, cross-correlation function for realization α .

Figs 7.D.2 through 7.D.10 show the results for these variances based on the computed values of eq(7.D.7) and the analytic expression of eq(7.D.6). Table 7.D.1 contains the parameters used in the process synthesis procedure. In these cases, the variance of the processes σ_{11}^2 and σ_{22}^2 was held fixed at 4 while λ_{11} and λ_{22} were varied from 0.1 to 0.99. The cross-correlation coefficient $|\rho_{12}|$ had values of 0.99, 0.5 and 0.0. Table 7.D.2 contains the A(1) and C coefficients. As noted previously, the off diagonal terms of the A(1) coefficients are negligible. We also note that as the temporal correlation coefficients λ_{ii} increase, the diagonal elements of A(1) increase; whereas, changes in $|\rho_{ij}|$ affect the c_{21} and c_{22} elements of C.

Fig.	σ_{11}^2	σ_{22}^2	λ_{11}	λ_{22}	λ_{12}	$ \rho_{12} $	N_T	N_R	l_{12}
7.D.2	4	4	0.1	0.1	0.1	0.99	100	1000	0
7.D.3						0.50			
7.D.4						0.00			
7.D.5			0.5	0.5	0.5	0.99			
7.D.6						0.50			
7.D.7						0.00			
7.D.8			0.9	0.9	0.9	0.99			
7.D.9						0.50			
7.D.10						0.00			

Table 7.D.1

Fig.	A(1)	C
7.D.2	$\begin{bmatrix} -0.1 & 4.7 \times 10^{-7} \\ 4.7 \times 10^{-7} & -0.1 \end{bmatrix}$	$\begin{bmatrix} 1.99 & 0.0 \\ 1.97 & 0.28 \end{bmatrix}$
7.D.3	$\begin{bmatrix} -0.1 & 0.0 \\ 0.0 & -0.1 \end{bmatrix}$	$\begin{bmatrix} 1.99 & 0.0 \\ 0.995 & 1.723 \end{bmatrix}$
7.D.4	$\begin{bmatrix} -0.1 & 0.0 \\ 0.0 & -0.1 \end{bmatrix}$	$\begin{bmatrix} 1.99 & 0.0 \\ 0.0 & 1.99 \end{bmatrix}$
7.D.5	$\begin{bmatrix} -0.5 & 0.0 \\ 0.0 & -0.5 \end{bmatrix}$	$\begin{bmatrix} 1.732 & 0.0 \\ 1.715 & 0.244 \end{bmatrix}$
7.D.6	$\begin{bmatrix} -0.5 & 0.0 \\ 0.0 & -0.5 \end{bmatrix}$	$\begin{bmatrix} 1.732 & 0.0 \\ 0.866 & 1.50 \end{bmatrix}$

Table 7.D.2

Fig.	A(1)	C
7.D.7	$\begin{bmatrix} -0.5 & 0.0 \\ 0.0 & -0.5 \end{bmatrix}$	$\begin{bmatrix} 1.732 & 0.0 \\ 0.0 & 1.732 \end{bmatrix}$
7.D.8	$\begin{bmatrix} -0.9 & 0.0 \\ 0.0 & -0.9 \end{bmatrix}$	$\begin{bmatrix} 0.872 & 0.0 \\ 0.863 & 0.123 \end{bmatrix}$
7.D.9	$\begin{bmatrix} -0.9 & 0.0 \\ 0.0 & -0.9 \end{bmatrix}$	$\begin{bmatrix} 0.872 & 0.0 \\ 0.436 & 0.755 \end{bmatrix}$
7.D.10	$\begin{bmatrix} -0.9 & 0.0 \\ 0.0 & -0.9 \end{bmatrix}$	$\begin{bmatrix} 0.872 & 0.0 \\ 0.0 & 0.872 \end{bmatrix}$

Table 7.D.2 (contin.)

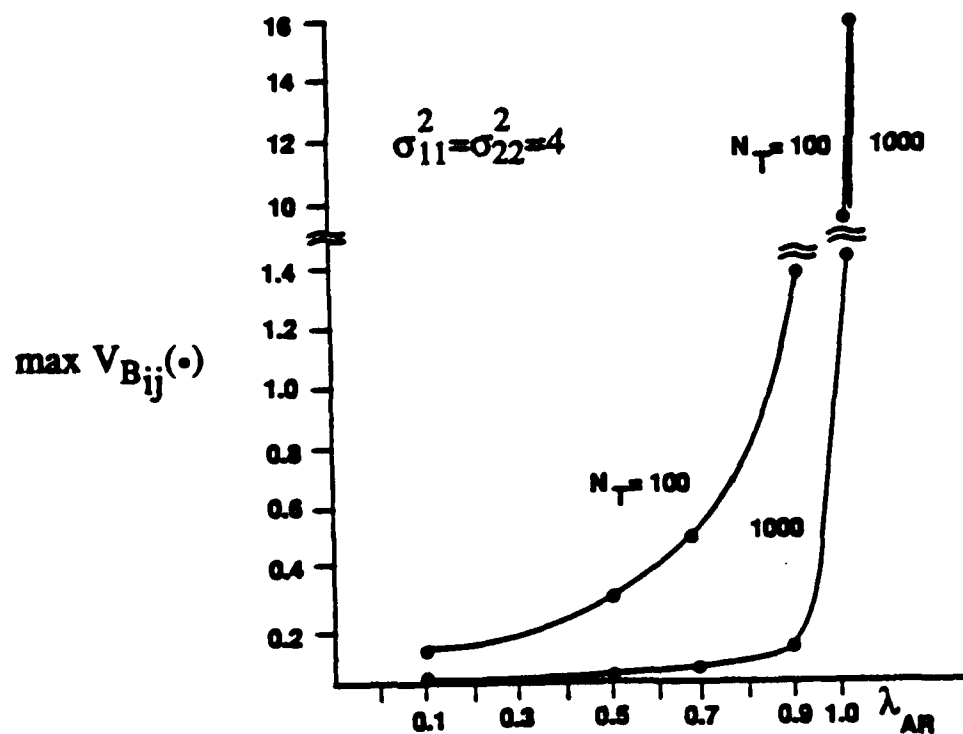


Fig 7.D.1 Maximum variance of the time-averaged exponentially shaped cross-correlation function with $\sigma_{11}^2 = \sigma_{22}^2 = 4$; analytic (—) and computed (\bullet).

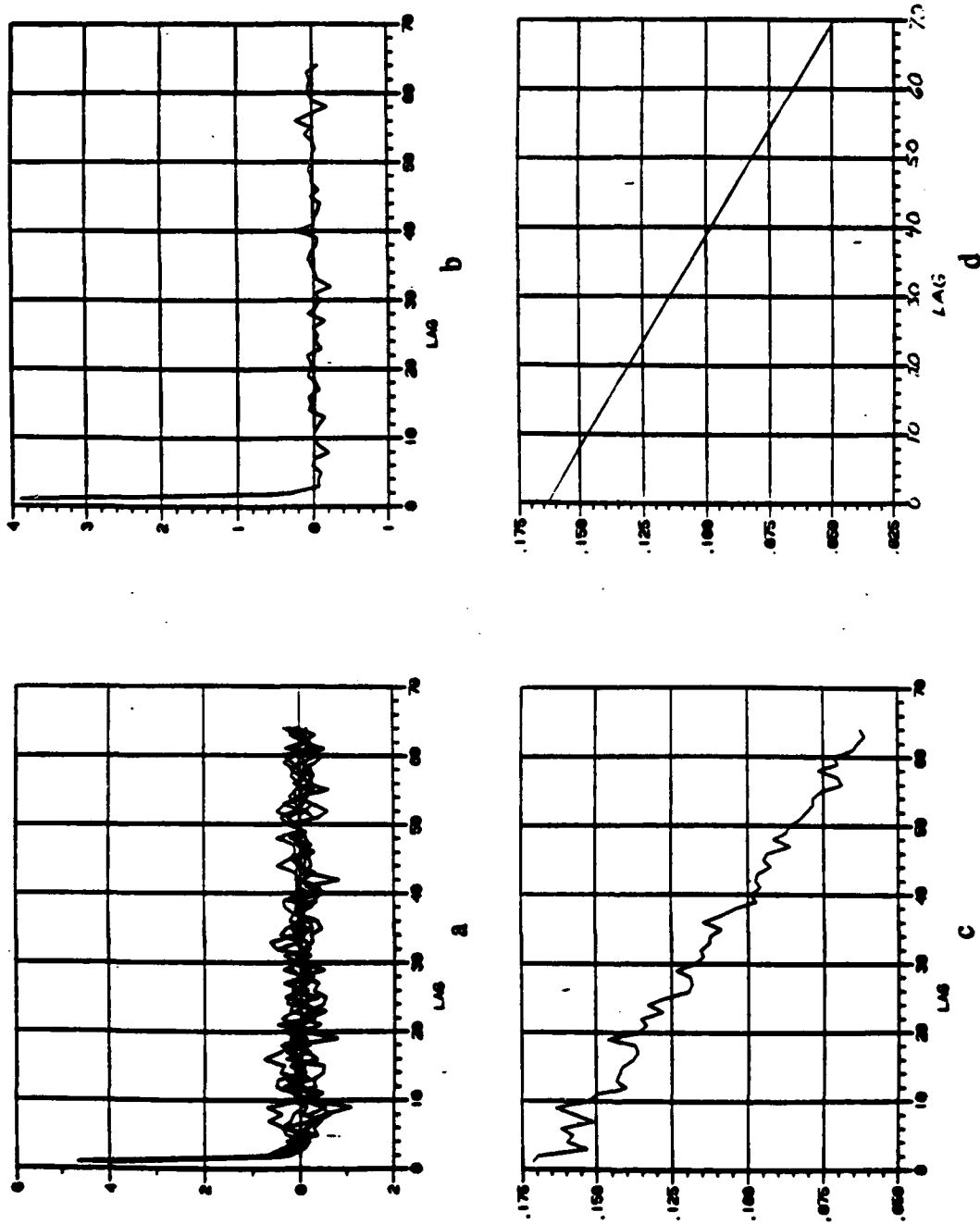


Fig 7.D.2 Time-averaged cross-correlation function and its variance for $|p_{12}|=0.99$, $\lambda_{11}=\lambda_{22}=\lambda_{12}=0.1$, $\sigma_{11}^2=\sigma_{22}^2=4$, $l_1 l_2=0$ a.) biased $R_T(l)$ (6 trials) using $N_T=100$ b.) ensemble averaged $R_E(l)$ (1,000 realizations) c.) sample variance of the biased $R_T(l)$ (1000 realizations) d.) analytical variance of biased $R_T(l)$.

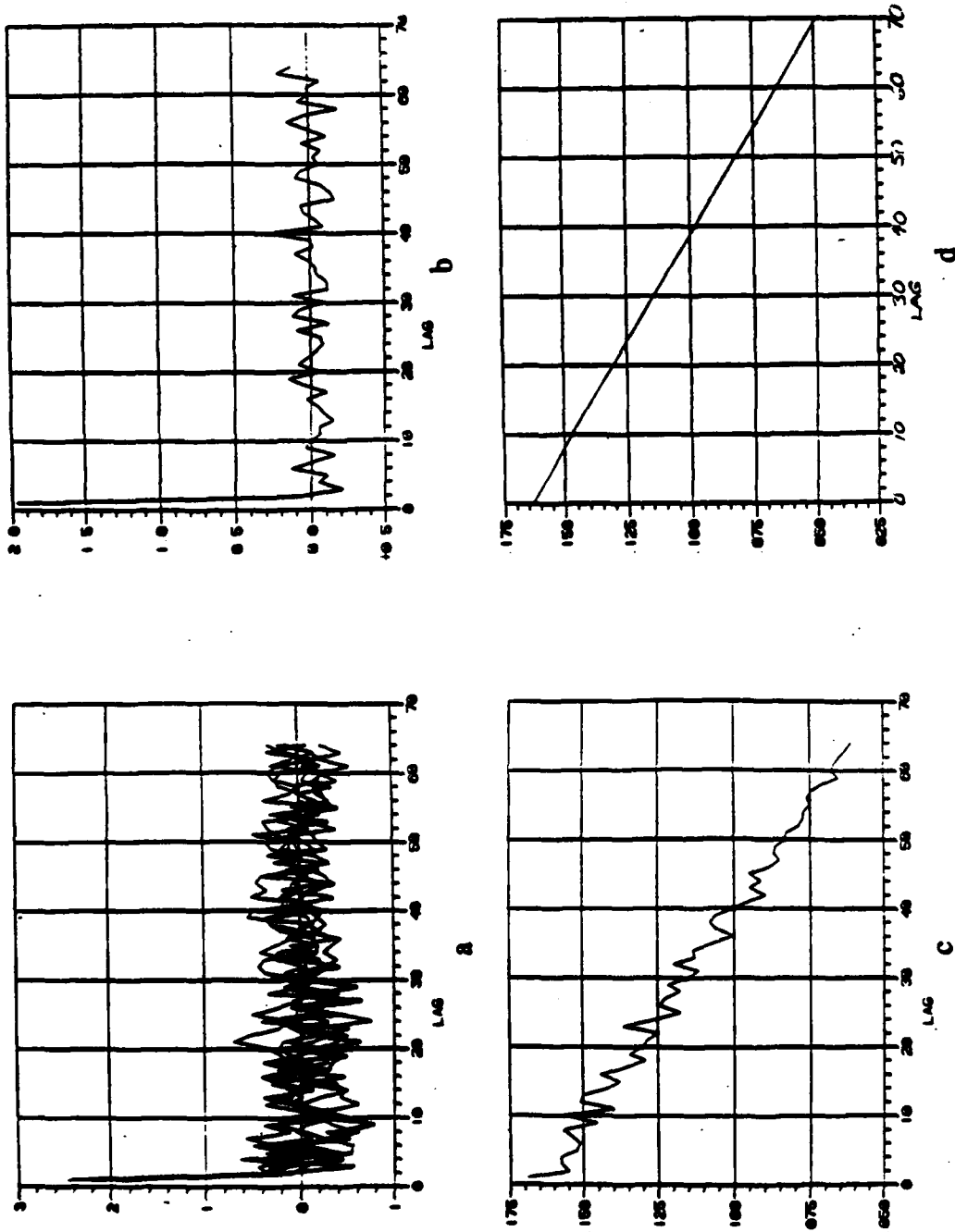


Fig 7.D.3 Time-averaged cross-correlation function and its variance for $|\rho_{12}|=0.5$, $\lambda_{11}=\lambda_{22}=\lambda_{12}=0.1$, $\sigma_{11}^2=\sigma_{22}^2=4$, $I_{12}=0$ a.) biased $R_T(l)$ (6 trials) using $N_T=100$ b.) ensemble averaged $R_E(l)$ (1,000 realizations) c.) sample variance of the biased $R_T(l)$ (1000 realizations) d.) analytical variance of biased $R_T(l)$.

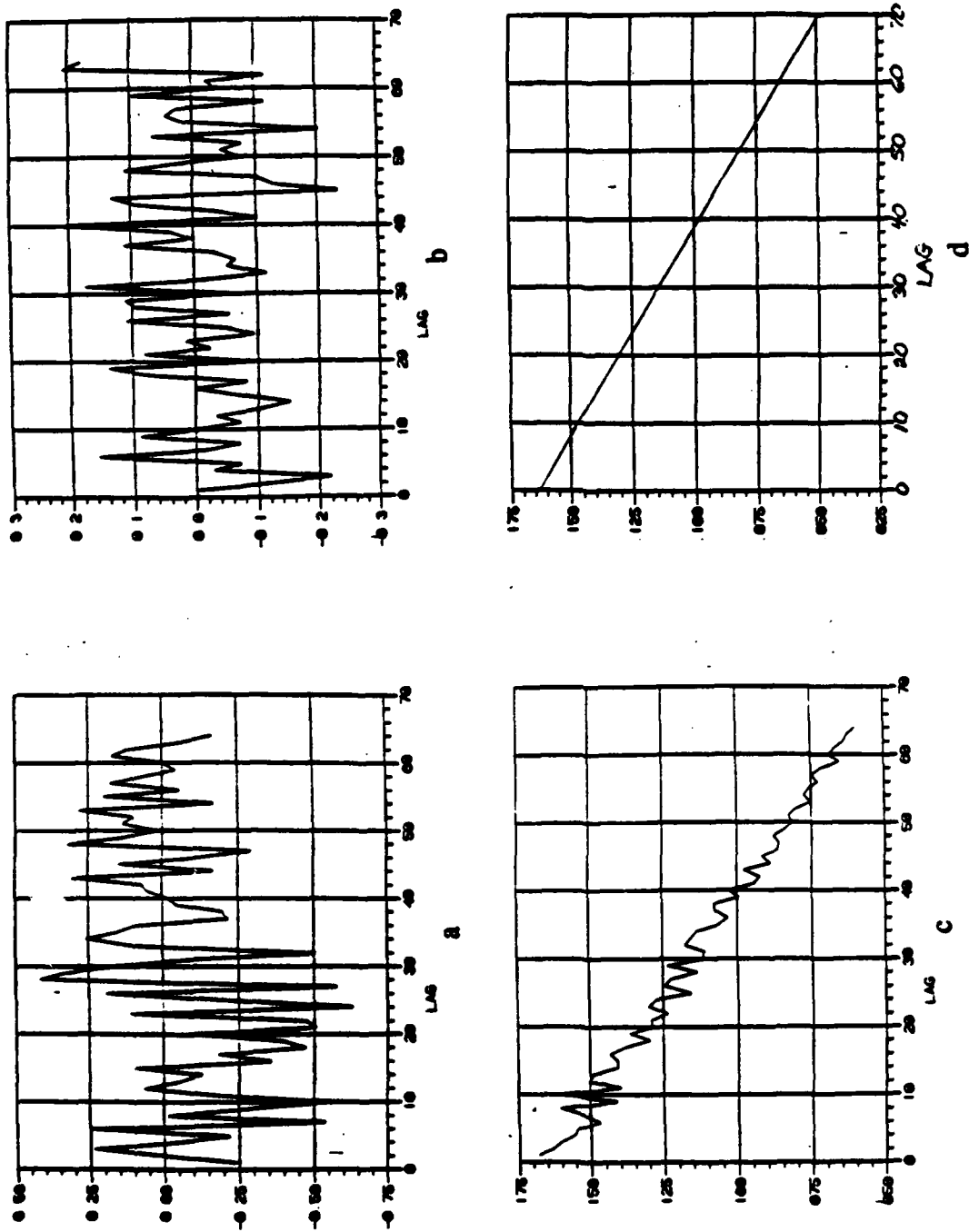


Fig 7.D.4 Time-averaged cross-correlation function and its variance for $|p_{12}|=0.0$, $\lambda_{11}=\lambda_{22}=\lambda_{12}=0.1$, $\sigma_{11}^2=\sigma_{22}^2=4$, $l_{12}=0$ a.) biased $R_T(l)$ (1 trial) using $N_T=100$ b.) ensemble averaged $R_E(l)$ (1,000 realizations) c.) sample variance of the biased $R_T(l)$ (1000 realizations) d.) analytical variance of biased $R_T(l)$.

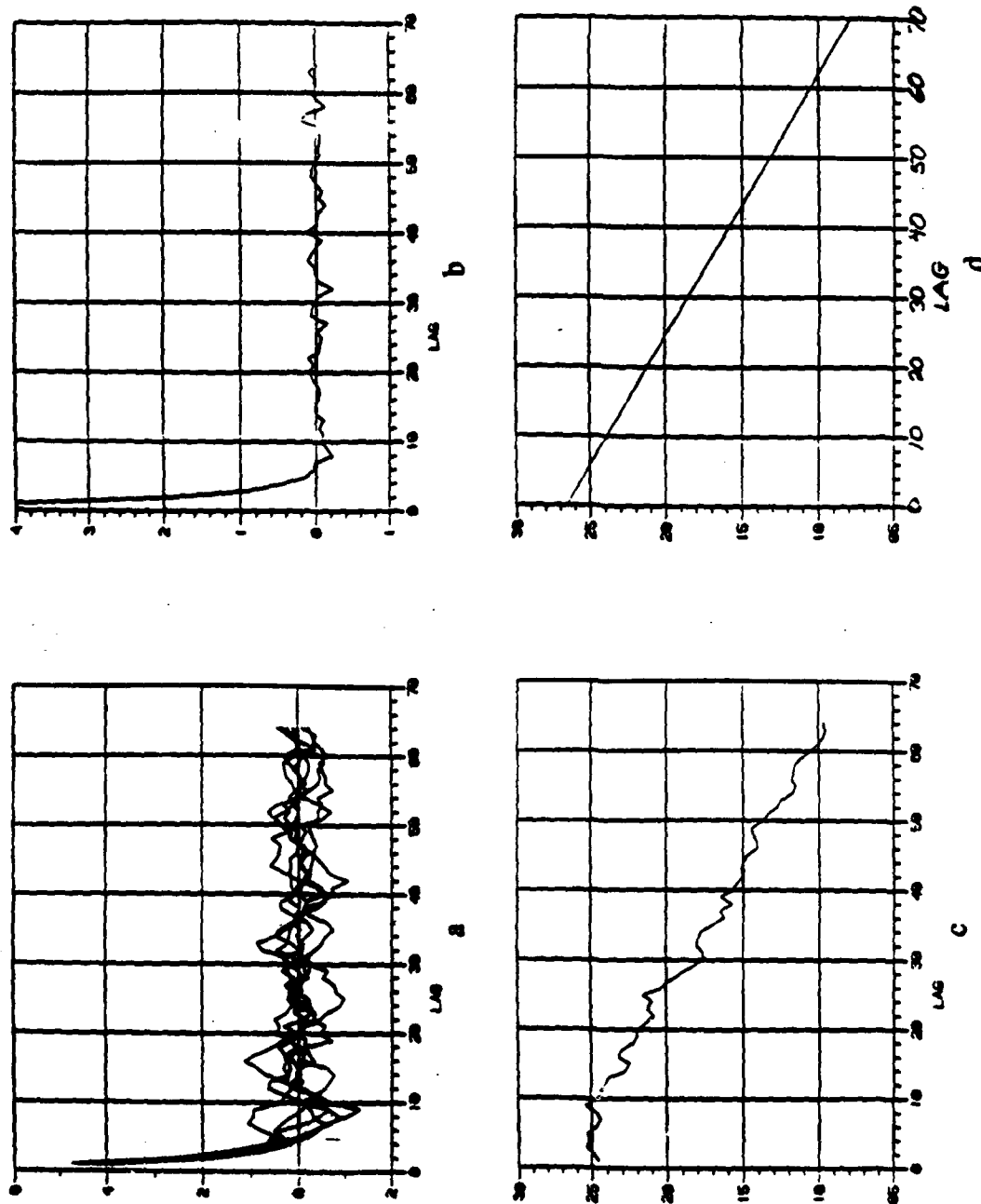


Fig 7.D.5 Time-averaged cross-correlation function and its variance for $\rho_{12}=0.99$, $\lambda_{11}=\lambda_{22}=\lambda_{12}=0.5$, $\sigma_{11}^2=\sigma_{22}^2=4$, $\lambda_{12}=0$ a.) biased $R_T(l)$ (6 trials) using $N_T=100$ b.) ensemble averaged $R_E(l)$ (1,000 realizations) c.) sample variance of the biased $R_T(l)$ (1000 realizations) d.) analytical variance of biased $R_T(l)$.

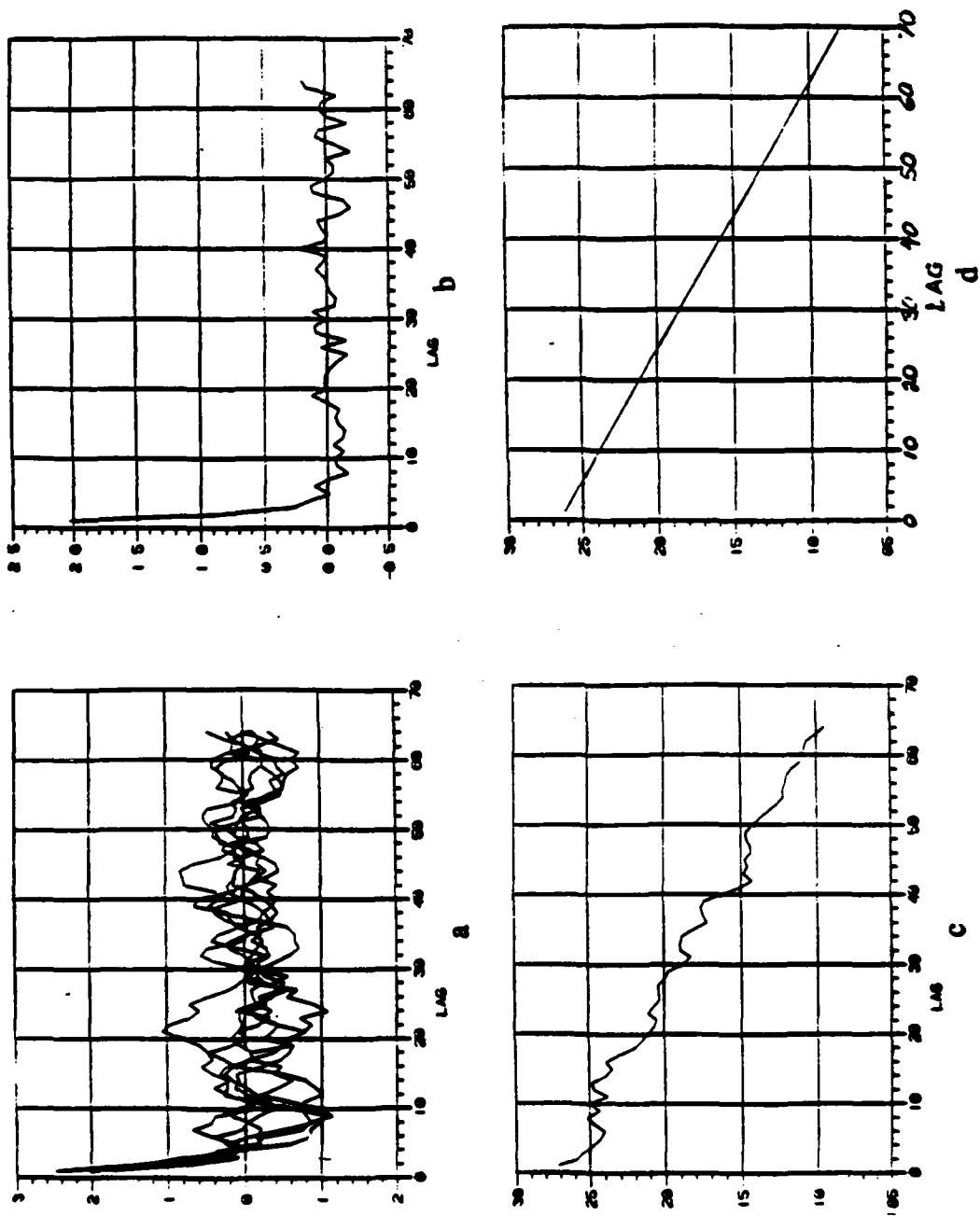


Fig 7.D.6 Time-averaged cross-correlation function and its variance for $|p_{12}|=0.5$, $\lambda_{11}=\lambda_{22}=\lambda_{12}=0.5$, $\sigma_{11}^2=\sigma_{22}^2=4$, $l_1 l_2=0$ a.) biased $R_T(l)$ (6 trials) using $N_T=100$ b.) ensemble averaged $R_E(l)$ (1,000 realizations) c.) sample variance of the biased $R_T(l)$ (1000 realizations) d.) analytical variance of biased $R_T(l)$.

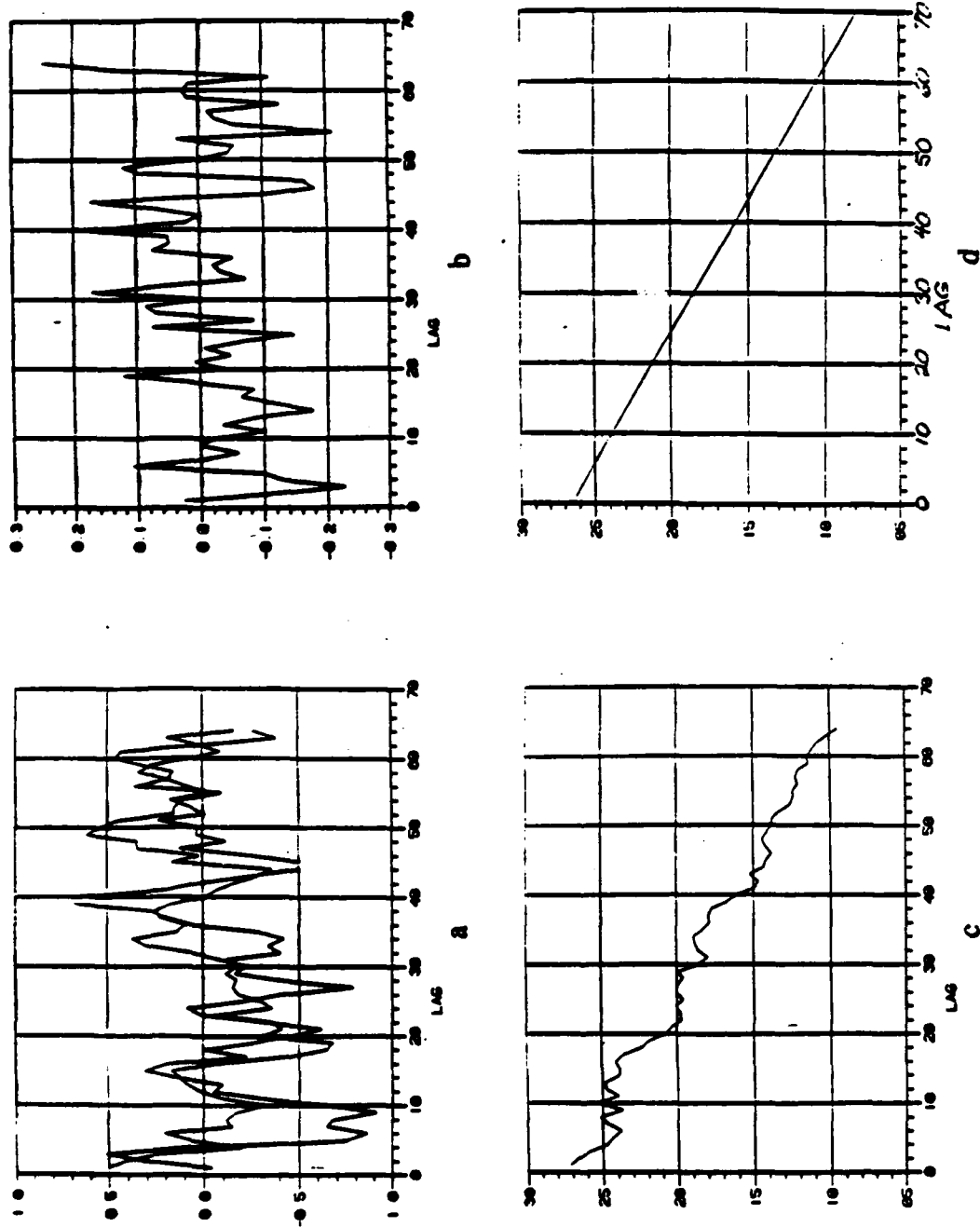


Fig 7.D.7 Time-averaged cross-correlation function and its variance for $\rho_{12} = 0.0$, $\lambda_1 = \lambda_2 = \lambda_{12} = 0.5$, $\sigma_{11}^2 = \sigma_{22}^2 = 4$, $\rho_{12} = 0$ a.) biased $R_T(l)$ (2 trials) using $N_T = 100$ b.) ensemble averaged $R_E(l)$ (1,000 realizations) c.) sample variance of the biased $R_T(l)$ (1000 realizations) d.) analytical variance of biased $R_T(l)$.

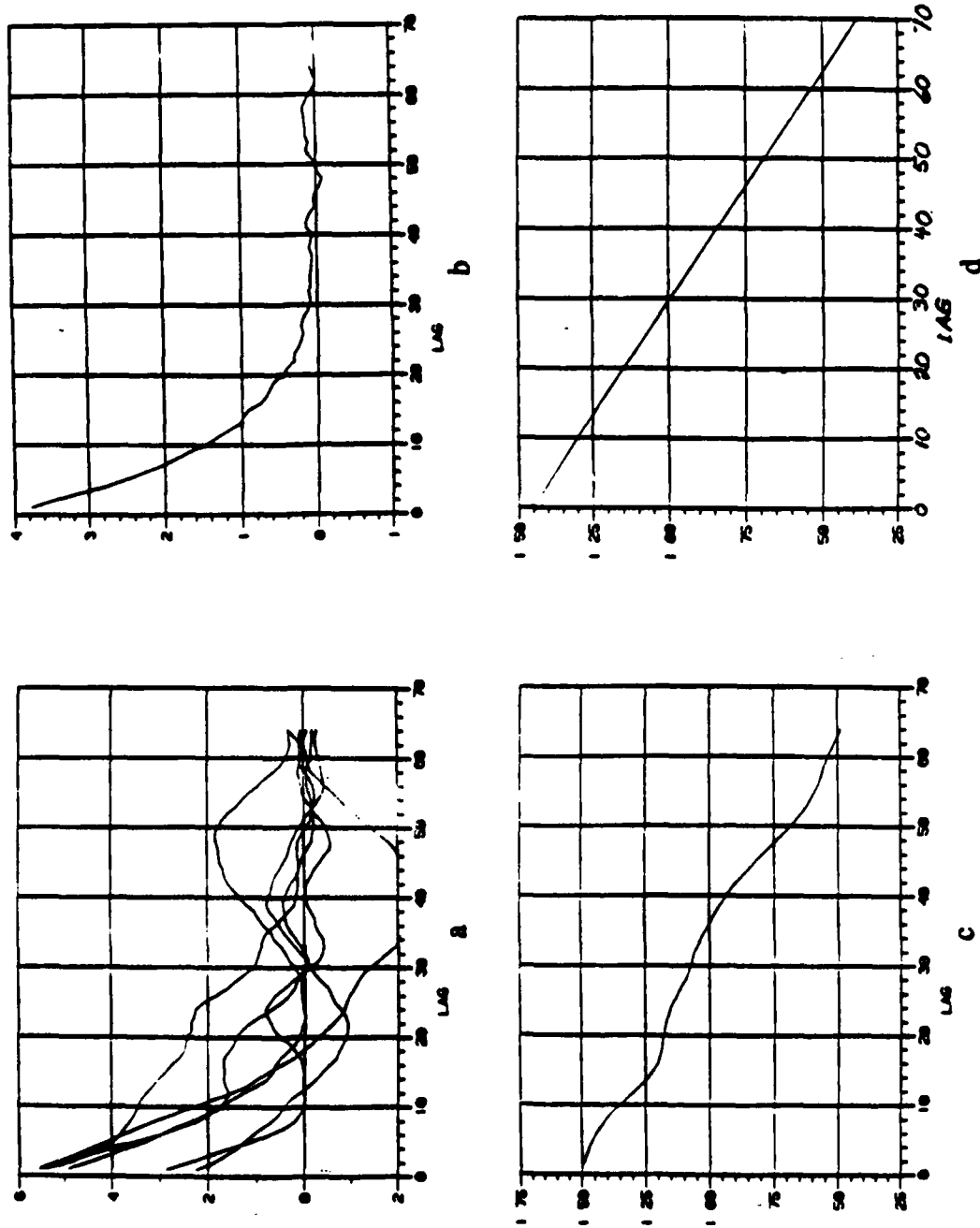


Fig 7.D.8 Time-averaged cross-correlation function and its variance for $|p_{12}|=0.99$, $\lambda_{11}=\lambda_{22}=\lambda_{12}=0.9$, $\sigma_{11}^2=\sigma_{22}^2=4$, $\lambda_{12}=0$ a.) biased $R_T(l)$ (6 trials) using $N_T=100$ b.) ensemble averaged $R_E(l)$ (1,000 realizations) c.) sample variance of the biased $R_T(l)$ (1000 realizations) d.) analytical variance of biased $R_T(l)$.

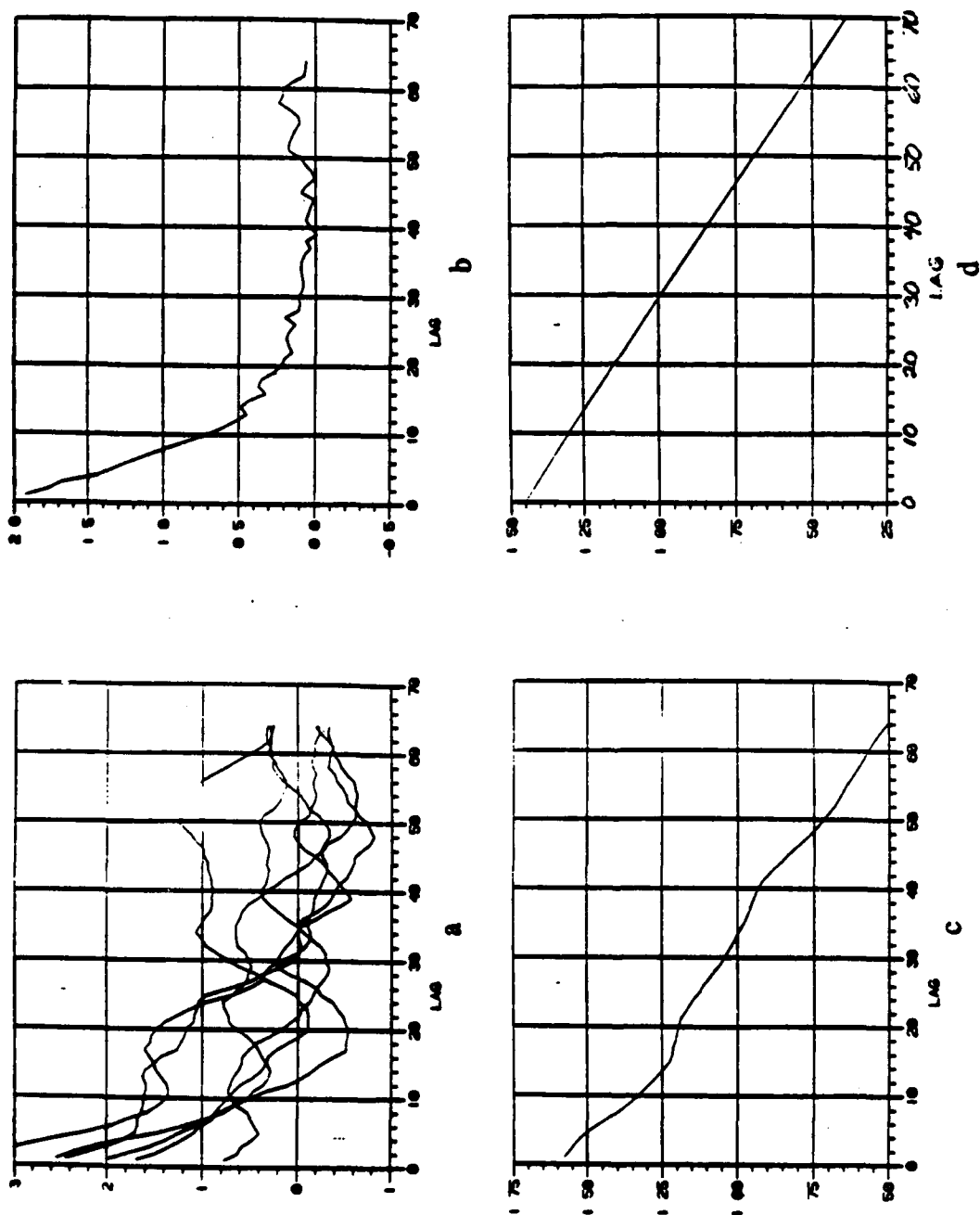


Fig 7.D.9 Time-averaged cross-correlation function and its variance for $|p_{12}|=0.5$, $\lambda_1=\lambda_2=0.9$, $\sigma_{11}^2=\sigma_{22}^2=4$, $\lambda_{12}=0$ a.) biased $R_T(l)$ (6 trials) using $N_T=100$ b.) ensemble averaged $R_E(l)$ (1,000 realizations) c.) sample variance of the biased $R_T(l)$ (1000 realizations) d.) analytical variance of biased $R_T(l)$.

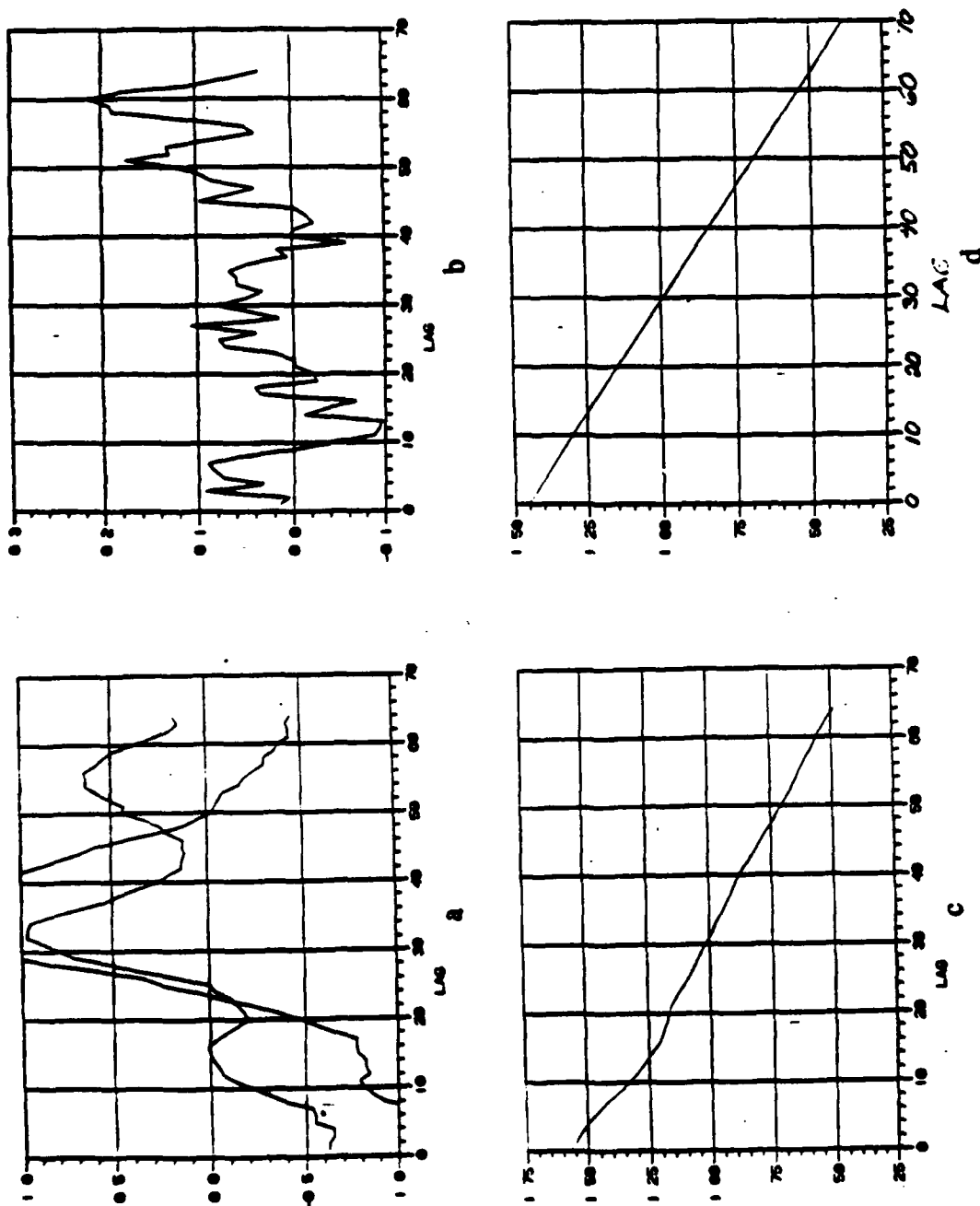


Fig 7.D.10 Time-averaged cross-correlation function and its variance for $|p_{12}|=0.0$, $\lambda_{11}=\lambda_{22}=\lambda_{12}=0.9$, $\sigma_{11}^2=\sigma_{22}^2=4$, $l_1 l_2=0$ a.) biased $R_T(l)$ (2 trials) using $N_T=100$ b.) ensemble averaged $R_E(l)$ (1,000 realizations) c.) sample variance of the biased $R_T(l)$ (1000 realizations) d.) analytical variance of biased $R_T(l)$.

REFERENCES

- [1] Michels, J. H., "A Parametric Detection Approach Using Multichannel Processes", RADC-TR-89-306, Nov. 1989, DTIC no. ADA - 219 -328.
- [2] Farina, A., Russo, A., "Radar Detection of Correlated Targets in Clutter", IEEE Trans. on Aerospace and Electronics Systems, vol AES-22, no 5, Sept. 1986.
- [3] Therrien, C.W., "The Analysis of Multichannel Two-Dimensional Random Signals", Naval Postgraduate School technical report NPS62-87-002, 31 Oct. 1986.
- [4] Haykin, S., Adaptive filter theory Prentice-Hall, 1986.
- [5] Papoulis, A., Probability. Random Variables and Stochastic Processes McGraw Hill, 1965.
- [6] Papoulis, A., Signal Analysis, McGraw-Hill Book Co., 1977.
- [7] Jenkins, G., Watts, D., Spectral Analysis and its applications, Holden-Day, 1968.
- [8] Bartlett, M.S., "On the Theoretical Specification and Sampling Properties of Autocorrelated Time Series." Jour. Royal Stat. Soc. B8, 27(1946).
- [9] Wiggins, R., Robinson, E., "Recursive Solution to the Multichannel Filtering Problem," JGR, Vol 70, 1965.
- [10] Marple, S. L., Digital Spectral Analysis with Applications, Prentice Hall, N.J., 1987.
- [11] Box, G. and Jenkins, G., Time Series Analysis -Forecasting and Control, Holden Day, 1976.

- [12] Prussing, J.E., "The Principal Minor Test for Semidefinite Matrices", *AIAA Journal of Guidance, Control, and Dynamics*, 9, 1, pp 121-122, Jan.-Feb. 1986.
- [13] Kerr, T.H. "Fallacies in Computational Testing of Matrix Positive Definiteness / Semidefiniteness", *IEEE Trans. AES*, vol. 26, no. 2, Mar.1990.
- [14] Swerling, P. "Detection of Fluctuating Pulsed Signals in the Presence of Noise", *IRE Trans.*, vol. IT-3, pp. 175-178, Sept. 1957.
- [15] Michels, J. H. "A Summary of Single and Multichannel Prediction Error Filters and Associated Algorithms", to be published as an RADC technical report.
- [16] Nuttall, A.H., *FORTTRAN Program for Multivariate Linear Predictive Spectral Analysis, Employing Forward and Backward Averaging*", Naval Underwater Systems Center TR-5419, New London, Conn., May 1976.
- [17] Nuttall, A.H., "Multivariate Linear Predictive Spectral Analysis Employing Weighted Forward and Backward Averaging: A generalization of Burg's algorithm, Naval Underwater Systems Center TR-5501, New London, Conn. Oct. 1976.

Appendix A

In this Appendix, we prove that

$$R_{\hat{n}_i \hat{n}_j}(\tau) = R_{n_i n_j}(\tau) \quad \text{for } i=j \text{ and } i \neq j \quad (\text{A.1})$$

where the symbol \wedge in this discussion refers to the Hilbert transform. Consider

$$R_{\hat{n}_i \hat{n}_j}(\tau) = E[\hat{n}_i(t) \hat{n}_j(t-\tau)] \quad (\text{A.2a})$$

$$= E \left[\frac{1}{\pi} \int_{-\infty}^{\infty} \frac{\hat{n}_i(t) n_j(\lambda)}{t-\tau-\lambda} d\lambda \right] \quad (\text{A.2b})$$

$$= \frac{1}{\pi} \int_{-\infty}^{\infty} \frac{E[\hat{n}_i(t) n_j(\lambda)]}{t-\tau-\lambda} d\lambda \quad (\text{A.2c})$$

But

$$E[\hat{n}_i(t) n_j(\lambda)] = E \left[\frac{1}{\pi} \int_{-\infty}^{\infty} \frac{n_i(\phi) n_j(\lambda)}{t-\phi} d\phi \right] \quad (\text{A.3a})$$

$$= \frac{1}{\pi} \int_{-\infty}^{\infty} \frac{E[n_i(\phi) n_j(\lambda)]}{t-\phi} d\phi \quad (\text{A.3b})$$

$$= \frac{1}{\pi} \int_{-\infty}^{\infty} \frac{R_{n_i n_j}(\phi-\lambda)}{t-\phi} d\phi \quad (\text{A.3c})$$

Let

$$\alpha = t - \lambda \quad (\text{A.4a})$$

and

$$\beta = \phi - \lambda \quad (\text{A.4b})$$

so that

$$E[\hat{n}_i(t)n_j^*(\lambda)] = \frac{1}{\pi} \int_{-\infty}^{\infty} \frac{R_{n_i n_j}(\beta)}{t-\beta-\lambda} d\beta \quad (\text{A.5a})$$

$$= \hat{R}_{n_i n_j}(t-\lambda) = \hat{R}_{n_i n_j}(\alpha). \quad (\text{A.5b})$$

Using eq(A.5b) in (A.2c), we have

$$R_{\hat{n}_i \hat{n}_j}(\tau) = \frac{1}{\pi} \int_{-\infty}^{\infty} \frac{\hat{R}_{n_i n_j}(\alpha)}{\alpha-\tau} (-d\alpha) \quad (\text{A.6a})$$

$$= \frac{1}{\pi} \int_{-\infty}^{\infty} \frac{\hat{R}_{n_i n_j}(\alpha)}{\tau-\alpha} d\alpha \quad (\text{A.6b})$$

$$= \hat{R}_{n_i n_j}(\tau) = R_{n_i n_j}. \quad (\text{A.6c})$$

These results also hold when $i = j$.

Appendix B

In this appendix, we derive the expression for the variance of $\hat{R}_{iiT}(l, N)$ expressed by eq(4.A.3a). Consider the time averaged estimate of the autocorrelation function; ie.,

$$\hat{R}_{iiT}(l, N) = \frac{1}{2N+1} \sum_{n=-N}^N x_i(n) x_i^*(n-l) \quad (B.1)$$

where the symbol \wedge in this discussion designates the quantity as an estimate. Let

$$\phi(n, l) = x_i(n) x_i^*(n-l) \quad (B.2)$$

Assuming stationarity, the covariance of $\phi(n, l)$ can be expressed as

$$C_{\phi\phi}(k, l) = E[\{ \phi(n, l) - E[\phi(n, l)] \} \{ \phi^*(n-k, l) - E[\phi^*(n-k, l)] \}] \quad (B.3a)$$

$$= E[\phi(n, l) \phi^*(n-k, l)] - E[\phi(n, l)] E[\phi^*(n-k, l)] \\ - E[\phi(n, l)] E[\phi^*(n-k, l)] + E[\phi(n, l)] E[\phi^*(n-k, l)] \quad (B.3b)$$

$$= R_{\phi\phi}(k, l) - E[\phi(n, l)] E[\phi^*(n-k, l)] \quad (B.3c)$$

where

$$R_{\phi\phi}(k, l) = E[\phi(n, l) \phi^*(n-k, l)]. \quad (B.4)$$

Assuming stationarity, we have from eq(B.2),

$$E[\phi(n, l)] = R_{ii}(l) \quad (B.5a)$$

and

$$E[\phi^*(n-k, l)] = R_{ii}^*(l) \quad (B.5b)$$

so that

$$C_{\phi\phi}(k,l) = R_{\phi\phi}(k,l) - |R_{ii}(l)|^2 \quad (\text{B.6a})$$

$$= E[x_i(n)x_i^*(n-l)x_i^*(n-k)x_i(n-l-k)] - |R_{ii}(l)|^2. \quad (\text{B.6b})$$

Now consider the variance of the complex estimate $\hat{R}_{iiT}(l,N)$ which can be expressed as

$$V_{ii}(l,N) = E \left\{ [\hat{R}_{iiT}(l,N) - E[\hat{R}_{iiT}(l,N)]] [\hat{R}_{iiT}^*(l,N) - E[\hat{R}_{iiT}^*(l,N)]] \right\} \quad (\text{B.7a})$$

$$= E[\hat{R}_{iiT}(l,N)\hat{R}_{iiT}^*(l,N)] - E[\hat{R}_{iiT}(l,N)]E[\hat{R}_{iiT}^*(l,N)]. \quad (\text{B.7b})$$

Using eq(B.1), we have

$$\hat{R}_{iiT}(l,N)\hat{R}_{iiT}^*(l,N) = \frac{1}{(2N+1)^2} \sum_{n=-N}^N \sum_{p=-N}^N x_i(n)x_i^*(n-l)x_i^*(p)x_i(p-l) \quad (\text{B.8})$$

so that

$$E[\hat{R}_{iiT}(l,N)\hat{R}_{iiT}^*(l,N)] = \frac{1}{(2N+1)^2} \sum_{n=-N}^N \sum_{p=-N}^N E[x_i(n)x_i^*(n-l)x_i^*(p)x_i(p-l)]. \quad (\text{B.9})$$

Also, from eq(B.1)

$$E[\hat{R}_{iiT}(l,N)] = \frac{1}{(2N+1)} \sum_{n=-N}^N R_{ii}(l) \quad (\text{B.10})$$

so that

$$E[\hat{R}_{iiT}(l,N)]E[\hat{R}_{iiT}^*(l,N)] = \frac{1}{(2N+1)^2} \sum_{n=-N}^N \sum_{p=-N}^N R_{ii}(l)R_{ii}^*(l). \quad (\text{B.11a})$$

$$= \frac{1}{(2N+1)^2} \sum_{n=-N}^N \sum_{p=-N}^N |R_{ii}(l)|^2. \quad (\text{B.11b})$$

Using eqs(B.9) and (B.11b) in (B.7b), we obtain

$$V_{ii}(l,N) = \frac{1}{(2N+1)^2} \sum_{n=-N}^N \sum_{p=-N}^N \left\{ E[x_i(n)x_i^*(n-l)x_i^*(p)x_i(p-l)] - |R_{ii}(l)|^2 \right\}. \quad (B.12)$$

Using eq(B.6b) in eq(B.12)

$$V_{ii}(l,N) = \frac{1}{(2N+1)^2} \sum_{n=-N}^N \sum_{p=-N}^N C_{\phi\phi}(n-p,l) \quad (B.13a)$$

$$= \frac{1}{(2N+1)^2} \sum_{k=-2N}^{2N} [2N+1-|k|] C_{\phi\phi}(k,l) \quad (B.13b)$$

$$= \frac{1}{(2N+1)} \sum_{k=-2N}^{2N} \left[1 - \frac{|k|}{2N+1} \right] C_{\phi\phi}(k,l). \quad (B.13c)$$

We now derive an alternate expression for the variance of $\hat{R}_{iiT}(l,N)$ using the biased time-averaged autocorrelation function. In this case, we use eq(7.C.1) with $M=N_T$ so that eq(B.8) becomes for positive and negative l

$$\hat{R}_{iiT_b}(l,N_T) \hat{R}_{iiT_b}^*(l,N_T) = \frac{1}{N_T^2} \sum_{n=0}^{N_T-l-1} \sum_{p=0}^{N_T-l-1} x_i(n)x_i^*(n-l)x_i^*(p)x_i(p-l) \quad (B.14a)$$

$0 \leq l \leq N_T - 1$

$$= \frac{1}{N_T^2} \sum_{n=0}^{N_T-|l|-1} \sum_{p=0}^{N_T-|l|-1} x_i(n)x_i(n-|l|)x_i^*(p)x_i^*(p-|l|) \quad (B.14b)$$

$-(N_T-1) \leq l \leq 0$

so that

$$E[\hat{R}_{iiTb}(l, N_T) \hat{R}_{iiTb}^*(l, N_T)] = \frac{1}{N_T} \sum_{n=0}^{N_T-l-1} \sum_{p=0}^{N_T-l-1} E[x_i(n) x_i^*(n-l) x_i^*(p) x_i(p-l)]$$

$$0 \leq l \leq N_T - 1 \quad (B.15a)$$

$$= \frac{1}{N_T} \sum_{n=0}^{N_T-l-1} \sum_{p=0}^{N_T-l-1} E[x_i(n) x_i(n-l) x_i(p) x_i^*(p-l)]$$

$$-(N_T-1) \leq l \leq 0 \quad (B.15b)$$

Also,

$$E[\hat{R}_{iiTb}(l, N_T)] = \frac{1}{N_T} \sum_{n=0}^{N_T-l-1} R_{ii}(l) \quad 0 \leq l \leq N_T - 1 \quad (B.16a)$$

$$= \frac{1}{N_T} \sum_{n=0}^{N_T-l-1} R_{ii}^*(l) \quad -(N_T-1) \leq l \leq 0. \quad (B.16b)$$

so that

$$E[\hat{R}_{iiTb}(l, N_T)] E[\hat{R}_{iiTb}^*(l, N_T)] =$$

$$= \frac{1}{N_T^2} \sum_{n=0}^{N_T-l-1} \sum_{p=0}^{N_T-l-1} |R_{ii}(l)|^2 \quad 0 \leq l \leq N_T \quad (B.17a)$$

$$= \frac{1}{N_T^2} \sum_{n=0}^{N_T-l-1} \sum_{p=0}^{N_T-l-1} |R_{ii}(l)|^2 \quad -(N_T-1) \leq l \leq 0. \quad (B.17b)$$

Using eqs(B.15) and (B.17) in the expression

$$V_{B_{ii}}(l, N_T) = E[\hat{R}_{iiTb}(l, N_T) \hat{R}_{iiTb}^*(l, N_T)] - E[\hat{R}_{iiTb}(l, N_T)] E[\hat{R}_{iiTb}^*(l, N_T)]$$

$$(B.18)$$

we obtain

$$V_{B_{ii}}(l, N_T) = \frac{1}{N_T^2} \sum_{n=0}^{N_T-l-1} \sum_{p=0}^{N_T-l-1} \{ E[x_i(n)x_i^*(n-l)x_i^*(p)x_i(p-l)] - |R_{ii}(l)|^2 \}$$

for $0 \leq l \leq N_T - 1$ (B.19a)

$$= \frac{1}{N_T^2} \sum_{n=0}^{N_T-||l|-1} \sum_{p=0}^{N_T-||l|-1} \{ E[x_i^*(n)x_i(n-||l|)x_i^*(p)x_i(p-||l|)] - |R_{ii}(l)|^2 \}$$

for $-(N_T-1) \leq l \leq 0$. (B.19b)

Using eq(B.6b) in (B.19)

$$V_{B_{ii}}(l, N_T) = \frac{1}{N_T^2} \sum_{n=0}^{N_T-l-1} \sum_{p=0}^{N_T-l-1} C_{\phi\phi}(n - p, l) \quad 0 \leq l \leq N_T - 1 \quad (B.20a)$$

$$= \frac{1}{N_T^2} \sum_{n=0}^{N_T-||l|-1} \sum_{p=0}^{N_T-||l|-1} C_{\phi\phi}^*(n - p, ||l|) \quad -(N_T-1) \leq l \leq 0. \quad (B.20b)$$

We now let $k = n - p$ where

$$-(N_T - l - 1) \leq k \leq N_T - l - 1 \quad \text{for} \quad 0 \leq l \leq N_T - 1 \quad (B.21a)$$

$$-(N_T - ||l| - 1) \leq k \leq N_T - ||l| - 1 \quad \text{for} \quad -(N_T-1) \leq l \leq 0. \quad (B.21b)$$

We also note that eq(B.21b) is equivalent to eq(B.21a) for all l so that

$$V_{B_{ii}}(l, N_T) = \frac{1}{N_T} \sum_{k=-(N_T-||l|-1)}^{N_T-||l|-1} [N_T - ||l| - |k|] C_{\phi\phi}(k, l) \quad 0 \leq l \leq N_T - 1 \quad (B.22a)$$

$$= \frac{1}{N_T} \sum_{k=-(N_T-|l|-1)}^{N_T-|l|-1} [N_T - |l| - |k|] C_{\phi\phi}^*(k, |l|) \quad -(N_T-1) \leq l \leq 0. \quad (\text{B.22b})$$

However, for negative lag l , we have

$$C_{\phi\phi}^*(k, |l|) = C_{\phi\phi}(k, l) \quad (\text{B.23})$$

so that after dividing the bracketed factor by one of the N_T terms in the denominator

$$V_{B_{ii}}(l, N_T) = \frac{1}{N_T} \sum_{k=-(N_T-|l|-1)}^{N_T-|l|-1} \left[1 - \frac{|l| + |k|}{N_T} \right] C_{\phi\phi}(k, l) \quad (\text{B.24})$$

for both positive and negative values of l . In Appendix C, we show that the imaginary terms in $C_{\phi\phi}(k, l)$ cancel when summed over positive and negative values of k so that

$$V_{B_{ii}}(l, N_T) = \frac{1}{N_T} \sum_{k=-(N_T-|l|-1)}^{N_T-|l|-1} \left[1 - \frac{|l| + |k|}{N_T} \right] \text{Re} \{ C_{\phi\phi}(k, l) \}. \quad (\text{B.25})$$

Appendix C

In this appendix, we consider the term $F_{ii}(l,k)$ in eq(4.A.11); ie.,

$$F_{ii}(l,k) = E[x_i(n)x_i(n-l-k)]E[x_i^*(n-l)x_i^*(n-k)]. \quad (C.1)$$

Expressing the process $x_i(n)$ in terms of its quadrature components

$$E[x_i(n)x_i(n-l-k)] = E\{[x_{iI}(n) + jx_{iQ}(n)][x_{iI}(n-l-k) + jx_{iQ}(n-l-k)]\} \quad (C.2a)$$

$$= \{R_{ii}^{II}(l+k) - R_{ii}^{QQ}(l+k)\} + j\{R_{ii}^{QI}(l+k) + R_{ii}^{IQ}(l+k)\} \quad (C.2b)$$

and

$$E[x_i^*(n-l)x_i^*(n-k)] = E\{[x_{iI}(n-l) - jx_{iQ}(n-l)][x_{iI}(n-k) - jx_{iQ}(n-k)]\} \quad (C.3a)$$

$$= \{R_{ii}^{II}(k-l) - R_{ii}^{QQ}(k-l)\} - j\{R_{ii}^{QI}(k-l) + R_{ii}^{IQ}(k-l)\} \quad (C.3b)$$

But

$$R_{ii}^{II}(k-l) = R_{ii}^{II}(l-k) \quad (C.4a)$$

$$R_{ii}^{QQ}(k-l) = R_{ii}^{QQ}(l-k) \quad (C.4b)$$

$$R_{ii}^{QI}(k-l) = R_{ii}^{IQ}(l-k) \quad (C.4c)$$

$$R_{ii}^{IQ}(k-l) = R_{ii}^{QI}(l-k) \quad (C.4d)$$

so that eq(C.3b) becomes

$$\begin{aligned}
E[x_i^*(n-l)x_i^*(n-k)] &= \\
&= \{R_{ii}^{II}(l-k) - R_{ii}^{QQ}(l-k)\} - j\{R_{ii}^{QI}(l-k) + R_{ii}^{IQ}(l-k)\}. \quad (C.5)
\end{aligned}$$

Substituting eqs(C.2b) and (C.5) into (C.1), we obtain

$$\begin{aligned}
F_{ii}(l,k) &= \{R_{ii}^{II}(l+k) - R_{ii}^{QQ}(l+k)\} \{R_{ii}^{II}(l-k) - R_{ii}^{QQ}(l-k)\} \\
&\quad + \{R_{ii}^{QI}(l+k) + R_{ii}^{IQ}(l+k)\} \{R_{ii}^{QI}(l-k) + R_{ii}^{IQ}(l-k)\} \\
&\quad - j \{R_{ii}^{II}(l+k) - R_{ii}^{QQ}(l+k)\} \{R_{ii}^{QI}(l-k) + R_{ii}^{IQ}(l-k)\} \\
&\quad + j \{R_{ii}^{II}(l-k) - R_{ii}^{QQ}(l-k)\} \{R_{ii}^{QI}(l+k) + R_{ii}^{IQ}(l+k)\}. \quad (C.6)
\end{aligned}$$

When the function $F_{ii}(l,k)$ is used in eq(4.A.12), and the limit as $N \rightarrow \infty$ is taken, it contributes the additional term in the summation

$$L_{ii}(l) = \lim_{N \rightarrow \infty} \frac{1}{2N+1} \sum_{k=-2N}^{2N} \left[1 - \frac{|k|}{2N+1} \right] F_{ii}(l,k). \quad (C.7)$$

By examination of eq(C.6), we note that the imaginary terms in eq(C.7) sum to zero. This can be seen by first noting that $F_{ii}(l,k)$ is real for $k=0$. We also note that imaginary terms evaluated with negative values of k serve to cancel the corresponding imaginary terms for positive values of k . And so, only the real part of the function $F_{ii}(l,k)$ contributes to the function $L_{ii}(l)$. Therefore,

$$L_{ii}(l) = \lim_{N \rightarrow \infty} \frac{1}{2N+1} \sum_{k=-2N}^{2N} \left[1 - \frac{|k|}{2N+1} \right] \text{Re}\{F_{ii}(l,k)\}. \quad (C.8)$$

Examination of the real terms in eq(C.6) indicate that identical terms are contributed by each positive and negative k value so that eq(C.8) can also be written

$$L_{ii}(l) = \lim_{N \rightarrow \infty} \frac{1}{2N+1} \sum_{k=0}^{2N} \left[1 - \frac{|k|}{2N+1} \right] \{ 2\text{Re}\{F_{ii}(l,k)\} - F_{ii}(l,0) \}. \quad (\text{C.9})$$

The term $F_{ii}(l,0)$ is subtracted in the above equation so that it is not counted twice. If we now define

$$R_{C_{ii}}(\alpha) = R_{ii}^{II}(\alpha) - R_{ii}^{QQ}(\alpha) \quad (\text{C.10a})$$

and

$$R_{D_{ii}}(\alpha) = R_{ii}^{QI}(\alpha) + R_{ii}^{IQ}(\alpha) \quad (\text{C.10b})$$

eq(C.8) becomes

$$L_{ii}(l) = \lim_{N \rightarrow \infty} \frac{1}{2N+1} \sum_{k=-2N}^{2N} \left[1 - \frac{|k|}{2N+1} \right] \text{Re}\{F_{ii}(l,k)\} \quad (\text{C.11a})$$

$$= \lim_{N \rightarrow \infty} \frac{1}{2N+1} \sum_{k=-2N}^{2N} \left[1 - \frac{|k|}{2N+1} \right] [R_{C_{ii}}(l+k)R_{C_{ii}}(l-k) + R_{D_{ii}}(l+k)R_{D_{ii}}(l-k)] \quad (\text{C.11b})$$

If the corresponding bandpass processes are stationary and narrowband, then (see Section III.E.2.a),

$$R_{ii}^{II}(\alpha) = R_{ii}^{QQ}(\alpha) \quad (\text{C.12a})$$

and

$$R_{ii}^{QI}(\alpha) = -R_{ii}^{IQ}(\alpha). \quad (\text{C.12b})$$

Using eqs(C.12a) and (C.12b) in (C.6), we obtain

$$F_{ii}(l,k) = 0. \quad (C.13)$$

In this case, eq(4.A.13b) becomes

$$V_{ii}(l,N) = \lim_{N \rightarrow \infty} \frac{1}{2N+1} \sum_{k=-2N}^{2N} \left[1 - \frac{|k|}{2N+1} \right] |R_{ii}(k)|^2. \quad (C.14)$$

Appendix D

In this appendix, we consider the terms $F_{ij}(l,k)$ and $R_{ii}(k)R_{jj}^*(k)$ in eq(4.B.10c). Consider,

$$F_{ij}(l,k) = E[x_i(n)x_j(n-l-k)]E[x_j^*(n-l)x_i^*(n-k)]. \quad (D.1)$$

Expressing the processes $x_i(n)$ and $x_j(n)$ in quadrature form, we have

$$E[x_i(n)x_j(n-l-k)] = E\{[x_{iI}(n) + jx_{iQ}(n)][x_{jI}(n-l-k) + jx_{jQ}(n-l-k)]\} \quad (D.2a)$$

$$= \{R_{ij}^{II}(l+k) - R_{ij}^{QQ}(l+k)\} + j\{R_{ij}^{QI}(l+k) + R_{ij}^{IQ}(l+k)\} \quad (D.2b)$$

and

$$E[x_j^*(n-l)x_i^*(n-k)] = E\{[x_{jI}(n-l) - jx_{jQ}(n-l)][x_{iI}(n-k) - jx_{iQ}(n-k)]\} \quad (D.3a)$$

$$= \{R_{ji}^{II}(k-l) - R_{ji}^{QQ}(k-l)\} - j\{R_{ji}^{QI}(k-l) + R_{ji}^{IQ}(k-l)\} \quad (D.3b)$$

But

$$R_{ji}^{II}(k-l) = R_{ij}^{II}(l-k) \quad (D.4a)$$

$$R_{ji}^{QQ}(k-l) = R_{ij}^{QQ}(l-k) \quad (D.4b)$$

$$R_{ji}^{QI}(k-l) = R_{ij}^{IQ}(l-k) \quad (D.4c)$$

$$R_{ji}^{IQ}(k-l) = R_{ij}^{QI}(l-k) \quad (D.4d)$$

so that eq(D.3b) becomes

$$\begin{aligned}
E[x_j^*(n-l)x_i^*(n-k)] &= \\
&= \{R_{ij}^{II}(l-k) - R_{ij}^{QQ}(l-k)\} - j\{R_{ij}^{QI}(l-k) + R_{ij}^{IQ}(l-k)\}. \quad (D.5)
\end{aligned}$$

Substituting eqs(D.2b) and (D.5) into (D.1), we have

$$\begin{aligned}
F_{ij}(l,k) &= \{R_{ij}^{II}(l+k) - R_{ij}^{QQ}(l+k)\} \{R_{ij}^{II}(l-k) - R_{ij}^{QQ}(l-k)\} \\
&\quad + \{R_{ij}^{QI}(l+k) + R_{ij}^{IQ}(l+k)\} \{R_{ij}^{QI}(l-k) + R_{ij}^{IQ}(l-k)\} \\
&\quad - j \{R_{ij}^{II}(l+k) - R_{ij}^{QQ}(l+k)\} \{R_{ij}^{QI}(l-k) + R_{ij}^{IQ}(l-k)\} \\
&\quad + j \{R_{ij}^{II}(l-k) - R_{ij}^{QQ}(l-k)\} \{R_{ij}^{QI}(l+k) + R_{ij}^{IQ}(l+k)\}. \quad (D.6)
\end{aligned}$$

When the function $F_{ij}(l,k)$ is used in eq(4.B.14), it contributes the additional term in the summation

$$L_{ij}(l) = \lim_{N \rightarrow \infty} \frac{1}{2N+1} \sum_{k=-2N}^{2N} \left[1 - \frac{|kl|}{2N+1} \right] F_{ij}(l,k). \quad (D.7)$$

As in the case for $L_{ii}(l)$ expressed by eq(C.7), the imaginary terms in eq(D.6) cancel in the summation of eq(D.7). Therefore, only the real part of $F_{ij}(l,k)$ contributes to the term $V_{ij}(l,N)$ so that

$$L_{ii}(l) = \lim_{N \rightarrow \infty} \frac{1}{2N+1} \sum_{k=-2N}^{2N} \left[1 - \frac{|kl|}{2N+1} \right] \text{Re}\{F_{ii}(l,k)\}. \quad (D.8)$$

Examination of the real terms in eq(D.6) indicate that identical terms are contributed by each positive and negative k value so that eq(D.8) becomes

$$L_{ij}(l) = \lim_{N \rightarrow \infty} \frac{1}{2N+1} \sum_{k=0}^{2N} \left[1 - \frac{|kl|}{2N+1} \right] \{ 2\text{Re}\{F_{ij}(l,k)\} - F_{ij}(l,0) \}. \quad (\text{D.9})$$

The term $F_{ij}(l,0)$ is subtracted in the above equation so that it is not counted twice. We now consider the second term in eq(4.B.10c); ie.,

$$R_{ii}(k)R_{jj}^*(k) = E[x_i(n)x_i^*(n-k)]E[x_j^*(n-l)x_j(n-l-k)]. \quad (\text{D.10})$$

Now

$$E[x_i(n)x_i^*(n-k)] = E\{[x_{iI}(n) + jx_{iQ}(n)][x_{iI}(n-k) - jx_{iQ}(n-k)]\} \quad (\text{D.11a})$$

$$= \{R_{ii}^{II}(k) + R_{ii}^{QQ}(k)\} + j\{R_{ii}^{QI}(k) - R_{ii}^{IQ}(k)\} \quad (\text{D.11b})$$

and

$$E[x_j^*(n-l)x_j(n-l-k)] = E\{[x_{jI}(n-l) - jx_{jQ}(n-l)][x_{jI}(n-l-k) + jx_{jQ}(n-l-k)]\} \quad (\text{D.12a})$$

$$= \{R_{jj}^{II}(k) + R_{jj}^{QQ}(k)\} - j\{R_{jj}^{QI}(k) - R_{jj}^{IQ}(k)\}. \quad (\text{D.12b})$$

And so

$$\begin{aligned} R_{ii}(k)R_{jj}^*(k) &= \{R_{ii}^{II}(k) + R_{ii}^{QQ}(k)\} \{R_{jj}^{II}(k) + R_{jj}^{QQ}(k)\} \\ &\quad + \{R_{ii}^{QI}(k) - R_{ii}^{IQ}(k)\} \{R_{jj}^{QI}(k) - R_{jj}^{IQ}(k)\} \\ &\quad - j\{R_{ii}^{II}(k) + R_{ii}^{QQ}(k)\} \{R_{jj}^{QI}(k) - R_{jj}^{IQ}(k)\} \\ &\quad + j\{R_{ii}^{II}(k) + R_{ii}^{QQ}(k)\} \{R_{ii}^{QI}(k) - R_{ii}^{IQ}(k)\}. \end{aligned} \quad (\text{D.13})$$

Consider the imaginary terms

$$\begin{aligned} \text{Im}\{R_{ii}(k)R_{jj}^*(k)\} = & -j R_{ii}^{II}(k)R_{jj}^{QI}(k) - j R_{ii}^{QQ}(k)R_{jj}^{QI}(k) + j R_{jj}^{II}(k)R_{jj}^{IQ}(k) \\ & + j R_{ii}^{QQ}(k)R_{jj}^{IQ}(k) + j R_{jj}^{II}(k)R_{ii}^{QI}(k) + j R_{jj}^{QQ}(k)R_{ii}^{QI}(k) \\ & - j R_{jj}^{II}(k)R_{ii}^{IQ}(k) - j R_{jj}^{QQ}(k)R_{ii}^{IQ}(k) \end{aligned} \quad (\text{D.14})$$

We now recall that

$$R_{ii}^{II}(k) = R_{ii}^{II}(-k) \quad (\text{D.15a})$$

$$R_{ii}^{QQ}(k) = R_{ii}^{QQ}(-k) \quad (\text{D.15b})$$

$$R_{ii}^{QI}(k) = R_{ii}^{IQ}(-k) \quad (\text{D.15c})$$

$$R_{ii}^{IQ}(k) = R_{ii}^{QI}(-k) \quad (\text{D.15d})$$

with equivalent expressions for the j channel processes. When $R_{ii}(k)R_{jj}^*(k)$ is used in the summation of eq(4.B.12), we recognize that the terms in eq(D.14) will cancel when the positive and negative k values are determined. For example, the first term in this equation becomes $-j R_{ii}^{II}(k)R_{jj}^{IQ}(k)$ when k is negative. This

term will cancel the third term in the equation for k positive. Similarly, the other terms cancel. A similar argument can be used to determine that the real terms in eq(D.13) for negative k equal those for positive k .

Finally, we note that if the corresponding bandpass processes are jointly stationary and narrowband, then (see Section III.E.2.b),

$$R_{ij}^{\Pi}(\alpha) = R_{ij}^{QQ}(\alpha) \quad (D.16a)$$

and

$$R_{ij}^{QI}(\alpha) = -R_{ij}^{IQ}(\alpha). \quad (D.16b)$$

Using these equations in eq(D.6), we obtain

$$F_{ij}(l,k) = 0. \quad (D.17)$$

In this case, eq(4.B.13) becomes

$$V_{ij}(l,N) = \frac{1}{2N+1} \sum_{k=-2N}^{2N} \left[1 - \frac{|k|}{2N+1} \right] \text{Re}[R_{ii}(k)R_{jj}^*(k)]. \quad (D.18)$$

Appendix E

In this appendix, we verify several of the equations noted in section III.C.4.b. From eq(3.C.60a)

$$A_1 = 1 + K_1^2 - 2(\lambda_{11})K_1 \quad (\text{E.1a})$$

$$= 1 + K_1[K_1 - 2\lambda_{11}]. \quad (\text{E.1b})$$

Taking the partial derivative of A_1 with respect to K_1 , we have

$$\frac{\partial A_1}{\partial K_1} = 2K_1 - 2\lambda_{11} \quad (\text{E.2a})$$

and

$$\frac{\partial^2 A_1}{\partial K_1^2} = +2. \quad (\text{E.2b})$$

Eq(E.2a) and the positive value of eq(E.2b) indicates that A_1 has a minimum value at $K_1 = \lambda_{11}$, so that

$$A_1 \geq 1 + \lambda_{11}^2 - 2\lambda_{11}^2 \quad (\text{E.3a})$$

$$\geq 1 - (\lambda_{11})^2. \quad (\text{E.3b})$$

Since $0 \leq \lambda_{11} \leq 1$, we have

$$A_1 \geq 1 - (\lambda_{11})^2 \geq 0 \quad (\text{E.4})$$

so that eq(3.C.61a) is verified. From eq(3.C.60e)

$$B = 1 - 2(\lambda_{12})^2 + (\lambda_{12})^4 \quad (\text{E.5a})$$

$$= [1 - (\lambda_{12})^2]^2. \quad (\text{E.5b})$$

Since $0 \leq \lambda_{11} \leq 1$, then $0 \leq B \leq 1$. From eq(3.C.60f)

$$C = (\lambda_{11})^2 + (\lambda_{22})^2 - (\lambda_{11})^2(\lambda_{22})^2 \quad (\text{E.6a})$$

$$= [\lambda_{11} - \lambda_{22}]^2 + (\lambda_{11})^2(\lambda_{22})^2 \quad (\text{E.6b})$$

so that $0 \leq C \leq 1$.

Appendix F

In this appendix, we validate eqs(7.C.8) and (7.C.9) of section VII. Consider the complex single channel i AR process of order M

$$x_i(n) = - \sum_{k=1}^M a^*(k) x_i(n-k) + u(n). \quad (F.1)$$

Expressed in quadratic form, we have

$$x_i(n) = x_{iI}(n) + j x_{iQ}(n) \quad (F.2a)$$

$$= - \sum_{k=1}^M [a_I(k) + j a_Q(k)]^* [x_{iI}(n-k) + j x_{iQ}(n-k)] + u_I(n) + j u_Q(n) \quad (F.2b)$$

$$= - \sum_{k=1}^M [a_I(k) x_{iI}(n-k) + a_Q(k) x_{iQ}(n-k)] + u_I(n) - j \left\{ \sum_{k=1}^M [a_I(k) x_{iQ}(n-k) - a_Q(k) x_{iI}(n-k)] + u_Q(n) \right\} \quad (F.2c)$$

so that

$$x_{iI}(n) = - \sum_{k=1}^M [a_I(k) x_{iI}(n-k) + a_Q(k) x_{iQ}(n-k)] + u_I(n) \quad (F.3a)$$

$$x_{iQ}(n) = - \sum_{k=1}^M [a_I(k) x_{iQ}(n-k) - a_Q(k) x_{iI}(n-k)] + u_Q(n). \quad (F.3b)$$

In general, $x_{iI}(n)$ and $x_{iQ}(n)$ will be correlated for $a_Q(k) \neq 0$ since they both contain terms involving $x_{iI}(n-k)$ and $x_{iQ}(n-k)$. However, for $a_Q(k)=0$, eqs(F.3a) and (F.3b) reduce to

$$x_{iI}(n) = - \sum_{k=1}^M a_I(k)x_{iI}(n-k) + u_I(n) \quad (F.4a)$$

$$x_{iQ}(n) = - \sum_{k=1}^M a_I(k)x_{iQ}(n-k) + u_Q(n). \quad (F.4b)$$

In this case, $x_{iI}(n)$ and $x_{iQ}(n)$ are uncorrelated provided their white noise driving terms are uncorrelated. In the process synthesis procedure described in Section VI, $a(k)$ will be real when the correlation function is specified to be real. And so, $a_Q=0$ and

$$R_{ii}^{IQ}(k) = R_{ii}^{QI}(k) = 0. \quad (F.5)$$

From eqs(F.4a) and (F.4b), we also note that both quadrature components are AR processes with the same coefficients and equal white noise driving variances. Therefore,

$$R_{ii}^{\Pi}(k) = R_{ii}^{QQ}(k). \quad (F.6)$$

We also note that in the simulation process described in section VI, we first solve for the white variance term σ_u^2 in the Yule-Walker equation. We then divide this quantity by 1/2 and apply this variance to each quadrature component of the white noise driving term. At $k=0$, we therefore expect to obtain the result

$$R_{ii}^{\Pi}(0) = R_{ii}^{QQ}(0) = \frac{\sigma_{ii}^2}{2}. \quad (F.7)$$

Appendix G

In this appendix, we validate eqs(7.D.4) and (7.D.5) of Section VII. Consider the complex two channel AR process of order M

$$\underline{\Delta}(n) = - \sum_{k=1}^M A^H(k) \underline{\Delta}(n-k) + \underline{u}(n) \quad (G.1)$$

Expressed in quadratic form, we have

$$\underline{\Delta}(n) = \underline{\Delta}_I(n) + j \underline{\Delta}_Q(n) \quad (G.2a)$$

$$= - \sum_{k=1}^M [A_I(k) + jA_Q(k)]^H [\underline{\Delta}_I(n-k) + j \underline{\Delta}_Q(n-k)] + \underline{u}_I(n) + j\underline{u}_Q(n) \quad (G.2b)$$

$$= - \sum_{k=1}^M [A_I^T(k) - jA_Q^T(k)] [\underline{\Delta}_I(n-k) + j \underline{\Delta}_Q(n-k)] + \underline{u}_I(n) + j\underline{u}_Q(n) \quad (G.2c)$$

$$= - \sum_{k=1}^M [A_I^T(k) \underline{\Delta}_I(n-k) + A_Q^T(k) \underline{\Delta}_Q(n-k)] + \underline{u}_I(n) \\ - j \left\{ \sum_{k=1}^M [A_I^T(k) \underline{\Delta}_Q(n-k) - A_Q^T(k) \underline{\Delta}_I(n-k)] + \underline{u}_Q(n) \right\} \quad (G.2d)$$

so that

$$\underline{\Delta}_I(n) = - \sum_{k=1}^M [A_I^T(k) \underline{\Delta}_I(n-k) + A_Q^T(k) \underline{\Delta}_Q(n-k)] + \underline{u}_I(n) \quad (G.3a)$$

$$\underline{\Delta}_Q(n) = - \sum_{k=1}^M [A_I^T(k) \underline{\Delta}_Q(n-k) - A_Q^T(k) \underline{\Delta}_I(n-k)] + \underline{u}_Q(n) \quad (G.3b)$$

In general, $\mathbf{x}_I(n)$ and $\mathbf{x}_Q(n)$ will be correlated for $A_Q^T(k) \neq 0$ since they both contain terms involving $\mathbf{x}_I(n-k)$ and $\mathbf{x}_Q(n-k)$. However, for $A_Q^T(k) = 0$, eqs(G.3a) and (G.3b) reduce to

$$\mathbf{x}_I(n) = - \sum_{k=1}^M A_I^T(k) \mathbf{x}_I(n-k) + \mathbf{u}_I(n) \quad (\text{G.4a})$$

$$\mathbf{x}_Q(n) = - \sum_{k=1}^M A_I^T(k) \mathbf{x}_Q(n-k) + \mathbf{u}_Q(n) \quad (\text{G.4b})$$

Written in expanded form, the two channel processes become

$$\mathbf{x}_I(n) = \begin{bmatrix} x_{1I}(n) \\ x_{2I}(n) \end{bmatrix} = - \sum_{k=1}^M \begin{bmatrix} a_{11}^I(k) & a_{21}^I(k) \\ a_{12}^I(k) & a_{22}^I(k) \end{bmatrix} \begin{bmatrix} x_{1I}(n-k) \\ x_{2I}(n-k) \end{bmatrix} + \begin{bmatrix} u_{1I}(n) \\ u_{2I}(n) \end{bmatrix} \quad (\text{G.5a})$$

and

$$\mathbf{x}_Q(n) = \begin{bmatrix} x_{1Q}(n) \\ x_{2Q}(n) \end{bmatrix} = - \sum_{k=1}^M \begin{bmatrix} a_{11}^I(k) & a_{21}^I(k) \\ a_{12}^I(k) & a_{22}^I(k) \end{bmatrix} \begin{bmatrix} x_{1Q}(n-k) \\ x_{2Q}(n-k) \end{bmatrix} + \begin{bmatrix} u_{1Q}(n) \\ u_{2Q}(n) \end{bmatrix} \quad (\text{G.5b})$$

In the process synthesis procedure described in Section VI.A and VI.B, the quadrature components of the white noise driving vectors are all uncorrelated. Therefore,

$$R_{12}^{IQ}(k) = R_{12}^{QI}(k) = 0. \quad (\text{G.6})$$

We also note from eqs(G.5a) and (G.5b) that the vector processes $\mathbf{x}_I(n)$ and $\mathbf{x}_Q(n)$ are AR processes which have identical parameters. We therefore have

$$R_{11}^{\Pi}(k) = R_{11}^{QQ}(k) \quad (G.7a)$$

$$R_{22}^{\Pi}(k) = R_{22}^{QQ}(k) \quad (G.7b)$$

and

$$R_{12}^{\Pi}(k) = R_{12}^{QQ}(k). \quad (G.7c)$$

These results validate eqs(7.D.4) and (7.D.5).

Appendix H

In this appendix, we validate eq(4.A.10c). Consider eq(4.A.9b) expressed as

$$R_{\phi\phi}(k,l) = E[x_i(n)x_i^*(n-l)x_i^*(n-k)x_i(n-l-k)]. \quad (H.1)$$

Consider

$$x_i(n) = x_{iI}(n) + j x_{iQ}(n). \quad (H.2)$$

Using eq(H.2) in (H.1), we obtain

$$R_{\phi\phi}(k,l) = E\{ [x_{iI}(n) + j x_{iQ}(n)][x_{iI}(n-l) - j x_{iQ}(n-l)] \\ \cdot [x_{iI}(n-k) - j x_{iQ}(n-k)][x_{iI}(n-l-k) + j x_{iQ}(n-l-k)] \} \quad (H.3a)$$

$$= E\{ [x_{iI}(n)x_{iI}(n-l) + x_{iQ}(n)x_{iQ}(n-l) + jx_{iQ}(n)x_{iI}(n-l) - jx_{iI}(n)x_{iQ}(n-l)] \\ \cdot [x_{iI}(n-k)x_{iI}(n-l-k) + x_{iQ}(n-k)x_{iQ}(n-l-k) + jx_{iI}(n-k)x_{iQ}(n-l-k) \\ - jx_{iQ}(n-k)x_{iI}(n-l-k)] \} \quad (H.3b)$$

$$= E[x_{iI}(n)x_{iI}(n-l)x_{iI}(n-k)x_{iI}(n-l-k)] + E[x_{iQ}(n)x_{iQ}(n-l)x_{iI}(n-k)x_{iI}(n-l-k)] \\ + E[x_{iI}(n)x_{iI}(n-l)x_{iQ}(n-k)x_{iQ}(n-l-k)] + E[x_{iQ}(n)x_{iQ}(n-l)x_{iQ}(n-k)x_{iQ}(n-l-k)] \\ - E[x_{iQ}(n)x_{iI}(n-l)x_{iI}(n-k)x_{iQ}(n-l-k)] + E[x_{iI}(n)x_{iQ}(n-l)x_{iI}(n-k)x_{iQ}(n-l-k)] \\ + E[x_{iQ}(n)x_{iI}(n-l)x_{iQ}(n-k)x_{iI}(n-l-k)] - E[x_{iI}(n)x_{iQ}(n-l)x_{iQ}(n-k)x_{iI}(n-l-k)] \\ + jE[x_{iI}(n)x_{iI}(n-l)x_{iI}(n-k)x_{iQ}(n-l-k)] - jE[x_{iI}(n)x_{iI}(n-l)x_{iQ}(n-k)x_{iI}(n-l-k)] \\ + jE[x_{iQ}(n)x_{iQ}(n-l)x_{iI}(n-k)x_{iQ}(n-l-k)] - jE[x_{iQ}(n)x_{iQ}(n-l)x_{iQ}(n-k)x_{iI}(n-l-k)] \\ + jE[x_{iQ}(n)x_{iI}(n-l)x_{iI}(n-k)x_{iI}(n-l-k)] + jE[x_{iQ}(n)x_{iI}(n-l)x_{iQ}(n-k)x_{iQ}(n-l-k)] \\ - jE[x_{iI}(n)x_{iQ}(n-l)x_{iI}(n-k)x_{iI}(n-l-k)] - j E[x_{iI}(n)x_{iQ}(n-l)x_{iQ}(n-k)x_{iQ}(n-l-k)] \quad (H.3c)$$

For Gaussian, zero-mean quadrature components, eq(H.3c) can be expressed as (dropping the i subscript)

$$\begin{aligned}
R_{\phi\phi}(k,l) = & R_{II}^2(l) + R_{II}^2(k) + R_{II}(l+k)R_{II}(k-l) \\
& + R_{QQ}(l)R_{II}(l) + R_{QI}^2(k) + R_{QI}(l+k)R_{QI}(k-l) \\
& + R_{II}(l)R_{QQ}(l) + R_{IQ}^2(k) + R_{IQ}(l+k)R_{IQ}(k-l) \\
& + R_{QQ}^2(l) + R_{QQ}^2(k) + R_{QQ}(l+k)R_{QQ}(k-l) \\
& - R_{QI}(l)R_{IQ}(l) - R_{QI}(k)R_{IQ}(k) - R_{QQ}(l+k)R_{II}(k-l) \\
& + R_{IQ}^2(l) + R_{II}(k)R_{QQ}(k) + R_{IQ}(l+k)R_{QI}(k-l) \\
& + R_{QI}^2(l) + R_{QQ}(k)R_{II}(k) + R_{QI}(l+k)R_{IQ}(k-l) \\
& - R_{IQ}(l)R_{QI}(l) - R_{IQ}(k)R_{QI}(k) - R_{II}(l+k)R_{QQ}(k-l) \\
& + j \{ R_{II}(l)R_{IQ}(l) + R_{II}(k)R_{IQ}(k) + R_{IQ}(l+k)R_{II}(k-l) \} \\
& - j \{ R_{II}(l)R_{QI}(l) + R_{IQ}(k)R_{II}(k) + R_{II}(l+k)R_{IQ}(k-l) \} \\
& + j \{ R_{QQ}(l)R_{IQ}(l) + R_{QI}(k)R_{QQ}(k) + R_{QQ}(l+k)R_{QI}(k-l) \} \\
& - j \{ R_{QQ}(l)R_{QI}(l) + R_{QQ}(k)R_{QI}(k) + R_{QI}(l+k)R_{QQ}(k-l) \} \\
& + j \{ R_{QI}(l)R_{II}(l) + R_{QI}(k)R_{II}(k) + R_{QI}(l+k)R_{II}(k-l) \} \\
& + j \{ R_{QI}(l)R_{QQ}(l) + R_{QQ}(k)R_{IQ}(k) + R_{QQ}(l+k)R_{IQ}(k-l) \} \\
& - j \{ R_{IQ}(l)R_{II}(l) + R_{II}(k)R_{QI}(k) + R_{II}(l+k)R_{QI}(k-l) \} \\
& - j \{ R_{IQ}(l)R_{QQ}(l) + R_{IQ}(k)R_{QQ}(k) + R_{IQ}(l+k)R_{QQ}(k-l) \}. \quad (H.4)
\end{aligned}$$

where we note that the first two terms in each parenthesis for the imaginary terms cancel. Since

$$R(l) = [R_{II}(l) + R_{QQ}(l)] + j [R_{QI}(l) - R_{IQ}(l)] \quad (H.5)$$

then

$$|R(l)|^2 = R_{II}^2(l) + 2R_{II}(l)R_{QQ}(l) + R_{QQ}^2(l) + R_{QI}^2(k) - 2R_{QI}(l)R_{IQ}(l) + R_{IQ}^2(l) \quad (H.6)$$

and similarly for $|R(k,l)|^2$ so that

$$R_{\phi\phi}(k,l) = |R_{ii}(l)|^2 + |R_{ii}(k)|^2 + F_{ii}(l,k) \quad (H.7)$$

where

$$\begin{aligned} F_{ii}(l,k) = & \{ R_{ii}^{II}(l+k) - R_{ii}^{QQ}(l+k) \} \{ R_{ii}^{II}(l-k) - R_{ii}^{QQ}(l-k) \} \\ & + \{ R_{ii}^{QI}(l+k) + R_{ii}^{IQ}(l+k) \} \{ R_{ii}^{QI}(l-k) + R_{ii}^{IQ}(l-k) \} \\ & - j \{ R_{ii}^{II}(l+k) - R_{ii}^{QQ}(l+k) \} \{ R_{ii}^{QI}(l-k) + R_{ii}^{IQ}(l-k) \} \\ & + j \{ R_{ii}^{II}(l-k) - R_{ii}^{QQ}(l-k) \} \{ R_{ii}^{QI}(l+k) + R_{ii}^{IQ}(l+k) \} \quad (H.8) \end{aligned}$$

as noted in eq(C.8b) of Appendix C.



MISSION of Rome Air Development Center

RADC plans and executes research, development, test and selected acquisition programs in support of Command, Control, Communications and Intelligence (C³I) activities. Technical and engineering support within areas of competence is provided to ESD Program Offices (POs) and other ESD elements to perform effective acquisition of C³I systems. The areas of technical competence include communications, command and control, battle management information processing, surveillance sensors, intelligence data collection and handling, solid state sciences, electromagnetics, and propagation, and electronic reliability/maintainability and compatibility.